# Elucidating a New Mode of Function for ERD2 (K/HDEL Receptor) at the cis-Golgi

**Robert Marshall Bolt**

*Submitted in accordance with the requirements for the degree of Doctor of Philosophy*

The University of Leeds

School of Biology

Faculty of Biological Sciences

December, 2022

The candidate confirms that the work submitted is his own and that appropriate credit has been given where reference has been made to the work of others.

Part of the work in this thesis was possible through the contribution of students completing projects in the host laboratory under my supervision and by previous laboratory members who kindly provided constructs. The authorship of each construct used is provided in Table 1.

Luis L.P. daSilva and Juan O. Concha are thanked for assisting with and sharing unpublished microscopy of HeLa cells transfected with mammalian vectors that I designed, produced and provided from the host laboratory. This work contributed to figures 9 and 14. The remainder of this thesis is my own work.

# Acknowledgements

The faith placed in me by family and friends has been a great source of inspiration throughout this project and as such, I would like to give a special mention to a few individuals as a gesture of my gratitude.

Firstly I'd like to thank my parents for their constant guidance, support and the trust bestowed in me to make it down the right path.

Secondly I'd like to say how grateful I am to have had Prof. Jurgen Denecke as my supervisor throughout this journey. Besides all of the ingenuity he has shared with me over the years, I can also walk away with the knowledge that I've gained a good friend.

Next I would like to offer my appreciation to Jing An for all the countless hours of company, lab support and last but not least, the treats. I am also thankful to the students who gave contributions; Matina Christaki, Dominique Hirsz, Meiyi Hu, Nicoletta Bencka, Emily Cooper and Ben Potter.

Finally, I could not have tackled many hurdles and reached the finish line without the emotional (and IT) support dedicated to me by the wonderful Amy West.

I would also like to thank the University of Leeds for supporting this project since October 2018 with the FBS Studentships initiative.

# Abstract

The secretory pathway is a network of organelles interfacing the endoplasmic reticulum (ER), the plasma membrane and the lysosomes/vacuoles. The Golgi apparatus plays a central role here, sending and receiving membrane carriers to and from these locations. The accumulation of soluble proteins in the ER is dependent on the K/HDEL receptor (ER retention defective 2 or ERD2), originally thought to capture ligands at the Golgi and recycle between these two compartments. In 2018 this model was challenged for the first time after discovery that the C-terminal fluorescent ERD2 fusions displaying the typical dual ER-Golgi localisation were biologically inactive. In this project I have systematically explored multiple lines of experiments, each of which had the potential to either support or refute the biological relevance of ERD2 recycling. I show that Golgi-residency of ERD2 is not a plant-specific feature but also applies to human ERD2. Furthermore, I could demonstrate that ligand-induced ERD2 recycling to the ER is an artefact caused by mutating, deleting or masking of a C-terminal di-leucine motif that is acting as a Golgi retention signal. Next, I illustrated the sensitivity of the ERD2 C-terminus to much smaller epitope fusions and even single residues, re-enforcing the requirement for a native C-terminus to enable meaningful functional studies. Approaching the subject from a different perspective, I discovered a strict correlation between biological activity and Golgi residency. This was substantiated by two complementary experiments; first I could show that the introduction of a COPII ER export signal can overcome the loss of Golgi retention. Secondly, fusing an alternative cis-Golgi retention signal can re-activate ERD2 when its own Golgi-retention motif is compromised. The combined experiments show that ERD2 does not recycle like other sorting receptors and must rely on a novel mechanism to capture ligands and segregate them into retrograde transport carriers without joining. To help dissect the as yet unknown sequence of events occurring upon ligand-binding and release at the cis-Golgi, I explored the subdomain structure of ERD2 and created dominant negative constructs which directly interfere with endogenous ERD2 function, strongly inducing the secretion of HDEL cargo. Whilst open ended, the tools generated will help elucidate the underlying mechanism conserved between plantae, mammals and protozoa that control the first and probably most ancient Golgi-mediated cargo sorting event in eukaryotes.

# Table of Contents

# List of Figures

# Abbreviations

| | |
|---|---|
| **Amy** | Barley alpha-Amylase |
| **AP** | Adaptor protein |
| **Arf1** | ADP ribosylation factor |
| **BFA** | Brefeldin A |
| **BIP** | Binding immunoglobulin protein |
| **CAMV35S** | Cauliflower mosaic virus 35S |
| **CCV** | Clathrin coated vesicles |
| **CHC** | Clathrin heavy chain |
| **CLC** | Clathrin light chain |
| **CLSM** | Confocal laser scanning microscopy |
| **CMV** | Cytomegalovirus |
| **COPII** | Coat protein complex II |
| **COPI** | Coat protein complex I |
| **CPY** | Carboxy peptidase Y |
| **DAPI** | 4′,6-diamidino-2-phenylindole |
| **DV** | Dual vector |
| **EE** | Early endosome |
| **ELP**-1 | ERD2-like protein |
| **ER** | Endoplasmic reticulum |
| **ERD2** | ER retention defective 2 |
| **ERAD** | ER associated degradation |
| **ERGIC** | ER-Golgi intermediate compartment |
| **FRAP** | Fluorescence recovery after photobleaching |
| **FRET** | Fluorescence resonance energy transfer |
| **GAP** | GTPase activating protein |
| **GEF** | Guanosine exchange factor |
| **GECCO** | Golgi entry core compartment GECCO |
| **GFP** | Green fluorescent protein |
| **GM130** | Golgi matrix protein 130 |

| | |
|---|---|
| **GRP78** | Glucose-regulated protein 78 |
| **GUS** | β-glucuronidase |
| **Hsp70** | Heat shock protein 70 |
| **HDEL** | His-Asp-Glu-Leu |
| **kDa** | Kilodalton |
| **KDEL** | Lys-Asp-Glu-Leu |
| **KDELR2** | K/HDEL receptor 2 |
| **LE** | Late endosome |
| **LPYS** | Leu-Pro-Tyr-Ser |
| **M-6-P** | Mannose-6-phosphate |
| **MANF** | Mesencephalic astrocyte-derived neurotrophic factor |
| **NSF** | N-ethylmaleimide-sensitive factor |
| **OST** | Oligosaccharyltransferase |
| **PAT** | phosphinothricin acetyl transferase |
| **PCR** | polymerase chain reaction |
| **PDI** | Protein disulphide isomerase |
| **PM** | Plasma membrane |
| **Rab** | Ras-related in brain guanosine triphosphatase |
| **RE** | Recycling endosome |
| **RFP** | Red fluorescent protein |
| **SI** | Secretion index |
| **SRP** | Signal recognition particle |
| **SNAREs** | Soluble NSF factor attachment receptor proteins |
| **TA** | Total activity |
| **TGN** | Trans Golgi network |
| **TM** | Transmembrane domain |
| **THB** | Triple helix bundle |
| **UPR** | Unfolded protein response |
| **VSR** | Vacuolar sorting receptor |
| **WT** | wild type |

| | |
|---|---|
| **YFP** | yellow fluorescent protein |

# Chapter 1 – Introduction

## 1.1 General Introduction to the Secretory Pathway

This dissertation focusses on protein sorting at the Golgi apparatus, the very core of the eukaryotic secretory pathway, the scale and complexity of which justifies a full appraisal of its cellular role to introduce the reader to the general context of my work. Keeping with tradition; the pathway can be described as a network of membrane-bound compartments offering an oxidative passage to the plasma membrane or vacuole/lysosome for lipids and proteins synthesised at the Endoplasmic reticulum. These intracellular organelles communicate via vesicular/tubular interfaces to preserve each functional domain, enabling a myriad of specific interactions for the correct maturation and localisation of numerous soluble and membrane-bound proteins.

Such cell dynamics were first considered almost 50 years ago in a *Sui generis* review of evidence alluding to a "secretory process", in which Palade (1975) humbly introduces the microscopy and fractionation techniques used to advance the field from pure descriptive observation to the molecular level and establishing the vectorial nature by which individual organelles cooperate. The analysis had a refreshing attitude towards the practical limitations of the era and by doing so shaped a modest, stepwise description of the secretory pathway which still holds merit today. The first steps considered were the synthesis and segregation of proteins in an environment separate from the cytosol, progressing from the ER via the Golgi apparatus to post-Golgi organelles. They were inspired by the identification of membrane-bound ribosomes which preferentially synthesised secreted trypsinogen (Siekevitz and Palade, 1960), and short specialised N-terminal peptide sequences which later shaped the signal peptide hypothesis (Blobel and Sabatini, 1971; Blobel and Dobberstein, 1975). These ribosomes are bound to specific membrane pores called translocons built from the sec61 complex (Johnson and Waes, 1999). The joining process is mediated by N-terminal signal peptides on nascent proteins which interact with the signal recognition particle (SRP) and its ER-membrane bound receptor, arresting any further translation until the ribosome complex is docked onto the ER (Keenan *et al*., 2001). Translocation

of peptides across the membrane occurs in synergy with mRNA translation, leading to protein folding in the ER lumen. Chaperone interaction in the lumen is highly regulated, enabling crosstalk with cytosolic translation factors in the event of ER stress and a requirement for the unfolded protein response (UPR) (Kaufman, 2004). BiP/GRP78 for example, is a key regulator and folding chaperone residing in the lumenal side of translocons awaiting the arrival of ribosome-bound nascent peptides. This positioning maintains ER integrity and separation from cytosol when pores are unoccupied on their cytosolic ER surface (Hamman *et al*., 1998).

Upon successful folding, proteins destined for export will progress to the outer most transitional portion of the ER, where cargo loading bays known as ER export sites form (DaSilva *et al*., 2004; Hammond and Glick, 2000). This progression is a passive, nonspecific migration of molecules defined as bulk-flow (Wieland *et al*., 1987; Denecke *et al*., 1990; Crofts *et al*., 1999) and it is in this manner that soluble proteins find themselves departing in transport vesicles from the ER (Vitale and Denecke, 1999). Membrane proteins are confined to the delimiting membrane of transport carriers and do not enjoy as much bulk-flow as soluble proteins. Specific ER export signals to speed up transport out of the ER were therefore mainly described for membrane spanning proteins with exposed cytosolic portions (Nishimura and Balch, 1997). Besides ER export, proteins need to be transported to the correct final compartment which required further sorting signals, and in some cases more than one. It is important to distinguish cargo proteins with sorting signals from the so-called sorting receptors that recognise these signals and mediate membrane transport. However, this is a simplified viewpoint because the sorting receptors themselves require signals to navigate the secretory pathway. Anterograde and retrograde sorting signals on membrane-bound proteins are a common occurrence as they are critical to the functioning of sorting receptors and organisation of the secretory pathway, so will be discussed at length throughout the introduction.

The aforementioned ER export sites are a gateway to the next stage of the classical route, which is the ER-Golgi interface (Weigel *et al*., 2021). A bi-directional highway, COPII and COPI membrane carriers contain anterograde and retrograde cargo, respectively (Brandizzi and Barlowe, 2013). These routes are co-dependent and heavily relied upon to regulate and maintain the membrane composition and

lumenal environment of each organelle, and in this dissertation the ER retention of lumenal chaperones is a cornerstone to the research mandate.

Upon entry and transport in COPII vesicles, proteins are delivered to the cis-Golgi and embark on a sorting process detailing their final destination. The elements necessary for secretion were recognised at the Golgi apparatus by Palade (1975) and categorized into concentration, compartmentalisation and then “discharge” of cargo beyond the plasma membrane. Pulse-labelling and tracking of radioactive amino acids in pig pancreatic slices showed a time-dependent increase in protein density of condensing vacuoles at the trans-Golgi which gradually matured into zymogen/secretory granules (Jamieson and Palade, 1967). Meanwhile, this location for secretion was further supported by Golgi fractions containing terminally glycosylated proteins (Schachter *et al*., 1970). Discharge of granules into glandular lamina (extra-cellular matrix) was captured as the membrane of zymogen granules fused with the plasma membrane, providing structural confirmation for the exocytosis of secretory proteins (Palade, 1975). Protein release of this manner is highly regulated and varies between specialised cells, but ultimately secretory granules act as hubs for concentration and continued proteolytic processing until their contents are required via external stimuli (Arvan and Castle, 1998). Much later it turned out that these “secretory granules” are in fact specialised endosomes/lysosomes.

Albeit Palade (1975) channelled great enthusiasm for intracellular transport of secretory proteins, advances in the field have expanded the pathway from a simple highway out of the cell to a busy interchange connecting diverse functional domains from the Golgi and beyond. In mammalian cells these destinations include the early endosome (EE), late endosome (LE), recycling endosome (RE) and lysosome, (Figure 1) which besides the RE are traditionally accessible from the Golgi and trans-Golgi network (Traub and Kornfeld, 1997). Post-Golgi trafficking is equally complex in plants, however nomenclature can differ for compartments and there is the structurally and functionally plant-specific vacuole (Rojo and Denecke, 2008). The key feature which draws separation from the classic pathway of secretion is that these organelles are all part of the endocytic pathway, transporting cargo into the cell via early endosomes for resources and environmental signals (Huotari and Helenius, 2011).

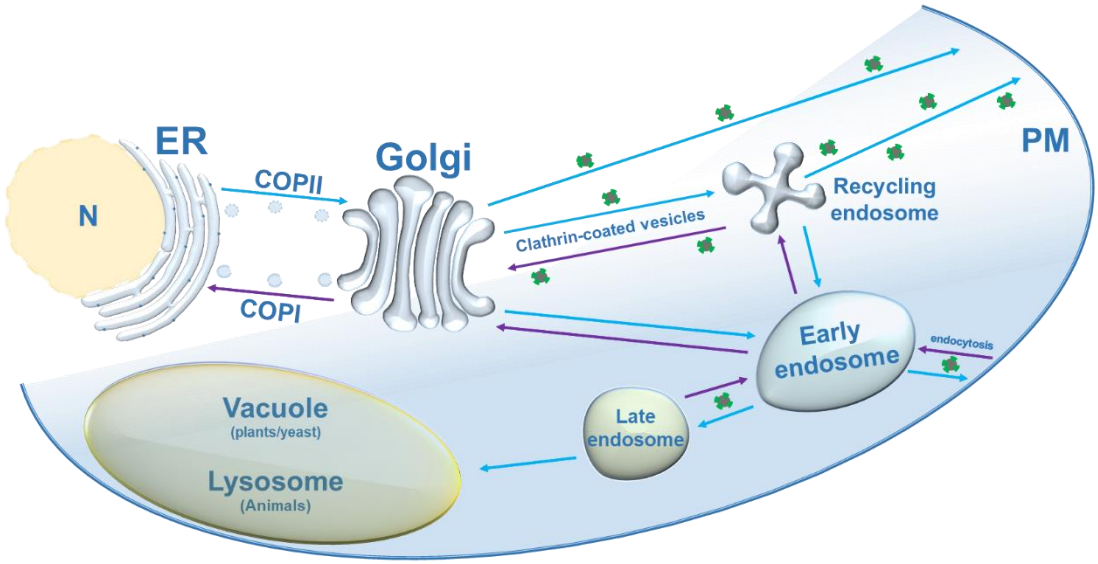


**Figure 1 – Transport routes in the secretory and endocytic pathways of eukaryotic cells.** In close proximity to the nucleus (N) is the Endoplasmic reticulum (ER). The ER shares the COPI/COPII transport network with the Golgi apparatus (Golgi). Proteins arriving at the Golgi may continue into default secretion at the plasma membrane (PM) or enter an interchange of routes provided by the endocytic pathway. Both routes are facilitated by clathrin-coated vesicles (green and gray-labelled vesicle structures), which are specific to post-Golgi sorting. Included in the endocytic pathway is the early endosome, late endosome, recycling endosome and lysosome (or vacuole depending on the species).

The correct delivery of cargo to each destination is crucial to the durability and cohesion of the secretory (exocytic) and degradation (endocytic) pathways. So much so, this property has earned its own space in research and is commonly described as protein sorting and targeting. I am interested in such events at the early secretory pathway which mediate homeostasis of the ER and retention of its lumenal components, a process comprising of sorting receptors and protein cargo packaging at the cis-Golgi. To help the reader delve into this subject, I will first introduce the fundamental elements which enable vesicles to depart from and fuse to membrane-bound compartments. This will be discussed alongside the discovery of prominent coat proteins, sorting receptors and transport pathways. Then I will move my focus to the early secretory pathway, describing the roles of the ER and Golgi in more detail and outline the overarching history of ERD2 (K/HDEL receptor) and how it maintains a high density of chaperones and functional integrity of the ER.

## 1.2 Cargo Carriers, the Late Secretory Pathway and Receptor Recycling Origins

### 1.2.1 Vesicle Structure and Composition

I have mentioned vesicles in terms of the synergy they provide to organelles in mediating secretion, so rather than giving a protracted description of these carriers over the course of the introduction, an individual section is better suited to explain the key targeting components (SNAREs, tethers and GTPases) universally found in the most common carriers to direct their transport and fusion with acceptor compartments. These components are separate to the individual molecular hetero-complexes of cytosolic vesicle coats, which are instead critical to the folding and budding of vesicles from donor membranes. More importantly, vesicle coats contain protein sorting domains which determine the proteomic profiles of their membrane and lumenal space, each being specific to a certain route in the secretory pathway. In this sense, targeting components themselves are sorted into vesicles at donor components, a process determined by the nature of the resident coat protein and the sorting signals needed for recruitment (Mossessova *et al*., 2003). The coat complexes associated with the ER-Golgi interface will be discussed in individual sections, as my research focusses heavily on receptor-cargo interaction here and transport associated with the COPII/COPI coats.

To continue with common themes, the general role of a vesicle is to package cargo at a point of origin, direct its transport to the appropriate target organelle and then finally deposit to the chosen destination via lipid membrane fusion. It should be noted that differential structures besides vesicles can be generated at donor membranes (Bonifacino and Lippincott-Schwartz, 2003; Weigel *et al*., 2021; Shomron *et al*., 2021), but they are newly emerging prospects and relatively uncharacterised compared to traditional vesicle formation. The joining of vesicles with organelles occurs after coat protein shedding, and the merging of membranes is mediated mostly by SNAREs and Rabs, resulting in membrane fusion and ultimately release of membrane proteins and lumenal proteins into the target organelle. In principle this also involves mixing of phospholipids, although it is possible that this is limited by kiss and go mechanisms to mediate immediate recycling of the vesicle membranes to the original donor membrane. There are at

least 65 and 57 genes for SNAREs and Rabs identified in *Arabidopsis*, respectively, divided into subgroups which helps to separate organelles into different protein targeting domains (Martiniere and Moreau, 2020). The activity of these protein families is facilitated by a variety of tethers during the initial steps of membrane fusion, in combination with regulatory co-factors which control the switch between "active" and "inactive" binding states.

#### *1.2.1.1 SNAREs (Soluble N-ethylmaleimide-sensitive factor attachment receptor proteins)*

Like many others, the name given to this protein family stems from the timeline of previous molecular discoveries which enabled their identification. It starts with NSF (N-ethylmaleimide-sensitive factor), a cytosolic protein which enables transport and membrane fusion between Golgi cisternae (Malhotra *et al*., 1988). It works in partnership with α-SNAP (soluble NSF association protein) when binding to membranes (Clary *et al*., 1990) and in subsequent pull-down assays the NSF:α-SNAP duo isolated four membrane proteins collectively known as SNAP receptors (SNAREs) (Sollner *et al*., 1993). SNAREs had actually been identified unwittingly in synaptic exocytosis (Walch-Solimena *et al*., 1993), later establishing that NSF and α-SNAP act as non-specific components to numerous SNARE donor/acceptor subsets.

Four membrane helices form the SNARE complex and consist of one vesicle SNARE (v-SNARE) and three target SNAREs (t-SNAREs) located at the destination membrane. They are typically anchored to membranes by C-terminal TM domains, with their N-terminal domains facing out into the cytosol (Fasshauer *et al*., 1998). The hydrophobic bundle generated from N-terminal combination contains an ionic portion consisting of one arginine and three glutamines, which is why these proteins have an alternative nomenclature of R-SNAREs and Q-SNAREs relating to the amino acids (Sutton *et al*., 1998). V-SNARES roughly correspond with R-SNAREs, likewise with t-SNAREs and Q-SNARES. The subgroups bind in parallel and create a *trans*-complex, which upon assisting membrane fusion mature into *cis*-SNARE complexes where the pair share the same orientation in a single membrane. α-SNAP binds to the *cis*-complex, recruiting NSF which functions as an ATPase to provide the energy necessary for

complex deactivation, and thus recycling of v-SNAREs to a point of origin for the next round of vesicle formation (Rice and Brunger, 1999; Mayer *et al*., 1996). This separation is facilitated by other accessory proteins such as LMA1 and GATE-16, which ensure SNAREs remain inactive in reverse transit, so as to not inhibit new fusion events on the way (Elazar *et al*., 2003).

#### *1.2.1.2 Rab GTPases (Ras-related in brain guanosine triphosphatases)*

Whilst SNAREs are critical to the actual fusion of vesicle and organelle membranes, it is the Rab family of GTPases which bind and usher vesicles from the cytosol to their correct location. This is via interactions with the cytoskeleton for more directional long distance transport compared to random diffusion, and via organelle tethering once in the vicinity of the target compartment. Initially discovered in yeast (*Ypt*), subsequent Rab clones were isolated from rat and human cDNA libraries (Touchot *et al*., 1987). GTP binding domains were highly conserved between clones but sequence variability was evident elsewhere, drawing suggestions that the *ras* superfamily may account for signal transduction in multiple domains along the pathway.

Rabs themselves undergo rounds of membrane-bound and free forms, regulated by association of accessory proteins at the GTPase C-terminus. Prenylation of this domain is a pre-requisite of the targeting capabilities of Rabs, as it enables initial incorporation into vesicle membranes (Martiniere and Moreau, 2020). To prevent membrane docking in the GDP-bound state, GDP dissociation inhibitors (GDI proteins) mask the C-terminus in the cytosol. Another family of accessory proteins, GDI displacement factors (GDF), dissociate GDIs when Rabs are required. GDFs are also available throughout the pathway in *Arabidopsis* and have regional specificity like Rabs (Kamei *et al*., 2008). Once Rabs have completed their own membrane attachment, they are able to facilitate vesicle-to-organelle fusion in a GTP-bound conformation. The occurrence of GTP-bound states will be addressed properly in the membrane recruitment of COPI/COPII coat proteins, but with respect to Rab proteins, the GTP conformation is necessary to pair vesicles to effector proteins associated with the acceptor membrane. The Golgin gene family serves as a good example of molecular tethers, as it encodes a family of coiled-coil membrane proteins found associated with Golgi stacks, forming a cytosolic

matrix speculated to help stabilise the Golgi stack structure. Six homologues exhibiting sequence similarity with yeast and human variants were identified in *Arabidopsis*, and equally conserved were the interactions taking place at the Golgi and Trans-Golgi Network (TGN) between the *Arabidopsis* Golgin candidate 5 (GC5) and the Rab6 homologues RabH1b and RabH1c (Latijnhouwers *et al*., 2007). This highlights the conservation and early evolution of tethering factors for vesicle fusion and structural maintenance of organelles.

### 1.2.2 Clathrin-Coated Vesicles, Endocytosis and Post-Golgi Sorting

As the first vesicle coat protein to be discovered, clathrin inherited its name from the clathrate appearance it displayed upon assembly (Pearse, 1975). Clathrin-coated vesicles (CCVs) provide a vessel for receptor-mediated endocytosis at the plasma membrane and protein sorting from the Golgi/TGN to lysosomes or vacuoles, with the former mechanism initially having more advanced characterisation in the field. They were also established as transport vehicles for membrane proteins, addressing a previously unknown mechanism and leading to the discovery of the subgroup of adaptor proteins (APs). APs simultaneously recruit cargo on the lumen-facing side of carriers whilst polymerising clathrin lattice formation on cytosol-facing domains, and they recruit protein sorting receptors such as the mannose-6-phosphate receptor (M-6-P) (Borgne and Hoflack, 1997) or vacuolar sorting receptor (VSR) (Sanderfoot *et al*., 1998). Packaging of these transmembrane proteins bridges the gap between soluble cargo in the lumen and cytosolic vesicle coat proteins which direct transport routes to endosomal compartments.

Endocytic and biosynthetic protein trafficking occurs via a number of post-Golgi compartments which fulfil a diverse range of protein sorting reactions, collectively referred to as endosomes. In mammalian cells we distinguish early endosomes from late endosomes and recycling endosomes (Lu and Hong, 2014). Endocytic cargo first reaches the early endosome where it may meet biosynthetic cargo arriving from the Golgi. From the early endosome cargo can either progress via the late endosome to the lysosome, or migrate via the recycling endosome back to the plasma membrane. This convergence is important for cellular signalling, nutrient

uptake, and turnover of membrane proteins, but the convergence of biosynthetic and endocytic routes involving joint organelles makes post-Golgi trafficking harder to study. In plants, and using Arabidopsis thaliana as principal model organism, the term TGN is often used to describe the early endosome or the recycling endosome (Viotti *et al*., 2010), but not everyone shares this nomenclature.

CCV budding from the plasma membrane incorporates extracellular material and makes way to the TGN/early endosomes, where they merge with newly synthesised commodities generated from the secretory pathway such as hydrolases and additional membrane constituents. Again facilitated by clathrin carriers, this cocktail of resources passes through a gradual degradation pathway in pre-vacuolar and pre-lysosomal compartments before reaching the ultimate lytic compartment (vacuole, lysosome). To maintain the efficiency of this system, the receptors responsible for selective cargo transport in CCVs have acquired a multi-use function through their ability to return to the original sorting domain for more proteins (Seaman, 2005). This mechanism has inspired the recycling model, a theory used to explain how few receptors can continuously relocate a much larger quantity of ligands. The model has been adapted for various other sorting receptors including ERD2, so an explanation of CCVs as cargo carriers also provides an introduction to receptor recycling and its origins.

#### *1.2.2.1 Clathrin and Vesicle Formation*

Structurally, a single unit of polymerised clathrin triskelion comprises of three hexameric heavy chains (CHCs) and three light chains (CLCs) (Kirchhausen *et al*., 1987; Brodsky *et al*., 1991; Kitakura *et al*., 2011; Wang *et al*., 2013). CLCs are responsible for modulating assembly; when bound to the central hub region of CHCs, a CLC charged domain prevents cytosolic clathrin self-polymerisation under physiological conditions, allowing it to occur only when CHCs are in association with APs near membranes (Ybe *et al*., 1998). For post vesicle-budding, CLCs recruit chaperones which induce coat disassembly (Brodsky *et al*., 1991). CHCs on the other hand are much larger in size and divided into functionally separate subdomains. The C-terminus mediates chain trimerization and is the focal point of clathrin triskelions, as this is where CLCs reside (Liu *et al*., 1995). From here extend

the proximal and distal segments which form the legs of the triskelion, characteristically having a slight bend in-between. These leg-like structures consist of highly repetitive α-helices and salt bridges (Ybe *et al*., 1999). Finally, a variety of binding sites for interacting proteins are found at the N-terminus, which is a globular terminal domain forming a beta-propeller structure with a large surface, similar to that of the WD40 domain (ter Haar *et al*., 2000). It is here that the structural clathrin helices contain most of their networking and protein recruiting capabilities.

*1.2.2.2 Adaptor Proteins and Sorting Signal Recognition*

The most widely studied adaptor proteins are heterotetrameric complexes and major contributors to cargo recruitment in CCVs. AP-2 (α, β2, μ2 and σ2 subunits) is seemingly the most abundant variant and associated with CCVs at the plasma membrane, whereas AP-1 (γ, β1, μ1 and σ1 subunits) is associated to the TGN (Kirchhausen, 1999; Pearse and Robinson, 1990).

As previously mentioned, the endocytic pathway has generated a great deal of interest and this applies to the lifecycle of AP-2 operating between “inactive” and “active” states. When left freely in the cytosol, AP-2 remains in an “inactive” closed conformation, exposing binding sites on its large α and β2 subunits for acidic phospholipid-binding to Phosphatidylinositol 4,5-bisphosphate (PtdIns(4,5)$P_2$), a minor phospholipid located at the plasma membrane (Kelly *et al*., 2014). Once recruited, the smaller μ2 subunit of AP-2 can also bind PtdIns(4,5)$P_2$, causing an open conformation. Importantly, this enables a C-terminal appendage extending from β2 to recruit clathrin and accessory proteins (Kelly *et al*., 2014; Kovtun *et al*., 2020).

As is the case with many regulatory proteins, the cycle between active and inactive states is another preventative measure against unbound coat formation in the cytosol. Another co-dependent structural and functional change is the exposure of receptor binding sites on the AP-2 complex once bound to the plasma membrane. A structural movement of β2 away from interfacing the α-σ2 hemi-complex and simultaneous opening up of the μ2 subunit causes the positioning of two “linear motif” binding sites to enter the open plane (Jackson *et al*., 2010). One is located at the C-terminus of μ2 and recognises the YXXΦ motif (Y = tyrosine, X = any amino acid, Φ = hydrophobic residue) (Ohno *et al*., 1995) and the other is shared

by α-σ2 subunits, recognising the [DE]XXXL[LI] motif (D = aspartic acid, E = glutamic acid, L = Leucine, I = isoleucine). The acidic D/E slots between basic residues on each of the AP-2 subunits, whilst the hydrophobic residues sit in hydrophobic pockets on σ2 (Kelly *et al*., 2008). These binding sites are integral to the recruitment of sorting receptors which enable the delivery of endocytosed material to storage compartments, or in the case of the secretory pathway, newly synthesised lipids and proteins with functional requirements in the lysosomal pathway.

For AP-1, the γ-subunit appears to be key for specialised protein sorting capabilities at the TGN, similar to other adaptors such as the Golgi-localized, γ ear-containing, ADP-ribosylation factor-binding proteins (GGAs) involved in hydrolase receptor trafficking (Page *et al*., 1999; Takatsu *et al*., 2000; Puertollano *et al*., 2001; Bonifacino, 2004). The signal sequences detected and the location of binding sites for cargo are very similar to AP-2, with μ1 and the γ-σ1 heterodimer detecting YXXΦ and [DE]XXXL[LI] motifs, respectively (Ohno *et al.,* 1995; Mattera *et al*., 2011). Where AP-1 differs quite substantially is in its membrane binding and conformation switching methods. It binds to the Golgi enriched PtdIns(4,5)$P_2$ precursor phosphatidylinositol 4 phosphate [PI(4)P] via the γ-subunit (Wang *et al*., 2003), however it also requires the GTPase Arf1 in its GTP bound form. Two binding sites for Arf1-GTP on AP-1 enable membrane recruitment and the conformational change that follows exposes the YXXΦ and [DE]XXXL[LI] binding domains (Ren *et al*., 2013), similar to the mechanism of AP-2.

### *1.2.2.3 Post-Golgi Receptor Targeting and Recycling*

Although the intricacies of sorting towards the lytic compartments in plants and mammals are not entirely conserved (Robinson and Neuhaus, 2016), the premise of hydrolase receptor recycling between the Golgi and endosome remains viable and is endorsed in both cell types.

Lysosomal proteins in mammalian cells are tagged with M-6-P residues and recognised in the Golgi by the cognate receptor (MPR) (von Figura and Hasilik, 1986). There are two individual receptors of varied sizes; MPR46/cation-dependent MPR (CD-MPR) of 46kDa size and MPR300/cation-independent MPR (CI-MPR) with a molecular mass of 300kDa. They are both type I transmembrane

glycoproteins and maintain sequence identity in the binding site-containing lumenal domains, regardless of their size differences (Kornfeld, 1992). The cytosolic C-terminus of both receptors contain sorting signals for packaging into CCVs and delivery to endosomal compartments, specifically the YXXΦ and [DE]XXXL[LI] motifs mentioned previously for interaction with AP-1. They also contain a C-terminal DXXLL signal recognised by the GGAs, a family of monomeric adaptor proteins which also harness clathrin at the TGN (for review see Braulke and Bonifacino, 2009). Once bound to lysosomal proteins at the Golgi, MPRs mediate cargo trafficking to acidic endosomal compartments via their C-terminal signals, whereby the pH gradient of the lumen shifts beyond favourable conditions for ligand binding, causing complex dissociation and downstream transport of hydrolases to lysosomes whilst MPRs are able to recycle to the TGN (Duncan and Kornfeld, 1988; Kornfeld and Mellman, 1989).

Research into the use of hydrolases as a defence mechanism against microbial pathogens identified that plants have secretory and vacuolar variants that are separated by the cleavage of N- and C-terminal sorting signals (Shinshi *et al*., 1988). The complexity of post-Golgi protein sorting in plants was expanded further upon the identification of different vacuolar compartments and more cargo sorting signals (Matsuoka and Neuhaus, 1999). It was suggested that hydrolase sorting may involve a general mechanism that is conserved across eukaryotes, which took the hunt for vacuolar sorting receptors (VSRs) to CCV-enriched fractions taken from developing pea cotyledons. Fractions were passed on affinity columns fixed with aleurain vacuolar sorting signal peptides, at neutral pH, then eluted at lower pH comparable to conditions in acidic endosomal compartments (Kirsch *et al*., 1994). From the elution profile an 80kDa binding protein (BP-80) was isolated. In follow up, this transmembrane protein was characterised for vacuolar cargo binding capabilities and determined as the plant VSR (Kirsch *et al*., 1996).

Agreeing upon a general model for VSR function has been arduous, as various findings suggest different collection and delivery compartments, complicated further by the fact the receptor also contains transport signals for numerous other trafficking routes, such as recovery from the plasma membrane (DaSilva *et al*., 2006; Foresti *et al*., 2010; Gershlick *et al*., 2014; Fruholz *et al*., 2018). Nonetheless and as per anterograde trafficking, a general mechanism for retrograde hydrolase

receptor recovery back to the original cargo collection points of the Golgi/TGN was also anticipated. This recycling avoids degradation in lytic compartments and thus reduces the necessity for *de novo* synthesis of M6P or VSR when sorting the next round of post-Golgi cargo (Seaman, 2012).

The retromer complex is the specialised domain responsible for this recycling, separating receptors into nascent tubules from the endosomes back upstream to the Golgi/TGN. Retromer was identified in *Saccharomyces cerevisiae* as a mediator for the retrieval of Vps10p, a sorting receptor seen to recycle from the endosome to the Golgi (Seaman *et al*., 1997). More specifically, Vps10p selects for carboxy peptidase Y (CPY), a hydrolase localised to the lysosome-like vacuole of yeasts. Retromer's initial characterization was also carried out in *S. cerevisiae*, shown to be comprised of five key proteins all encoded for by vacuolar protein sorting (*VPS*) genes. Divided into two sub-complexes, the first contains a trimer of Vps35p, Vps29p and Vps26p for cargo selection. The other contains Vps17p and Vps5p and is responsible for tubule and vesicle formation (Seaman *et al*., 1998). The trimer is conserved in mammals and plants and Vps5p has two homologs known as SNX1 and SNX2 from the sorting nexin (Snx) family. Meanwhile for Vps17p there is no direct homolog, but orthologues Snx5 and Snx6 have been identified in mammalian cells (Seaman, 2012; Heucken and Ivanov, 2018).

It is easy to understand why the receptor-recycling principle is attractive, and the identification of specific anterograde and retrograde transport mutants of plant VSRs (Foresti *et al*., 2010) provides compelling experimental evidence in support. As such it is also understandable why the recycling principle has been the dominant model for the study of sorting receptor function in general. The remainder of this introduction illustrates how this dogma has guided the field for the last 30 years on the very core of the pathway, the ER-Golgi interface, which will now be discussed in detail.

## 1.3 The Early Secretory Pathway and Bi-Directional Transport

Because organelles of the late secretory/endocytic pathway appear more conditioned and proximal to direct trading of membranes and cargo with the plasma membrane (PM), grouping in parallel the Endoplasmic reticulum (ER) and Golgi apparatus as an “early” secretory pathway can mislead how developmentally related they are with post-Golgi compartments and the cell exterior itself. The course of evolution has segregated various cellular functions into distinct organelles like the ER and Golgi, generating a total membrane surface in cells which is far greater than that of the PM alone. One pertinent theory for this is that eukaryotic cell complexity developed beyond that of simple prokaryotes through continual invagination of the PM which gradually progressed into the formation of individual bodies. Internalised membranes gave rise to more expansive subcellular capabilities to support synthesis and translocation of specialised proteins in an environment similar to the external environment but separate from the cytosol, ultimately resulting in the secretory pathway of current eukaryotes. This brings us to the bearer of the first subset of specialised proteins to be segregated in the secretory pathway – the Endoplasmic reticulum.

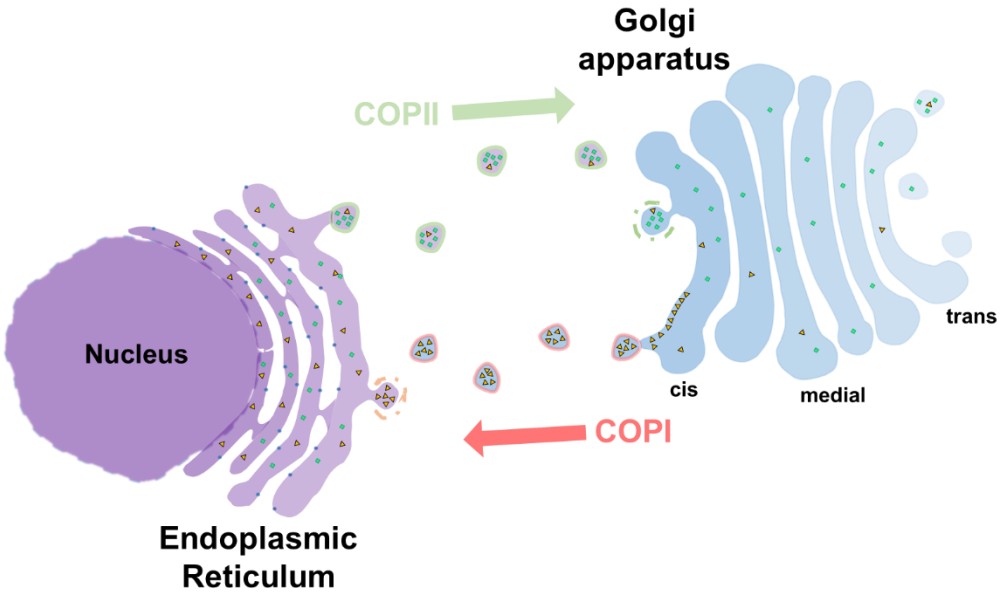


**Figure 2 – The early secretory pathway and the ER-Golgi interface.**
Anterograde transport (green) is mediated by COPII vesicles, travelling from the ER to the cis-Golgi. These carriers contain soluble cargo (green squares) destined for the trans-Golgi via medial stacks and also ER chaperones (yellow triangles). Both populations are transported via passive bulk flow. Most of the chaperones are sorted from other soluble cargoes at the cis-Golgi and returned to the ER in COPI vesicles (red).

### 1.3.1 The Endoplasmic reticulum: A Factory for Protein Synthesis

Whilst prokaryotes translocate secretory proteins directly across the plasma membrane, eukaryotes utilise the ER membrane for this function, but this organelle is also critically involved in a diverse range of cellular roles including lipid biogenesis for membranes and $Ca^{2+}$ ion storage for signalling cascades such as cell movement. From the context of this research project, its most important feature is its oxidative lumen for the synthesis and correct folding of soluble and transmembrane proteins.

#### *1.3.1.1 Structure*

The ER is a highly dynamic organelle and remains proximal to transcriptional events by way of enveloping the nucleus. This external nuclear bilayer is a small component relative to the nearby expansions of flat stacked sheets/cisternae, otherwise known as peripheral ER. Particularly in mammals, these extensive sheets are recognised as rough ER due to the abundance of attached ribosomes acting as hubs for protein synthesis (Shibata *et al*., 2010). The ER also has thin and extended tubules, or in some cases smooth ER which does not widely accommodate ribosomes but instead interlinks sheets and enables connections to other organelles throughout the cell. In certain cases such as plant epidermal cells, high cortical ER levels can be found sandwiched between the PM and vacuole and exhibit restricted mobility. This type of ER is of hybrid cisternal/tubular structure and has indiscriminate membranes for protein synthesis (Hawes *et al*., 2015). Whilst mobile ER stretches are controlled by the actomyosin system, other stationary portions such as perinuclear ER in mammalian cells are typically connected to the microtubule network (Schwarz and Blower, 2016).

Reticulons are a specific subset of ER-localised integral membrane proteins distinguishing the curved structures of tubules and stacked cisternae edges from vast flat sheets of rough ER (Sparkes *et al*., 2010). So much so, reticulon levels are directly proportional to the quantity of tubules or cisternae. Overexpression of reticulons caused elongation and reduced tubular branching, whilst gene knockouts exhibited increased sheet formation (Voeltz *et al*., 2006). They act alongside ER DP1/YOP1/REEP family proteins, crucially sharing the same hairpin structure of TM domains to form wedge shapes which enforce curvature. Finally,

the signature polygonal three-way junctions of ER tubules require the atlastin GTPase family to mediate branching and fusion events between them (Hu *et al*., 2009). Without atlastins, the tubular ER would consist merely of singular, extended elongations rather than a network.

As for the maintenance of cisternal sheets, there are a combination of potential mechanisms in play. It is possible that the fixed curvature of reticulons at cisternae edges is sufficient to maintain the overall ER structure of stacked sheets. However it is more likely that intraluminal “bridges” or flattened cytosolic scaffolds maintain the width of sheets across broad spaces (Shibata *et al*., 2009), which would explain why they do not exhibit swelling in central regions. CLIMP-63 has been identified as a potential bridge protein and p180 or kinectin as external flattening scaffolds, and all three candidates localise heavily to ER sheets.

#### *1.3.1.2 Protein Folding and chaperones*

Based on the origins of the early secretory compartments, it may not come as much of a surprise that the lumen of the ER has an oxidising nature, very similar to the extracellular space, hence its suitability for the maturation of secretory cargo containing numerous disulphide bridges. The lumenal space is a protein rich environment, not least due to the high rates of translocation of newly synthesised peptides across the ER membrane. It also provides residency for a host of protein folding assistants collectively known as chaperones. They help to reduce aggregation and mediate numerous enzymatic and physical configuration changes to nascent peptides that allow them to be transported out of the ER. The main structural issues that chaperones identify in nascent peptides are hydrophobic stretches, partially processed glycans and exposed cysteine residues (Anelli and Sitia, 2008). In each instance there are prominent chaperone families and physical modifications dedicated to remedying these undesirable properties, which is further assisted by the unique chemical environment of the ER.

A chaperone of the heat shock protein 70 (hsp70) family is widely conserved across eukaryotes and responsible for the recognition of hydrophobic regions common at first in most peptides. Its nomenclature includes BiP (binding immunoglobulin protein), GRP78 (glucose-regulated protein 78) or Kar2p in yeast. First isolated when bound to dissociated Ig-H chains (Haas and Wabl, 1983), BiP essentially

holds new amino acid chains in a stabilised manner akin to the internalisation of hydrophobic residues in a fully folded protein (Flynn *et al*., 1991). It comprises of an ATP/ADP nucleotide binding N-terminus and a substrate binding C-terminus. When in the active ATP conformation the N-terminus engages in interactions with hydrophobic regions, and hydrolysis to ADP shortly after fixes BiP into a longer-lived inactive complex. This provides adequate time for the energy released from ATP-hydrolysis to be transferred to the folding intermediate for potential unfolding, followed by subsequent re-folding. ATP hydrolysis of BiP is facilitated by Hsp40 co-chaperone family members known as J-domain proteins or ERdjs (Otero *et al*., 2010) who also help position ATP-bound BiP at translocons in anticipation of new peptide arrivals.

Asparagine-linked glycosylation (N-glycosylation) is a stabilising modification unique to secretory proteins, occurring at NXS/T sequence sites (where X is any amino acid). Initiated by interaction with oligosaccharyltransferase (OST) the preformed complex saccharide $Glc_3Man_9GlcNac_2$ is bound to the asparagine sidechain (Khalkhall and Marshall, 1975) with the intention of regulating protein maturation through rounds of glycan changes. Glucosidase I and II are the earliest sequential modifiers, removing a glucose residue each and leaving an intermediate glycan recognised by the lectins calreticulin and the membrane-bound paralog calnexin (Schrag *et al*., 2001). It is these chaperones which provide stability by preventing aggregation and stratifying folding steps by interaction with other assisters such as the oxidoreductase ERp57 which facilitates disulphide bonding (Ellgaard *et al*., 2001). Upon removal of the final glucose residue by glucosidase II, the lectins can dissociate and the protein can take its final configuration. However if an unfolded intermediate persists, any irregularities nearby N-glycan sites are detected by UDP-glucose glycoprotein glucosyltransferase (UGGT), which places an individual glucose residue back on to aberrations (Taylor *et al*., 2004). This acts as a round of quality control for glycoproteins and by returning the terminal glucose residue, these lectins are able to initiate a second attempt of successful folding.

Oxidative conditions within the ER are preferential for the maturation of secreted proteins, instigated in part by the much larger ratio of oxidised glutathione compared to average cytosolic levels (Hwang *et al*., 1992). Glutathione disulphide thus acts as a nucleation point for oxidoreductases such as protein disulphide

isomerase (PDI), a folding enzyme which also chaperones hydrophobic regions of nascent peptides (Wilkinson and Gilbert, 2004). Because nonspecific disulphide bridges will repeatedly form under the supervision of all chaperones, PDI not only promotes their formation, but also isomerises and reduces bonds if necessary to reconvene the native folding of proteins. The oxidation of thiol groups on newly synthesised proteins to stable disulphide bridges is important for avoiding retention and potential degradation in the early secretory pathway, which can be triggered by exposed cysteine residues (Fra *et al*., 1993).

#### *1.3.1.3 ER Homeostasis and the Unfolded Protein Response (UPR)*

Whilst there are numerous components enabling the ER to maintain a rigorous synthesis regime, the high protein density within the lumen and mostly inept folding capabilities of unsupervised nascent peptides end up as recurring reasons for misfolding and protein aggregation. If not dealt with promptly, the disruption can lead to a state of ER stress symbolised by an inability to keep up with folding demands. There are transmembrane proteins which act as sensors for a struggling ER, such as inositol-requiring enzyme 1α (IRE1α) which is conserved across eukaryotes, designed to install adaptive measures such as reducing translation, increasing chaperone concentrations, initiating ER-associated degradation (ERAD) or in the most critical cases inducing apoptosis (Chen and Brandizzi, 2013).

IRE1α is inactivated through interaction with BiP on the lumenal side of the membrane, but when this chaperone population becomes overly occupied with malfolded proteins IRE1α may passively undergo conformational changes caused by multimerization and autophosphorylation, ultimately activating the RNAse and splicing activity intended to combat ER stress (Hetz *et al*., 2011). Xbp-1 is a bZIP transcription factor that is spliced to increase chaperone expression, targeting what can be collectively described as UPR genes. Regulated IRE1 dependent decay (RIDD) involves targeted RNase activity towards translocon-encoding mRNA (Chen and Brandizzi, 2013). Combined, this is an immediate attempt to alleviate ER stress by simultaneously increasing folding abilities and reducing the volume of translocation, respectively.

A mammalian sensor that activates in a very similar fashion is PERK, which is responsible for the phosphorylation and thus inactivation of eukaryotic translation initiation factor 2 (eIF2α) causing widespread reduction in translation (Harding *et al*., 1999). EIF2α is also capable of influencing UPR gene expression in its phosphorylated form by increasing levels of the ATF4 transcription factor (Vattem and Wek, 2004). ATF6, a sensor which is conserved between mammals and plants, is again geared towards the increased expression of UPR genes in an attempt to expand the folding potential of the ER. Typically residing in the ER, when ATF6 disassociates from BiP it is translocated to the Golgi where the cytosolic portion is cleaved and converted into a transcription factor destined for the nucleus (Haze *et al*., 1999; Shen and Prywes, 2005).

Whilst the UPR avoids resorting to apoptosis, the methods discussed so far do not relieve the lumen of stubborn aggregates which may have triggered ER stress in the first place. Even though induced synthesis of ER chaperones and boosted traffic between the ER and the Golgi will certainly contribute to dealing with an increase amount of folding intermediates that can still fold properly, only the ERAD machinery can dispose of permanently misfolded proteins. The transcription factors generated from ATF6 cleavage and XBP-1 splicing are also implicated in the upregulation of ERAD machinery (Sicari *et al*., 2019). Here, problematic folding intermediates are identified and retro-translocated out of the ER into the cytosol, followed by ubiquitination to direct disposal of troublesome peptides at the proteasome.

### 1.3.2 Anterograde Transport in COPII Vesicles

Taking into account the variability between specialised cell types, on average the synthesis of secretory, vacuolar and transmembrane proteins at the ER constitutes around a third of the total cellular proteome. Once newly synthesised proteins pass the folding criteria enforced by the previously described ER quality control chaperones, they are destined for transport to the next stage of maturation, the Golgi apparatus. As is the case with post-Golgi trafficking, this route of cargo export has adapted its own membrane-budding scaffold which is collectively known as the Coat Protein Complex II (COPII).

*1.3.2.1 The COPII Coat*

Residing in the cytosol, COPII sub-units are sequentially recruited to ER membranes beginning with the GTPase Sar1p (Barlowe *et al*., 1993). The gene for Sar1p in yeast (*SAR1*) was identified as a multi-copy suppressor in mutant cell lines where vesicle formation and protein transport was inhibited (Nakano and Muramatsu, 1989). The mutant phenotype was associated with Sec12p, an essential and specific guanosine nucleotide exchange factor (GEF) for Sar1p (Barlowe and Schekman, 1993). Sec12p is a 70kD type II integral membrane protein with a large 354 residue cytosolic domain (d'Enfert *et al*., 1991a), although fidelity to the membrane is most important with respect to COPII formation, as Sec12p does not require its lumenal domain to recruit cytosolic Sar1p onto the ER membrane (d'Enfert *et al*., 1991b). Likewise, the transition of cytosolic GDP-bound Sar1p to vesicle forming Sar1p-GTP requires the presence of a lipid membrane (Antonny *et al*., 2001) as GTP activation and membrane anchoring are co-dependent.

Sar1p contains a Sar1-$NH_2$-terminal activation recruitment (STAR) motif which is necessary for ER-membrane embedding and mediating GTP transfer from Sec12p (Huang *et al*., 2001). This motif is an evolutionary conserved N-terminal extension of bulky hydrophobic amino acids in an amphipathic α-helix designed for membrane interaction, separating Sar1p from other members of the Ras superfamily which typically receive modifications such as N-terminal myristoylation to integrate with membranes (Nakano and Muramatsu, 1989). The conformational change from GTP binding leading to membrane association of Sar1p involves two structural switch regions (Bi *et al*., 2002). Switch region 1 bonds with the gamma phosphate of GTP and cofactor $Mg^{2+}$, whilst the second switch region co-ordinates gamma phosphate positioning. GTP binding causes an approximate 7 angstrom displacement of a β2-β3 hairpin within Sar1p, preventing the formation of hydrogen bonds between β3 and β1 strands typical of GDP-bound Sar1p. Combined, these structural changes eliminate a surface pocket where the N-terminal amphipathic α-helix would previously reside unexposed, instead forcing the motif to protrude which is then stabilised by entry into the membrane (Bi *et al*., 2002). It is proposed that insertion by Sar1-GTP causes membrane perturbation and curvature, with subsequent addition of coat proteins causing further constriction at the budding

neck before Sar1p is released and vesicle fission occurs (Bielli *et al*., 2005). GTP hydrolysis which leads to fission is enhanced when the COPII coat is more stabilized by recruitment of correctly folded proteins, suggesting a proof-reading mechanism which ensures vesicle release only occurs with suitable contents (Sato and Nakano, 2004; 2005).

GTP binding and membrane association of Sar1p are synergistic in recruitment of the first COPII complex components, the Sec23p-Sec24p heterodimer. Sec23p is a ~84kD protein originally identified in a 260kD multimeric complex alongside p105, a 105kD protein later titled Sec24p (Hicke and Schekman, 1989; Hicke *et al*., 1992). Although there is high sequence divergence, they share similar structure combining to form a bow-tie shaped complex with a concave inner face lined with basic residues (Lee *et al*., 2004). The curvature and internal positive surface charge combined with an extending Sar1 N-terminal interaction enables large coverage of the outer ER membrane by a single heterodimer (Bi *et al*., 2002). The heterodimer is crucial for vesicle budding at the ER membrane, as inhibition is seen after the addition of polysera against both proteins (Hicke *et al*., 1992). Increased expression on the other hand increases the GTPase activity of Sar1p substantially, however it is Sec23p that acts as the specific GTPase activating protein (GAP), as titration with polysera alone for sec24p made no effect on Sar1p activation (Yoshihisa *et al*., 1993). Sec23p inhibition reduced GTPase activity and membrane budding, identifying that Sar1p activity is critical to vesicle formation. The precise catalysis of GTPase activity is induced by the insertion of an arginine finger from Sec23p into the Sar1p active site, neutralizing the overpowering charges across the phosphate groups to enable a transition to GDP (Bi *et al*., 2002). Sec24 is responsible for equipping COPII vesicle-specific proteins such as the SNARE Sec22p for fusion at the Golgi (Mossessova *et al*., 2003). On a similar note, the Sec23/24 complex is phospho-regulated on approach to the acceptor compartment to ensure correct directionality and fusion of COPII vesicles (Lord *et al*., 2011).

The construction of the COPII complex is concluded upon the addition of the Sec13p-Sec31p heterodimer. The necessity of this heterodimer in ER vesicle budding was established in a similar manner to Sec23p-Sec24p, using polysera to inhibit transport and then showing Sec13p as part of a complex alongside a 150kD protein now identified as Sec31p (Salama *et al*., 1993; Pryer *et al*., 1993; Salama

*et al*., 1997). Sec13p and Sec31p are mostly identified in heterotetramers independent of membrane interaction, containing two globular domains and a central rod (Matsuoka *et al*., 2001). These heterotetramers polymerise to form cubo-octahedral cages, with the Sec13p globular domains acting as vertices and the Sec31p rods as the cross-bridging edges (Stagg *et al*., 2006). COPII vesicles are highly pleomorphic and can cater for a range of differently sized cargo, most likely due to the polyhedral nature of Sec13p-Sec31p (Stagg *et al*., 2006). For example, membrane curvature and export of the secretory marker tsO45-G-YFP is unaffected by Sec13p-Sec31p depletion, however collagen secretion in fibroblasts is severely affected, suggesting the heterodimer accounts for vesicle flexibility (Townley *et al*., 2008). The discovery of *bypass-of-sec-thirteen* (*bst*) mutants following knockout has helped identify that although not essential, Sec13p offers rigidity to the COPII cage, improving its ability to bend membranes (Copic *et al*., 2012). Besides acting as a nucleation site for cage polymerisation, Sec13p-Sec31p recruitment also enhances the GAP activity of Sec23p up to ten-fold (Antonny *et al*., 2001; Bi *et al*., 2007). A highly conserved 50 amino acid stretch within Sec31p is responsible for this, strengthening the interaction between Sec23p-Sec24p and Sar1p necessary for GTP hydrolysis (Bi *et al*., 2007).

In conclusion, these coat components provide insight into how COPII vesicles assemble at the ER. The built in mechanism of GTP-hydrolysis explains the synergistic coat release and unveiling of vesicle SNAREs for fusion with the Golgi membrane, recycling individual coat components for renewed vesicle budding from the ER.

### 1.3.3 Sorting at the Golgi and Retrograde transport

#### *1.3.3.1 The Golgi apparatus*

Situated at the intersection between endosomal and biosynthetic transport pathways, the Golgi is a master protein sorting station within the cell and most likely evolved early in the history of the secretory pathway. Yet it is highly pleomorphic and handles continuous waves of exo- and endocytic membrane traffic not only on external sides but also between cisternal layers, offering a mechanistic complexity that remains in open debate (Glick and Luini, 2011). The rate of flux at this organelle is embodied by its response to Brefeldin A (BfA) treatment, a protein

transport inhibitor, which causes the Golgi's devolution into neighboring structures such as the ER as it is unable to maintain individual integrity (Lippincott-Schwartz *et al*., 1990). This transition under stress raises questions on whether the Golgi should be considered structurally independent or rather a cumulative body generated from various transport routes. Such a question brings additional complexity to understanding the mechanisms in place which retain transmembrane proteins to different cisternae.

The intricacies of this organelle differ between eukaryotes, adding difficulty for the field in proposing a general mode of function which can tie in structure. The Golgi is split into three subdomains where the *cis* side typically faces towards the ER, the *trans* towards post-Golgi compartments and sandwiched in between is the *medial* region. For the budding yeast *S. cerevisiae,* these cisternae exist individually and can be identified across the cell by differences in their coat protein profiles (Beznoussenko *et al*., 2016). Meanwhile in plant cells the *cis*, *medial* and *trans* sub-compartments hold together forming miniature, motile Golgi stacks, also termed Golgi-bodies. They move rapidly throughout cells along actin filaments (Boevink *et al*., 1998). In most mammalian cells, the Golgi is visibly much larger and described as having a ribbon structure where many stacks, held together by tubular connections accumulate in the vicinity of the nucleus, whilst the ER is spread out more towards the cell periphery. The uninterrupted pattern is maintained by membrane association with microtubule motor proteins dynein and kinesin close to the centrosome (Thyberg and Moskalewski, 1999). A special mention should also be given to the mammalian-specific ER-Golgi intermediate compartment (ERGIC), a collection of vesicles and tubules containing COPII and COPI coatomer acting almost as a half-way house for the comparatively larger journey in mammalian cells. The compartment is characterised by a unique marker protein ERGIC53 (Appenzeller-Herzog and Hauri, 2006) and unlike the Golgi it is able to maintain itself upon BfA exposure (Lippincott-Schwartz *et al*., 1990). Although no ERGIC 53 orthologue has been identified in plants, a similar structure is emerging here termed GECCO (Golgi entry core compartment), which retains some *cis*-Golgi components in smaller punctate structures upon BfA treatment and appears to be traversed by the rest of the Golgi components upon reconstruction (Ito *et al*., 2018).

In plants the Golgi also has the important role of synthesising many cell wall polysaccharides (Hoffmann *et al*., 2021) and across all eukaryotes it sequentially generates mature glycoproteins from the initial sugar branches acquired in the ER, courtesy of glycoenzymes segregated by cisternae (Stanley, 2011). However and as previously noted, this organelle undergoes continuous rounds of protein sorting which and on the *cis* side of the Golgi this is of particular importance to ER homeostasis. A retrograde pathway here is key for recycling the lipid membrane, transmembrane proteins and lumenal constituents of the ER which have been delivered in COPII vesicles, and in not doing so would be detrimental to ER stability due to large increases in *de novo* synthesis demands.

#### *1.3.3.2 COPI vesicles*

As is the case with many research findings, the chronology of discovery doesn't necessarily align with the actual order of biological steps. For transport at the ER-Golgi interface this has led to somewhat confusing nomenclature. Vesicles localised to the Golgi besides those relating to endocytosis were originally classified as "non-clathrin coated", then after isolation the associated membrane proteins of these carriers were collectively named "coatomer" (Waters *et al*., 1991). It was not until the discovery of COPII vesicles at the ER that coatomer was renamed COPI, mainly to acknowledge their close relationship (Barlowe *et al*., 1994). It was in the same year the field came to terms with COPI/coatomer actually controlling Golgi to ER retrograde transport (Cosson and Letourneur, 1994; Letourneur *et al*., 1994), rather than intra Golgi anterograde transport (Orci *et al*., 1986) a fact that stirred up the field for at least another decade (Orci *et al*., 1997). Hence, coat nomenclature relates to the order of discovery rather than the progression stage in the secretory pathway. Nonetheless, the two structural coats share mechanistic synergy, with any compromise to just one of these transport routes having a potentially detrimental effect to the overall function of the ER-Golgi interface (Phillipson *et al*., 2001).

With the exception of the coat proteins which are released into the cytosol, the rest of the COPII machinery remains bound in vesicles upon arrival at the *cis*-Golgi alongside the ER lipid membrane that they are encased in. In this respect, much of the responsibility of COPI vesicles is to provide safe return for this machinery and

membrane (Manneville *et al*., 2008) to allow for future rounds of ER export. Importantly, there are many well-established sorting signals associated with COPI-mediated retrograde transport which mediate the segregation of cargoes.

Yet a less-defined role of COPI vesicles is their relationship with cisternae beyond the *cis*-Golgi. They have been considered responsible for the correct localisation of Golgi enzymes between cisternae and in fact were originally suggested as anterograde carriers within the Golgi (for review see Rabouille and Klumperman, 2005). There is some evidence for concentrated anterograde cargo in COPI vesicles, however this means there would have to be the capability of recruiting multiple variants of sorting, targeting and fusion machinery by one individual set of coat proteins. This is difficult to rationalise when considering the vectorial evolution of the secretory pathway and the purpose of different coats such as COPII and clathrin. Structural differences have been recognised between retrograde COPI vesicle formation at the *cis*-Golgi and in downstream *medial* and *trans* compartments using tomography and electron microscopy, (Donohoe *et al*., 2007) which again suggests separate sub-populations, but their contents have not been discussed in any detail and such differences have not been as intensively studied in reliable mammalian models. Much of the work on in vitro generated COPI-vesicles stems from the use of GTPgammaS, a non-hydrolysable analogue of GTP. This prevents un-coating and thus accumulation of COPI vesicles, the nature of which have never been proven representative of living cells (Pelham, 1994) The very nature of Golgi-localised anterograde and retrograde COPI vesicles means that in each case they support a different model of Golgi morphology and trafficking, which as previously discussed is still debated due to the contradictions in supporting evidence. If in the end only one model for the Golgi can prevail, in equal measure it is likely that there will only be one trafficking function for COPI vesicles.

Whilst the topic of intra-Golgi COPI vesicles is not a focal point of this research, the COPI coat itself is of much more interest due to its role in Golgi-to-ER recycling of ER resident proteins. Similarly to COPII, the initial recruitment of COPI to the membranes occurs following the activation of a GTPase (Garcia-Mata *et al*., 2003). This being Arf1-GTP (Spang *et al*., 1998), the same G protein responsible for clathrin recruitment at the Golgi, requires myristoylation of its amphipathic N-terminal for insertion into the membrane. COPI itself exists as a cytosolic heptamer,

which certainly facilitated its purification and functional testing using semi-intact cells in vitro (Malhotra *et al*., 1989). However, COPI is often split structurally into two sub-complexes even though it is recruited onto the Golgi membrane in its entirety (Hara-Kuge *et al*., 1994). The trimeric α-, β'-, ε-COP is described as cage-like and named the B-complex based on early comparisons drawn with clathrin and the outer COPII structure, whilst the tetrameric β-, δ-, γ-, ζ-COP is considered similar to adaptor complexes and otherwise known as the F-complex. However the unique quality which separates COPI is that both arrangements make contact with the membrane (Dodonova *et al*., 2015), as the α- and β'- subunits of the cage-like complex form an overarching α-solenoid across the adaptor-like tetramer. Another particular quality is that COPI complexes form leaf-shaped triads containing six molecules of Arf1-GTP that interact primarily with β- and γ-COP (β-Arf and γ-Arf, respectively) (Dodonova *et al*., 2017). Between these triads there are different combinations of interactions that can occur between α-, β- and δ- subunits, in turn generating vesicles of varying size (for review see Bethune and Wieland, 2018). In the case of COPI disassembly, a separate family of proteins namely the ArfGAPs are recruited to trigger the GTPase activity of Arf1 (Cukierman *et al*., 1995). As is the situation of two separate binding sites between Arf1-GTP and the COPI complex, two separate forms of ArfGAP have been identified in humans that are separately suited to binding each of the G protein-COPI complex conformations (Frigerio *et al*., 2007).

*1.3.3.3 Transport between the ER and the Golgi*

ER export has already been touched on briefly, but the idea of cytosolic signalling for recruitment into transport vesicles also applies at the cis-Golgi.

Two of the most prominent and well characterised COPI sorting signals are the C-terminal KKXX (Nilsson *et al*., 1989) and KXKXX (Jackson *et al*., 1990) motifs found on transmembrane proteins. Much like the manner of clathrin-mediated recruitment, the COPI coat contains WD-repeat domains with large surface areas designed to interact with the cytosolic domains of other proteins. More specifically, β'-COP preferentially binds to the KXKXX motif and the same is proposed for α-COP and the KKXX motif (Eugster *et al*., 2004; Jackson *et al*., 2012). The p24 family of proteins are an abundant group of type I transmembrane proteins

localised to the ER-Golgi interface conserved between yeasts, plants and mammals. Interestingly, a subgroup carry this putative COPI sorting signal in their C-terminus alongside a diaromatic motif consisting of phenylalanines which interacts with COPII (Fiedler *et al*., 1996; Dominguez *et al*., 1998; Contreras *et al*., 2004), suggesting a bidirectional mode of function. Pinpointing the exact function of p24 proteins remains difficult and is possibly due to the sequence variability across subfamilies (Strating *et al*., 2009), however the abundance of p24 variants in the early secretory pathway advocates their importance in itself. A crystallographic study identified the proteostasis regulator 4-phenylbutyrate (4-PBA) as a binder of Sec24p in a region called the B site, mimicking the interaction with an ER export signal known as the ΦC motif (Ma *et al*., 2017). Mutation of key residues in the B site or incubation with 4-PBA saw a reduction of p24 proteins captured into COPII vesicles in assays containing permeabilised mammalian cells and enriched recombinant COPII coat proteins. Alongside this effect was an increase in the packaging of ER resident proteins and malfolded mutant receptors into COPII vesicles. The authors inferred this as a knock-on effect from the exclusion of p24 proteins, either because p24 may directly exclude such molecules from leaving the ER, or rather the sorting of other proteins for ER export simply limits space in COPII vesicles for the bulk flow of any proteins which aren’t associated with p24. In either instance, this suggests that the p24 family may be another group of transmembrane proteins that bridge the gap between lumenal cargo packaging and coat protein sorting.

Not only that, the traits held by this family in utilizing both pathways of the ER-Golgi interface shows the closely intertwined alliance held by COPI and COPII coats in sustaining their perpetual genesis of transport carriers.

## 1.4 Retention of Soluble Proteins in the Endoplasmic Reticulum

### 1.4.1 Bulk Flow – a Rationale for ER Retention

Great advances were made in the decade following Palade's discovery of the secretory pathway (for review see Pfeffer and Rothman, 1987), particularly the notion that any proteins not destined for the plasma membrane or beyond must be pulled out of the export stream by presentation of specific signals. Lysosomal sorting via the mannose-6-P receptor is the earliest supporting evidence for this and became the driver for connecting coat proteins to certain transport routes for lumenal cargo, such as clathrin and post-Golgi compartments. However, a pertinent question still yet to be pursued was how this strategy applies to the Endoplasmic reticulum. It did not seem fathomable that the ER protein fraction of folding chaperones would continue non-specifically along the pathway with secretory cargo, but a mechanism to prevent this was yet to be identified.

One theory was that export is signal-mediated, based on the varying rates at which different membrane and soluble proteins were seen leaving the ER in human hepatoma HepG2 cells (Lodish *et al*., 1983). At the same time it emerged that intermediates such as the heavy and light chains of IgM could be trapped in the ER when synthesised without their partnering subunits (Mains and Sibley, 1983), suggesting that unassembled or unfolded proteins may traverse the ER over different periods of time to attain their correct configuration. Signal-mediated ER export at least offered the potential for a set of associated receptors, as the alternative outcome was that all contents of the ER lumen are in fact shipped out in a passive, non-specific manner. To bring together the two opposing models, Wieland *et al*. (1987) set out experiments which quantified the transit of trivial proteins out of the ER which were designed to avoid any folding or sorting signal bias. CHO and HepG2 cells were incubated with tripeptides containing the N-glycosylation recognition sequence (N-X-S/T), which after diffusion caused them to be trapped in the ER through attachment of preformed saccharide chains. The rate of secretion was then calculated by the time taken to leave the ER and reach the cell surface. This ranged between 5-20 minutes which was at the same rate of any other soluble or membrane proteins studied, essentially showing that no signal is necessary for efficient transport out of the ER. This study was expanded on in plant

cells. Cytosolic proteins of prokaryotic origin were fused to eukaryotic signal peptides from both plants and animals, to show that these could be secreted from protoplasts to the culture medium after successful translocation into the ER lumen (Denecke *et al*., 1990).

### 1.4.2 Discovery of the K/HDEL retention sequence

Although it became apparent that correct folding is the only requirement for secretory cargo to exit the ER, the field were still left contemplating how a known portion of soluble chaperones could seemingly remain behind all the while. The gradual sequence availability of chaperones including BiP, endoplasmin and PDI led researchers to muse over conserved regions and it was not long before the C-terminal Lys-Asp-Glu-Leu (KDEL) found in all three proteins was tested for function (Munro and Pelham, 1987). They found that expressing the rat BiP with varying C-terminal truncations in COS cells caused its accumulation in culture supernatant when compared to a wild type transfection. This provided strong arguments for the bulk flow theory of soluble protein secretion, because it was unlikely that ER retained proteins would contain cryptic ER export signals to accommodate the event of man-made mutants lacking the retention signal. Evidence that the putative retention signal was sufficient arose from the fact that re-attaching a short SEKDEL C-terminal peptide to the mutants would re-establish ER retention. Not only that, the same addition to the typically secreted chicken lysozyme caused its accumulation in the ER of COS cells. Finally it was shown that the KDEL sequence had to position at the extreme C-terminus, as an extension of two residues (Gly-Leu) led to the same levels of secretion out of COS cells as the truncated BiP mutants (Munro and Pelham, 1987).

The KDEL sequence was a landmark discovery for ER retention and offered the field a tangible research tool for characterising protein transport in the early secretory pathway. Munro and Pelham (1987) also deliberated on their direction of follow up research, sharing that they did not envision any candidates that could mediate retention within the ER. This was based on the sheer volume of chaperones which so far had not been matched in abundance by any other proteins for possible binding (Macer and Koch, 1988). Not only that, BiP, endoplasmin and PDI were frequently solubilised upon ER homogenization in other studies

suggesting no membrane anchoring. Instead, they theorised that perhaps rather than being held in the ER, these chaperones were continually recovered from a downstream compartment.

Mannose-6-phosphorylation occurs in the Golgi and directs the correct localisation of lysosomal enzymes. The initial incorporation of phosphate is carried out by GlcNAc-P-transferase at the *cis*-Golgi, a domain that is functionally separated from the ER (Waheed *et al*., 1981). The side chains of the Cathepsin D are known substrates of this process, therefore to test the theory of downstream sorting Pelham (1988) attached the KDEL sequence and studied the modification profile of the enzyme. It was immediately clear that fusing KDEL at the C-terminus retained Cathepsin D in the ER. Labelling with the radioactive isotope $^{32}P$ showed that ER-retained and lysosome-bound Cathepsin D had the same degree of $^{32}P$ incorporation from side chains, identifying that they both reached the *cis*-Golgi. It cannot be excluded that phosphorylated Cathepsin D-KDEL was that which had been sorted to the lysosomes, as pure ER was never isolated. This data, combined with a study by Ceriotti & Colman (1988) showing that removing KDEL from BiP does not alter its rate of diffusion in the ER lumen of *Xenopus* oocytes posed another strong case that there is no receptor to anchor these proteins within the ER.

### 1.4.3 Identification of the prophesised receptor

Exploration into this recovery mechanism escalated to the yeast *S. cerevisiae* (Pelham *et al*. 1988), a species also showing conserved C-terminal residues amongst ER residents that have Golgi-specific modifications. Here the tetrapeptide signal was His-Asp-Glu-Leu (HDEL). In an elegant genetic screen, any yeast mutants with a reduced ability to retain ER residents could be identified by expression of an HDEL-tagged invertase (invertaseHDEL) knock-in, in place of the endogenous invertase gene. Pre-cultured transformants were plated on medium where sucrose was the sole carbon source, thus requiring invertase to convert the disaccharide into fructose and glucose monomers. The availability of monosaccharides was crucial to yeast growth as it is unable to take up sucrose, therefore only the colonies secreting substantial amounts of invertaseHDEL would be capable of surviving. Simultaneously, an ER retention deficiency would be

exposed. Truly defective mutants were then confirmed with a secondary screen detecting the secretion of endogenous HDEL proteins. To do this, nitrocellulose filters were placed in contact with colonies during growth, then probed with anti-HDEL antibodies and radiolabelled with $^{125}$I-protein A. The outcome was two complementation groups presenting strong secretion phenotypes, named *erd1* and *erd2* (ER retention defective) (Hardwick *et al*. 1990). The corresponding genes *ERD1* and *ERD2* were cloned via restriction mapping shortly after and then analysed in separate studies.

Strains where *ERD1* was disrupted or deleted did allow secretion of ER resident proteins, but this phenotype was subdued in conditions where growth was severely slowed (Hardwick *et al*. 1990). *ERD1* mutants also appeared to be implicated in downstream compartments beyond the *cis*-Golgi where carboxypeptidase Y (CPY) is processed and complex glycan modifications occur (Hardwick *et al*. 1990), raising questions as to whether this gene was primarily involved in sorting at the *cis*-Golgi or not. A silencing effect by reducing the rate of growth could be explained when considering that mannose side chain additions at the cis-Golgi were not prevented in the *erd1* phenotype (Pelham *et al*., 1988). This meant the cis-Golgi retained some function and only when growth rates were higher could HDEL proteins reach beyond into more defective regions and end up secreted. At this stage the deficit in ER retention exhibited by *erd1* was not deemed detrimental to the functioning of the secretory pathway.

Semenza *et al*. (1990) investigated *ERD2* under the same strategies and the immediate observation was that *erd2* mutants also caused BiP to be secreted, yet CPY processing and glycosylation was not compromised. *ERD2* now appeared more likely to have a specific association with the ER retention mechanism. Overexpression of ERD2 C-terminally tagged with a *myc*-epitope reduced the secretion of HDEL proteins in a variety of mutants including *erd1*. Removal of ERD2 proved to be lethal, showing essentiality for growth in yeast. This was surprising and in contrast to findings on *ERD1* (Hardwick *et al*., 1990), which had initially led to assumptions that the HDEL retention system may not be as important as first thought, since *erd1* and HDEL removal from BiP had not prevent growth in yeast.

The twin studies were closely followed by the identification of a human ortholog based on similar sequence, size and structure to yeast *ERD2* (Lewis & Pelham, 1990). Interestingly, complementation assays between humans and *S. cerevisiae* proved unsuccessful. Nonetheless, the conservation of genes initiated a motion of acknowledgement that ERD2 coded for the receptor which is responsible for sorting and returning ER resident proteins from a downstream compartment.

### 1.4.4 Initial ERD2 characterization and the Recycling Concept

Compelling evidence for chaperone recycling between the *cis*-Golgi and ER combined with the identification of ERD2 opened speculation as to whether the receptor was recycling too (Dean & Pelham 1990; Hardwick *et al*. 1990). In the process of hunting for any indication of this mechanism, structural and functional properties of ERD2 continued to gather.

#### *1.4.4.1 Ligand Specificity*

Differences in retention ligand specificity between species were explored further by comparing this mechanism in two closely related budding yeasts, *Kluyveromyces lactis* and *S. cerevisiae*. The BiP homolog in *K. lactis* contains a DDEL C-terminal sequence unlike the HDEL found in *S. cerevisiae* (Lewis *et al*., 1990). The cloned gene from *K. lactis* shared 59% amino acid similarity and could complement growth in *S. cerevisiae erd2* mutants, identifying itself as the receptor. Three retention sequences (FEHDEL, YFDDEL and SEKDEL) were fused to invertase as a representation of the known *S. cerevisiae*, *K. lactis* and mammalian retention signals and secretion was measured for *S. cerevisiae* strains expressing either of the yeast variants. In agreement with Pelham *et al*., 1988, the *S. cerevisiae* ortholog only efficiently retained the HDEL ligand. However, when strains instead expressed *K. lactis* ERD2, proteins bearing either DDEL or HDEL were both retained (Lewis *et al*., 1990). These results were reproducible with prepro-alpha factor as cargo in place of invertase. More interestingly, multi-copy vector overexpression of *S. cerevisiae* ERD2 in chromosomal knock-out strains mediated low level retention of KDEL and DDEL proteins, showing increased promiscuity for the first time. In these conditions retention of HDEL-tagged proteins was also much improved relative to wild type levels. This suggested that under normal conditions endogenous receptors are saturated, but by increasing the availability of ERD2 there is a better

chance of retention for proteins with less preferable retention sequences. Interaction with the -5 and -6 residues of tested signal sequences was not ruled out and it should be mentioned that they have been proposed to effect the strength of retention in a more recent study (Mei *et al*., 2017). Regardless, the outcomes still supported an association between ligand specificity and ERD2 orthologs.

In a comparison of the two yeast sequences, Lewis *et al*. (1990) recognised a mutation at residue 51 in the *S. cerevisiae erd2* phenotype which is naturally present in *K. lactis*. To follow up, Semenza and Pelham (1992) studied changes in the specificity of *K. lactis ERD2* after substituting certain residues for those found in the *S. cerevisiae* homolog. When Asn-51 was converted to aspartic acid (N51D), DDEL retention was maintained however HDEL retention was severely impaired. In another mutant, a gap-lysine (-K) was replaced with phenylalanine-histidine (FH) at positions 55-56 and this caused reduced retention for both DDEL and HDEL, but retention was still more evident relative to the negative control (KDEL). A third phenotype was seen when both mutations were combined; DDEL retention was comfortably above background whilst HDEL retention was weakened. It appeared that residue 51 in *K. lactis* was crucial for HDEL binding and less important for DDEL, however the region of interaction for both ligands was clearly shared. Coinciding was very similar mutational research in human ERD2, altering residues 51, 55 and 57 in accordance to the *K. lactis* sequence (Lewis & Pelham, 1992b). HDEL binding was not tested, but affinity was lost for KDEL and increased for DDEL in the human *ERD2* triple mutant. The joint outcomes on this small stretch of amino acids suggested they may dictate the specificity of retention between species, more specifically residue 51 having particular importance to HDEL-binding in yeast and KDEL-binding in humans.

ER Retention signals were also established in plants, where phosphinothricin acetyl transferase (PAT) was the test cargo representing passive bulk flow in *Nicotiana tabacum* (Denecke *et al*., 1992). The characteristics of retention were slightly different to yeast and mammalian cells, as three C-terminal tetrapeptides (HDEL, KDEL and RDEL) were all accepted as retention sequences in this pathway. After little success with conventional approaches such as polymerase chain reaction amplification, random clones from the *Arabidopsis thaliana* cDNA library with homology to *S. cerevisiae* were sequenced in order to identify ERD2 in

plants serendipitously (Lee *et al*., 1993). The protein shared 52% homology with human ERD2 and 49% homology with the *S. cerevisiae* ERD2. Interestingly, it was capable of complementing the yeast *erd2* mutant whilst containing closer sequence similarity to the human receptor in the previously studied 51-56 amino acid stretch.

### *1.4.4.2 Localisation and structure*

Alongside the original discovery of the receptor, preliminary indirect immunofluorescence assays in *S. cerevisiae* were undertaken on ERD2 modified with a C-terminally fused c-*myc*-epitope tag (ERD2-c-myc) (Semenza *et al*., 1990). The receptor presented punctate structures comparable to the antibody-targeted YPT1 Golgi-marker, visibly separate to the ER localisation of anti-HDEL antibodies (Hardwick *et al*., 1990). This suggested an ERD2 localisation in the Golgi under steady state conditions, but authors' exercised caution given the interpretation was with a modified receptor. The ERD2 fusion protein remained membrane-bound after centrifugation, was not removed from microsomes following sodium carbonate treatment and generated a large yield from Triton X-114 detergent extracts, all of which reflect the behaviour of an integral transmembrane protein (Semenza *et al*., 1990). Hydropathy plots of *S. cerevisiae* and human ERD2 homologs (Semenza *et al*., 1990; Lewis & Pelham, 1990) helped visualise the high structural similarity and projected seven transmembrane domains from the identification of seven distinct hydrophobic regions. The charged residues amongst hydrophobic regions were also predicted to be components of the binding site, as this trend is seen in other members of the seven-transmembrane (TM)-domain class (Lewis & Pelham, 1990). A second human ERD2 (ERD2.2) (Lewis & Pelham, 1990) with 83.5% amino acid homology to the first discovered human ERD2 also had seven hydrophobic regions and appeared to accumulate mainly in the Golgi (Lewis & Pelham, 1992a), consistent with the previous findings.

Evidence that ERD2 may not permanently reside in the Golgi arose when KDEL cargo overexpression was studied in fixed COS7 cells. Overexpressed KDEL and DDEL-tagged lysozyme caused redistribution of ERD2.2-c-myc to the ER in stained cells, and much more so in the case of KDEL (Lewis & Pelham, 1992b). This redistribution was exclusive to ERD2 and ligand overexpression, as other Golgi markers were not influenced and the same response could not be induced

by the mock signal sequence AARL. ERD2 redistribution advocated the idea that the receptor and retention sequences directly interact and it now also raised questions as to what structural features would enable this new found function.

The localization and dynamics of endogenous ERD2 in multiple mammalian cell types was detected with the use of polyclonal antibodies targeting the C-terminus in fixed cells (Tang *et al*., 1993). It is the only study of its kind which may be due to the technical limitations associated to very low endogenous ERD2 levels, which we have recently confirmed in *Physcomitrium patens* (not published) and also found from previous experience in the laboratory. Nonetheless, in this study stable KDEL-ligand expression had no effect on localization, whilst transient KDEL-overexpression in COS cells led to slightly less distinguishable ERD2 staining. The authors did not comment whether this diffuse pattern was ER rather than post-ER and it is true that the labelled structures do not share a typical ER pattern, but perhaps instead a morphologically altered Golgi/ERGIC.

#### *1.4.4.3 Ligand Binding and Receptor Transport*

Further mutational analysis of human ERD2.1 was undertaken to identify other important regions and residues involved in transport to the Golgi, ligand binding and retrograde transport (Townsley *et al.,* 1993). A good portion of these research employed novel *in vitro* assays (Wilson *et al*., 1993). Here, rat liver Golgi enriched fractions extracted from cells overexpressing human ERD2 or mutant versions were treated with sodium carbonate to expose the lumenal Golgi surface and then incubated with different retention peptides. An interesting find with control assays was that human ERD2 had equally affinity for HDEL and KDEL sequences in this study, which was also supported by redistribution detected with immune-fluorescent staining. This assay also identified that ERD2 has preferential and optimum ligand binding in more acidic conditions.

Certain mutations in predicted cytosolic loops (see figure 1 in Townsley *et al*., 1993) caused complete ER retention and for five out of seven mutants studied, also led to a 2- to 3-fold reduction in KDEL binding *in vitro* compared to wild type ERD2. A second phenotype appeared to reduce ligand-induced redistribution of ERD2 to the ER, presumably indirectly due to the cytosolic nature of mutations. All mutations of conserved acidic and basic residues within transmembrane (TM) domains also

prevented ligand-induced redistribution of ERD2. The final phenotype of note was the abolishment of retrograde transport when altering a charged residue in TM7 (D193N), even though binding ability to KDEL was not affected. The composition appeared to be key, as mutating this residue and positioning aspartic acid elsewhere in TM7 also prevented ER recycling. When combined with mutations which caused an ER accumulation, D193N reduced ER staining, suggesting that those mutations do not actually cause permanent ER residency, but instead may change the rate of bidirectional transport. However, when combined with mutations that caused complete ER residency D193N did not change this phenotype, implying that these double mutants never reach the Golgi most likely due to malfolding.

The same mutation in yeast (D200N) was unable to support growth in yeast and also did not appear to recycle, however C-terminal additions to this mutant including KKXX, LSK or the c-myc epitope appeared to suppress this effect (Townsley *et al*., 1994). Because an ER localisation re-appeared after the addition of these C-terminal peptides, it was concluded that inhibition of recycling was the reason the Asp-193/200 mutation was problematic, especially since it was still able to bind ligands *in vitro*. Yet, there were still some phenotypes that were left uncategorised by Townsley *et al.* (1993) as they muddied the basic principle of a ligand-induced redistribution associated to the recycling model. These included mutants that did not recycle but could bind KDEL, or redistributing receptors that showed a complete lack of binding.

#### *1.4.4.4 Reaching the Limits of Understanding Ligand-Receptor Interaction*

Research endeavours into the binding pocket of ERD2 came later, using the maleimidation of ectopic cysteines to study any interference this may cause (Scheel & Pelham, 1998). There was a large focus on the four residues Arg-5, Asp-50, Tyr-162 and Asn-165, because their replacement by cysteine caused a substantial reduction in ligand binding which was further exacerbated from binding to maleimide variants. Topological studies were also carried out using membrane impermeant biotinylators and the insertion of cysteine residues predicted to be facing the lumen or cytoplasm. The premise here is that cysteines on the lumenal side can only be biotinylated after membrane permeabilization, whereas cytosolic

residues should not have this problem. Their findings were in agreement with previously reported orientations (Semenza & Pelham, 1992; Townsley *et al.*, 1993) that ERD2 has a lumenal N-terminus and cytosolic C-terminus with 7 transmembrane domains. Reporting on the topology of ERD2 with different techniques in each study was necessary due to the proposals that ERD2 may have just six TM domains, with the N- and C-terminus both being cytosolic (Singh *et al*., 1993; Brach *et al*., 2009). Finally, in competitive binding assays Asp-50 appeared to be key for interaction with the positive charge in HDEL, KDEL and RDEL at position -4, as binding to DDEL was unaffected.

Another study generated decapeptide portions of ERD2 with a particular focus on lumenal loop portions, covalently binding them to cellulose membranes before exposing them to KDEL proteins (Janson *et al*., 1998). Here it was found that the essential sequence for ligand binding was $^{22}$KIWK$^{25}$, not in agreement to the aforementioned amino acids. Another set of separate conclusions on this topic have also been made, after using computer simulation to select structures in ERD2 for biochemical analysis (Mei *et al*., 2017). Here the conclusions were that aromatic residues in the first three lumenal loops of ERD2 are believed to interact with the aromatic residues of HDEL/KDEL including a residue at -6, during binding. The variation in findings for amino acids associated with receptor binding suggests there is still a lot to be investigated on this function.

A potential association of ERD2 with COPI-mediated transport was recognised after overexpression of an *ERD*-like protein (ELP-1) led to the perturbation of the Golgi system in a manner indistinguishable from BFA treatment (Hsu *et al*., 1992). In this study, degenerate oligonucleotide primers targeting the most conserved regions of other ERD2 sequences were mixed with cDNA from a human erythroleukemia cell line (K562), identifying the previously reported human ERD2 and ELP-1 which shared 75% sequence similarity. When tagged with a C-terminal c-myc epitope both receptors exhibited the typical ER-Golgi localisation described in the field previously, but with increased expression saw an obvious redistribution to an ER-only state. In the same manner as BFA incubation, overexpression also led to the inhibition of constitutive secretion and saw glycan processing on the side chains of ER residents that could be explained by a migration of Golgi lumenal proteins to the ER. Meanwhile, endocytosis at the plasma membrane was not

disrupted by the overexpression of ELP-1. In both cases β-COP is driven off the Golgi membrane into the cytosol and in follow up (Aoe *et al*., 1997), ARF1 displays an inactive phenotype. This suggested ELP-1 overexpression had a detrimental effect on linked components of COPI vesicle formation, whereby the β-COP coatomer forming protein is recruited to the Golgi membrane by the GTPase ARF1. The cyclical activity of ARF1 is determined by the GEF and GAP, and Aoe *et al*. (1997) found that 6xhistidine-tagged GAP and C-terminally c-myc epitope-tagged ERD2 co-precipitated, an interaction further enhanced by ERD2 oligomerisation. Unfortunately, no experiments were presented to confirm that 6xhistidine-tagged GAP overexpression could mediate the same effects as the wildtype at the ER-Golgi interface. Binding to KDEL ligands also strengthened the interaction between human ERD2 and ARF1GAP, suggesting bound receptors more readily engaged in this interaction (Aoe *et al*., 1998). Based on these findings they proposed that ERD2 regulates ARF1-mediated COPI vesicle formation through recruitment of GAP to the Golgi membrane, subsequently controlling ARF1 inactivation and vesicle disassociation from the membrane. This interaction was supported using fluorescence resonance energy transfer (FRET) with ERD2 modified with CFP and YFP at the C-terminus, adding that ligand-bound ERD2 enhances the recruitment of GAP (Majoul *et al*., 2001). In one of the human homologs it was also suggested that phosphorylation of a serine residue in the C-terminus of ERD2 is critical for the recruitment of ARF1-GAP and coatomer (Cabrera *et al*., 2003). These lines of research supported a mechanism for how ERD2 could shuttle at least in a retrograde fashion between the ER and Golgi when recycling ER resident proteins.

### 1.4.5 Findings of ERD2 in Plants

Over the course of characterising ERD2 in plants, many traits of the modified receptors appear to mirror those in yeast and mammalian homologs. The relationship between the ER and Golgi was analysed in living cells for the first time using an ERD2 homolog from *A. thaliana,* C-terminally fused to green fluorescence protein (GFP) and visualised in *Nicotiana clevelandii* leaves (Boevink *et al*., 1998). Following BFA treatment this marker was reported to disappear from the Golgi and simultaneously increase in localisation at the ER, characteristic of the response

seen with mammalian and yeast homologs. A similar phenotype has been described following the overexpression of HDEL-ligands alongside *A. thaliana* ERD2a and b C- or N-terminally fused to yellow fluorescent protein, respectively (Montesinos *et al*., 2014). The sequence divergence across these isoforms is most likely the reason Southern blotting with a probe designed around the one known isoform failed to identify others during the initial investigation of *A. thaliana* (Lee *et al*., 1993). ERPs have also not been found in mammalian or yeast genomes, suggesting a biological role that is plant-specific.

More recent characterisation was carried out following the identification of *Nicotiana benthamiana ERD2a* and *ERD2b* (Xu *et al*., 2012). These homologs had 73% identity with each other, 83% with *A. thaliana ERD2b* and 44-50% with yeast and human *ERD2*. It should be noted that plant homologs had previously been successful in yeast mutant complementation (Lee *et al*., 1993), confirming the identified sequences represented ERD2. *N. benthamiana* variants had a dual ER-Golgi localisation upon C-terminal fluorescent tagging, maintaining the theme with other homologs. The study itself focussed on the role of ERD2 in ER stress and programmed cell death, therefore the impact of ERD2a/b silencing on the ER was studied. Silencing caused an increase in BiP mRNA levels when just one of the homologs were silenced, but total BiP protein only saw an increase after silencing both. Silencing also exacerbated the rates of cell death following incubation with the ER stress inducer DTT, highlighting the role of ERD2 in maintaining normal levels of ER resident proteins and minimising ER stress. Other studies have also supported that silencing ERD2 in plants caused ER lumenal proteins to escape (Xu & Liu, 2012; Wang *et al*., 2018).

It has been postulated that the different ERD2 isoforms may have arose from specificity to different retention signals, given plants have independent traits such as promiscuity towards H/K/DDEL ligands and an ability to complement both yeast and human mutants. However a an inactive *A. thaliana ERD2b* mutant was shown to exclusively reduce calreticulin3 retention, even though calreticulin1, calreticulin2 and calreticulin3 all contain a HDEL sequence (Li *et al*., 2009). The retention of other chaperones containing HDEL such as BiP were also unaffected in this mutant, suggesting that such an effect is unrelated to the ER retention ligand. This study also generated a novel intra-molecular tagged ERD2b fluorescent construct

by placing YFP in the first predicted lumenal loop and found it to be Golgi-localised. There are some findings which suggest ERD2 isoforms may have higher specificity to certain retention ligands. In two studies using *N. benthamiana* (Xu & Liu, 2012; Xu *et al*., 2012), Silencing of ERD2b did not affect GFP-HDEL fluorescence but did cause the loss of that for GFP-KDEL. Using firefly luciferase complementation imaging assays (LCI), Xu & Liu (2012) presented ERD2a and ERD2b self- and co-interacting, as well as interacting with ARF1 and ARF1-GAP. The findings led the authors to propose that ERD2 may function as an oligomer and interact heavily with COPI-mediated transport vesicles. This would be in agreement with the recycling model for ERD2 function.

### 1.4.6 The most recent developments and inconsistencies in the field, leading to the current project aims

#### *1.4.6.1 A novel validation system for ERD2 function*

My host laboratory introduced a quantitative gain-of-function assay which was developed in plants to study and directly quantify ERD2 function, specifically the model organisms *N. tabacum* and *N. benthamiana* (Silva-Alvim *et al*., 2018). Such a tool has not previously been employed in the field, thus bringing a number of novel findings which may bring some accepted principles of ERD2 under question. Using barley α-amylase (Amy) as a model cargo molecule, total secretion and cellular retention could be quantified via the use of a quantitative colorimetric assay. The ratio of extracellular/intracellular enzyme levels offers a calculation for the secretion index (SI) to monitor reduced or increased secretion at a glance. This method was applied to a model ER resident, Amy-HDEL, thus enabling ER retention to be monitored and the biological activity of any co-expressed ERD2 variants. Such variants were then directly compared under normalised conditions by using the internal expression marker β-glucuronidase (Gershlick *et al*., 2014).

The legitimacy of the assay was displayed when Amy-HDEL overexpression clearly saturated the retention system and could be reversed by co-transfection with increasing amounts of *A. thaliana* ERD2a, thus massively reducing the secretion index of Amy-HDEL. To confirm this was not a cause of BFA-like effects (Hsu *et al*., 1992), the Golgi-marker ST-CFP was expressed in a dual vector (DV) with ERD2a and a normal punctate morphology of the Golgi was apparent. A control

vector expressing Amy alone showed the level of ERD2a expression in this study also did not impact constitutive secretion. Similarly, a mock protein (phosphinotricine acetyl transferase) in place of ERD2a covered the potential of ST-CFP having an impact on Amy-HDEL transport, which it did not. Finally, the isoforms of *N. benthamiana* and *A. thaliana* ERD2b were compared alongside the two retention signals, HDEL and KDEL. Results showed species isoforms and retention signals were completely interchangeable and that *A. thaliana* ERD2b could complement knockdown of ERD2a and b in *N. benthamiana*, reiterating conserved function between species.

The method was so powerful that some of the most prominent point-mutations affecting ERD2 function could be interrogated via this assay and revealed an unexpected complexity (An, 2015). Some mutants were loss of function mutants that simply failed to reduce the secretion of Amy-HDEL (R5A, N167A) or caused partial effects (D50A, D195N). Interestingly, other mutants revealed an induced secretion of Amy-HDEL, suggesting altered functions leading to dominant or co-dominant effects. To characterise the different classes of mutations, it was important to complement the secretion assay with direct subcellular localisation of the ERD2 mutants, relative to the wild type. Only as a precaution, the commonly used C-terminal fusion ERD2-YFP was tested in the Amy-HDEL secretion assay. To the dismay of all laboratory members involved, ERD2-YFP exhibited no biological activity at all, although the in-situ analysis of this fusion protein reported localisations consistent with what is frequently observed in the field, a dual ER-Golgi localisation. The N-terminal fusion YFP-ERD2 was completely retained in the ER and expressed at low levels. Attaching a signal peptide to N-terminally YFP-tagged ERD2 (secYFP-ERD2) increased expression levels drastically and caused total localisation to the Golgi. This suggested that YFP-ERD2 had a flipped topology, whilst forcing YFP into the lumen aligned with the preferred topology of the receptor. However, both YFP-ERD2 and secYFP-ERD2 were still completely inactive in the Amy-HDEL secretion assay (An, 2015; Silva-Alvim *et al*., 2018).

A further fusion protein was ultimately developed where an extra transmembrane domain (sourced from ERP1) was added to the N-terminus between YFP and ERD2 (YFP-TM-ERD2), placing the bulky fluorescent protein into the cytosol instead. This novel modification yielded a functional ERD2 fusion which was

localised exclusively to the cis-Golgi (Silva-Alvim *et al*., 2018). The same modification was attempted at the C-terminus, but this led to an ER-Golgi localisation and abolished function, highlighting the fragility of the C-terminus. Structurally the predicted topology of a lumenal N-terminus and a cytosolic C-terminus was confirmed by the use of a proteinase K protection experiment identifying peptides of particular length from microsomes containing ERD2 fusions after exposure to detergent.

Finally, when HDEL saturation was induced in protoplasts, YFP-TM-ERD2 localised entirely to the cis-Golgi, in contradiction to the reports of redistribution that the recycling model is based on (Lewis & Pelham, 1992b). Since the alteration of the C-terminus in the ERD2-YFP fusion led to a loss of biological activity, mutations were studied within the C-terminus in an attempt to identify important functional residues. The mutation of two leucine residues at position -5 and -3 from the C-terminus (LLGG) reproduced the typical dual ER-Golgi localisation of ERD2-YFP, but in the YFP-TM-ERD2 configuration instead, suggesting that these residues were masked in C-terminal fluorescent fusions. More importantly, the fact that the point mutations rendered the native untagged ERD2 molecule inactive as it failed to mediated increased retention of Amy-HDEL clearly established their importance (Silva-Alvim *et al*., 2018). The results presented important residues in ERD2 which had not been previously reported and a phenotype which questions the mode of function assumed by the field. Interestingly, none of the lysine residues of the ERD2 C-terminus were important in mediating increased retention of Amy-HDEL (An, 2015, Silva-Alvim *et al*., 2018).

#### *1.4.6.2 The Crystal Structure of the Chicken Ortholog*

Yeast and human coding regions containing a C-terminal c-myc-epitope enabled the isolation of ERD2 from cell lysates in some of the earliest studies. Here ERD2 was determined to be ~26kDa from western blot analysis, behaved like a transmembrane protein and contained seven distinct hydrophobic regions (Semenza *et al*., 1990; Lewis and Pelham, 1990). A type I transmembrane protein with seven transmembrane domains has since been proven (Scheel and Pelham, 1998; Silva-Alvim *et al*., 2018).

The most recent structural development is the crystal structure of the chicken KDEL receptor (Brauer *et al*., 2019). Besides confirming seven transmembrane domains, the key unveiling was a close structural relationship between ERD2 and SWEET transporters, contrasting from previous suggestions that ERD2 is structurally related to G-protein coupled receptors (Cancino *et al*., 2014). The structures of SWEET transporters, G-protein coupled receptors and ERD2 are compared in Figure 2, with the closer relationship between ERD2 and SWEET transporters evident by segregation of transmembrane domains into two internalised triple helix bundles (THB). Although the mechanism of SWEET transporter function remains poorly understood (Tao *et al*., 2015), other properties have been characterised. This includes the identification of two PQ-loop domains (Xuan *et al*., 2013), one of which is conserved in ERD2. PQ-loops are associated with vesicle packaging and protein trafficking (Saudek, 2012), thus further characterization could clarify the functional divergence brought about by the different location and quantity of PQ-loop domains.

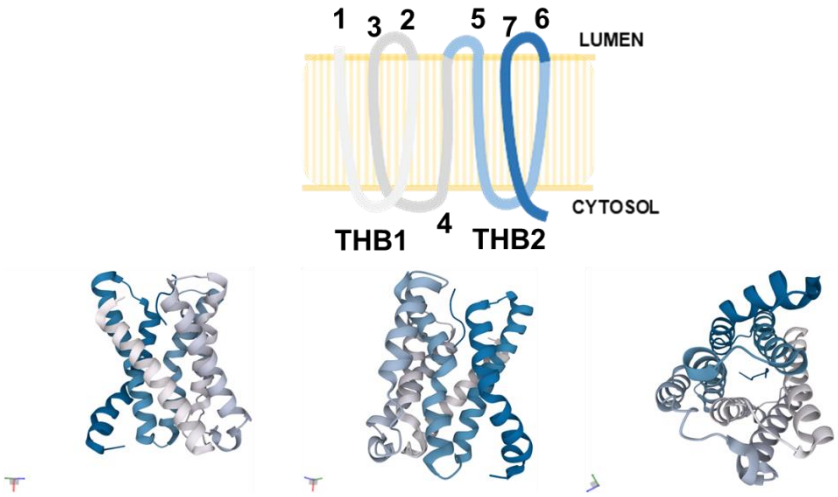


**Figure 3 – Triple Helix bundle subdomains of ERD2 identified from an analysis of the crystal structure (Brauer *et al*., 2019).**
A schematic diagram of the transmembrane domains in ERD2 is provided above ribbon structures (Brauer *et al*., 2019) to show their positioning within the membrane. The colouring of membranes in the diagram is replicated in ribbon structures. Crucially the order of TMs in the THB subdomains is not sequential from left to right. A short peptide containing the KDEL ligand is also visible in the ribbon structures, displaying how it may position in the cavity between THB1 and THB2. Notice the TM4 linker is visibly separate from the hexagonal shape of the combined THBs.

Although the earlier study by Silva-Alvim *et al*. (2018) raised questions with respect to ERD2 recycling and the use of C-terminal tags when studying the receptor, Brauer *et al*. (2019) presented other interesting structural findings with a rationale

which was in support of the recycling model. Immediately highlighted was a large polar cavity on the lumenal side, setting a precedent for ligand-binding. Combined with prior research in the field proposing a pH dependence on ligand binding (Wilson *et al*., 1993; Scheel and Pelham, 1998), two separate configurations were identified defining a bound and unbound receptor state. Bound ERD2 was analysed at pH 6, whilst the unbound (Apo) state was analysed at a pH of 9. Unfortunately ERD2 was not also crystallised at a higher pH alongside the TAEKDEL peptide, nor alone at pH 6, so two variables determining the bound and unbound configurations have limited the ability to make direct conclusions on the individual structural effects caused by pH or ligand-binding. It is also unlikely that pH 6 and 9 are representative of the steady-state conditions at the ER-Golgi interface, given the highly dynamic nature of lumenal components here. Nonetheless, a robust explanation on the differences in positioning of transmembrane domains and the specific residues enabling stability for bound and unbound states was accumulated from the crystallography data. Key residues in the binding pocket of ERD2 for ligand interaction were also elucidated, but explored more deeply in a sequential publication (Gerondopoulos *et al*., 2021). This follow up also considered the residues responsible for differences in binding affinity to the variant ligands K/H/A- and D-DEL in Mammalia.

Returning back to data supporting the recycling model, a configurational change in the bound receptor state proposed that a key movement in TM7 exposes a “cluster of lysine residues” (Brauer *et al*., 2019), reminiscent of the established KKXX motif which causes recruitment into COPI-mediated retrograde transport. The insinuation was that this amino acid stretch is only available upon ligand binding and may assist the receptor in returning ER residents. In this study mutation of the cluster (KGKK-AGAA) and overexpressing KDEL ligands did not cause a redistribution of the receptor form the Golgi to the ER, which in respect to the recycling model assumes they must hold importance in ERD2 function. Yet, authors did not test this mutant in their own KDEL binding assay to remove the possibility that such changes may simply compromise ligand binding. Likewise, microscopy studying a redistribution of this mutant was in an expression vector containing a C-terminal 20 amino acid linker followed by GFP, a modification which when considering the findings of Silva-Alvim *et al*. (2018) should be approached

with caution. The crystal structures have massively advanced the understanding of intramolecular and ligand-specific interactions which define the separate configurations of ERD2, however there is still much to be learned on the collective mechanism which ensures efficient ERD2-mediated ER retention at the ER-Golgi interface.

### *1.4.6.3 ERD2 at the plasma membrane?*

A more controversial study discusses ERD2 recycling between the Golgi and plasma membrane via clathrin coated vesicles (Jia *et al*., 2021). Here it is proposed that a portion of the KDELR1 population act as bona fide cell surface receptors, possibly inspired by mammalian research claiming that ERD2 may provide an endocytic route for growth factors such as mesencephalic astrocyte-derived neurotrophic factor (MANF). This is after observation that HDEL ligand-binding causes receptor clustering at the cell surface (Henderson *et al*., 2013; Becker *et al*., 2016). Taking a closer look at methodologies, it is clear that in all three publications there is no functional validation for modified ERD2 constructs, which include a variety of N- and C-terminal fusions ranging from large HaloTags to smaller dual myc-FLAG epitope tags. One modification even includes a btx binding site for cell surface binding situated between transmembrane domains four and five (Becker *et al*., 2016). Unless N-terminal fusions are linked via an extra transmembrane domain to prevent any lumenal interference, our experience has shown that such changes are detrimental to ERD2 function (Silva-Alvim *et al*., 2018, unpublished data). As the HaloTag is much larger than ERD2 and YFP, it is likely that fusing it to the N-terminus will render the receptor inactive. The same authors raise hesitancy over the use of C-terminal modifications too. Overall, the techniques associated with plasma membrane trafficking give reason to approach with caution on the topic, as the biological relevance of modified receptors remain to be validated by the authors.

## 1.5 Outlook to Future Research and Objectives

Whilst a host of different research groups have adopted new experimental techniques over the 30 years of ERD2 research, there is a case to be made that the degree of technological innovation has not been met by equivalent advancement in the story of ERD2 function. As such, 15 years after its discovery Pfeffer (2007) praised the efforts leading to a consensus that ERD2 interacts with COPI components when recycling HDEL cargo, but simultaneously delivered a review of clear gaps in the overall story that would need addressing before closing the book on receptor recycling. The main concerns were associated with the Golgi localisation of ERD2, for example what enabled this localisation? What prevented ERD2 from traversing beyond this compartment? And what occurred under KDEL saturation to prevent even a hint of Golgi residency? Considering the Golgi was the dominant localisation for steady-state ERD2, elucidating a mechanism for this had lacked consideration compared to the efforts for retrograde transport. Not only this, scepticism towards a pH dependency on ligand release was also aired, since any experimental conditions so far did not identify different outcomes between the very similar physiological conditions found at the ER and cis-Golgi (Llopis *et al*., 1998).

Another 15 years of research later and the field has gained the crystal structure for ERD2, but the answers to Pfeffer's questions still go begging. More research has amassed with propensity towards the recycling model, often citing and reiterating the same findings presented in section 1.4.4. In many cases the choice of C-terminal ERD2 fusion remains the same, but novelty is brought about by introducing a modernised experimental platform (Xu *et al*., 2012; Xu & Liu, 2012; Montesinos *et al*., 2014; Brauer *et al*., 2018). A crucial component of ERD2 research which has escaped modernisation is the method of biological validation following ERD2 modification. The ERD2-c-myc was first tested in yeast (Semenza *et al*., 1990) and validated by its ability to complement *erd2* mutants, although data was not shown. Other notable points from yeast studies were that high biological activity is not required for growth since yeast mutants exhibiting low levels of retention were isolated (Townsley *et al*., 1994), and the detrimental leakage of ER residents in the *erd2* phenotype could be suppressed by SED genes (Hardwick and Pelham, 1992).

Combined, these suggest that yeast complementation may not be the most appropriate technique to identify highly active ERD2.

Since then C-terminal ERD2 fusions have been adopted by numerous research groups even though the supporting evidence for biological activity is very limited. Silva-Alvim *et al*. (2018) sought to give the field a more robust method of validating ERD2 constructs by introducing their gain-of-function assay. The intention was to fill in the gaps identified by Pfeffer (2007) and select for anterograde transport mutants by combining microscopy with functional assays. If wild type ERD2 was a baseline for biological activity in the gain-of-function assay, it was appropriate to check the activity of all other tools including ERD2-YFP, which could be marginally compromised due to such a large addition. In turn these read-outs would act as positive controls for detecting mutations which affect biological activity and localisation. What was not anticipated was the complete inactivity of ERD2-YFP, which has caused a complete redirection of research.

### 1.5.1 Research aims

The recycling model had become dogma long before I commenced research into ERD2 function, therefore a great deal of push-back has been received since questioning its legitimacy in 2018. In response I have prepared an extensive panel of results in support of a new stance on ERD2 modality. I begin by exploring ligand-induced redistribution and why the field has been so easily mislead by the dual ER-Golgi localisation of ERD2-YFP. Indeed Silva-Alvim et al. (2018) never considered further work with ERD2-YFP once it was clear that its biological activity was destroyed. Hence the necessity to establish that experimental conditions in the host laboratory actually allowed for redistribution assays. Once confirmed I could start dissecting the behavioural properties of ERD2 constructs which support the recycling model and challenge any biological relevance they previously held (Chapter 2). This analysis highlighted the fragility of the ERD2 C-terminus, which must avoid alteration if the receptor is to function to its full potential (Chapter 3). In the process of finding inconsistencies with the recycling model a large amount of data was generated showing a strict preference towards a permanent Golgi residency for ERD2, which is brought together in chapter 4. After confirmation of a new localisation for ERD2 the final results section (chapter 5) was dedicated to

generating new reagents to manipulate ERD2 function and consolidate all leads I have on the cis-Golgi residency of ERD2. This would lead to a number of non-anticipated findings and new molecular tools that point to a fast internal recycling mechanism within the cis-Golgi. The new tools aimed to disrupt key-steps other than mechanisms for Golgi retention and instead those which mediate K/HDEL sorting and delivery from the cis-Golgi. From here the reagents could be adapted for identification of novel protein-protein interactions occurring with ERD2 that normally escape detection due to their short lived nature.

# Results

# Chapter 2 - ERD2 recycling is an artefact and caused by a compromised C-terminus

## 2.1 Introduction

ERD2-recycling is the primary model for explaining how ER resident K/HDEL proteins accumulate at their point of origin, inspired by endosomal receptors that transport cargo to compartments beyond the Golgi apparatus (Dean and Pelham, 1990; Hardwick *et al*., 1990; Robinson and Aniento, 2020). A Golgi-to-ER migration of the receptor following ligand overexpression was the first evidence to support such a model, as authors suggested it showed continuous, cyclical transportation between compartments (Lewis and Pelham, 1992b). Much of the research since has been a proponent of recycling, including some fluorescent-ERD2 fusions which exhibit a dual ER-Golgi localisation and ligand-mediated redistribution in plant and mammalian cells (Boevink *et al*., 1998; Majoul *et al*., 2001; Montesinos *et al*., 2014). With regard to understanding the induced ER localisation, an interaction between ERD2 and coatomer is suggested to facilitate retrograde transport of the receptor from the Golgi to the ER (Hsu *et al*., 1992; Aoe *et al*., 1998; Majoul *et al*., 2001; Cabrera *et al*., 2003; Xu and Liu, 2012; Bräuer *et al*., 2019).

Where many studies have followed suit and continued to characterise the behaviour of large ERD2-fusion constructs, my host laboratory followed a completely different approach and established a novel validation system defining the ability to increase the retention of ER residents as a signature of wild type receptor activity. This was based on monitoring secretion of barley α-amylase modified with an HDEL tetrapeptide as ER-retention signal (Amy-HDEL) in function of co-expressed ERD2. Increased Amy-HDEL cell retention in *N. Benthamiana* protoplasts directly reports on receptor function and is highly quantitative (Silva-Alvim *et al*., 2018). As a control and display of efficacy for this assay, both wild type gene isoforms encoding *Arabidopsis thaliana* ERD2 (AT1G29330 and AT3G25040) caused a remarkable reduction in Amy-HDEL secretion when co-expressed.

Unexpectedly, when frequently used C-terminal fluorescent ERD2-fusions such as ERD2-GFP or ERD2-YFP (Boevink *et al*., 1998; Majoul *et al*., 2001; Montesinos *et al*., 2014) were tested under the same conditions, no increase in Amy-HDEL retention was observed (Silva-Alvim *et al*., 2018). As most of the field's understanding of ERD2 recycling hinged on localisation studies with such C-terminal fusions, it was imperative to establish a fluorescent receptor with retained biological function. After several unsuccessful alternative attempts, this was finally achieved by placing an additional transmembrane domain between an N-terminal YFP and the ERD2 coding region (YFP-TM-ERD2). The new chimera was only detected in the Golgi, even when co-expressed with HDEL-ligands, and also facilitated increased Amy-HDEL retention. Critically, it was determined to be due to a previously unreported di-leucine motif at the C-terminus, which when mutated led to a return of an ER-Golgi distribution and abolished biological activity (Silva-Alvim *et al*., 2018). The most plausible explanation was that fusion of a bulky fluorescent protein would simply mask this signal.

Whilst this information has been disseminated, the field appeared to be somewhat discouraged in uptake (Aniento and Robinson, 2020), perhaps in part because the ramifications compromise numerous lines of early secretory pathway research. It was also popular to dismiss the findings as a plant specific phenomenon among the wider cell research community. This is illustrated by the reported crystal structure of chicken ERD2, which still included C-terminal fluorescent ERD2 fusions for recycling experiments (Brauer *et al*., 2019). Nevertheless, there were still valid reasons why these findings have not gained the desired traction beyond the preconceived biases mentioned. One of those reasons, to be addressed in this chapter, is what underpins the vastly different properties of our functional ERD2 fusion protein when compared to other fusions used to study ERD2 for the previous three decades.

In this process I have determined the biological relevance of ligand-induced redistribution (Lewis and Pelham, 1992; Majoul *et al*., 2001, Brauer *et al*., 2019). In considering the wider reach of this research I have highlighted the functional conservation within eukaryotes by analysing modifications in both *A. thaliana* and *H. sapiens* ERD2 orthologs, alongside studies of the active and inactive human and plant fluorescent fusions in mammalian HeLa cells.

## 2.2 Results

### 2.2.1 Ligand-overexpression in leaves permits ERD2-YFP redistribution to the ER

Ligand-induced ERD2 redistribution to the ER has been repeatedly reported as a functional attribute in mammalian and plant cells, but exclusively shown with C-terminal YFP or c-myc fusions (Lewis and Pelham, 1992b; Majoul *et al*., 2001, Montesinos *et al*., 2014, Brauer *et al*., 2019). As Silva-Alvim *et al*. (2018) only tested the effects of ligand-overdose on YFP-TM-ERD2 and saw no effect, I first wanted to establish if the experimental conditions in house actually permitted for ligand-induced redistribution of non-functional ERD2 derivatives. To do so I co-expressed the non-functional ERD2-YFP fusion (Figure 4A) either with control cargo amylase (Amy) or the ER-retained Amy-HDEL cargo in *Nicotiana tabacum* leaf mesophyll cells (Figure 4C). For consistent molecular concentrations of cargo in infiltrated mesophyll cells, dual expression T-DNA constructs were created combining Amy or Amy-HDEL coding regions under control of the strong Cauliflower Mosaic Virus 3SS (CaMV35S) promoter, together with ERD2-YFP under control of the weak TR2 promoter (Figure 4B).

When co-expressed with Amy, ERD2-YFP was readily detected in the Golgi-bodies, but also in the ER network (Figure 4C). In sharp contrast, co-expression of Amy-HDEL resulted in an almost complete shift of ERD2-YFP to the ER. This is particularly clear at high magnification; whilst ERD2-YFP results in bright saturating signals at the Golgi bodies when co-expressed with Amy (Figure 4D), only remnant fluorescence is left with Golgi bodies when Amy-HDEL is co-expressed (Figure 4E). This shows that HDEL overdose provided suitable experimental conditions to observe a clear re-distribution of ERD2-YFP. Repeating the same experiment with YFP-TM-ERD2 confirmed that HDEL-overdose was unable to cause detectable levels in the ER (Figure 4F), confirming the initial observation (Silva-Alvim *et al*., 2018).

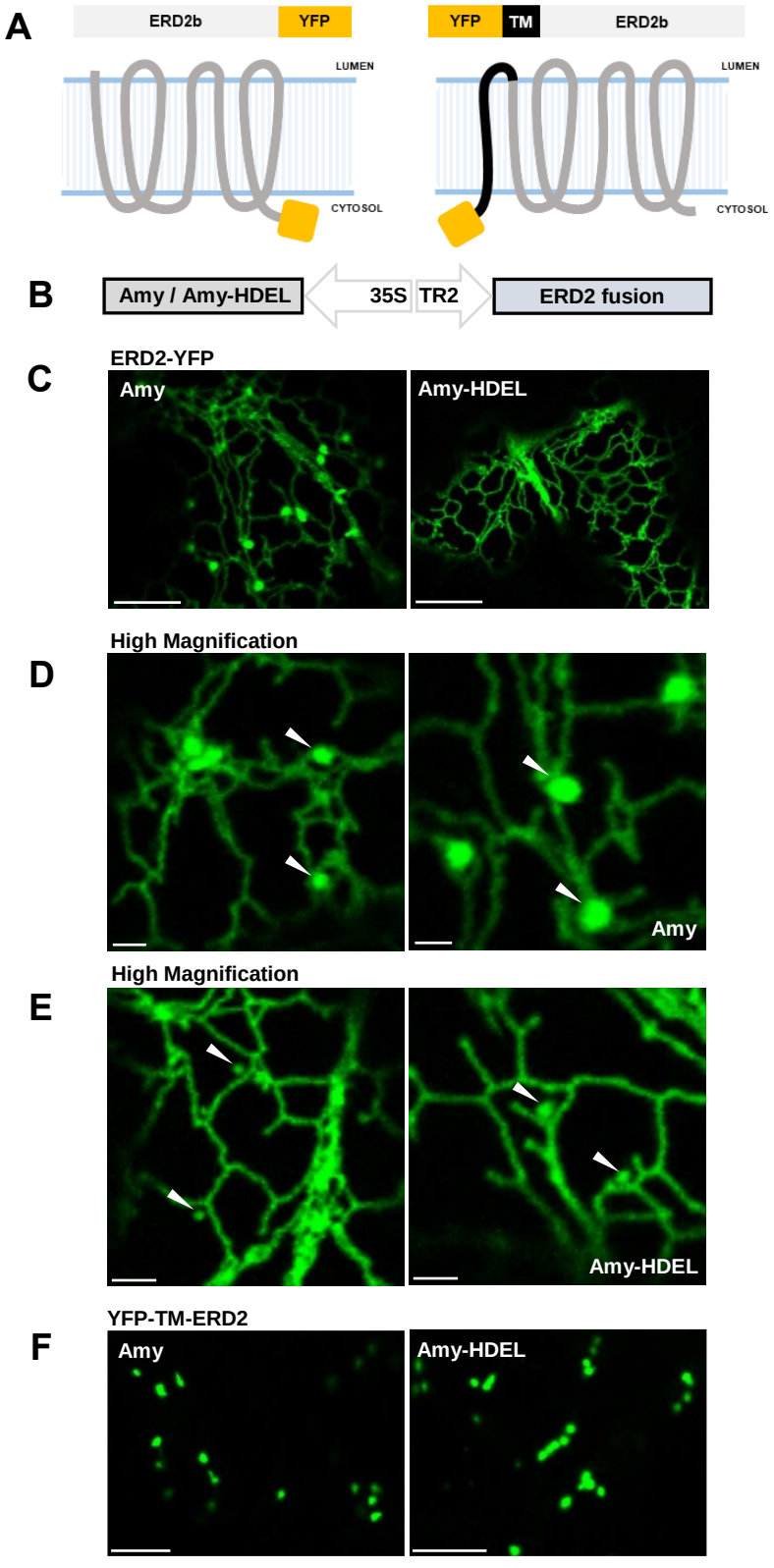


**Figure 4: ERD2-YFP co-expression with Amy and Amy-HDEL identify suitable conditions to carry out redistribution assays.**

**(A)** Visual representation of the novel N-terminal and classic C-terminal ERD2 fusion protein variants. Notice the additional TM domain (black) and yellow fluorescent protein (YFP) (yellow square - not to scale). The ERD2 triple helix bundle (THB) structures (grey) are shown integrated into the membrane (light blue).

**Figure 4: ERD2-YFP co-expression with Amy and Amy-HDEL identify suitable conditions to carry out redistribution assays (cont.)**
**(B)** Diagram of T-DNA dual vectors used to co-express the fluorescent ERD2 fusions with either secreted Amylase (Amy) or ER-retained Amy-HDEL. **(C)** Confocal laser scanning microscopy (CLSM) of transiently expressing gene cassettes from infiltrated *Agrobacterium tumefaciens* in leaf epidermis cells of *N. tabacum* (Size markers are 10 microns throughout this thesis unless otherwise stated). Dual ER-Golgi localisation of ERD2-YFP co-expressed with Amy and Amy-HDEL. The re-distribution of ERD2-YFP to the ER by co-expressed Amy-HDEL is drastic. **(D)** ERD2-YFP co-expressed with control cargo Amy at higher magnification (size marker is 2 microns). Notice that with co-expressed Amy, Golgi bodies show bright saturating signals (white closed arrow heads) compared to weak ER fluorescence. **(E)** ERD2-YFP co-expressed with the model ligand Amy-HDEL at higher magnification (size marker is 2 microns). When co-expressed with Amy-HDEL, ER fluorescence is slightly stronger, but the Golgi fluorescence intensity is no longer saturating and comparable to the ER fluorescence (white closed arrowheads). **(F)** Golgi localisation of YFP-TM-ERD2 co-expressed with Amy and Amy-HDEL. Distribution is solely within the Golgi remains unchanged for both cargo. Dual ER-Golgi localisation of YFP-TM-ERD2ΔC5 co-expressed with Amy and a more prominent ER localisation when co-expressed with Amy-HDEL.

### 2.2.2 ERD2-YFP cannot complement ERD2 antisense knockdown

The finding that ERD2-YFP is inactive and does not promote the retention of Amy-HDEL (Silva-Alvim *et al*., 2018) was repeatedly challenged by peers (Robinson and Aniento, 2020), because the same ERD2-YFP had earlier been reported to increase the retention of YFP-HDEL in plant protoplasts (Montesinos *et al*., 2014). Prior to my dissertation, Alvim (2018) provided genetic evidence demonstrating that YFP-TM-ERD2 is biologically active after generating viable plants co-expressing this fusion under control of the TR2 promoter together with a CaMV35S-driven *N. benthamiana* ERD2a/b hybrid antisense construct from a dual T-DNA expression construct. Here I repeated this experiment but with the ERD2-YFP fusion to explore every attempt to detect weak residual biological activity that may have been below the detection limit in Amy-HDEL transport experiments in protoplasts.

In contrast to the positive control expressing YFP-TM-ERD2, only very few calli formed on the leaf discs when ERD2-YFP was tested via Agrobacterium-mediated stable plant transformation. Even fewer shoots formed on the calli that were successfully propagated. When leaf samples of these shoots were tested via CLSM, ERD2-YFP was initially only detected in guard cells where it labelled the nuclear envelope and ER (Figure 5B, panel b1), as well as Golgi bodies (panel b2). With very high laser and detector gain settings, the ER network and weak Golgi punctae could also be seen in the surrounding epidermis pavement cells (Figure 5C). Curiously, in these cells most of ERD2-YFP was detected in the ER, and only weak punctae were observed that could be Golgi bodies. This is in sharp contrast to the

Golgi patterns typically observed for C-terminal fluorescent ERD2 fusions in leaf epidermis cells (Boevink *et al*., 1998).

Invariantly, the shoots co-expressing ERD2-YFP and NbERD2ab antisense were unable to develop roots and were rapidly lost due to wilting, without exception. It is likely that this was caused by the lethal effect of the co-expressed *Nb*ERD2ab antisense inhibition construct. Since position effect and copy number of insertions affect both ERD2-YFP and *Nb*ERD2ab antisense in a similar fashion as they are present on the same T-DNA, I hypothesize that only very weak expressing lines reached the shoot stage whilst higher expressing lines were most likely already lost at the earlier callus forming stage due to ERD2 knockdown. To provide absolute confirmation, an analysis using reverse transcriptase (RT)-PCR to determine the RNA expression levels of both insertions could have been carried out on tissues taken from transgenic lines, however this was not within the scope of this line of research.

### 2.2.3 ERD2-YFP segregation between ER and Golgi is influenced by expression levels alone

Whilst functional YFP-TM-ERD2 was exclusively Golgi-localised in transgenic plants when co-expressed with the *Nb*ERD2a/b hybrid antisense construct (Alvim *et al*., 2023) and under all conditions when co-expressed transiently with HDEL cargo (Figure 5F), the ER pattern of ERD2-YFP in transgenic shoots was most astonishing. For this reason I tried to test the effect of ERD2-YFP expression alone by taking advantage of the natural variation of transient expression in infiltrated leaf samples. Figure 5C shows that cells expressing very low levels of ERD2-YFP also show a much weaker signal in Golgi bodies relative to the ER network. For this purpose, cells with low expression (low E) were imaged with higher detector gain settings (Figure 5D). Under these conditions it was obvious that low-expression results in an apparent re-distribution to the ER, whilst high expression (High E) favours Golgi-localisation. This phenomenon will have gone unnoticed in the plant field because most laboratories work with the strong CaMV35S promoter (Boevink *et al*., 1998, Montesinos *et al*., 2014). It is possible that high expression of ERD2-YFP results in an excess of this fusion protein relative to endogenous K/HDEL proteins such as BiP, calreticulin or PDI. At low expression, endogenous K/HDEL

proteins might provide sufficient ligands for increased recycling to the ER. I conclude that whilst I can reproduce ligand-induced redistribution of ERD2-YFP to the ER, its non-functional properties suggest that this redistribution is an artefact caused by compromising the C-terminus.

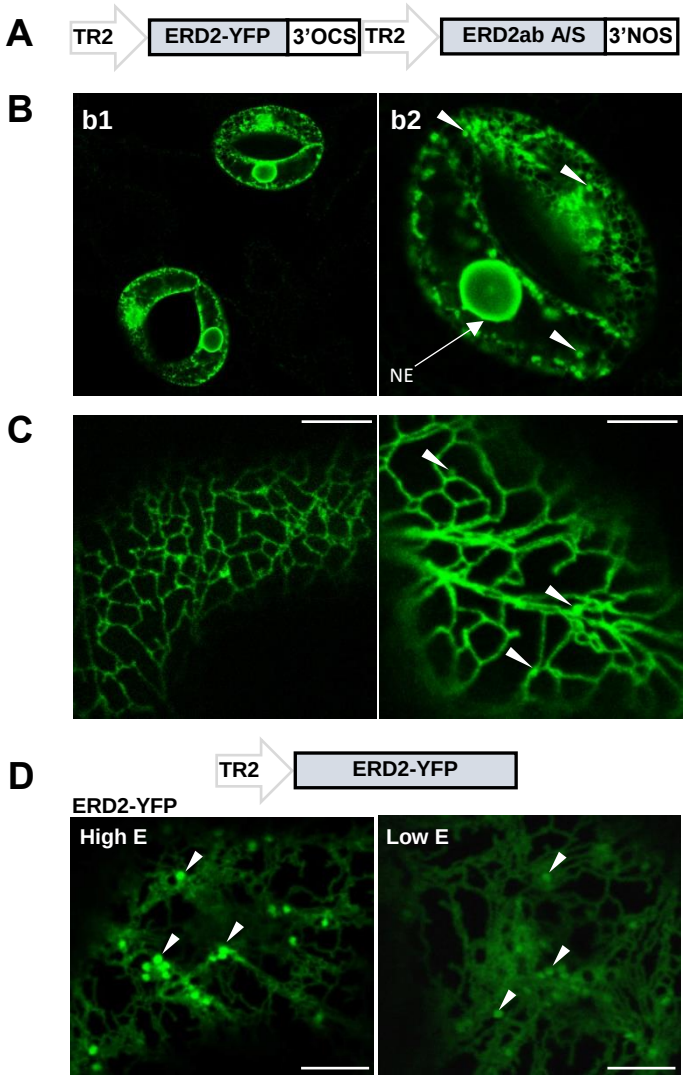


**Figure 5: ERD2-YFP redistribution in transgenic *N. benthamiana* lines and transient differentially expressing mesophyll cells.**

**(A)** Diagram of T-DNA dual vector used to co-express ERD2-YFP and *N. benthamiana* ERD2a/b antisense. **(B)** ERD2-YFP fluorescence in leaf cells of regenerating transgenic plants with low expression. Guard cells of the lower epidermis layer (b1, b2) show nuclear envelope (NE) staining as well as ER and Golgi bodies (white closed arrow heads). **(C)** Adjacent pavement cells had to be imaged with much higher detector gain to visualise a predominant ER fluorescence with very low Golgi fluorescence remaining (closed white arrow heads). **(D)** The final diagram is the T-DNA vector used to study high and low expression levels of ERD2-YFP. Golgi bodies (white closed arrowheads) are labelled by ERD2-YFP more visibly during high cellular expression (High E), whereas punctae are much fainter relative to the ER fluorescence at low expression (Low E, imaged at higher detector gain).

### 2.2.4 YFP specifically masks the C-terminal di-leucine motif

As it was established that two leucine-residues at position -3 and -5 from the stop codon are required for both Golgi-localisation and the cargo-sorting activity of ERD2 (Silva-Alvim *et al*., 2018), I hypothesized that ligand-induced ERD2 redistribution may also be observed with the YFP-TM-ERD2 fusion, as long as the last 5 amino acids (LQLPA) are deleted. I therefore tested the truncated fluorescent fusion (YFP-TM-ERD2ΔC5) in the co-expression experiment with Amy and Amy-HDEL as introduced in Figure 4. In the control infiltration with Amy a partial localisation to the ER is clearly visible, but less extreme than that of ERD2-YFP (Figure 6B). Upon Amy-HDEL co-expression, there is a strong shift to a dominant ER localisation in correlation with the behaviour of the C-terminal ERD2-YFP fusion, albeit slightly weaker. It is possible that in addition to masking the C-terminus, the large YFP-portion has a more damaging influence on ERD2, possibly by preventing homotypic interactions with endogenous wild type ERD2 that could yet provide a level of Golgi retention for YFP-TM-ERD2ΔC5 even when HDEL proteins are co-expressed.

Initial redistribution assays suggest that preventing exposure of the ERD2 C-terminus causes a dual steady-state localisation at the ER and Golgi. Next I wanted to determine if this was specific to the di-leucine motif by co-expressing receptors with the visual PVC/vacuolar and ER markers Aleu-RFP and RFP-HDEL, respectively. Varying the format of HDEL cargo would confirm that redistribution is a receptor-specific occurrence and not specific to our model cargo Amy-HDEL. It would also help to show comparable conditions of cargo expression where Amy and Amy-HDEL are typically not visible. As a control ERD2-YFP was tested first with the two markers and as expected, redistribution occurred when co-expressing RFP-HDEL but the typical ER-Golgi dual localisation was maintained with Aleu-RFP (Figure 6C). A general vacuolar stain and extra punctate structures were also observed for Aleu-RFP, typical for a vacuolar model marker (Foresti *et al*., 2010). When deleting the last 5 amino acids of ERD2 (YFP-TM-ERD2ΔC5) or mutating the di-leucine motif (YFP-TM-ERD2LLGG), the receptor redistributed in the same manner as ERD2-YFP when co-expressed with RFP-HDEL, while remaining predominantly Golgi-localised when co-expressed with Aleu-RFP (Figure 6D, E). It appears the functional domain compromised by C-terminal tagging can be

narrowed down to the di-leucine motif. It is important to note that the partial ER localisation of YFP-TM-ERD2LLGG under control conditions is also less intense than that of ERD2-YFP, as seen for YFP-TM-ERD2ΔC5.

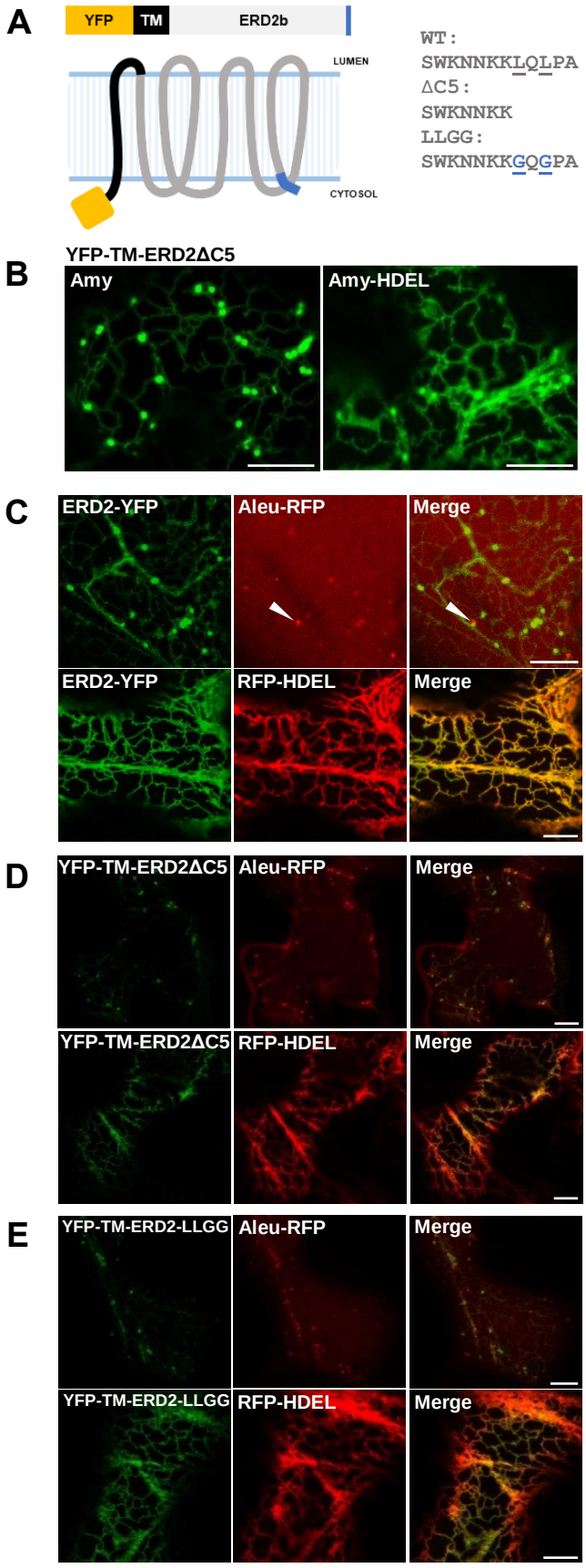


**Figure 6: Redistribution assays with visible cargoes identify masking of the di-leucine motif.** CLSM and infiltration as in Figure 4 with the additional capture of RFP.

**Figure 6: Redistribution assays with visible cargoes identify masking of the di-leucine motif (cont.).** CLSM and infiltration as in Figure 4 with the additional capture of RFP.

**(A)** Visual representation of the novel N-terminal ERD2 fusion C-terminal mutant variants visualised in blue and included are C-terminal sequences of the ΔC5 and LLGG variants. **(B)** Dual ER-Golgi localisation of YFP-TM-ERD2ΔC5 co-expressed with Amy and a more prominent ER localisation when co-expressed with Amy-HDEL. **(C)** ERD2-YFP presents a dual ER-Golgi localisation when co-infiltrated with a control cargo Aleu-RFP. Notice this marker labels the Golgi and post-Golgi compartments (closed arrowheads, middle panel) and is partially in the vacuole. The re-distribution of ERD2-YFP occurs when co-infiltrated with RFP-HDEL. This marker is only visible in the ER. ERD2-YFP confirms that both markers are suitable as visible negative and positive controls, respectively. **(C)** Dual ER-Golgi localisation of YFP-TM-ERD2ΔC5 under control conditions with Aleu-RFP. A redistribution occurs when co-infiltrated with RFP-HDEL, with any Golgi punctate very difficult to detect. **(D)** YFP-TM-ERD2LL^GG shows an ER-Golgi localisation when co-infiltrated with Aleu-RFP comparable to **(B)**. When co-infiltrated with RFP-HDEL the di-leucine mutant visibly shifts to a dominant ER localisation, showing that this motif is the compromised domain.

### 2.2.5 A knockout mutant does not redistribute upon HDEL overexpression

The case presented so far is that compromising the di-leucine motif enables ERD2 transit between the ER and Golgi, which is further exacerbated by an increase in ligand concentration. What remains to be investigated is why the availability of HDEL protein affects the rate of redistribution; is it simply an increase in passive retrograde transport because of a heightened demand for COPI vesicles at the *cis*-Golgi, or are receptors collecting in the ER because they are dragged back by HDEL proteins?

To study whether HDEL binding causes the change to receptor localisation via influencing the structure of the receptor itself, I introduced an N-terminal mutation into YFP-TM-ERD2ΔC5. The conserved Arg-5 (R5) was previous shown to be important for ligand-binding (Townsley *et al*., 1993). This was shown by incubating crude membrane fractions from COS cells transformed with ERD2 mutants with iodinated KDEL peptides followed by pelleting the membranes. Ligand-binding was quantified based on co-pelleted peptide and found to be strongly reduced to a mere 10-30% compared to wild type ERD2. In gain-of-function assays in tobacco protoplasts this mutant also exhibited very low levels of additional Amy-HDEL retention (An, 2015). More recently the crystal structure elucidating the binding pocket has determined that Arg-5 is part of a critical arginine ladder guiding the entry of KDEL/HDEL (Gerondopoulos *et al*., 2021). So, by introducing the R5A mutation into the YFP-TM-ERD2ΔC5 format I postulated that the mutant receptor may no longer redistribute upon HDEL overexpression if this phenomenon is dependent on ligand-induced conformational changes of ERD2 itself. YFP-TM-

ERD2ΔC5 (R5A) has the typical ER-Golgi localisation of the C-terminal mutant under control conditions without ligand (Figure 7A). Co-infiltrated RFP-HDEL showed a strict ER localisation (Figure 7B) and expression levels were suitable to induce a redistribution as seen previously (Figure 6). However by introducing the R5A mutation into the fusion it remained heavily in Golgi bodies and was directly comparable to control conditions, in other words very much lacking a redistribution (Figure 7B). This would suggest that a direct interaction with HDEL is key to the ligand-induced redistribution of non-functional ERD2 fusions.

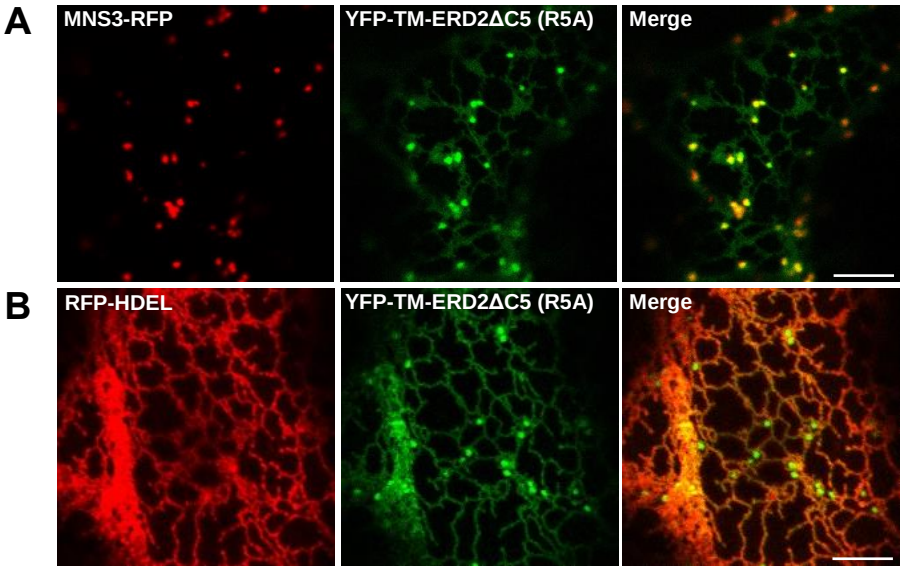


**Figure 7: The R5A binding mutant does not redistribute upon HDEL overexpression when lacking the di-leucine motif.**
**(A)** MNS3-RFP is seen to label Golgi bodies and YFP-TM-ERD2ΔC5 (R5A) is visible in the typical dual ER-Golgi distribution of the ΔC5 mutant. MNS3 is a strictly cis-Golgi localised glycan-modifying mannosidase used as a control to separate the labelling of punctate from ER tubules and sheets, although this is already quite visible in the R5A mutant. **(B)** An almost identical localisation is observed for YFP-TM-ERD2ΔC5 (R5A) when co-infiltrating the ER-localised RFP-HDEL. Expression levels of RFP-HDEL are comparable to Figure 6, where a redistribution was induced for YFP-TM-ERD2ΔC5. Most importantly is the labelling of Golgi bodies which maintain strong fluorescence in both conditions. ER fluorescence is also comparable, but there is an increase of ER sheets in **(A)** relative to **(B)** where ER tubules are more prominent.

### 2.2.6 The activity and localisation of Human KDELR2 fluorescent fusions can be determined in plant expression systems

The importance of the di-leucine motif and its high degree of conservation in different eukaryotic kingdoms has previously been reported (Alvim, 2018), a good example being the human ERD2 form (KDELR2) which can mediate increased retention of HDEL proteins in plant protoplasts (C-terminal sequence comparison is displayed in Figure 8A). For consistency, KDELR2 is hereafter referred to as HsERD2.

Since a large portion of ERD2 modelling has been driven in mammalian research systems, I decided to repeat the most important key-findings surrounding the role of the di-leucine motif and the influence of YFP-tagging with HsERD2 instead of AtERD2 as the model (Figure 8B). Here the coding regions of wild type KDELR2 (WT) and its LLGG mutant variant (LLGG) were first transferred into GUS reference vectors to establish comparable expression levels in *N. benthamiana* protoplasts (Gershlick *et al*., 2014) and monitor the effect on Amy-HDEL model cargo retention in a quantitative gain-of-function assay (Silva-Alvim *et al*., 2018). Increased Amy-HDEL cell retention relative to basal secretion of the cargo when expressed alone demonstrates receptor activity. The activity of different receptors can then be compared when the GUS internal references are equivalent. Figure 8B shows that the LLGG mutant has completely lost the ability to increase the retention of Amy-HDEL.

Next I generated fluorescent fusions mirroring the earlier constructs of Silva-Alvim *et al.* (2018) but using HsERD2 and inserted the coding regions for YFP-TM-HsERD2 and HsERD2-YFP into the same GUS reference vector. YFP-TM-HsERD2 mediated high levels of Amy-HDEL retention similar to the wild type, whilst HsERD2-YFP was almost inactive (Figure 8B). Notice at higher concentrations HsERD2-YFP mediates slightly increased Amy-HDEL retention levels, suggesting the detection of a minor retention activity that was not previously observed with AtERD2 (Silva-Alvim *et al*., 2018). It is possible that a portion of the fusion protein is prone to proteolytic cleavage, releasing minor quantities of free YFP and an active untagged HsERD2 but this was not investigated since the measured activity is minor compared to that of the YFP-TM fusion at the N-terminus. The experiments

confirmed that obstruction of the C-terminus is undesirable also for the human receptor molecule.

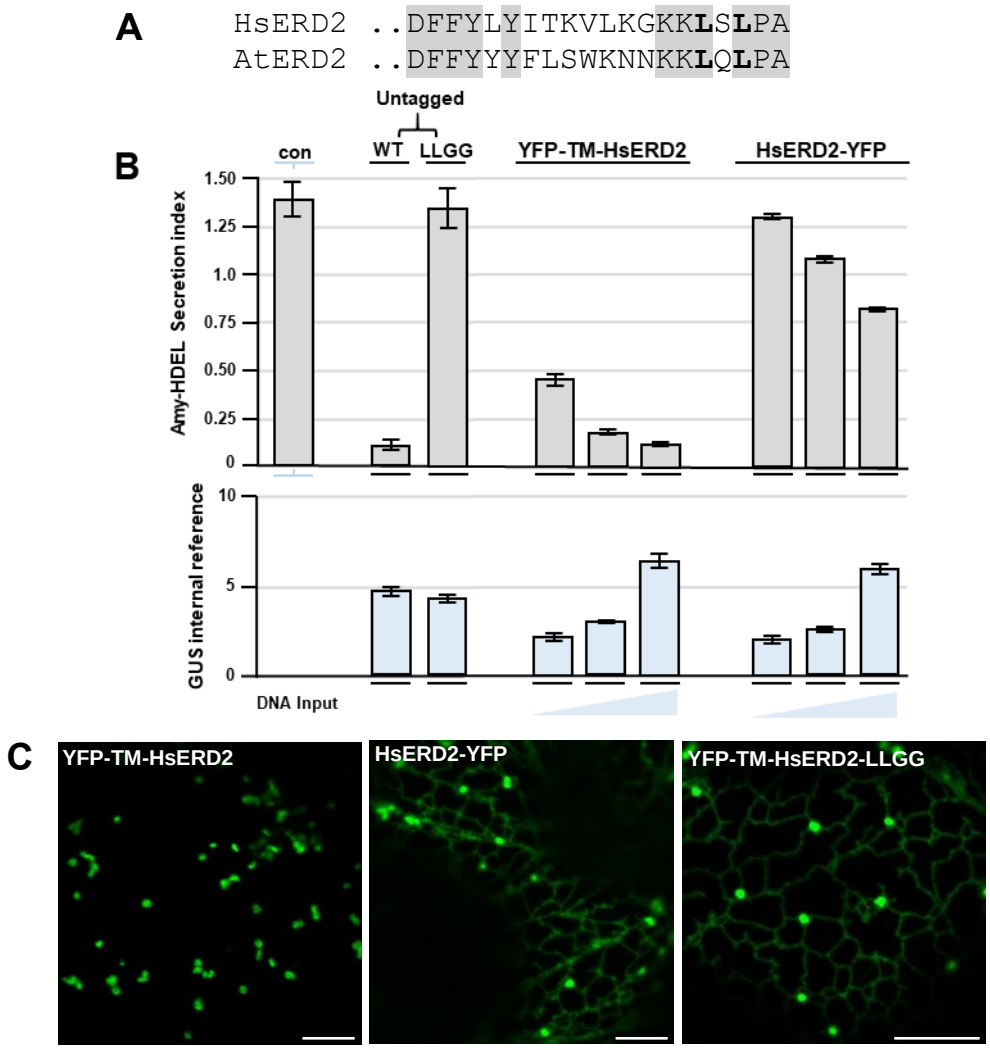


**Figure 8: Localisation and Function of Human ERD2 Fluorescent Fusion Variants in plant expression systems.**

**(A)** C-terminal amino acid sequences of plant and human ERD2 (*At*ERD2b and KDELR2). Conserved residues are highlighted in grey including the di-leucine motif in bold. **(B)** Functional assays carried out in *N. Benthamiana* mesophyll protoplasts to determine the secretion index (SI) of Amy-HDEL from cell and medium samples. Here Amy-HDEL is co-expressed with wild type KDELR2 and the LLGG mutant then compared with the two fluorescent fusion variants, respectively. The control experiment for Amy-HDEL without any effector plasmid is labelled (con). Comparable levels of KDELR2 and LLGG mutant encoding plasmids were co-transfected at equal levels (see GUS internal reference, Methods section 7.5.5). KDELR2 exhibits strong retention of Amy-HDEL in cells whilst LLGG mutant is virtually non-functional and comparable to the SI of the control. The SI of YFP-TM-huERD2 and huERD2-YFP were tested in comparable dose responses (see GUS internal reference). YFP-TM-HsERD2 is very active throughout the dose response, whereas HsERD2-YFP is unable to mediate a meaningful SI until very high plasmid concentrations and even then the activity is heavily compromised. **(C)** CLSM analysis of three human ERD2 fluorescent fusions in plant mesophyll cells (YFP-TM-HuERD2, HuERD2-YFP and YFP-TM-HuERD2-LLGG). Notice exclusive Golgi punctate for functional YFP-TM-HuERD2. Meanwhile the C-terminal YFP fusion and LLGG mutant both cause partial ER localisations.

Next I subcloned the YFP-TM-HsERD2 and HsERD2-YFP coding regions into Agrobacterium vectors for expression under the transcriptional control of the weak TR2 promoter (Silva-Alvim *et al*., 2018). Transient expression in leaf epidermis cells revealed that YFP-TM-HsERD2 and HsERD2-YFP mirrored their *A. thaliana* counterparts with a strict Golgi and ER-Golgi co-localisation, respectively (Figure 8C). To determine if these differences were also caused by C-terminal masking of the di-leucine motif, an additional YFP-TM-HsERD2-LL^GG construct was transiently expressed and displayed a dual ER-Golgi localisation (Figure 8C), in complete agreement with the previously presented data on *At*ERD2b fluorescent fusions. In summary, all earlier findings could be reproduced with human ERD2 in plant cells and it is remarkable that the wild type human receptor strictly accumulates in the Golgi apparatus of plant cells.

### 2.2.7 Active and inactive fluorescent fusions in HeLa cells

As there is only little over 50% sequence identity between human KDELR2 and *A. thaliana* ERD2b, the conservation of Golgi retention and functionality when expressed in plant cells is fascinating and highlights the propensity of ERD2 retention between eukaryotes. I was therefore curious how the fluorescent plant ERD2 fusions would behave in a mammalian cell system. The two fluorescent variants of either human or Arabidopsis ERD2 fusions were subcloned in a mammalian expression vector under the transcriptional control of the cytomegalovirus (CMV) promoter and transfected in HeLa cells. Figure 9A and B shows the fluorescent pattern of AtERD2-YFP and YFP-TM-AtERD2, respectively, when co-transfected with RFP-KDEL in fixed HeLa cells, staining endogenous Golgi matrix protein 130 (GM130) as a cis-Golgi marker present in all cells. ERD2-YFP is mostly found in the ER, although partial overlap with the cis-Golgi marker was visible and more pronounced when expressed at higher levels. In sharp contrast, YFP-TM-ERD2 was almost perfectly co-localised with GM130. Regardless of expression levels and the presence of RFP-KDEL, YFP-TM-ERD2 could not be detected in an ER network. The same results were obtained with the two human ERD2 fusions YFP-TM-HsERD2 and HsERD2-YFP (Figure 9C, D). This corresponds entirely with my findings in plant cells and suggests the mechanism of ERD2 Golgi localisation is conserved between plants and mammals.

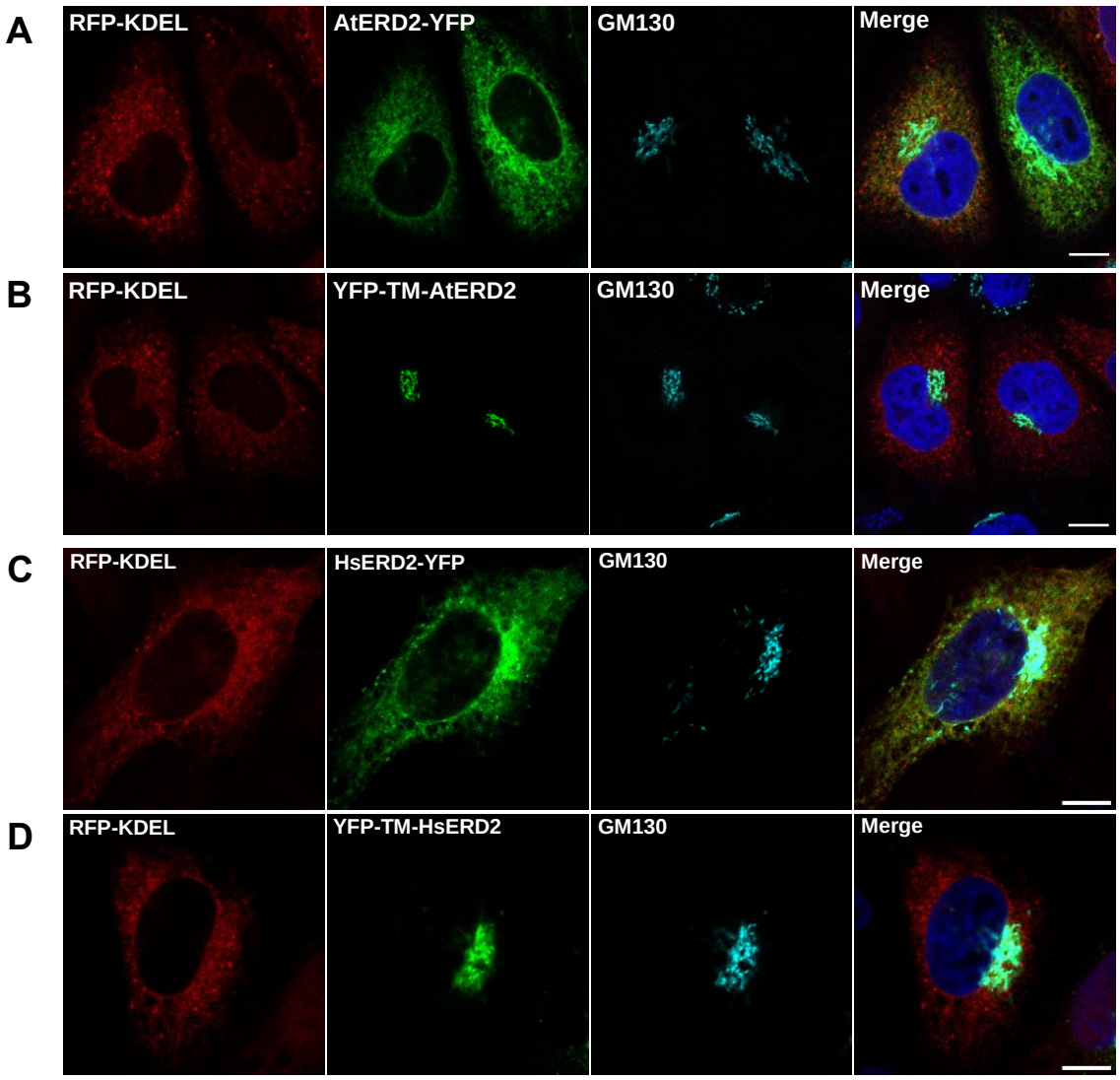


**Figure 9: Localisation and Function of Human and Plant ERD2 Fluorescent Fusion Variants in HeLa cells.**

**(A)** CLSM analysis of AtERD2-YFP (green) co-expressed with the ER marker RFP-KDEL (shown in red) in HeLa cells (size markers are 10 microns throughout this thesis unless otherwise stated). The endogenous cis-Golgi marker GM130 was detected via immunocytochemistry (shown in light blue) and the nucleoplasm is stained with DAPI (dark blue). Notice the heavy ER staining in the green channel. **(B)** CLSM analysis of YFP-TM-AtERD2 (green) co-expressed with the ER marker RFP-KDEL (shown in red) in HeLa cells. Notice that YFP-TM-AtERD2 is not detected in the ER and shows the best co-localisation with GM130. **(C)** and **(D)** same as in **(A)** and **(B)** using Hs ERD2 in place of At ERD2. Localisation of each fusion for both species is consistent.

## 2.3 Discussion

The systematic style of this chapter has taken shape as an exhaustive evaluation of findings and techniques associated with the ERD2 recycling model. Originally, conservative concerns were shared by Silva-Alvim *et al*. (2018) in an attempt to alter the trajectory of ERD2 research, rather than wipe the slate clean. However, this approach has failed its main objective in curbing the use of C-terminal modifications. Instead it has caused unwanted conflict in the field (Aniento and Robinson, 2020) and the use of these fusions has continued without validation (Brauer *et al*., 2019; Gerondopoulos *et al*., 2021; Yue *et al*., 2021). It has also brought a very negative reception for proposing a new mode of function in grant proposals and future publications, leaving no option but to first dismantle any remaining validity to the ERD2 recycling model with a multifaceted dataset, summarised in this discussion.

### 2.3.1 Golgi-to-ER Redistribution is a symptom of di-leucine motif masking

In honour of ERD2 validation methods in the field prior to our secretion assays, I carried out redistribution experiments with the aim of determining why non-functional and functional ERD2 fluorescent fusion proteins present different phenotypes. By using varied ligands, I wanted to make clear there was no discrepancy between what is observed for ERD2-YFP, but instead what I deem to be biologically relevant. As expected, I was able to induce a clear migration of the inactive ERD2-YFP from a dual ER-Golgi state to entirely ER after HDEL-ligand saturation. This demonstrated that the failure of biologically active YFP-TM-ERD2 to show ligand-induced redistribution and remain entirely Golgi-localised was not due to insufficient ligands, but simply due to the fact that it's C-terminus was not compromised by masking the Golgi retention signal. The fact that ERD2-YFP could not suppress the lethal effect of ERD2 knockdown by anti-sense inhibition may reflect that multicellular life could be more sensitive to insufficient cellular ERD2 compared to yeasts, but mainly it illustrates the non-functional nature of the C-terminal fusion. The mutants YFP-TM-ERD2ΔC5 and YFP-TM-ERD2LL^GG also showed ligand-induced redistribution to the ER. Since the C-terminus and di-leucine motif were known to be critical for ERD2 function in retaining Amy-HDEL,

the experiments establish a clear correlation between compromised function and exacerbated ER residency.

An entire series of experiments was devoted to the use of a human ERD2 ortholog previously shown to mediate increased retention of HDEL proteins in plants which exhibits the same signature di-leucine motif at the C-terminus. Interestingly, the human gene is also sensitive to C-terminal fusions and retains much more of its activity when expressed in the YFP-TM-ERD2 configuration (Figure 8B). A minor activity was detected for the C-terminal YFP fusion of human ERD2 (Figure 8B), which was never seen for the plant fusion protein (Silva-Alvim *et al*., 2018). It is possible that minor differences in the way ERD2 was fused to fluorescent proteins could contribute to the partial biological activity earlier reported when using the cargo GFP-HDEL (Montesinos *et al*., 2014). If proteolysis has occurred and released active ERD2 this would be accompanied by a release of GFP, which would have migrated at the same position as GFP-HDEL on the protein gel (Figure 5 of Montesinos *et al*., 2014). Although these are minor effects, my results remain clear in that the YFP-TM-ERD2 configuration retains most of the original activity whilst C-terminal fusions either retain minor activity or none at all.

Crucially, the human receptor localises to the Golgi apparatus and only shows partial ER localisation when the di-leucine motif is masked or mutated (Figure 8C). Notably, both plant and human receptors accumulated at the cis-Golgi of human HeLa cells when their C-termini were unobstructed, whilst the C-terminal fusions showed strong additional labelling of the ER. This rules out a species-specific property of fluorescent fusions in plants and instead shows a highly conserved mechanism between two Eukaryotic kingdoms. The structural relationship between migrating constructs is a compromised C-terminus and it appears that masking with YFP exacerbates changes in localisation at least as much and probably more than mutating or removing the di-leucine motif completely, due to the additional steric hindrance.

### 2.3.2 Golgi-to-ER redistribution of ERD2-YFP is influenced by receptor expression levels and endogenous ligands

A fundamental prerequisite of redistributions assays is that the steady-state localisation of modified ERD2 remains unchanged except for HDEL-ligand

saturation. However, I witnessed an unreported phenomenon of a change in ER-Golgi distribution depending on expression levels alone. Townsley *et al*. (1993) have a similar claim, reporting a tendency for ER localisation to increase when receptor expression levels are 10-fold higher relative to their test conditions, but this is most likely due to saturation of the ER-Golgi interface. In my case, it was clear that at as ERD2-YFP expression levels decreased, more of the fusion protein resided at the ER and the fluorescence intensity in Golgi-bodies was reduced. Meanwhile higher expression led to a dominant Golgi localisation.

As it is highly unlikely that ERD2-YFP overexpression leads to faster ER export, I postulate that Golgi to ER retrograde transport becomes rate limiting. Since ligand-mediated recycling should be regarded as an accidental transport that would not normally occur when the di-leucine motif is properly exposed, the results support the idea that Golgi-retention is promoted by the prevention of retrograde recycling. At low expression levels the relative quantity of endogenous ER chaperones to ERD2-YFP are higher, therefore a larger proportion of these receptor fusions migrate to the ER. At higher expression levels the interaction of endogenous ER chaperones with total ERD2-YFP is smaller, thus the majority of receptors remain at the Golgi. Given expression levels alone can determine the outcome of redistribution assays, more caution should be taken when considering the rather high variance of transient expression levels in transfected mammalian cells, especially as they are called upon to draw conclusions on ERD2 function (Brauer *et al*., 2019).

What is consistent with distributions, regardless of expression levels, is that they are induced by ligand-binding. Because ERD2 does not migrate to the ER deliberately it is conceivable that its positioning at the interface without the di-leucine motif to anchor it at the cis-Golgi may have been enough for the receptor to be sequestered into retrograde COPI carriers. However, because a redistribution was prevented following the mutation of Arg-5, a known binding mutant, it is evident the association with ligands is the key element allowing for the receptor to be mistakenly dragged back to the ER. It will be interesting to identify how a cytosolic signal can prevent such transport when it is triggered by ligand-binding in the lumen, and how ERD2 is capable of releasing its ligand into retrograde transport structures without joining them.

## 2.4 Conclusion

The C-terminus of ERD2 was deemed of little importance from the very beginning of research into the receptor (Townsley *et al*., 1993). Combined with the field's reluctance to deviate from redistribution assays with non-functional receptors, a complete oversight of a highly conserved di-leucine motif has occurred. Deletion, mutation, replacement or masking of this motif significantly impairs biological activity and enables receptors to redistribute from the Golgi to the ER. Due to this, receptors exhibiting an ER localisation should not be considered as wild type. All future ERD2 studies containing modified receptors must provide evidence of biological activity without the use of redistribution assays as this method holds no biological relevance to the mode of function. Ultimately, a definitive wild type localisation for ERD2 still needs to be determined if better antibodies become available.

# Chapter 3 - The ERD2 C-terminus is sensitive to minor fusions and does not harbour signals for COPI-mediated recycling

## 3.1 Introduction

Whilst I have settled the dispute on the biological unsuitability of ERD2-YFP as a research tool, a key practical aspect mentioned earlier which I am yet to address is that pioneering research building up to the recycling hypothesis involved the human receptor C-terminally fused to a c-myc epitope (Dean and Pelham, 1990; Hardwick *et al*., 1990; Semenza *et al*., 1990; Townsley *et al*., 1993). It was indeed this alteration which has since encouraged a generalised use of C-terminal tags and ligand-mediated redistribution assays, with the only validation of any new modifications coming in a referral to the aforementioned research articles containing the original c-myc epitopes (Boevink *et al*., 1998; Majoul *et al*., 2001; Montesinos *et al*., 2014; Bräuer *et al*., 2019).

It is true that the C-terminal c-myc epitope tag by comparison is only a fraction in size to the fluorescent proteins that have since been used more frequently, so it may actually avoid negative effects on ER retention mediated by ERD2. To provide background on what we know about the original c-myc tagged receptor so far, the first attempt of validation is also the only measure ever to be taken to verify that ERD2 with a C-terminal c-myc fusion has biological activity (Semenza *et al*., 1990). The method was simplistic by nature, requiring *erd2* mutant strains transfected with ERD2-c-myc-containing vectors to grow on minimal media, so much so that any evidence confirming this was deemed unnecessary to present at the time. In spite of that, continued research in yeast did characterise the species' capability in circumnavigating the stresses brought about by severely compromised ERD2 function. For example, a mutational analysis indirectly confirmed that yeast growth does not necessarily confer high biological activity, as growth was the prerequisite for identifying certain yeast mutants which were later categorised as having a lower ER retention efficiency (Townsley *et al*., 1994). Moreover, some mutant *erd2* phenotypes were later identified to contain "suppressors of the ERD2-deletion" otherwise known as SED genes, which when isolated and expressed as multi-copies in other mutants returned the ability to grow (Hardwick *et al.,* 1992). The

original SED expressing mutants still secreted the chaperone BiP and contained visible abnormalities in morphology, suggesting that ER retention in these strains was still very poor. All in all it was evident that yeast complementation was in fact multifactorial, so to avoid future difficulties in ERD2 research the ligand-induced redistribution of C-terminal ERD2 fusions was instead chosen to be the signature of wild type ERD2 activity, and mammalian cells transfected with C-terminal ERD2 fusions gained preference for modelling (Lewis and Pelham,1992a, b).

In this chapter I have chosen to investigate just how sensitive the receptor C-terminus is by analysing the effects a fusion of such epitope tags have on function. This will involve a more elaborate panel of constructs compared to the first chapter in order to fairly characterise the intricacies of the native C-terminus and the changes it can withstand. In addition, I have explored elements of the C-terminus to test more recent ideas about certain sequences involved in ERD2 recycling that are at odds with the permanent residency of ERD2 at the Golgi, notably the role of a non-conserved serine at position -4 from the C-terminus and two lysines at position -7 and -6 from the C-terminus. The former was reported to mediate conditional ERD2 recycling based on inducible serine-phosphorylation (Cabrera *et al*., 2003), and the two lysines were very recently introduced as a “lysine cluster” and proposed to act as inducible COPI transport signals that are revealed upon ligand-binding (Brauer *et al*., 2019). This entailed the characterisation of more mutations and the fusion of other putative transport signals.

## 3.2 Results

### 3.2.1 Small C-terminal epitope tags can compromise ERD2 function

It is clear that C-terminal fluorescent fusions compromise the exposure of a Golgi-retention signal close to the ERD2 C-terminus, not just in plants but also in mammals. It is important to notice that the first evidence for ligand-induced redistribution of ERD2 was obtained using an ERD2 fusion containing a C-terminal c-myc epitope (Lewis and Pelham, 1992a) which is much smaller compared to YFP. It is possible that adding only a small number of amino acids has very little impact on activity when compared to a 24kD fluorescent protein, therefore the only certainty I have obtained so far is that a YFP C-terminal fusion is inherently bad for

ERD2 function and the leading cause of redistribution. Previously we have shown that fusion of the HA tag to the C-terminus of *At*ERD2b has very little effect on Amy-HDEL retention in *N. tabacum* protoplasts (An, 2015), therefore I chose to carry out the same functional assay in *N. benthamiana* protoplasts along with c-myc and FLAG fusions to determine if any variability may be generated, creating fusions with both *At*ERD2b and HsERD2 (Figure 10A). New coding regions at the C-terminus were constructed using specifically designed primers and polymerase chain reaction (PCR), then transferred into GUS vectors for normalising expression levels prior to functional assays.

The newly generated FLAG- and original c-myc-tagged ERD2 exhibited much weaker biological activity when compared to untagged ERD2 in both human and plant variants (Figure 10B, C). In the case of the c-myc epitope, it is likely that the residual activity observed will still have been sufficient for complementation experiments in yeast (Semenza *et al*., 1990), as none of the epitope tags cause a complete knock out. Interestingly, I could confirm that fusing the HA tag caused only a minor reduction in either plant or human ERD2 activity, as previously illustrated for the *A. thaliana* ortholog in *Nicotiana tabacum* protoplasts (An, 2015). It is apparent that C-terminal fusions may be able to maintain biological activity on a contextual basis and must be tested individually in each case. It is also astonishing that the varying sensitivity to these tags is highly conserved between plant and human ERD2, with c-myc and FLAG having strong negative effects on ERD2 activity and HA tag the opposite.

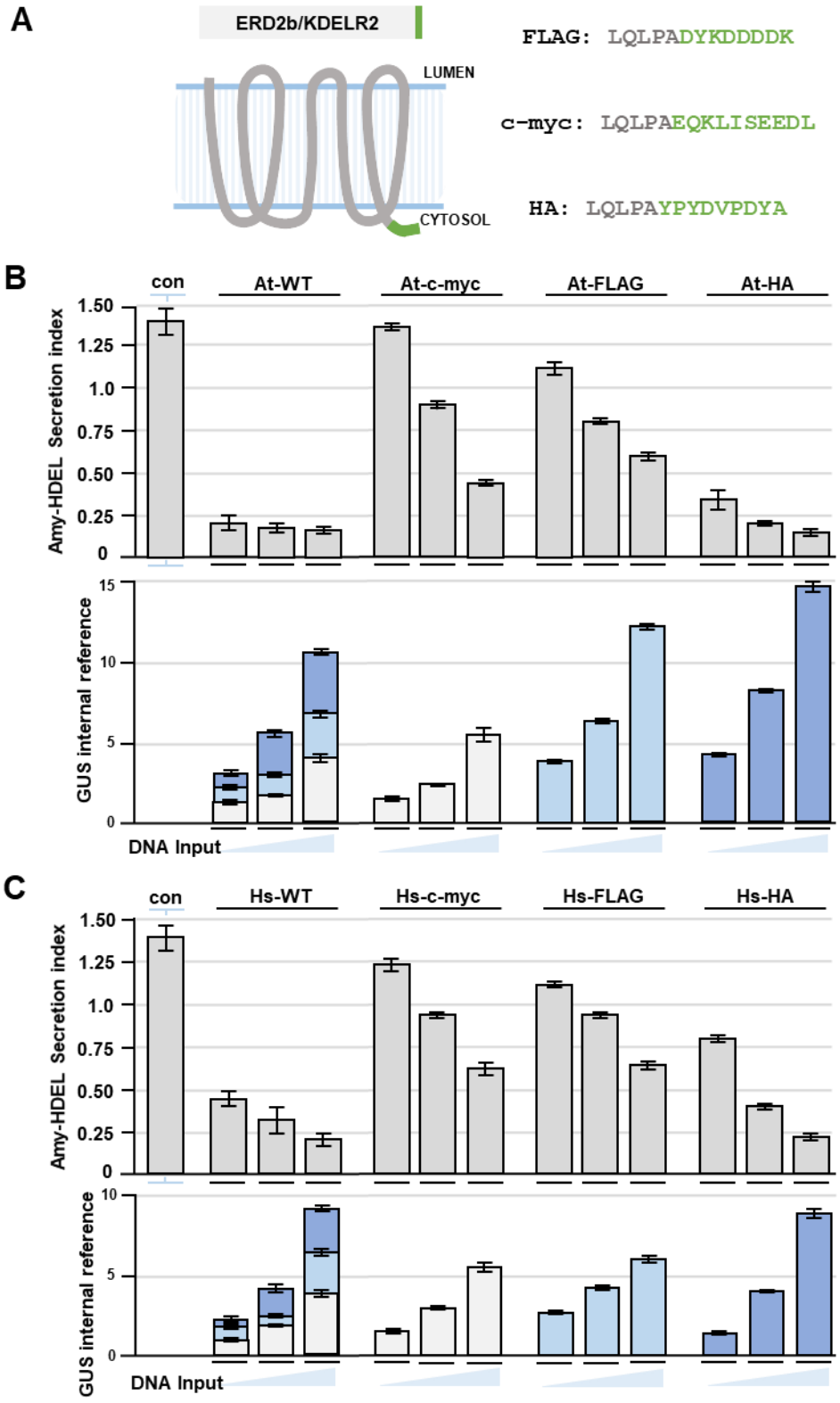


**Figure 10: Function of ERD2 following minor C-terminal modifications.**

**(A)** Visual representation of C-terminal fusions to plant and human ERD2 (*At*ERD2b and KDELR2) for functional assays. Epitope sequences after *At*ERD2b sequence are provided in green text. **(B)** Secretion index of Amy-HDEL when co-expressed with wild type *At*ERD2b or KDELR2 and then compared with the three different C-terminal modifications, respectively. Comparable dose responses for each C-terminal tag against the wild type receptor are colour co-ordinated in the GUS internal reference data (e.g. white bars for wild type are compared with white bars for c-myc tag).

**Figure 10: Function of ERD2 following minor C-terminal modifications (cont.)**

**(B cont.)** Notice in every instance the wild type expression is slightly lower than that of C-terminal fusions, yet the secretion index always remains lower. Medium expression levels in each dose response therefore reflect the biological activity of each variant most realistically. The addition of a FLAG or c-myc tag strongly reduced function, whilst most of the activity was maintained for each ortholog after adding the HA tag. **(C)** As in **(B)** but At ERD2 is replaced with Hs ERD2.

### 3.2.2 Compromising epitope tags also cause an ER-Golgi Dual Localisation

At this point the variation in biological activity from the different epitope tag fusions raised the possibility that they may localise differently too, considering this is the common theme between the choices of inactive and inactive fluorescent fusion configurations. To test if compromised function was accompanied by a reduced Golgi residency, the three C-terminal epitope tags were introduced into the YFP-TM-ERD2 format for both plant and human ERD2 coding regions (Figure 11A) and infiltrated as in 1.2.1. In agreement with the loss-of-function C-terminal YFP fusion, FLAG- and c-myc-tagged YFP-TM-ERD2 fusions were both distributed between the ER and Golgi, whilst both of the HA-tagged fluorescent fusions exhibited a predominant Golgi localisation with none visible at the ER under the same conditions, as expected for functional constructs (Figure 11). This supports the strict correlation between di-leucine motif masking and induced ER-Golgi distribution, reiterating that the context of modification is important. Crucially, this feature is not specific to the plant kingdom and is equally presented for the human receptor. It is important to focus on the fact that the additional ER staining of the c-myc fusions with human or plant ERD2 (Figure 11B) are similar to those obtained with mutated or deleted di-leucine motifs (Chapter 2). Hence it is likely that the original reporting on ligand-induced redistribution was indeed due to masking or compromising this motif by the c-myc epitope. The FLAG tag is smaller than the HA tag but has a much more negative effect on function similar to the c-myc tag, so size alone does not seem to be the direct cause of compromised activity.

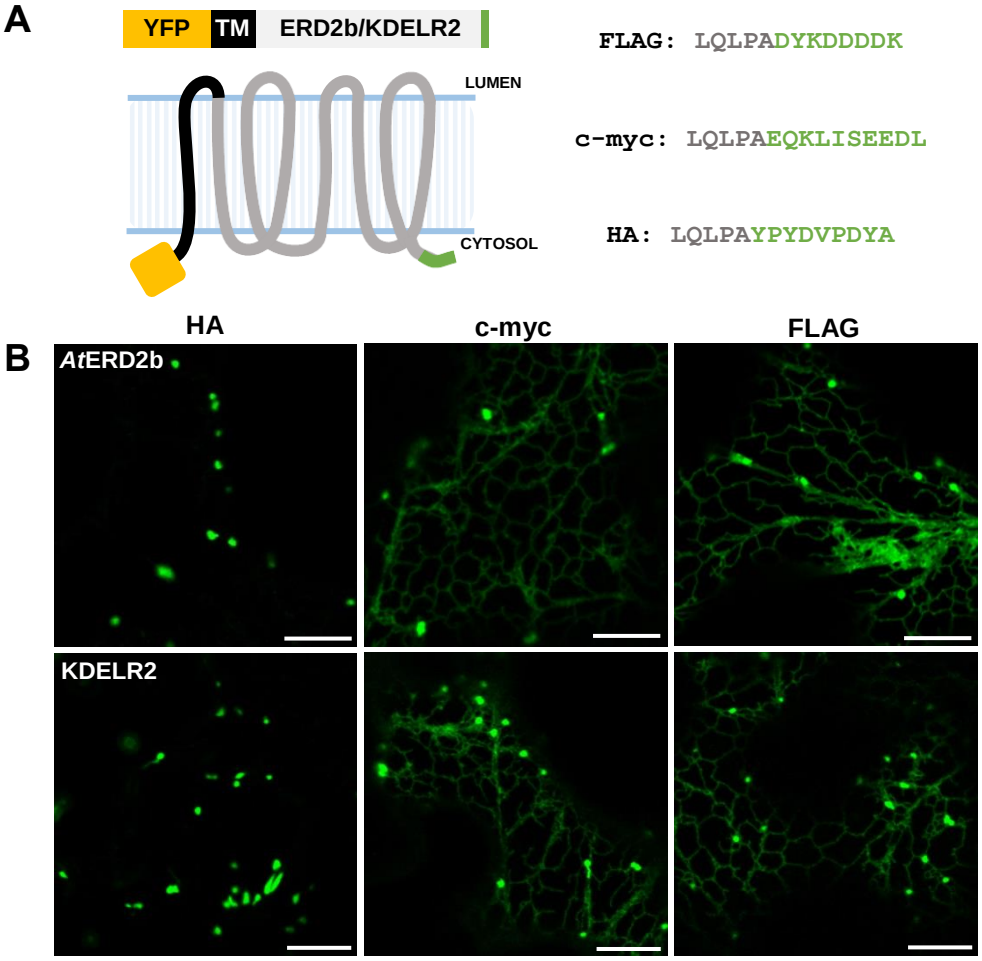


**Figure 11: Localisation of ERD2 following minor C-terminal modifications.**
**(A)** Visual representation of C-terminal fusions to plant and human ERD2 (*At*ERD2b and KDELR2) for fluorescence microscopy. The epitope sequences are provided in green text. **(B)** Localisation of *At*ERD2b and KDELR2 fluorescent fusions with C-terminal FLAG, c-myc and HA tags. Notice that FLAG and c-myc additions cause an ER-Golgi localisation, whilst the addition of an HA tag does not affect the Golgi localisation of YFP-TM-ERD2 for both orthologs.

### 3.2.3 One more C-terminal residue can strongly reduce function

Due to the varying effect C-terminal modifications can have on ERD2, it was important to establish how much change can be made before large reductions in function are seen. Similar experiments have been done with other C-terminal signals to determine how sensitive the location of the signal is. Prominent examples are the KDEL motif (Munro and Pelham, 1987) and the KKXX motif (Jackson *et al*., 1990). In both cases the signals could be knocked out by addition of just one or two amino acids.

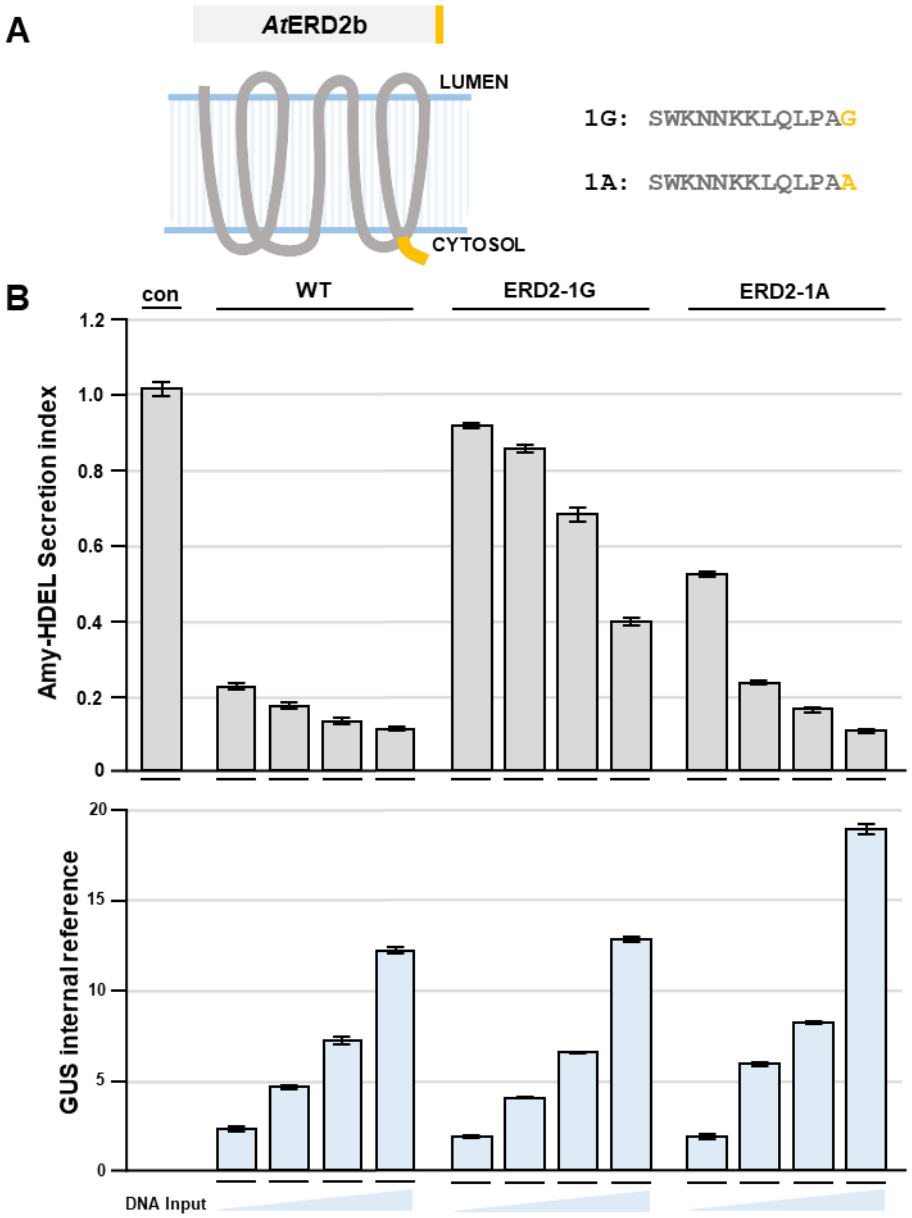


**Figure 12: Reduced Biological Function of ERD2 following single amino acid additions.** **(A)** Visual representation of the C-terminal additions of one glycine and one alanine used in functional assays, highlighted yellow. **(B)** Secretion index of Amy-HDEL when co-expressed with the receptors in **(A)** in dose response assays. Notice again that even at low expression levels (GUS internal reference) the wild type receptor immediately reduces the secretion index. Expression of ERD2-1A is higher in the upper range of the dose response, however where expression is comparable with ERD2-1G in the lower range it is clear that a single alanine addition allows for higher biological activity than a single glycine.

Working with *A. thaliana* receptor only, I started by adding a single C-terminal glycine or alanine residue (ERD2-1G, ERD2-1A), the simplest structures among amino acids (Figure 12A). Examined in a dose response format of increasing plasmid transfection, it is clear that just a single glycine addition to the C-terminus caused a staggering reduction in activity compared to the wild type receptor.

Interestingly, a single alanine addition had much less of a negative effect on Amy-HDEL retention and displayed almost wild type activity (Figure 12B). In this instance, a relatively small probe has highlighted the fragility towards changes at the receptor C-terminus on a single amino acid scale, regardless of any similarity the additions may have to the native structure. The results also illustrate neatly the high sensitivity of the Amy-HDEL transport assay in protoplasts, allowing researchers to monitor minor changes in the biological activity of this class of sorting receptors which may go unnoticed in overexpressed conditions.

### 3.2.4 Functional serine mutants remain at the Golgi

After determining that small C-terminal fusions are context dependent, I wanted to establish how pertinent certain C-terminal residues discussed in the literature were to function and localisation. Serine-209 has drawn interest in the mammalian field after suggestion that it controls Arf1-GAP recruitment after PKA phosphorylation and thus COPI vesicle tethering (Cabrera *et al*., 2003). This feature was debated in my laboratory as the serine residue is not conserved between human alleles nor species, yet other important features at the C-terminus are. When tested in functional assays mutation to alanine (S209A) or aspartic acid (S209D) had no effect on retention of Amy-HDEL (Alvim, 2018). The consensus with my research so far associates a Golgi localisation to functional ERD2 fusions and mutants, therefore I rounded off the analysis of these mutants by transferring the coding regions into the YFP-TM-HsERD2 format for microscopy. As anticipated staining was present in punctate structures only (Figure 13B). Thus the mutants are not only silent with respect to the ability to mediate Amy-HDEL retention, but also silent with respect to subcellular localisation of ERD2.

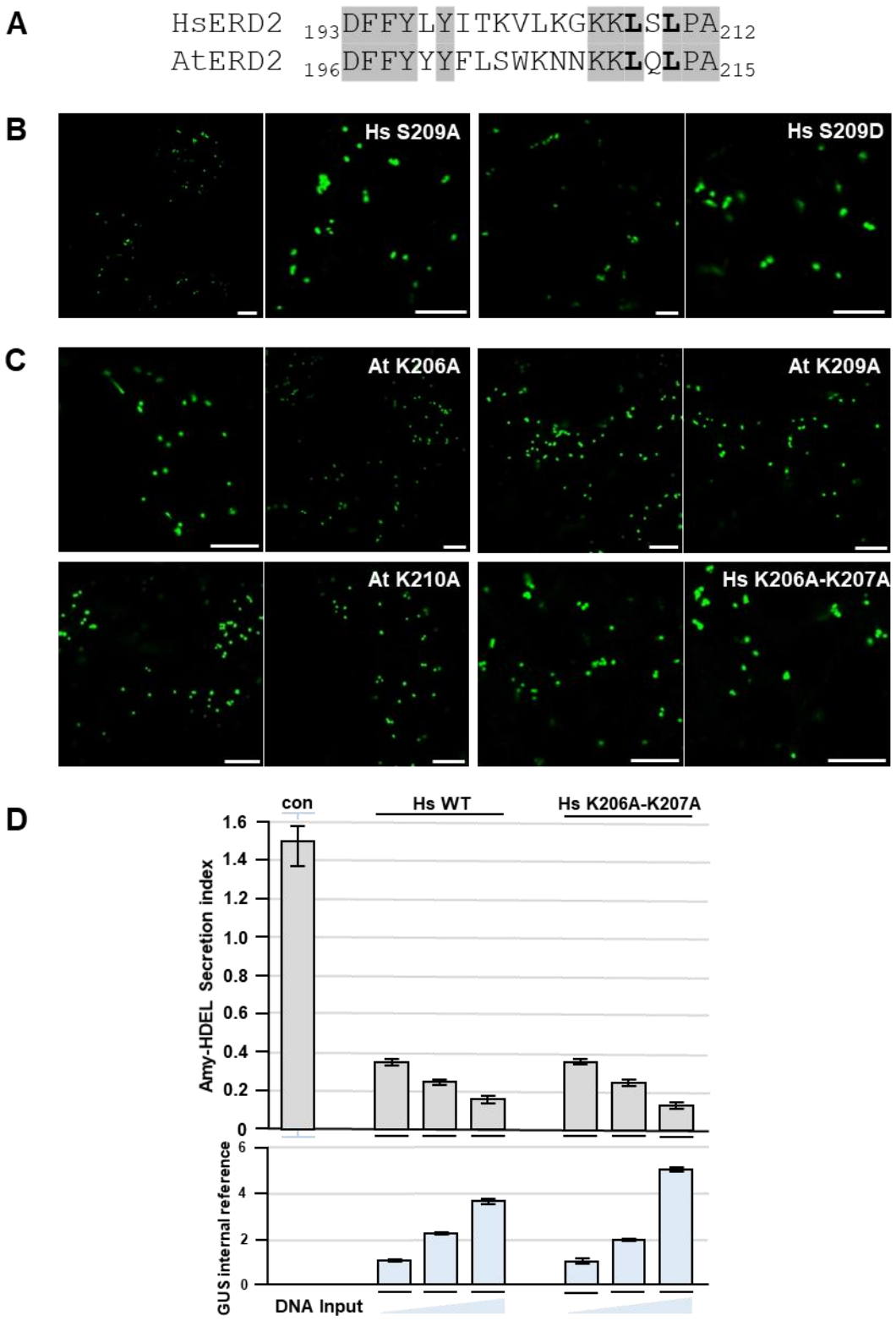


**Figure 13: ERD2 Function and Golgi Residency is Conserved Amongst Eukaryotes.**
**(A)** C-terminal amino acid sequences of plant and human ERD2 (*At*ERD2b and KDELR2). Conserved residues are highlighted in gray including the di-leucine motif in bold. Also visible is the non-conserved At Lys-206. **(B)** CLSM analysis of the two serine mutants S209A and S209D in the functional YFP-TM-HsERD2 fluorescent fusion format imaged in tobacco leaf epidermis cells. Notice that only a Golgi localisation is present and this is shown at different magnifications.

**Figure 13: ERD2 Function and Golgi Residency is Conserved Amongst Eukaryotes (cont.)**

**(C)** Same as in **(B)** but for the mutations K206A, K209A and K210A in *A. thaliana* and the double mutant K206A-K207A in *H. sapiens*. In every instance a strict Golgi-only localisation is visible. Two separate images are provided for each mutant to help observe this localisation at different magnification. **(D)** Functional assays as in Chapter 2 comparing wildtype HsERD2 with the K206A-K207A double mutant. The double mutant is highly active and exhibits the same levels of retention as the wild type receptor at equivalent expression levels.

### 3.2.5 Mutation of "Dilysine Clusters" have no effect on localisation or activity of ERD2

AtERD2 and HsERD2 share 52% sequence homology including the aforementioned di-leucine motif and also two lysines just prior at position -7 and -6 from the stop codon (Figure 13A). In each homolog there is one other lysine upstream where the position is not conserved, lending themselves to being described as "lysine clusters" (Montesinos *et al*., 2014; Brauer *et al*., 2019) and drawing comparison with the canonical COPI transport KKXX motif (Jackson *et al*., 1993). In the case of AtERD2b, the three lysines (K206, K209, K210) when individually mutated to alanines had no effect on retention of Amy-HDEL (An, 2015, Silva-Alvim *et al*., 2018). To confirm localisation, again I transferred the mutants of HsERD2 into the functional fluorescent fusion format (YFP-TM-AtERD2K206A, YFP-TM-AtERD2K209A, YFP-TM-AtERD2K210A) and when infiltrated in leaves only a strict Golgi pattern was observed in all cases (Figure 13C), directly comparable to all other functional receptors. To see if lysines were actually critical to ERD2 function when in combination, the two conserved residues were mutated together in HsERD2 and then studied in functional assays. As displayed in Figure 13D, biological activity in the K206A-K207A double mutant is almost indistinguishable from wildtype HsERD2 in the dose responses at comparable GUS levels, meaning no change to function without the "lysine cluster". Similar to the single mutations in Arabidopsis, the double mutant YFP-TM-HsERD2K206A-K207A localised to the Golgi only (Figure 13C). It is clear these residues do not play an important role in ERD2-mediated retention nor do they influence the localisation of ERD2.

## 3.3 Discussion

### 3.3.1 Redistribution and dominant ER localisation occurs in receptors with a lack of biological function

The recycling model was founded from redistribution assays with ERD2 C-terminally tagged with a c-myc epitope, therefore I studied its effect alongside the FLAG and HA tag to gain a better understanding of smaller fusions. This was a large piece of research as all experiments were carried out with both Arabidopsis and human ERD2 orthologs to gain further evidence for a conserved mechanism between species. Although all three tags were roughly equal in size, the FLAG and c-myc tags were severely disruptive for both species whilst the HA tag had only a weak negative impact on biological activity. Perhaps the structural nature of HA is less obstructive to interactions with the di-leucine motif due to two proline residues keeping the epitope away from causing harm, however this is purely conjecture and any structural analysis is beyond the scope of this research. The detrimental impact of the c-myc tag is at odds with complementation assays of ERD2-c-myc (Semenza *et al*., 1990), however I have shown that at high expression levels there is residual activity which may be enough to support growth in yeast. Nonetheless, the most important outcome was the correlation between wild type activity and Golgi localisation. The functional HA fusion is entirely Golgi-localised just like YFP-TM-ERD2 with a native C-terminus, whereas the inactive c-myc and FLAG fusions have ER-Golgi dual localisations, as if the di-leucine motif were deleted or mutated, or indeed masked as in ERD2-YFP. Considering this is the case across two species, it is fair to conclude that for ERD2 to mediate strong retention of HDEL ligands, it must not visibly redistribute back to the ER, but be confined to the Golgi-apparatus. This working hypothesis will form the motivation for a number of experiments to specifically test this in chapter 4.

### 3.3.2 Receptor integrity is highly susceptible to C-terminal changes

In this chapter I have determined the functional integrity of various ERD2 constructs based on activity in secretion assays and the degree of ER localisation. Dose responses with wild type ERD2 (Figure 10, 12) show only a subtle increase in retention with increasing expression levels; the point being that very little of the

receptor is required to immediately cause a strong reduction in secretion. Given this consideration, it is at low expression levels where the effect of modification is most dramatic, as most constructs can reduce secretion to some degree if available in large quantities at the ER-Golgi interface.

At high concentrations it is evident that ERD2 with a C-terminal addition of glycine or alanine still operates to some extent. The reality at low expression levels is in vast contract to wild type ERD2 however, particularly with the addition of a single glycine which is virtually non-functional. While a single alanine addition still eventually allows for wild type levels of retention, its weaker functionality manifests itself only at lower expression levels. The difference may in part be due to the ERD2 protein sequence already ending with an alanine residue, so any C-terminal interactions may only be hindered sterically but less so biochemically, compared with the glycine. Regardless, the point here is that even the smallest of additions to the receptor C-terminus can be detrimental to function and this should be seen as a strict argument to avoid any further experiments carried out with C-terminal ERD2 fusions such as ERD2-YFP.

### 3.3.3 ERD2 function and localisation is not affected by other functional domains proposed for the C-terminus

A more or less permanent Golgi residency of functional ERD2 fusions (Silva-Alvim *et al*., 2018, this study) is at odds with its presumed necessity to recycle in COPI and COPII vesicles (Montesinos *et al*., 2014; Brauer *et al*., 2019, Aniento and Robinson, 2020). The experiments surrounding the proposed lysine cluster (Brauer *et al*., 2019) did not openly take into account that it does not form a canonical KKXX or KXKXX motif. In fact the native human and plant ERD2 C-terminus contains a KKXXXXX configuration, sporting 3 additional amino-acids beyond the consensus. It is already known that the extension of canonical KKXX by just two serines abolishes its function completely (Jackson *et al*., 1990), so the functioning of the proposed lysine cluster would have to be intrinsically coupled to the ligand-induced conformational changes of ERD2 leading to a less strict requirement for the KKXX signature, permitting not only 3 additional amino acids, but in fact an entire fluorescent protein as well (Brauer *et al*., 2019). Since C-terminal ERD2 fusions

already show ER localisation which is dependent on expression levels, microscopy alone would be a poor choice to obtain reliable data.

Having established that the Amy-HDEL secretion assays are extremely sensitive and even disclose minor changes in ERD2 activity (Figure 12), I interrogated the role of the lysine cluster in human ERD2 using this direct method to study functionality of ERD2. I failed to detect any noticeable change in activity, even when a double lysine mutant was tested (Figure 13D). As these experiments were carried out with untagged ERD2, they should have revealed an effect if the proposed lysine were essential for receptor function. Thus, localisation data supported by functional validation leaves no doubt that what I observe reflects native ERD2 behaviour.

Another issue eluding proper explanation from the crystal structure is that the last 5 amino acids are not included, which on independent inspection appears to be due to it being a region of high mobility (Brauer *et al*., 2019). This region contains the crucial di-leucine motif and by removing it may also have placed the “lysine cluster” in an unwarranted spotlight. Overall, the conclusions taken from the crystal structure regarding the ERD2 C-terminus should not be considered highly until the full data set is acquired. Validation of structural models should always be accompanied with directed mutational analysis of the native ERD2 backbone, testing its ability to mediate ligand retention, and such direct assays have been avoided in the rest of the field.

## 3.4 Conclusion

The previous chapter suggested that the true steady-state localisation of ERD2 was unknown now that supporting evidence for the recycling model containing ERD2-YFP had been disproven. For thoroughness I have further characterised the properties of redistribution by investigating the other key player of this model, ERD2-c-myc. Whilst structurally very different, the outcomes on localisation and function were consistent with ERD2-YFP results and therefore not reflective of true ERD2 function. I continued by expanding on small C-terminal additions and found that even a single glycine can severely compromise ERD2, highlighting the fragility of this domain and adding additional caution to any such modifications in the future. Finally I addressed all residues reported in connection to enabling COPI-mediated

transport and confirmed that native lysines at the C-terminus do not contribute to ERD2 function.

# Chapter 4 - ERD2 Golgi Residency is Critical to the ER Retention of HDEL Proteins

## 4.1 Introduction

The recycling model for protein sorting receptors has been extremely popular in the field because it explains how a single protein can mediate the sorting of many ligands. Whilst what I have presented in the previous chapters clearly refutes the accepted dual ER-Golgi localisation and COPI-mediated recycling of ERD2, I do not dispute the key K/HDEL receptor recognition of chaperones such as BiP and calreticulin (Lewis *et al.,* 1990, Semenza and Pelham, 1992, Denecke *et al*., 1992), which has since been verified in crystal structures (Brauer *et al*., 2019; Gerondopoulos *et al*., 2021). However, the sequential steps mediating ER retention are now much less clear (Silva-Alvim *et al.,* 2018; Robinson & Aniento, 2020) and need an investigative lead.

How ERD2 can shuttle between ligand-free and ligand-bound conformations and yet remain in the Golgi apparatus is a formidable question, and it is not surprising that the field has bias against this idea. So far Alvim and co-workers have shown that the di-leucine motif of ERD2 is not only highly conserved amongst eukaryotes but it is clearly not an ER export signal (Alvim, 2018). This was accomplished with Fluorescence recovery after photobleaching (FRAP) experiments showing that mutation of the di-leucine motif does not lead to a slower recovery indicative of a block in ER export. The premise that ERD2 may have very short periods of residence in the ER, due to unusually fast ER export to the Golgi (Robinson and Aniento, 2020) can therefore be ruled out. The only alternative explanation is that the motif prevents ERD2 from entering the Golgi to ER retrograde route. Yet it should be noted even though an ER localisation is induced, that deletion, mutation or masking of the di-leucine motif still results in a partial Golgi-localisation of ERD2. So the fact that ERD2-YFP, and YFP-TM-ERD2ΔC5 cannot be detected in any post-Golgi structures suggest that the ERD2 core has another Golgi retention signal that prevents anterograde leakage.

The presence of an independent Golgi-retention mechanism was specifically tested using the C-terminus of the type I membrane spanning plant vacuolar sorting receptor (VSR) which harbours a YMPL signal required for recycling between the Golgi and the prevacuolar compartment (Foresti *et al*., 2010, Gershlick *et al*., 2014). When the cytosolic tail of VSR was fused to ERD2 in order to replace its own C-terminus, it was still mostly found in the Golgi apparatus and failed to reach the prevacuolar compartment. This either means that the ERD2-C-terminus does not display the YMPL motif in an adequate way to trigger clathrin coated vesicle formation, or that the ERD2 core is intrinsically incompatible with Golgi-export in these vesicles.

It is also important to note that the ERD2 C-terminus is necessary but not sufficient for permanent Golgi residency. Transplantation experiments in which the ERD2 C-terminus replaced the native Vacuolar Sorting Receptor (VSR) C-terminus failed to mediate Golgi-retention (Alvim, 2018), suggesting that the di-leucine motif does not function independently. Clearly other components of the ERD2 core are involved in preventing post-Golgi trafficking and mediating adequate display of the di-leucine motif.

In this chapter I wanted to explore the Golgi retention of ERD2 in much more detail in order to set the stage for a functional analysis of ERD2. This involves a closer interrogation of the proposed cis-Golgi residency of ERD2 that remained to be proven after the initial discovery that ERD2 resides mainly at the Golgi (Silva-Alvim *et al*., 2018). In addition, I critically explored all avenues to test the influence of COPI-mediated sorting and explored alternative Golgi-retention motifs. The results clearly establish ERD2 as a cis-Golgi marker and raise questions over the proposed involvement of COPI-mediated transport in the targeting of the receptor itself. Instead, I can demonstrate via independent highly complementary experiments that Golgi residency is the key to the biological function of ERD2.

## 4.2 Results

### 4.2.1 Functional ERD2 resides at the cis-Golgi in plants and mammals

Earlier work has shown that functional fluorescent fusions of ERD2 do not completely co-localise with a sialyl transferase (ST) RFP fusion (Silva-Alvim *et al*., 2018). Since ST-RFP is known to reach the trans-Golgi (Boevink *et al*., 1998) and Amy-HDEL has been shown to mainly transit the cis-Golgi before being returned to the ER (Phillipson *et al*., 2001), it was postulated that YFP-TM-ERD2 is mainly restricted to the cis-Golgi (Silva-Alvim *et al*., 2018). The recent characterisation of a new cis-Golgi marker MNS3 (Schoberer *et al*., 2019) allowed me to test this hypothesis directly. I constructed a new MNS3-RFP fusion that contains the N-terminal cytosolic domain with the LPYS (Leu-Pro-Tyr-Ser) signal for cis-Golgi retention and the TM domain at the RFP-N-terminus.

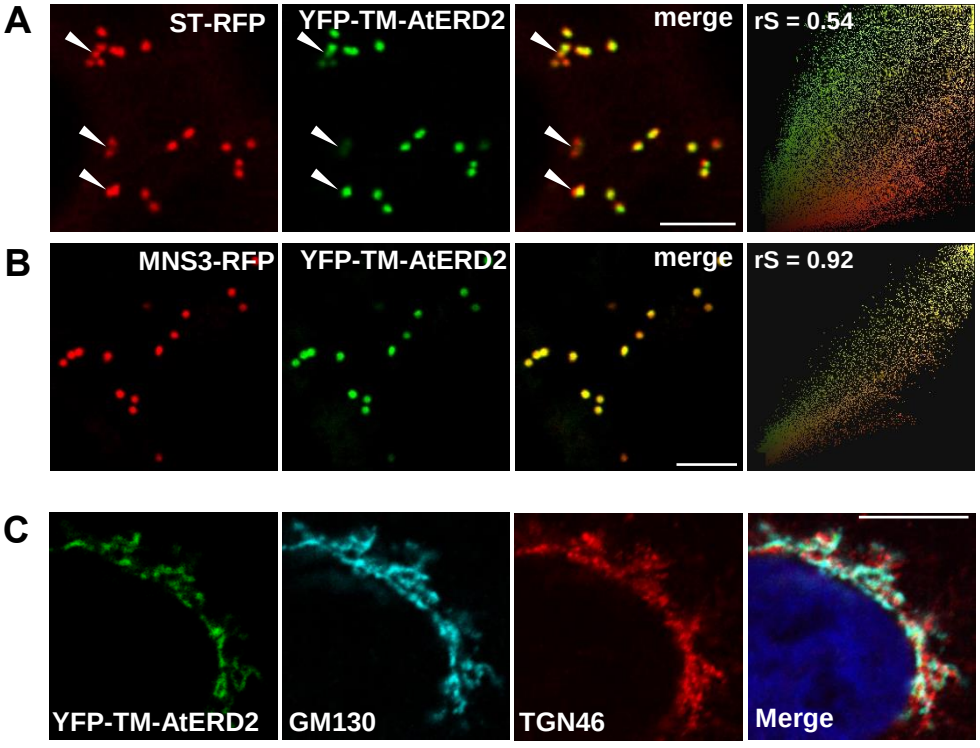


**Figure 14: Functional ERD2 fluorescent fusions localise to the cis-Golgi.**
**(A)** Comparative Golgi distribution between ST-RFP and YFP-TM-AtERD2. Although both labelling punctae, an rS value of 0.54 highlights a cis-trans Golgi segregation of YFP-TM-AtERD2 and ST-RFP, respectively. This is also visible in regions identified with white arrow heads. **(B)** When compared with the cis-Golgi marker MNS3-RFP instead, the shared cis-Golgi localisation of YFP-TM-AtERD2 is clearly demonstrated by an rS value of 0.92. **(C)** CLSM analysis at higher magnification to compare YFP-TM-AtERD2 with two different Golgi markers. Notice that the trans-Golgi marker TGN46 is clearly distinct from the ERD2-fusion and GM130 based on the red staining in the merge. Nucleus is labelled dark blue using DAPI.

Figure 14A confirms that ST-RFP partially segregates from YFP-TM-AtERD2 leading to a Spearman's correlation score of 0.54. Golgi regions with mostly red fluorescence (closed white arrow heads) were postulated to be trans-Golgi domains. In sharp contrast, MNS3-RFP almost completely overlaps with the ERD2 fusion (Figure 14B) leading to a very high Spearman's co-efficient of 0.92. This provides direct evidence that YFP-TM-ERD2 is accumulating in the cis-Golgi cisternae, the same region from which recycling of HDEL-proteins was initially proposed in plants (Phillipson *et al*., 2001).

Due to the observed conservation of ERD2 function between plants and human, the plasmid I constructed for transient expression of YFP-TM-AtERD2 in HeLa cells was used to compare its subcellular localisation with that of the cis-Golgi marker GM130 as well as the trans Golgi marker TGN46. Fixed HeLa cells probed with antibodies to either marker revealed that ERD2 is much more closely localised to GM130 in the merged panel based on the large amount of TGN46 staining alone that remains (Figure 14C). This confirms that plant ERD2 is capable of accumulating in the cis-Golgi of human cells. The results suggest that the di-leucine motif at the ERD2 C-terminus must mediate Golgi-retention via a highly conserved mechanism.

### 4.2.2 Removal of the di-leucine motif abolishes preferential cis-Golgi residency of ERD2

Having shown that removal or masking of the di-leucine motif leads to retrograde transport of ERD2 back to the ER (exacerbated further by overproduced ligands), I wanted to test if the cis-Golgi preference is also affected. For this purpose, I co-expressed MNS3-RFP with the deletion mutant YFP-TM-ERD2ΔC5. Figure 15 shows that in contrast to the wild type fusion, the deletion mutant did not completely overlap with the cis-Golgi marker. When analysing punctate structures only to avoid the additional ER staining typical for the ΔC5 mutant, a much lower Spearman's co-efficient of just 0.68 was obtained. The scatterplot illustrates that some structures are enriched for YFP fluorescence, whilst other structures are enriched mainly in RFP fluorescence.

The results suggest that deletion of the last 5 amino acids harbouring the di-leucine motif does not only lead to recycling to the ER, but it also abolishes the ability of

ERD2 to strictly co-localise with the cis-Golgi marker, leading to accidental leakage to the medial- and trans-Golgi. However, it remains clear that the deletion mutant does not progress to post-Golgi structures and there was no evidence for entirely separate structures that only contained YFP fluorescence, except for the ER. In contrast, some structures were seen that contained exclusively MNS3-RFP without YFP-TM-ERD2ΔC5 (Figure 15, closed white arrowheads), represented by red only regions very close to the X-axis in the scatterplot. Since MNS3 contains a highly efficient Golgi retention signal (Schoberer *et al*., 2019) it is possible that it displaces a Golgi-protein that has lost its cis-Golgi retention signal, simply by competitive exclusion.

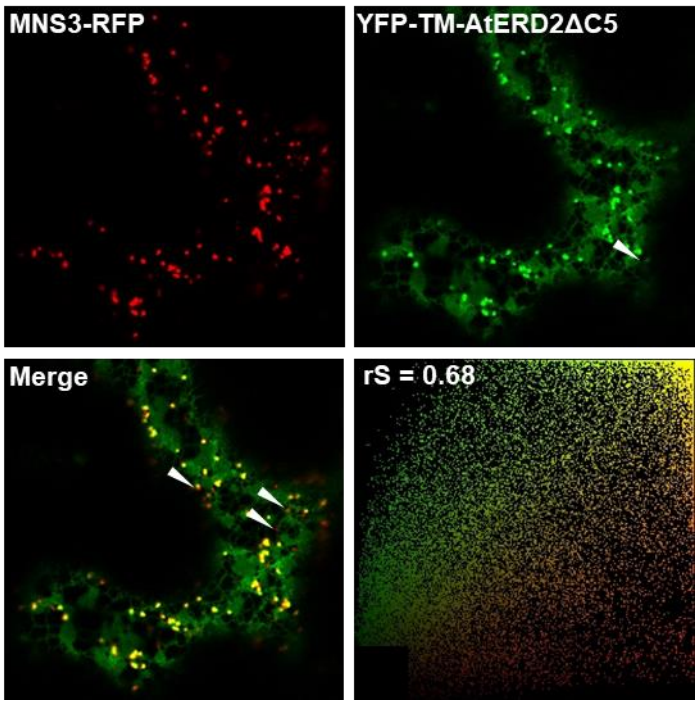


**Figure 15: YFP-TM-ERD2ΔC5 is unable to localise in the cis-Golgi to the same extent as MNS3-RFP.**

A comparison between the Golgi distribution of MNS3-RFP and YFP-TM-AtERD2ΔC5. Whilst YFP-TM-AtERD2ΔC5 is labelling some punctae alongside the ER, the rS value of 0.68 shows a larger segregation than what was observed with the functional YFP-TM-ERD2. Not only that, there are visible RFP only punctate identified with white arrow heads, which are also visualised by the red only region in the scatterplot. The green only regions are also indicative of areas in the Golgi where MNS3-RFP does not co-localise.

### 4.2.3 KKXX-mediated COPI transport is incompatible with ERD2 function

An interesting finding surrounding the localisation of MNS3 was an experiment with a chimera containing the cis-Golgi retention signal on the cytosolic N-terminus, and the HDEL signal on the luminal C-terminus, which revealed that cis-Golgi retention was dominant (Schoberer *et al*., 2019). To explore this further for ERD2, I have fused the last five amino acids of p24δ5 (KKKLI) to the ERD2 C-terminus, which generates a fusion protein that has both the di-leucine motif as well as the KKXX motif for ER retention (Figure 16A). The construct was created in the untagged form for functional studies in protoplasts, and in the YFP-TM-ERD2 configuration for subcellular localisation.

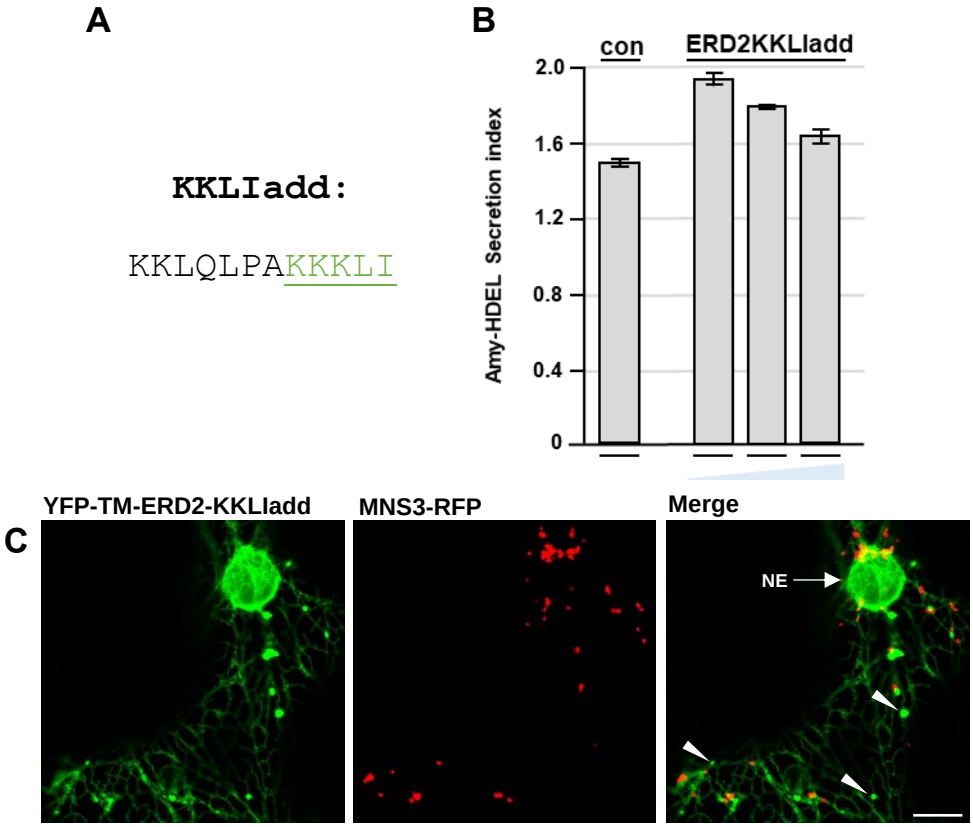


**Figure 16: Addition of the COPI KKXX motif to the ERD2 C-terminus induces HDEL secretion and punctate separate to Golgi bodies.**
**(A)** A simple diagram of the C-terminal amino acid sequence of this ERD2 mutant following the KKKLI fusion (underlined and green). **(B)** Functional dose response assay of the ERD2KKLIadd mutant compared against control conditions. At higher expression levels the induction in Amy-HDEL secretion decreases, thus the effect is seen mostly at lower concentrations. **(C)** CLSM analysis of YFP-TM-ERD2KKLIadd co-expressed with the cis-Golgi marker MNS3-RFP. This fusion is exclusively in the ER with apparent punctate forming in ER tubules, separate to cis-Golgi punctate labelled by MNS3-RFP. This separate population of punctate is clear in the merge (Closed white arrowheads). The nuclear envelope (NE) is visible in the YFP channel.

A dose-response assay with Amy-HDEL as cargo molecule revealed an unexpected mixed response (Figure 16B). At low dosage of the chimeric receptor fusion, a weak but reproducible increase of Amy-HDEL secretion was observed. This effect progressively subsided at higher dosage but never approached levels below control secretion (Figure 16B). Subcellular localisation of the chimaera in the YFP-TM-ERD2 configuration revealed a typical ER pattern with some punctate structures that were strictly ER-associated. This is evident when co-expressed with MNS3-RFP, where separate punctate representative of the Golgi are present (Figure 16C). Although small C-terminal extensions can partially compromise the Golgi retention signal (Figure 10, 12), the resulting ER localisation cannot be the only explanation for the resulting pattern. It is more likely that the KKXX signal takes precedence and does not permit Golgi-residency. However, this hybrid is not ideal for this analysis as there are too many unknowns.

### 4.2.4 An ER export signal to the Golgi can support the loss of the di-leucine motif

To avoid the constraints of the previous chimera, I explore an earlier fusion in which the 9 C-terminal amino acids of ERD2 were replaced by the equivalent C-terminal residues of p24δ5 (Alvim, 2018). This hybrid no longer contained the Golgi retention signal, and instead contains a di-hydrophobic ER export signal (YF) and a canonical di-lysine motif (KKXX), earlier verified to use both COPI and COPII-mediated transport to recycle (Contreras *et al*., 2004a,b). The resulting construct was fully ER retained and biologically inactive with respect to Amy-HDEL retention assays (Alvim, 2018). Interestingly, mutating the critical lysines (Langhans *et al*., 2008) in the C-terminal replacement construct (p24KK^SS, Figure 18C) brought the return of a Golgi-only localisation, but functional studies with Amy-HDEL assays were never carried out.

To test if the remaining COPII signal in the KK^SS could suppress the lack of a Golgi-retention signal, I subcloned the ERD2 fusion without the fluorescent N-terminal extension to the GUS reference vector for comparison in dose response assays with wildtype ERD2. Interestingly, at higher concentrations of the receptor constructs, the increase in Amy-HDEL retention was comparable between wild type and KK^SS chimaera (Figure 17B). Only at lower concentrations could a reduction

in the biological activity be observed for the chimaera. The results suggest that the introduction of the COPII signal from p24δ5 overcomes the lack of the Golgi-retention signal and resulted in one of the most biologically active chimeras so-far. I hypothesise that accelerated ER export to the Golgi can shift the steady state levels in favour of the Golgi (Alvim, 2018) and this seems enough to re-gain biological activity when the di-leucine motif is not present. Similar to the previous chapters, the data show a clear correlation between Golgi-residency and activity for ERD2, whilst COPI-mediated recycling remains fatal to biological activity.

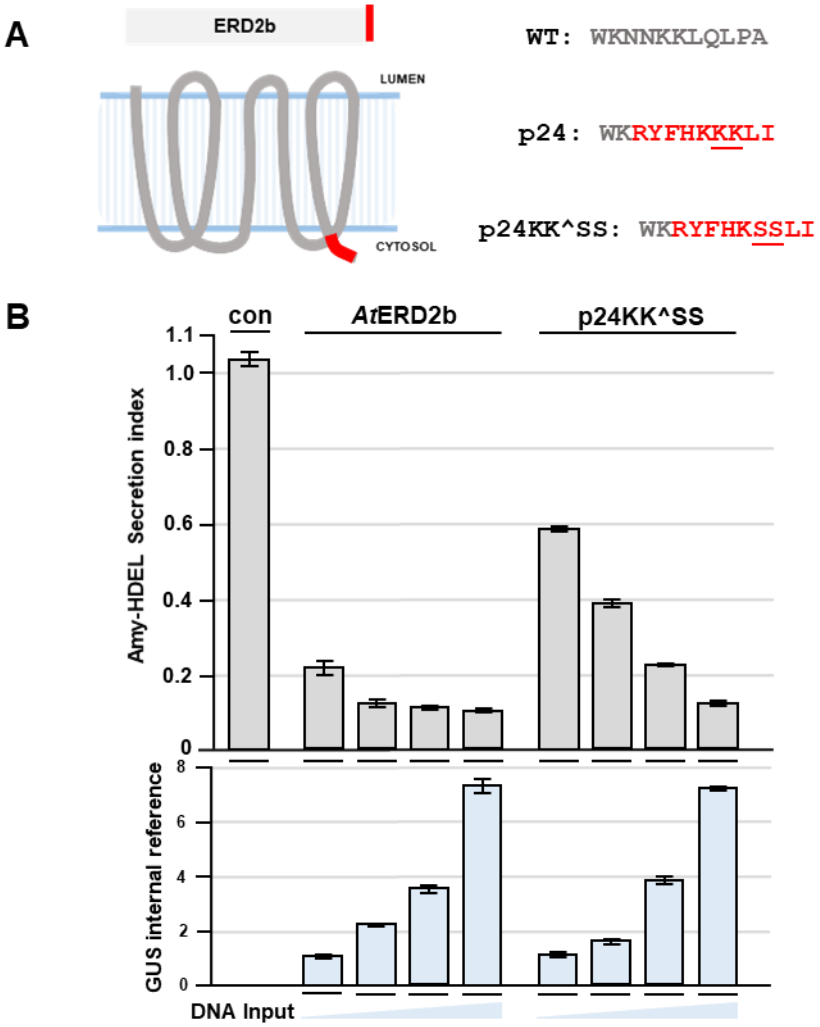


**Figure 17: A p24 COPII ER export signal (YF) boosts the biological activity of ERD2 lacking a di-leucine motif.**

**(A)** C-terminal amino acid sequences of wildtype ERD2 and two p24 variants in which the last 9 amino acids of ERD2 is replaced by the corresponding region of P24 (highlighted red). The proposed COPII ER export signal of p24 (Contreras *et al*., 2004b) is shown and the relevant lysines of the canonical COPI transport motif or the mutant serines in the KK^SS variant are underlined. **(B)** Dose-response assay measuring the influence of co-transfected C-terminal ERD2 variants (given in standard GUS OD units below each lane) on Amy-HDEL secretion. ERD2WT mediates strong cell retention whilst the P24 fusion shows no retention activity. The KK^SS mutant of the p24 fusion restores the retention activity at the highest dose.

### 4.2.5 ERD2p24KK^SS biological activity is attributable to its persistent ER export rather than Golgi retention

To exclude the remote possibility that the ERD2p24KK^SS construct created an unexpected cryptic Golgi-retention signal, I wanted to test the fluorescent configuration of the construct under conditions of HDEL saturation. I first co-infiltrated the original p24 tail fusion harbouring the wild type KKXX motif together with a dual expression construct encoding ST-CFP together with either the control cargo Amy or the test cargo Amy-HDEL (Figure 18B). RFP-TM-ERD2p24 was entirely ER-localised, regardless of the co-expression with either Amy or Amy-HDEL, confirming the absolute dominance of the KKXX signal. The visible expression of ST-CFP confirms that a suitable amount of Amy or Amy-HDEL was also expressed during these assays. However, the mutant RFP-TM-ERD2KK^SS was almost exclusive found at the Golgi apparatus when co-expressed with ST-CFP and Amy (Figure 18C), and weak ER staining could only be detected at high detector gain settings when the Golgi signals are extremely saturated (not shown). When RFP-TM-ERD2KK^SS was co-expressed with ST-CFP and Amy-HDEL, there was a noticeable increase in ER fluorescence using normal detector gain settings (Figure 18C), albeit still less intense than the Golgi bodies. This suggests that unlike wild type ERD2 which is strictly retained at the Golgi via its di-leucine motif regardless of the level of HDEL saturation (Silva-Alvim *et al*., 2018, Alvim 2018), ERD2KK^SS remains sensitive to the ligand-induced accidental leakage into retrograde transport carriers.

The results show that the introduced COPII transport signal really suppresses the lack of the Golgi-retention signal, as it provides an alternative strategy to support high steady state levels at the Golgi apparatus. In the wild type receptor, ER export does not have to be supported by specific export signals as its cis-Golgi retention signal appears to be highly effective.

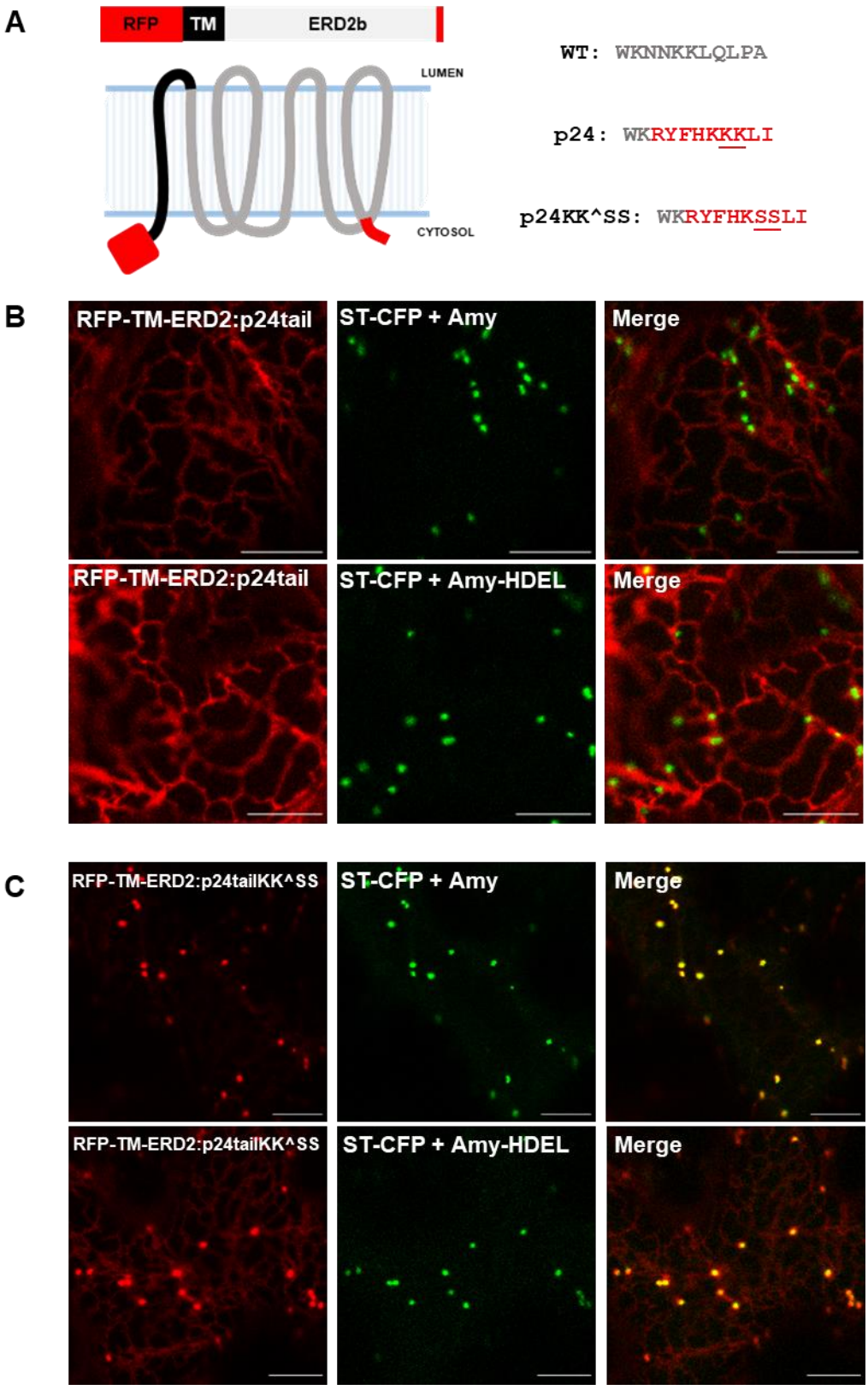


**Figure 18: The KK^SS mutant can redistribute upon HDEL overexpression and thus does not contain a Golgi retention motif**

**(A)** Schematic of the fluorescent fusions containing the two p24 variants in which the last 9 amino acids of ERD2 is replaced by the corresponding region of P24 (highlighted red).

**Figure 18: The KK^SS mutant can redistribute upon HDEL overexpression and thus does not contain a Golgi retention motif (cont.)**

**(B)** And **(C)** Localisation of p24 and KKSS chimaeras when co-infiltrated with the Golgi marker ST-CFP and either secreted Amy or the model ER cargo Amy-HDEL. The p24 C-terminus mediates complete ER localisation of the resulting ERD2 fusion regardless of Amy or Amy-HDEL co-infiltration. Meanwhile the KK^SS mutant shifts from a predominant Golgi localisation under Amy control conditions to having a partial redistribution of receptors in the ER. Golgi punctae are still highly fluorescent.

### 4.2.6 The KXD/E Golgi Retention Motif is not sufficient for ERD2 and other type I transmembrane proteins

The data so far suggest that Golgi localisation of ERD2 is critical to biological function, therefore it was necessary to establish if localisation alone is enough to support activity or whether there are other important properties associated to the di-leucine motif. This could be tested by fusing other published Golgi retention motifs to ERD2 which differ from the di-leucine motif, then observing how localisation and biological activity are affected. Such experiments may also reveal an as yet unappreciated subdomain structure of the Golgi apparatus.

The first Golgi retention motif I considered was the C-terminal KXD/E motif found in the plant EMP protein family, proposed to be necessary and sufficient for Golgi localisation (Woo *et al*., 2015). This is also known as the TM9 family proteins that contain a large luminal domain followed by 9 TM domains and a short cytosolic tail. It was shown experimentally that the KCD sequence of EMP12 had to be exposed at the C-terminus and was shown to be sufficient to redirect non-Golgi localised membrane proteins to the Golgi apparatus (Gao *et al*., 2012). It therefore appeared to be the perfect choice to test the requirement for ERD2 Golgi localisation.

I first replaced the 10 most C-terminal residues of ERD2 by the equivalent 10 C-terminal residues of EMP12, exposing the KCD at the C-terminus as in the native protein (Figure 19A). As an alternative, I fused the 10 residues to the C-terminus of ERD2, so that it may contain two Golgi-sorting signals that could potentially compete with each other, or to test if the KCD signal could rescue the masking of the di-leucine motif (Figure 19A). Unexpectedly, in both cases the fusion protein was exclusively detected at the ER. This either suggests that the KCD tetrapeptide is not sufficient to direct any membrane protein with an exposed cytosolic C-terminus (Gao *et al*., 2012), or that the ERD2 C-terminus may not be compatible

with providing the correct structural environment for KCD-display to the Golgi-retention machinery.

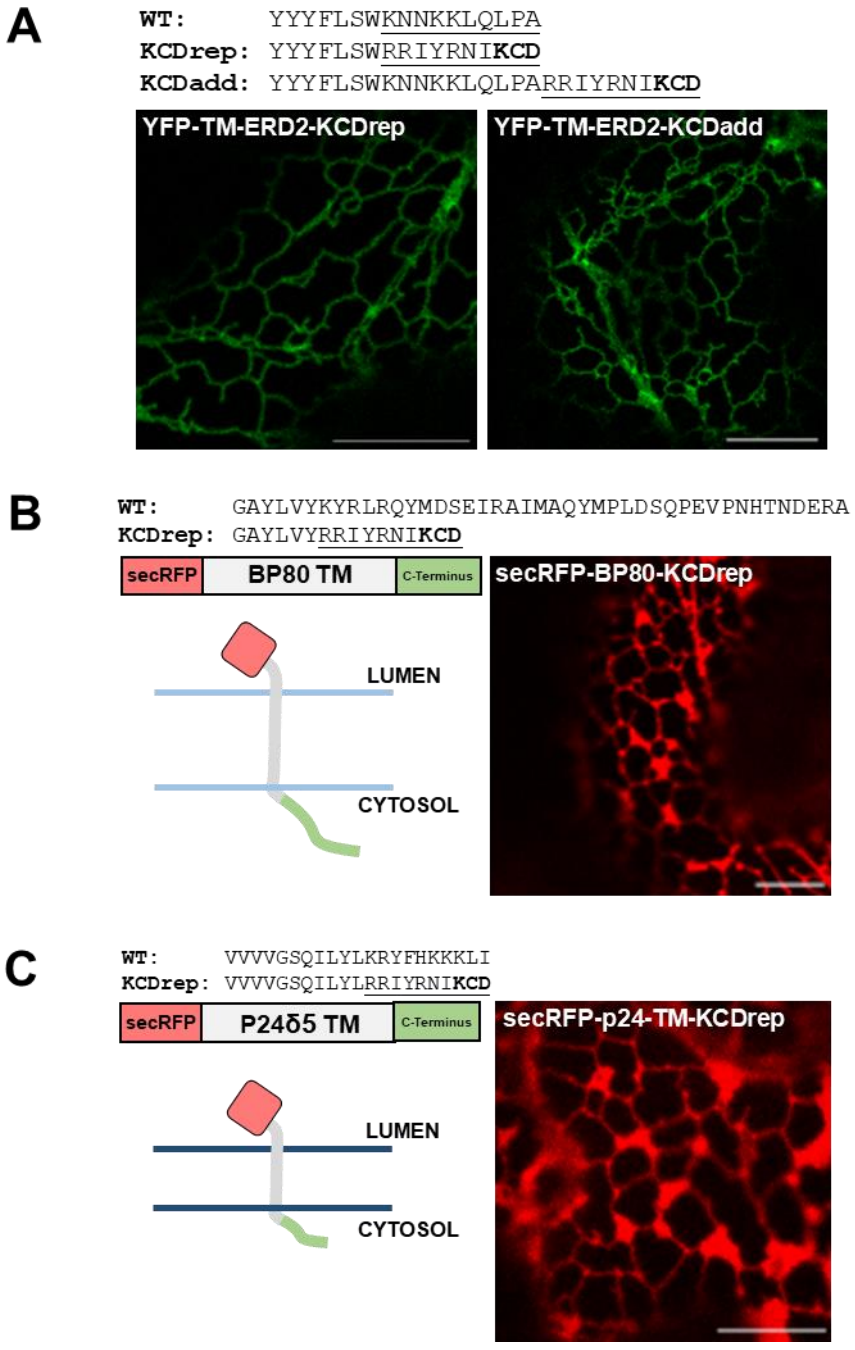


**Figure 19: The reported KCD Golgi retention motif is context dependent and does not mediate a Golgi localisation for ERD2, p24δ5 and VSR/BP80.**
**(A)** CLSM analysis of YFP-TM-ERD2-KCDrep and YFP-TM-ERD2KCDadd, with sequences provided for the C-terminus. In both cases the fluorescent fusions exclusively label ER structures. **(B)** Illustration shows the replacement at the C-terminus for the post-Golgi sorting receptor VSR/BP80 accompanied by the C-terminal sequences of wild type and the KCD replacement. This fusion is also exclusively localised to the ER. **(C)** As in **(B)** but for p24δ5. Again, a complete localisation to the ER is observed.

Even though the experiment failed, I still wanted to test the merits of the KCD signal as original proposed (Gao *et al*., 2012). For this reason I created additional fusion proteins based on the Type I membrane proteins p24δ5 (Contreras *et al*., 2004a, b) and the vacuolar sorting receptor BP80/VSR (Kirsch *et al*., 1994), both of which carry short cytosolic tails suitable for transplantation studies (Figure 19B, C) and have been used for protein targeting studies with RFP replacing the luminal domains (Langhans *et al*., 2008; Foresti *et al*., 2010). In both instances the localisation of the hybrid C-terminal replacements were exclusively in the ER. Given these results, the proposed KXD/E Golgi-retention motif (Gao *et al*., 2012) can no longer be considered as being sufficient for Golgi-retention as originally claimed and must therefore be context dependent.

### 4.2.7 An alternative Golgi-retention signal can partially re-activate ERD2-YFP and ERD2-LLGG

Although the MNS3 cis-Golgi retention motif LPYS (Schoberer *et al*., 2019) is very different from the di-leucine motif of ERD2 due to its N-terminal cytosolic location, it was an ideal candidate because MNS3-RFP co-localised extremely well with YFP-TM-ERD2. In addition the LPYS signal was shown to exhibit a strong tendency to resist redistribution into a merged ER-Golgi compartment and MNS3 is one of the earliest proteins to be visible in the reformation of Golgi-puncta after BFA wash out, with these structures recently being described as Golgi entry core compartments (GECCO) (Ito *et al*., 2018). As a type II membrane protein, the N-terminal LPYS presents itself on the cytosolic side of the membrane like the di-leucine motif. However, its position at the opposite end compared to the C-terminal di-leucine motif permitted a competition to play out two Golgi-retention signals against each other. I thus built the MNS3 N-terminus harbouring the LPYS signal by oligonucleotide self-assembly and replaced the YFP portion in YFP-TM-ERD2, yielding LPYS-TM-ERD2 (Figure 20A). The TM-ERD2 control was generated previously (Silva-Alvim *et al*., 2018). Biological activity was tested by sub-cloning into the GUS reference vector. Figure 20B confirms that the additional TM domain had hardly any effect on the functioning of ERD2, as established earlier (Silva-Alvim *et al*., 2018). The additional LPYS containing peptide resulted in a slightly stronger reduction of ERD2 activity, but the effect is still weak and could simply be

due to creating a larger fusion protein that is slightly harder to synthesize, an assumption that was earlier made for the much larger YFP-TM-ERD2 fusion. It is also possible that LPYS causes partial segregation to a slightly different cis-Golgi subdomain beyond the detection limit of my earlier subcellular localisation experiments, but this is a far more speculative scenario compared to the earlier explanation. Nonetheless, this fusion is still very active at higher expression levels and therefore suitable for testing whether Golgi-localisation alone is sufficient for ERD2 function.

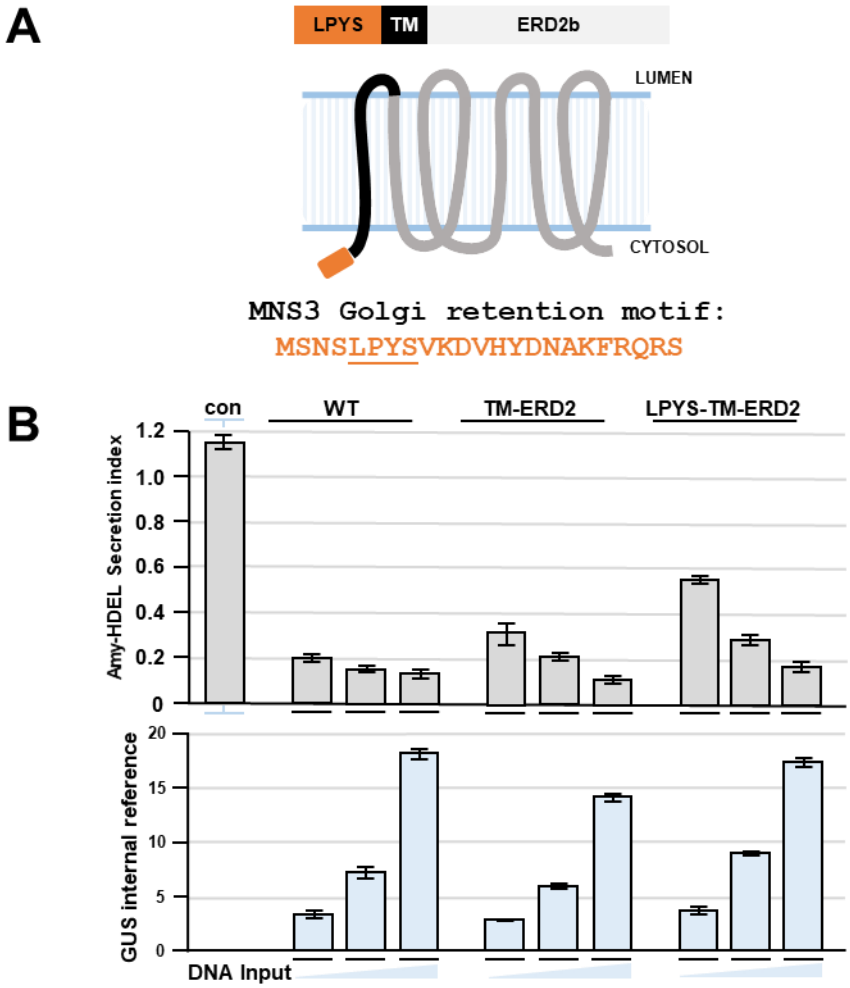


**Figure 20: ERD2 still effectively retains Amy-HDEL after the addition of LPYS at the N-terminus.**

**(A)** Schematic diagram presenting the N-terminal sequence addition to TM-ERD2b containing the LPYS motif from *At*MNS3. **(B)** Functional dose-response assays comparing the effect on activity of an N-terminal addition including the LPYS cis-Golgi retention signal, a TM domain and ERD2 alone (wt). There is a slight decrease in biological activity as the N-terminal additions increase in size, however all activity displayed is still comparable with high functioning ERD2.

The obvious constructs to determine the effectiveness of an alternative Golgi retention motif were the inactive C-terminal variants combined with LPYS, creating LPYS-TM-ERD2-YFP and LPYS-TM-ERD2-LL^GG. As a control, I also created TM-ERD2-YFP. Figure 21A shows that TM-ERD2-YFP is unable to confer increased Amy-HDEL retention, as expected due to the inactive nature of ERD2-YFP (Silva-Alvim *et al*., 2018). It was not expected that the additional TM domain would rescue activity when the di-leucine motif is masked. The fusion protein also shows the typical ER-Golgi dual localisation as observed for ERD2-YFP when expressed in tobacco leaf epidermis cells (Figure 21B). A dose response was also produced with ERD2-LLGG to show the inactivity of this construct (Figure 22) when comparing with the LPYS fusion.

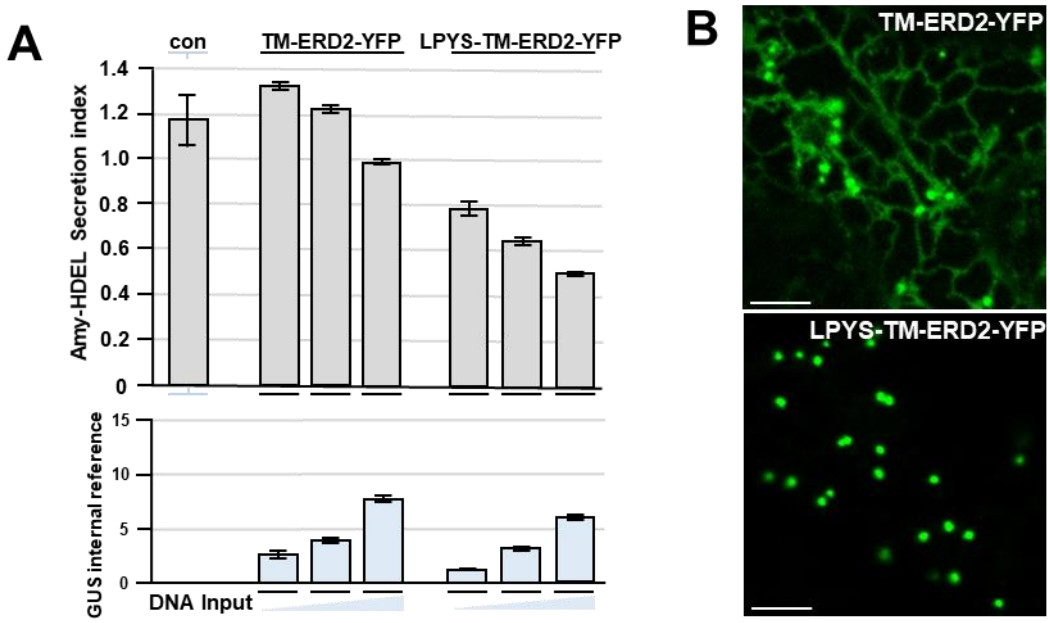


**Figure 21: Reactivation of ERD2-YFP with an ectopic cis-Golgi retention motif.**
**(A)** Dose-response assays of ERD2-YFP and LPYS-TM-ERD2-YFP. ERD2-YFP is unable to mediate retention even at higher expression levels, as previously shown. However there is a clear decrease in the S.I of LPYS-TM-ERD2-YFP. This construct still exhibits low activity relative to receptors with a native C-terminus, most likely due to masking by YFP. **(B)** TM-ERD2-YFP presents the expected ER-Golgi dual localisation similar to the inactive ERD2-YFP fusion. The N-terminal addition of LPYS causes complete retention of TM-ERD2-YFP at the cis-Golgi, in agreement with the reactivation observed in functional assays. Size bars 10 µm**.**

In sharp contrast the LPYS containing constructs were significantly re-activated despite the masked C-terminus, showing a clear dose-dependent reduction of Amy-HDEL secretion relative to the inactive controls (Figure 21A, 22A). In both cases they are much weaker than wild type ERD2, which in respect to the much larger LPYS-TM-ERD2-YFP could have been due to a resulting lower number of

synthesized molecules. It is however more likely reflective of the importance of exposing the di-leucine motif, given the same result in LPYS-TM-ERD2-LLGG. In tobacco leaf epidermis cells, LPYS-TM-ERD2-YFP was fully localised to the Golgi bodies with no detectable ER network under any condition, confirming the dominant nature of the LPYS Golgi retention signal.

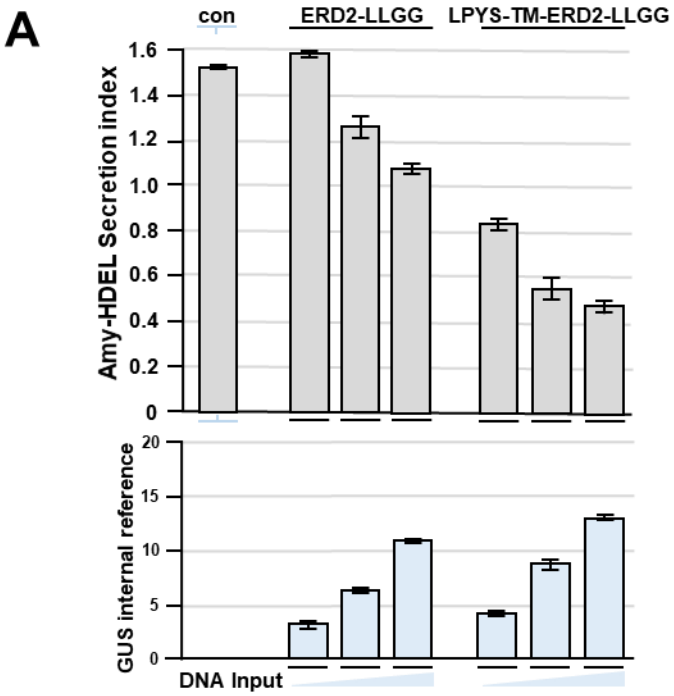


**Figure 22: Reactivation of ERD2-LLGG with an ectopic cis-Golgi retention motif**
**(A)** Same as in (Figure 21A) but comparing the mutant ERD2-LLGG with LPYS-TM-ERD2-LLGG. The ERD2-LLGG construct exhibits poor retention of Amy-HDEL comparable to ERD2-YFP in **(B)**. However by adding the LPYS-TM N-terminal domain a substantial amount of biological activity returns.

Of all the data so far, this is perhaps the most convincing suggestion that Golgi retention is critical to ERD2 function, It provides positive evidence for introducing a Golgi-retention signal in mutants where the native di-leucine motif is compromised, thus directly refuting the recycling model.

### 4.2.8 ERD2 does not persist at the Golgi under stressed conditions

As referred to earlier, GECCOs are an emerging structure in plant cells which seemingly host a sub-population of cis-Golgi membrane proteins during BFA treatment (Ito *et al*., 2018; Schoberer *et al*., 2019). These structures are thought to be Golgi remnants which offer a port of entry for ER proteins upon BFA wash out. Given the cis-Golgi localisation established for functional ERD2 it would be interesting to see how the receptor responds under the same conditions. As a control ST-YFP was co-infiltrated with RFP-TM-ERD2 and in the top panels of Figure 23A and B residencies in the frequently observed Golgi punctate are presented by both. The bottom panel of Figure 23A shows that after 3 hours of BFA treatment (50mM solution infiltrated into leaves) a complete redistribution to the ER is seen for ST-YFP and RFP-TM-ERD2 with no obvious or dominant punctate structures in either case. An interesting phenomenon observed at lower magnification was the increased staining of the vacuole by RFP-TM-ERD2 following BFA treatment (Figure 23B). The top panel shows Golgi bodies near the cell edges and then very little fluorescence elsewhere, with the focus set to capture within the vacuolar plane. Meanwhile in the bottom panel the general red fluorescence of the transformed cell is evident compared to neighbouring cells, which are dark or showing ER depending on the plane. This fluorescence in the vacuole is especially clear when compared with the YFP channel. It should be noted that YFP fluorescence is quenched in the acidic conditions of the vacuole, therefore observations for ST remain inconclusive. Nonetheless, the outcomes of BFA treatment were unexpected and did not follow suit with other cis-Golgi membrane proteins. Instead they presented a potential localisation of ERD2 in post-Golgi compartments for the first time, which would require a previously unreported mode of transport for the receptor.

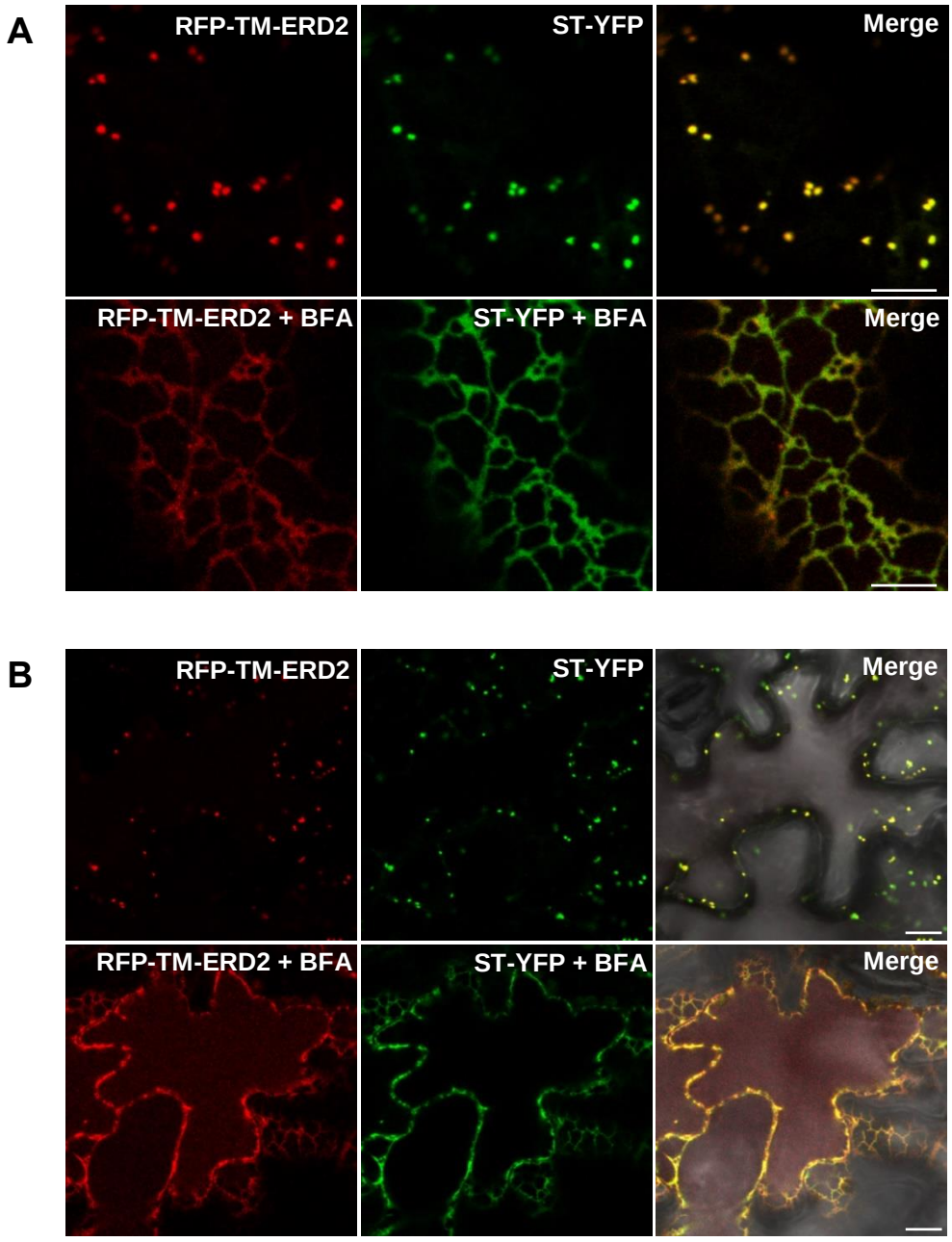


**Figure 23: The effect of Brefeldin A on the transport of RFP-TM-ERD2 and ST-YFP in N. tabacum mesophyll cells. BFA incubation for 3 hours.**

**(A)** The typical Golgi pattern is seen for RFP-TM-ERD2 and ST-YFP in the upper panel, but after a 3hr incubation with BFA both fusions have re-distributed to the ER (lower panel). **(B)** The same CLSM analysis at lower magnification. Again punctate structures can be seen for both RFP-TM-ERD2 and ST-YFP pre-incubation with BFA (upper panel). What is more noticeable in expressing cells at lower magnification is the increased vacuolar staining by RFP, which is accentuated by the dark regions of surrounding cells. Importantly, this fluorescence is not highly visible in control cells before BFA incubation.

## 4.3 Discussion

### 4.3.1 The di-leucine motif enables ERD2 to maintain a cis-Golgi localisation

Strong co-localisation with MNS3 confirmed the cis-Golgi residency of ERD2 and what remains clear is that the functional receptor is not observed in post-Golgi compartments under normal conditions. Exactly how ERD2 and other proteins are efficiently prevented from reaching post-Golgi compartments remains a mystery (Pfeffer 2007), as does a full understanding of the mechanisms that maintain the spatial polar organisation of the early Golgi stacks themselves (Lujan and Campelo, 2021). What is more telling is that masking, mutating or even deleting the di-leucine motif still does not lead to a leakage into post-Golgi compartments, meaning there must be a separate mechanism in the body of ERD2 preventing anterograde transport.

However, the co-localisation of YFP-TM-ERD2ΔC5 and MNS3-RFP has shown more than just a reduced cis-Golgi residency, as besides localising in the ER the ΔC5 mutant was also able to traverse the entirety of the Golgi. Less visibility in the cis-Golgi and additional fluorescence in the medial and trans stacks is something that only a cis-Golgi marker such as MNS3 is able to highlight. For example, co-localisations with ST have unintentionally hid such a novel finding due to its shared ability to enter the medial- and trans-Golgi. This significantly adds value to the use of MNS3 in future localisation studies as it offers an additional parameter of localisation to these compartments. Meanwhile, the reduced residency of YFP-TM-ERD2ΔC5 in the cis-Golgi may hint that this region is in high demand from sorting receptors and their chosen machinery, so any proteins lacking the assets to reserve space for identifying ligands may be forced into neighbouring compartments.

### 4.3.2 COPI transport is not suitable in conjunction with cis-Golgi retention

Whilst ERD2 function has been proven to be abolished after replacing the native C-terminus with a small stretch of amino acids containing the well characterised COPI/COPII transport signals (Nilsson *et al*., 1989, Cosson and Letourneur, 1994), these transport signals have never been studied alongside the di-leucine motif to detect a functional partnership between Golgi retention and COPI transport. A fusion of the putative KKXX motif to the native C-terminus caused a minor induction

in Amy-HDEL secretion and thus is not co-operative with ERD2 function, suggesting the native sequence is also unlikely to mediate retrograde transport. Conflicting signals at the C-terminus of this chimaera may be the reason for partial secretion, for example a small portion of receptors could remain at the Golgi via the di-leucine motif and simultaneously titrate an equal quantity of COPI coat proteins with the attached KKXX motif, reducing retrograde transport.

However the microscopy suggests that the KKLI addition is completely dominant, as no co-localisation of YFP-TM-ERD2KKLIadd is detected at the cis-Golgi with MNS3-RFP. Also, the additional punctate structures visible within the ER network have not been observed for any constructs harbouring a di-leucine motif or KKXX motif only. The generation of novel subdomains indicates that a protein hosting both signals is not compatible with the typical morphology of the ER-Golgi interface, but an analysis of ERD2 mutants in the same construct may reveal some context as to what causes them and what they may contain.

### 4.3.3 Increased Golgi Localisation improves the biological activity of retention mutants

It is apparent that the ER export signal (YF) is able to compensate for a large portion of activity lost when the di-leucine motif is removed, even if it is still less functional overall than the wild type receptor. Importantly, this construct seems capable of maintaining a predominant Golgi localisation even under saturated HDEL conditions, which is the total opposite to the other C-terminal mutants tested. This presents an almost linear correlation between the increased degree of Golgi fluorescence and increased ability to retain HDEL cargo. It also further highlights that increasing the receptor population can compensate to some degree for the reduced biological activity, considering this mutant can exhibit wild type levels of retention at higher expression, as seen for ERD2-1A (Figure 12).

Having observed how effective a di-leucine motif replacement with ER export was to biological activity, it was important to test if cis-Golgi retention by other means could also support function. Applying the Golgi retention motif proposed by Gao *et al*. (2012) onto ERD2 delivered an unexpected ER localisation across three varied transmembrane proteins put an end to this particular pursuit. Whilst it is of no interest to discredit the findings associated to the KXD/E localisation signal, my

findings seriously question the integrity of this tool as a cis-Golgi anchor. Our efforts were better placed instead by working with a Golgi retention motif identified in MNS3 (Schoberer *et al*., 2019) and in fact the outcomes were greater than anticipated. It was immediately apparent in dose response assays that the N-terminal LPYS enforced Golgi retention and this was later confirmed in the microscopy of LPYS-TM-ERD2-YFP. Most importantly, this Golgi retention motif proved sufficient for some reactivation of the non-functional ERD2-YFP and ERD2-LLGG, providing the strongest evidence so far that Golgi residency is a key component for ERD2 in mediating HDEL retention.

The fact that a Golgi-only localisation was mediated from the LPYS motif but both constructs still lacked substantial activity suggests that the context of Golgi retention via the di-leucine motif may still be more suitable to ERD2 function. This would explain the reduced activity of LPYS-TM-ERD2 which is detectable at lower expression levels, if for example a sub-population of receptors are captured by the less preferable Golgi retention mechanism mediated from the N-terminus. However investigating the separate mechanisms of the LPYS and di-leucine motif were beyond the scope of this research.

### 4.3.4 Vacuolar disposal under stressed conditions?

The emergence of GECCOs has brought an additional degree of separation to the cis-Golgi proteins localising to them. They are reportedly the earliest structure of the Golgi forming upon recovery from BFA treatment without a requirement for COPII transport and therefore made up of elements from the cis-most cisternae (Ito *et al*., 2018). My data suggests the latter to be true in the case of ERD2 localisation, however a three hour incubation with BFA eradicated any structures reminiscent of punctate unlike what is observed for MNS under similar conditions (Schoberer *et al*., 2019), therefore it is unlikely the receptor partakes in the formation of these structures.

Besides removing the possibility of ERD2 recruitment into GECCOs, the BFA results have generated new questions as to how ERD2 navigates the secretory pathway, particularly in stressed conditions. The fluorescent protein in the RFP-TM-ERD2 configuration is located on the cytosolic side of the cis-Golgi, therefore

to be visible in the vacuole but not the tonoplast means at some point the receptor must have flipped in the membrane. The most likely explanation for this is membrane internalisation at the cis-Golgi, however the reasons for this are unknown. Whether this is a BFA-specific event or a process accelerated by BFA incubation still remains unclear, but regardless the data presents a previously unreported form of trafficking and mechanism within the membrane for ERD2.

## 4.4 Conclusion

In many instances the localisation of transmembrane proteins within the secretory pathway are determined by retention and export signals (Jackson *et al*., 1993; Nishimura *et al*., 1999). The bi-directional nature of certain sorting receptors has also lead to the identification of more than one transport signal (Gershlick *et al*., 2014). In the case of ERD2, an objective identification of transport signals has been stifled by the overbearing dogma that the receptor must recycle. Here, the outcome of functional assays and CLSM has consistently shown that dominant Golgi residency enables the most effective retention of HDEL proteins, therefore not requiring ER export or retrograde transport to function. Establishing that native ERD2 maintains a cis-Golgi localisation with a single mode of signalling gives support to the conceptual problems of the recycling model that have not been discussed previously. It also paves the way for establishing a completely new mode of function, a topic which is explored in the next chapter.

# Chapter 5 - Triple helix bundles and other tools to identify ERD2-cycling machinery within the Golgi

## 5.1 Introduction

Conclusions from the previous chapters carefully considered all the previously published findings under the umbrella of biological relevance as a prime directive. The results explain how the field was systematically mislead by a very popular characteristic of C-terminal fusions, in particular those with a large fluorescent protein such as GFP or YFP. Once this conceptual difficulty was overcome, all data systematically pointed at a new mechanism based on a cis-Golgi-residency of ERD2 as prerequisite for function. Other researchers in the lab established that ERD2 does not have unusually fast ER export properties and is likely to contain a Golgi-retention signal. I could show that this is indeed the case by using an alternative Golgi-retention signal to reactivate non-functional ERD2-YFP (Figure 21). It is now time for the field to be brave; move on from the recycling model and consider a new mode of function for the K/HDEL receptor.

Whilst the field has mostly overexpressed inactive C-terminal ERD2 fusions using strong promoters in mammals and plants, subcellular localisations at Leeds were carried out with the weak TR2' promoter (Silva-Alvim *et al*., 2018 and my current work). That this is relevant was established by a collaborating laboratory at Leeds, using a Physcomitrium patens knock-in line expressing YFP-TM-ERD2 under control of its native promoter whilst the second gene was knocked out completely (Kamisugi and Cuming, unpublished). The resulting lines showed that extremely low levels of YFP-TM-ERD2 were capable of supporting multicellular growth with wild type phenotypes, but also illustrated that endogenous expression levels for ERD2 are notoriously low. This makes sense because if ERD2 is actively retained in the Golgi apparatus, its turnover should be small. It also explains why direct observation of endogenous ERD2 using antibodies has not been a main driver in the field.

The new results obtained at Leeds cause problems on two fronts, one to convince the field that a new model is required, and the second more important challenge to

identify adequate experimental approaches. In order to function as a more or less permanent Golgi-resident in low copy numbers, ERD2 would have to capture K/HDEL cargo almost instantly upon arrival. However, due to the low number of ERD2 molecules, it would have to equally rapidly release them again into a specialised sub-compartment to initiate COPI-mediated retrograde transport. ERD2 would have to recycling within the Golgi apparatus itself and switch binding-partners extremely fast.

Protein-protein interaction studies can be used to identify completely new key-players but low quantity of receptors and the transient nature of the interactions would be a formidable battle to success. I have generated an excellent bait by replacing the YFP-portion in YFP-TM-ERD2 with a small triple FLAG tag. The resulting fusion protein exhibits almost wild type activity similar to TM-ERD2 alone, and the ΔC5 variant forms the ideal control as it lacks the Golgi-retention signal (not shown). However, the advantage ends here because isolation of Golgi membranes and partial enrichment into cis-, medial and trans Golgi fractions is very challenging indeed (Parsons *et al*., 2019) and separating hypothesized subdomains within the cis-Golgi is probably beyond hope. Even if it were possible to pull down endogenous proteins from lysates, the assets required to properly identify these binders would involve specialist native separation techniques and mass spectrometry. In recent years, protein-protein interaction studies followed a protocol of extraction and immunoprecipitation, where the key elements for success are robust capture elements and predetermined co-IP candidates. However, as there is no knowledge on any functional partners associated to the new mode of function, and the di-leucine signal is only one of several elements contributing to conditional binding partner proteins, there are too many open questions at this stage to consider this approach.

Given these limitations, it seemed appropriate to build on the new information generated from the ERD2 crystal structure (Brauer *et al*., 2019) when considering new ways of creating tools to understand ERD2 function. The most impactful development was that ERD2 is composed of two THBs connected by a linker (TM4), unlike the G-protein coupled receptors it has previously been compared with. Its structure is actually much more closely related to the SWEET (sugars will eventually be exported transporter) family of membrane proteins whose main role

is to translocate sugar molecules across the plasma membrane (Tao *et al*., 2015). SWEETs are known to cycle between open and closed conformational states with respect to the cytosol and extracellular matrix during this, however the process of translocation is still poorly understood. Similarly, the crystal structure of ERD2 implies the same for when the receptor undergoes rounds of ligand-bound and -free states. It has been proposed that SWEETs likely came from gene duplication in prokaryotes, which have smaller three-TM proteins known as SemiSWEETs and can dimerise. SWEETs and SemiSWEETs only function when assembled into oligomers and in the case of plants this typically consists of hexameric trimers (Hu Xuan *et al*., 2013). Compromised sugar translocation upon the co-expression of defective and functional mutants supports the idea that monomers are dependent on one another to combine and create translocation pores large enough for sugar molecules.

The idea of ERD2 containing two THBs is completely novel and as such has not been investigated. I found myself in the fortunate position of holding a monopoly on the idea of ERD2-recycling within the Golgi, and having access to a very reliable experimental system for the identification of receptor modifications that lead to dominant-negative effects (Foresti *et al*., 2010, Gershlick *et al*., 2014). Dominant-negative mutants often help to exacerbate interactions that would normally be below the detection limit. The quantitative nature of the Amy-HDEL transport assay in protoplasts does not only permit visualisation of induced cargo retention, but it has the potential to reveal induced secretion as well, as illustrated in figure 16 (KKLI add) even though the effect was subtle. With such resources there is a natural inclination to revisit previous experiments in the literature like the mutational analyses. Here the redundant fusions and redistribution assays could be replaced with the gain-of-function validation system, as well as altered-function assays based on interference with endogenous ERD2. In fact, a full re-characterization of published mutants has almost been completed by other lab members and now requires only a small contribution from myself. No other research groups can directly quantify the influence these structures have on ER retention in vivo and in situ, so this opportunity was not to be missed.

This chapter is dedicated to elucidating the individual and combined effects of each THB in the experimental system utilised throughout this thesis. In the process I

generated novel engineered constructs which inhibited endogenous ERD2 function, possibly through competition for unknown machinery residing at the cis-Golgi. The long term aim is to generate a larger portfolio of baits and control baits for proteomic studies, which may form the basis of follow-up research.

## 5.2 Results

### 5.2.1 Isolation and analysis of THB1 and THB2 from ERD2

The triple helix bundles identified from the ERD2 crystal structure are connected by a 4$^{th}$ transmembrane domain which enables their symmetrical topology within the membrane (Brauer *et al*., 2019). In SWEET transporters TM4 must be co-expressed with the first THB (THB1) in order to mediate sugar transport whilst THB2 is preferentially left alone (Hu Xuan *et al*., 2013). As for ERD2 the 4$^{th}$ TM domain seems to be positioned more neutrally, so I have initially chosen not to include it in the isolation of either triple helix bundle.

For THB1 I amplified the sequence Met-1:Glu-91 out of AtERD2b as template, which stretches from the absolute N-terminus to the cytosolic loop between TM3 and TM4. Primers included flanking sites for sub-cloning of this sequence directly into a GUS vector for analysis in gain-of-function assays. For THB2 I isolated Glu-113:Ala-215 from the same template and employed the same method of sub-cloning for activity assays. This sequence begins in the shorter lumenal loop between TM4 and TM5 and finishes at the end of the ERD2 coding region. Additionally for THB2 I subcloned the sequence into a vector that included an N-terminal signal peptide (SP) to ensure the correct orientation of the protein. Outside the context of the whole receptor there is a risk that during synthesis of TM5, 6 and 7 the THB may flip in the membrane, however a signal peptide would prevent this. This problem could also apply to THB1, but often the membrane orientation of multiple membrane spanning proteins is determined by the first TM domain (von Heijne, 1992). In addition, THB1 navigates the N-terminus into the lumen independently when synthesised as part of the native ERD2 protein, which I hoped would also be the case here.

With these constructs I intended to determine if THB1 and 2 could oligomerise to mediate retention of HDEL cargo at the cis-Golgi even when synthesised

separately, in the same manner that SWEET transporters combine into multimers to form translocation pores at the plasma membrane. Similarly, expressing individual THBs may allow for interactions with endogenous ERD2 which may enhance or even inhibit HDEL retention if they hetero-oligomerise in the same manner as bacterial and plant SWEETs (Hu Xuan *et al*., 2013). As a control I separately expressed AtERD2b for comparison.

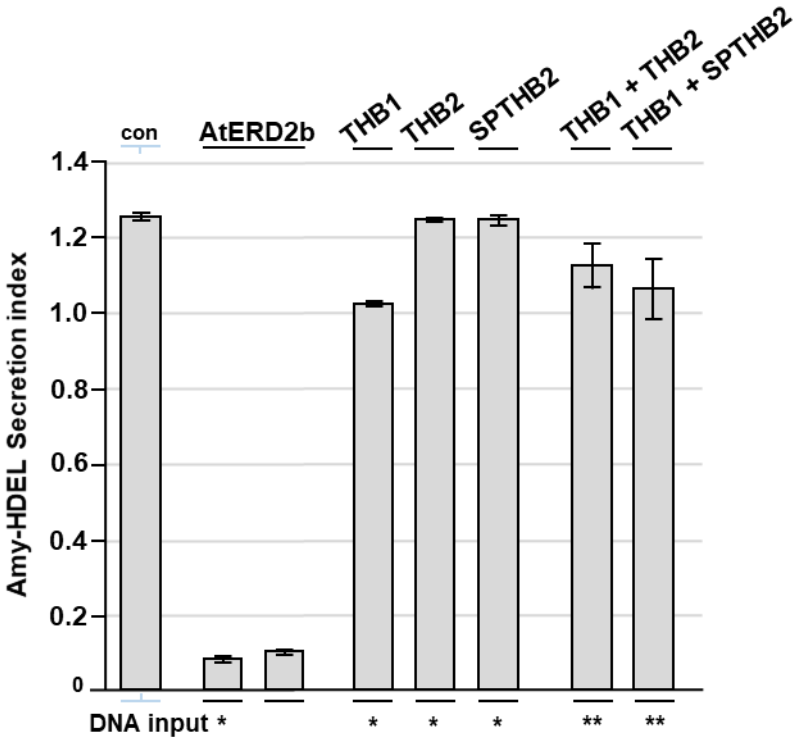


**Figure 24: THB1 and THB2 have no effect on ER retention when expressed individually or together.**

Functional assays comparing AmyHDEL retention mediated triple helix bundles. Normalised expression levels are equivalent between all constructs labelled (*) and likewise for all constructs labelled (**), hence there are two AtERD2b wildtype activity controls. THB1 causes a marginal reduction in secretion relative to the AmyHDEL control, however the difference is negligible when considering the activity of AtERD2b. Neither THB2 nor SPTHB2 are able to have any effect on AmyHDEL secretion. THB1 in combination with THB2 or SPTHB2 causes a minor but insignificant change to AmyHDEL retention.

Figure 24 shows that electroporated samples expressing either THB1, THB2 or SPTHB2 alone had no meaningful impact on the secretion index of Amy-HDEL relative to the control. Comparable expression levels are denoted by * or **. Even though there was a visible decrease in THB1, when considering how many magnitudes higher the SI is relative to fully functional AtERD2b, then the data is clearly not indicative of a biologically influential protein. When combining THB1 with

THB2 or SPTHB2 the effect on Amy-HDEL was equally unfruitful, with the SI for both combinations landing in the same range as the individual THBs.

Whilst the choices of sequences are biologically sound, it is very likely that the manner I have chosen to isolate THBs lacking any supporting structure is unsuitable for their topology within membranes. If the truncated proteins are retained in the ER, they are unlikely to offer any assistance to K/HDEL ligands in returning from the Golgi apparatus. Given ERD2 itself contains an additional TM4, some consideration should be given to the stability this may offer to the smaller subdomains.

### 5.2.2 The additions of a Golgi retention motif and an N-terminal ERP TM-domain onto THB1 allow for two separate influences on Amy-HDEL

I was not convinced that THB1 alone was a suitable construct to reflect any individual properties of this structure given the outcomes in Figure 24. There is the possibility that THB1 is at risk of flipping in the membrane when it is without the linker TM and THB2, or it may be unable to permanently reside in the Golgi without a Golgi retention motif. Earlier deletion experiments also suggested that individual TM domains of ERD2 were unable to mediate stable membrane insertion, with the exception of additional TM domain of ERP1 which also dictates a cytosolic N-terminus (Silva-Alvim, unpublished). I thus decided that adding this TM domain from ERP may help anchoring THB1 in the membrane in such a way that its topology is identical to when it is part of the native ERD2 structure. Not only that, the TM addition also enables the N-terminal addition of the LPYS Golgi retention motif from MNS3 for adequate exposure in the cytosol, which might cause separate properties again if TM-THB1 and THB1 alone do not localise to the Golgi.

I thus built TM-THB1 and LPYS-TM-THB1 to test in our gain-of-function assays and the outcome was much more encouraging compared to expression of THB1 alone. Figure 2 shows that TM-THB1 leads to a mild but dose-dependent gradual increase in Amy-HDEL retention correlated with increased expression of the chimeric construct, which reduces cargo secretion by almost 50% at the highest expression levels. The same decrease in Amy-HDEL secretion is seen for LPYS-TM-THB1, albeit it at a slightly steeper rate when comparing dose responses (Figure 25A).

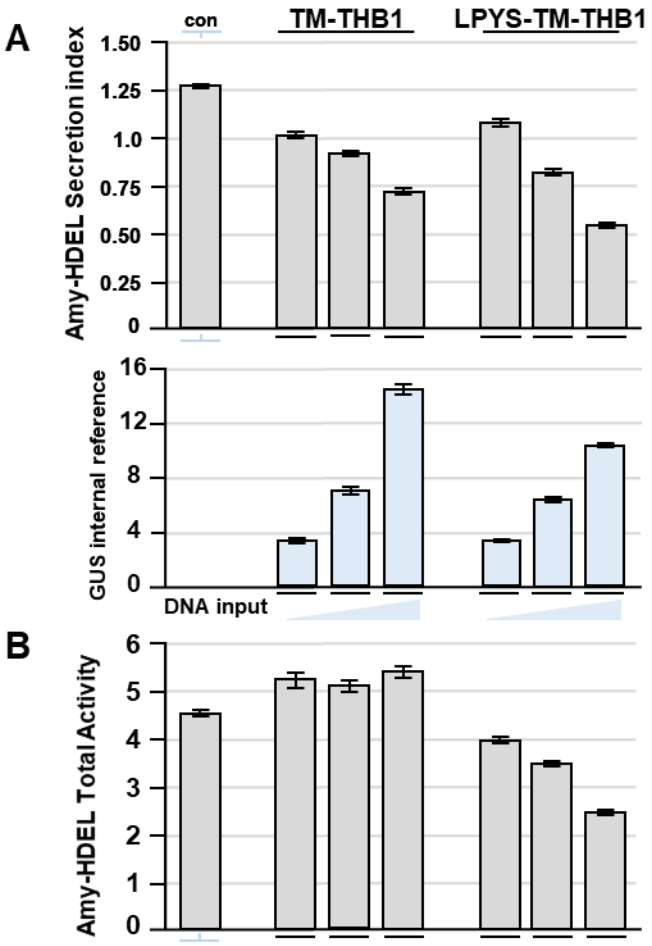


**Figure 25: A TM domain addition at the N-terminus of THB1 with and without a Golgi retention signal causes different effects.**

**(A)** Dose response assays measuring Amy-HDEL retention when co-expressed with TM-THB1 and LPYS-TM-THB1. Equivalent decreases in the SI are seen for each, but a steeper response is seen for THB1 provided with a Golgi retention signal (LPYS). GUS activity between TM-THB1 and LPYS-TM-THB1 is similar therefore expression levels are comparable in dose responses. **(B)** The total Amy-HDEL activity for samples in each of the dose responses, which are presented as in **(A**). Total activity is the combined amylase activity in cell samples and medium samples from one individual electroporation, which is calculated when determining the secretion index. The total activity for TM-THB1 remains consistent and comparable with the Amy-HDEL control throughout the dose response. However as LPYS-TM-THB1 from the beginning and as expression levels increase, there is a clear reduction in the total activity of Amy-HDEL in this dose response.

On the secretion indexes alone each response appears quite similar, yet when inspected further there is an obvious difference between the total activities of Amy-HDEL (Figure 25B). The total activity (TA) is determined by combining amylase activities from cell samples and medium samples generated in one individual electroporation, which are primarily used to calculate the secretion index. In contrast to TM-THB1, the presence of the Golgi-retention signal in LPYS-TM-THB1 leads to a very clear reduction in the total yield of Amy-HDEL. The gradual

decrease of Amy-HDEL occurs in both the cells and medium, which is why the effect originally goes undetected in the secretion index. Nonetheless, this additional effect on total activity may be specific to THB1 that is forcibly retained in the cis-Golgi, which would also imply that TM-THB1 localises in a separate manner.

### 5.2.3 The effect of LPYS-TM-THB1 may be related to the BFA-like effect of overexpressed full length ERD2

The reduction of Amy-HDEL total yield by LPYS-TM-THB1 was reminiscent of effects observed earlier by a previous lab member. This was when comparing the SI and TA for Amy-HDEL and the control cargo Amy when co-expressed with ERD2. Not only did Amy-HDEL systematically underperform relative to Amy when it came to TA, but the effect appeared to be related to ERD2 expression because ERD2-knockdown in protoplasts by anti-sense inhibition then boosted Amy-HDEL yield whilst having no effect on the control cargo Amy (Alvim, 2018). Moreover, ERD2-overexpression was previously shown to cause a Brefeldin A-like effect in mammalian cells (Hsu *et al*., 1992), caused by an exacerbated recruitment of ARF1-GAP and release of COPI complexes from the Golgi apparatus (Aoe *et al*., 1997). This was recently substantiated by demonstrating that ERD2 overexpression also causes a redistribution of the GTPase ARF1 from Golgi membranes to the cytosol (Alvim, 2018).

I therefore tested the influence of drastic ERD2 overexpression on either Amy or Amy-HDEL. Figure 26 shows that constitutive secretion of Amy is compromised when ERD2 is drastically overexpressed. This is accompanied by a mild reduction in the total activity. This effect is normally not detected, because our gain-of-function assays require only low levels of ERD2, and were originally developed to avoid disintegration of the Golgi apparatus (Silva-Alvim *et al*., 2018). When Amy-HDEL was tested, the reduction of the secretion index is stronger as it occurs with much lower ERD2 concentrations already, but the effect on the total activity is clearly stronger than for Amy.

It was originally suggested that HDEL-cargo may follow a route to degradation that is not available for constitutively secreted cargo such as Amy, and may be part of a quality control mechanism that operates when ER stress leads to increase recycling of HDEL proteins in general (Alvim, 2018). The current data appear to

support this model. Therefore it is possible that LPYS-TM-THB1 may also influence the COPI machinery or endogenous receptors located at the cis-Golgi.

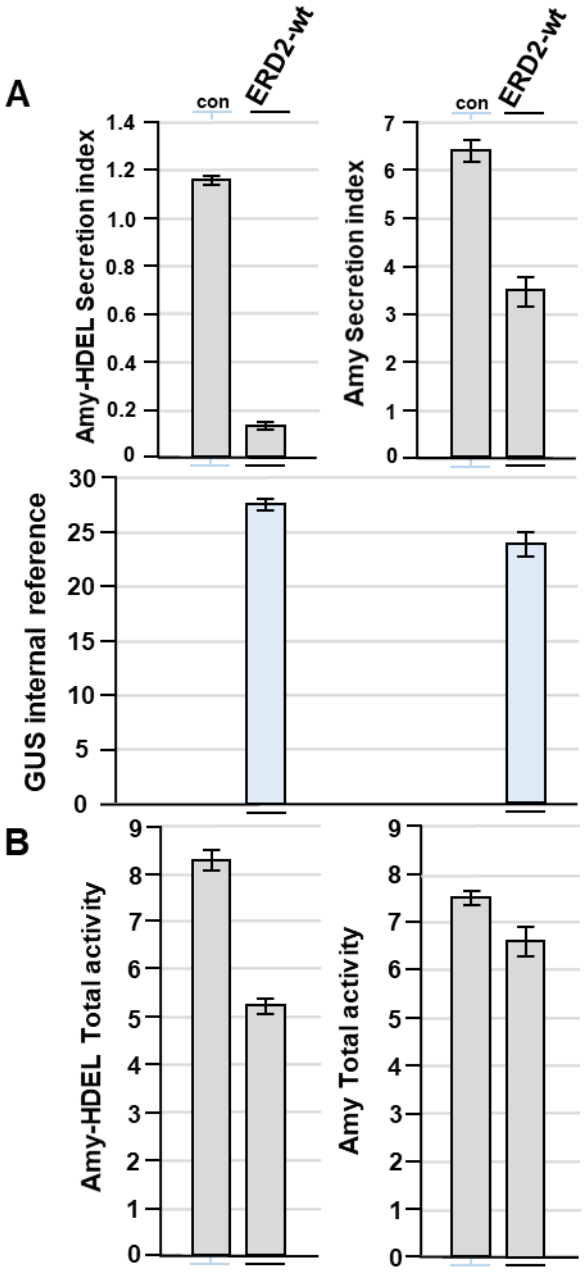


**Figure 26: ERD2 overexpression reduces the yield of Amy-HDEL and the constitutive secretion of control cargo Amy.**

**(A)** Individual high doses of wildtype ERD2 co-expressed with Amy-HDEL (left), or control cargo Amy (right). Notice the exceedingly high GUS levels representing ERD2 overexpression. Amy-HDEL secretion is reduced to levels expected for wildtype ERD2, whilst Amy secretion is reduced by approximately 50% compared to the control. **(B)** The total Amy-HDEL activity (left) and total Amy activity (right) with and without an individual high dose of wildtype ERD2. Notice the large reduction in total activity for Amy-HDEL, whilst the effect on Amy activity is much smaller.

To test if LPYS-TM-THB1 expression also influences the two cargoes differently, I repeated the previous experiment with Amy-HDEL and Amy. The effects so far caused by LPYS-TM-THB1 were visible at lower expression levels than what was tested for wildtype ERD2, therefore I opted for lower expression levels in this experiment too.

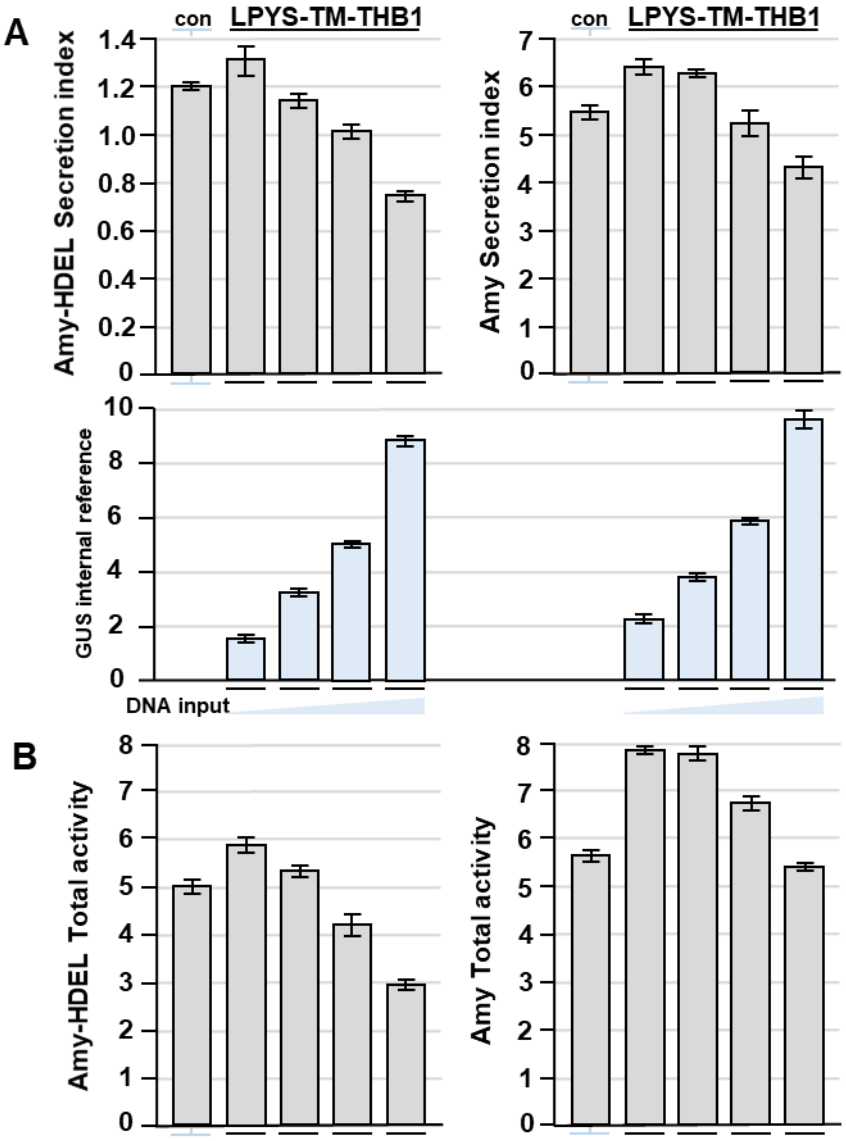


**Figure 27: LPYS-TM-THB1 has a similar influence to ERD2 overexpression on the secretion index and total activity of Amy-HDEL and Amy.**
**(A)** Comparable dose-response assays expressing LPYS-TM-THB1 with ER cargo Amy-HDEL (left) and secretory cargo Amy (right). In both cases cargo secretion is reduced but the effect is greater for Amy-HDEL compared to Amy, with a reduction of almost half and then less than a quarter, respectively. **(B)** The total activity of Amy-HDEL (left) and Amy (right) across both dose responses with LPYS-TM-THB1. Whilst the total activity of Amy-HDEL reduces by over a third, the total activity of Amy clearly increases and is then comparable to control levels at the highest expression levels of LPYS-TM-THB1.

Figure 27A shows that the effect on the secretion index for each cargo is similar when compared to control conditions where cargo is expressed on its own, but slightly more intense for Amy-HDEL. However, whilst LPYS-TM-THB1 expression progressively leads to a reduction in the total yield of Amy-HDEL, the yield of Amy was induced except for the highest expression levels of LPYS-TM-THB1 where it was comparable to control conditions (Figure 27B). This means that in addition to a BFA-like effect, Golgi-retained THB1 may be responsible for triggering a pathway for the increased degradation of HDEL-proteins but not constitutive secreted cargo. THB1 could play the same role when part of the native ERD2 molecule.

### 5.2.4 YFP-TM-THB1 produces BFA-bodies

The localisation of THB1 is yet to be determined and as I've shown in previous chapters the method of tagging can influence this, therefore a panel of provisional modifications were tested. As a first attempt I directly fused RFP to the N-terminus of THB1 but could not generate suitable levels of expression in leaf infiltrations (data not shown). It has been found previously that N-terminal ERD2 fluorescent fusions are trapped in the ER due to flipping in the membrane (Silva-Alvim *et al*., 2018), which may also be the case for THB1 and THB2. Cleavage of the fluorescent protein or faster degradation of the THBs could thus explain why these constructs were difficult to detect.

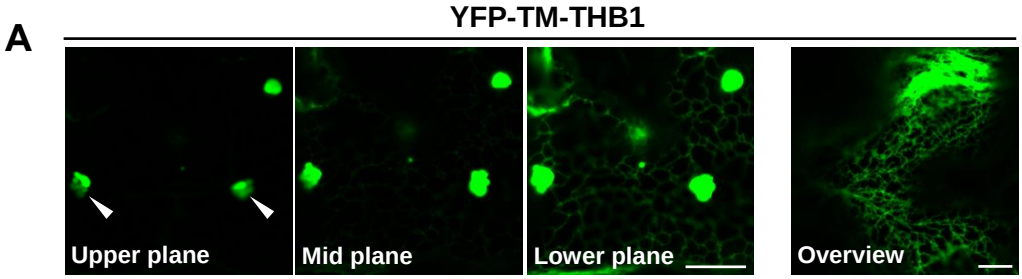


**Figure 28: Localisation of YFP-TM-THB1 in the ER and BFA bodies.**
**(A)** CLSM analysis of the fluorescent fusion YFP-TM-THB1. Notice in the first three panels a cluster of punctate structures reminiscent of Golgi bodies, which is most visible in the upper plane (closed white arrowhead). As the visual plane enters further into the cell the ER becomes visible and the cluster becomes less define (mid plane, lower plane). An overview at lower magnification shows that YFP-TM-THB1 localises mainly to the ER and cannot be seen in single Golgi bodies.

Next I replicated the biologically active ERD2 fluorescent fusion structure to create YFP-TM-THB1 (Figure 28A). This yielded much better expression levels, with the

construct being localised mostly in the ER (overview, Figure 28A). More interesting however was the detection of novel structures appearing to be clustered Golgi bodies. The upper plane (Figure 28A) presents individual Golgi bodies at the top of the cluster before the fluorescence signal is quickly saturated in lower layers. Saturation is also maintained with the ER in the field of view. I have observed these structures previously in cells saturated with biologically active ERD2 fusions (data not shown), leading me to theorise that they may be indicative of an intermediate BFA effect. It should be noted that only a small portion of YFP-TM-THB1 is likely reaching the Golgi based on the data for TM-THB1, which shows it to be a much less disruptive protein compared to LPYS-TM-THB1. Nonetheless the effect TM-THB1 is having on Golgi bodies can still be indicative of the behaviour of LPYS-TM-THB1. As the BFA-like effect was not of main interest to me, further experiments on this topic (i.e. construction of LPYS-TM-THB1-YFP) were not prioritised, which will become clear after presenting data on the second domain of ERD2, the THB2 (see below).

### 5.2.5 LPYS-TM-THB2 causes a strong induction in Amy-HDEL secretion

After seeing the benefits an additional ERP TM domain and LPYS Golgi retention motif has on the ability for THB1 to influence Amy-HDEL secretion, it was obvious to test the same parameters with THB2, so I constructed TM-THB2. Additionally I wanted to test TM4 from ERD2 itself, to see if this would create a more native context. Unlike the individual TM domains of the two THB domains, TM4 stands out as it provides an independent inversion loop within the membrane to create the THB dimer. Figure 29 compares the effect of THB2 alone with the effect of the two fusions with additional TM domains. TM4-THB2 expression caused a mild induced secretion of Amy-HDEL. For TM-THB2 this effect was marginally stronger, perhaps offering slightly higher stability of the fusion protein compared to that offered by TM4, however the differences were really minor. Addition of the LPYS signal however caused a very strong induction of Amy-HDEL secretion, revealing a staggering three-fold increase in the secretion of Amy-HDEL. In contrast to the earlier two constructs, the secretion index continued to increase with higher effector dosage. This can only be explained by a dominant-negative interference with endogenous ERD2, and it is remarkable because it exceeds that of ERD2

knockdown itself in transient assays (Silva-Alvim *et al*., 2018). This sparks questions in terms of its relevance to ERD2 function, it presents a completely new "altered-function" phenotype in our Amy-HDEL secretion assays, and it could lead to interesting tools for future work.

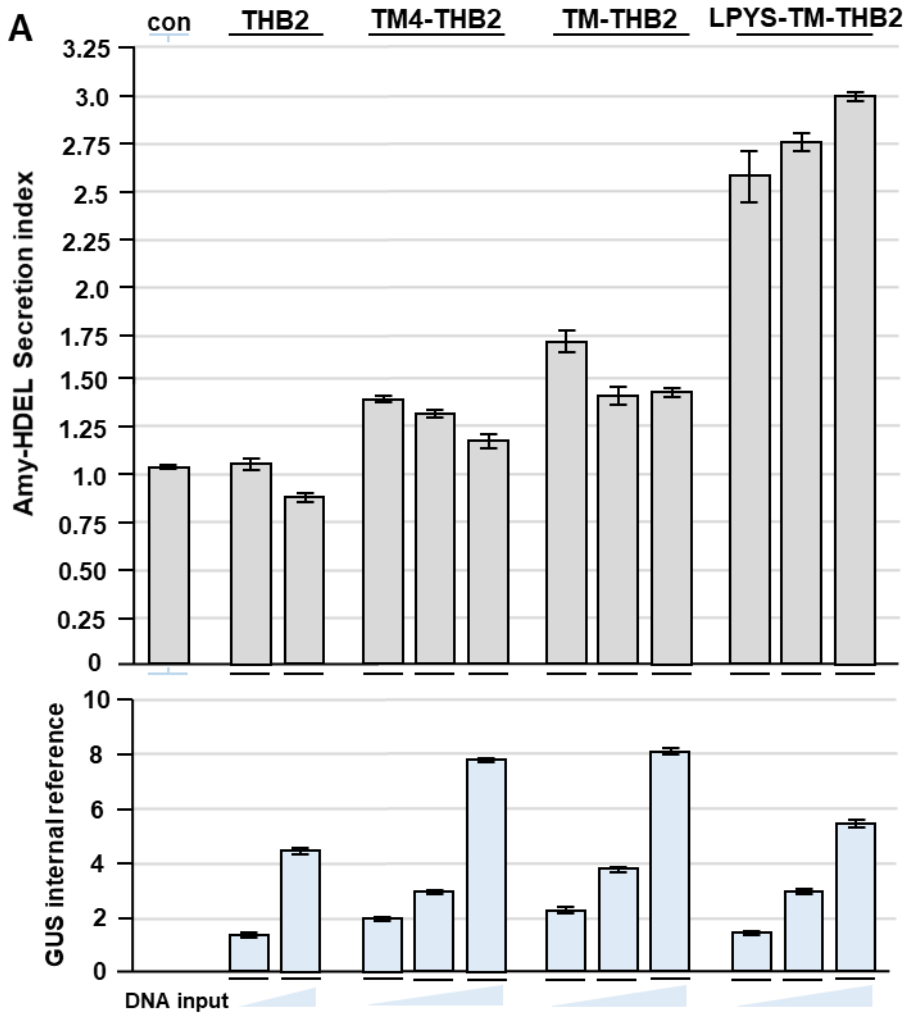


**Figure 29: TM domain additions at the N-terminus of THB2 cause a staggering induction in secretion when combined with a Golgi retention signal.**
**(A)** Dose response assays comparing Amy-HDEL retention when co-expressed with THB2 alone, TM-THB2, TM4-THB2 and LPYS-TM-THB2. Again no effect is seen for THB2 alone, however a small induction in secretion is seen when THB2 is given an N-terminal TM domain from ERP and slightly less so with the native TM4 from ERD2. In the final dose response the addition of LPYS and the ERP TM causes a 3-fold induction in secretion of Amy-HDEL.

### 5.2.6 The C-terminus of THB2 is not responsible for the induction in Amy-HDEL

Given the importance of the di-leucine motif to the Golgi-localisation and function of ERD2 and the importance of the LPYS signal in revealing the effect of THB1 on Amy-HDEL yield, it is reasonable to assume that the induction caused by THB2

could be competitive inhibition of the interactions usually taking place with the ERD2 C-terminus during ligand hand-over. To assess if this was the case or if THB2 is engaging with a different mechanism, I removed the last 5 amino acids generating the construct LPYS-TM-THB2(ΔC5) and compared it with the full length THB2 in a dose response assay (Figure 30). Whilst the dose response is slightly more staggered for LPYS-TM-THB2(ΔC5), its effect on Amy-HDEL is very comparable and the induction caused by both constructs is 3.5-4-fold at the highest concentration. There were also no differences in the total activity from either construct even at the high expression levels (Figure 30B). The results clearly suggest that the LPYS-TM-THB2 must be titrating a machinery component that supports ERD2 via another aspect of its cycling between receptor conformations and not Golgi-retention per-se.

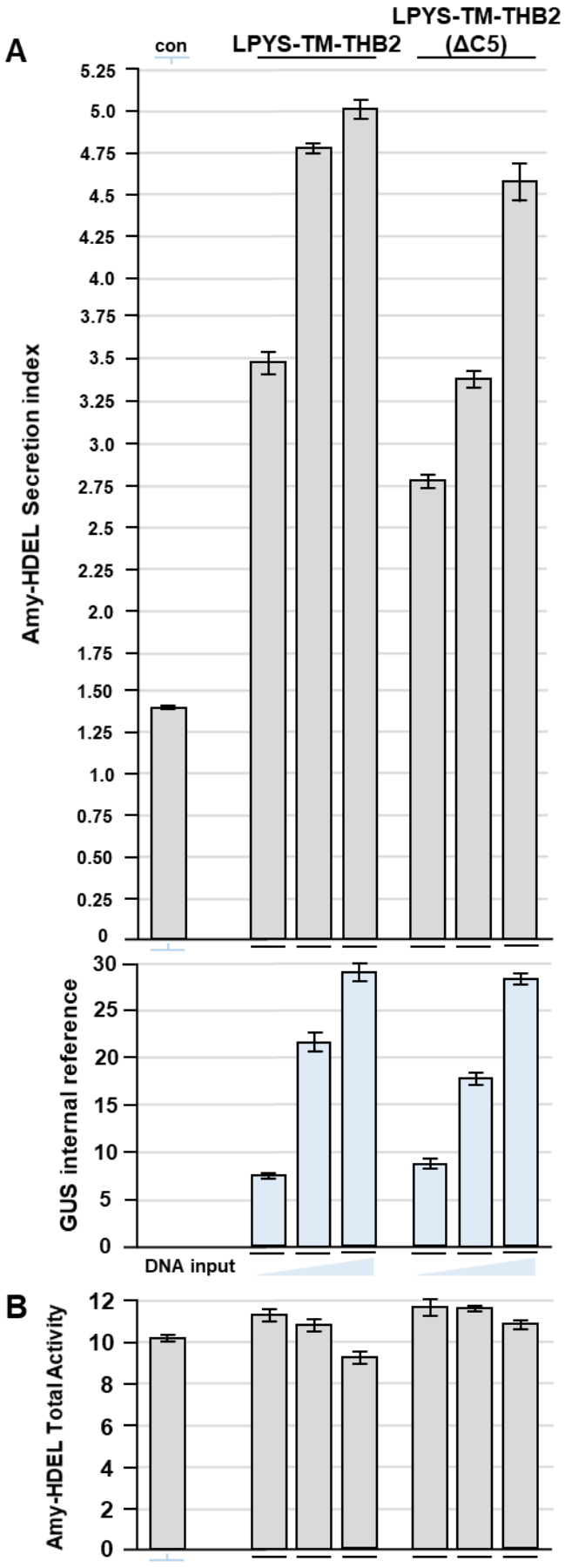


**Figure 30: the di-leucine motif is not required to cause an induction in Amy-HDEL secretion.**
**(A)** Comparable dose response assays of LPYS-TM-THB2 and LPYS-TM-THB2(ΔC5) confirms that the di-leucine motif nor the C-terminus is necessary to induce a three-fold increase in Amy-HDEL secretion. **(B)** The total activity is not effected in either dose response.

### 5.2.7 THB2 does not independently localise to the Golgi

THB2 was also localised with fusions where YFP-TM- and RFP-TM- were applied to the N-terminus after the improved response seen for THB1. This meant co-localisations with different markers could be tested and also allowed for the identification of any potential influences different fluorescent proteins may have.

When co-expressed with the cis-Golgi-marker MNS-RFP (Figure 31A), YFP-TM-THB2 appeared exclusively in the ER. This was especially noticeable by the lack of overlap with MNS3-RFP. Not only that, the fluorescence of YFP-TM-THB2 was weaker throughout all samples, suggesting that the protein was not well expressed.

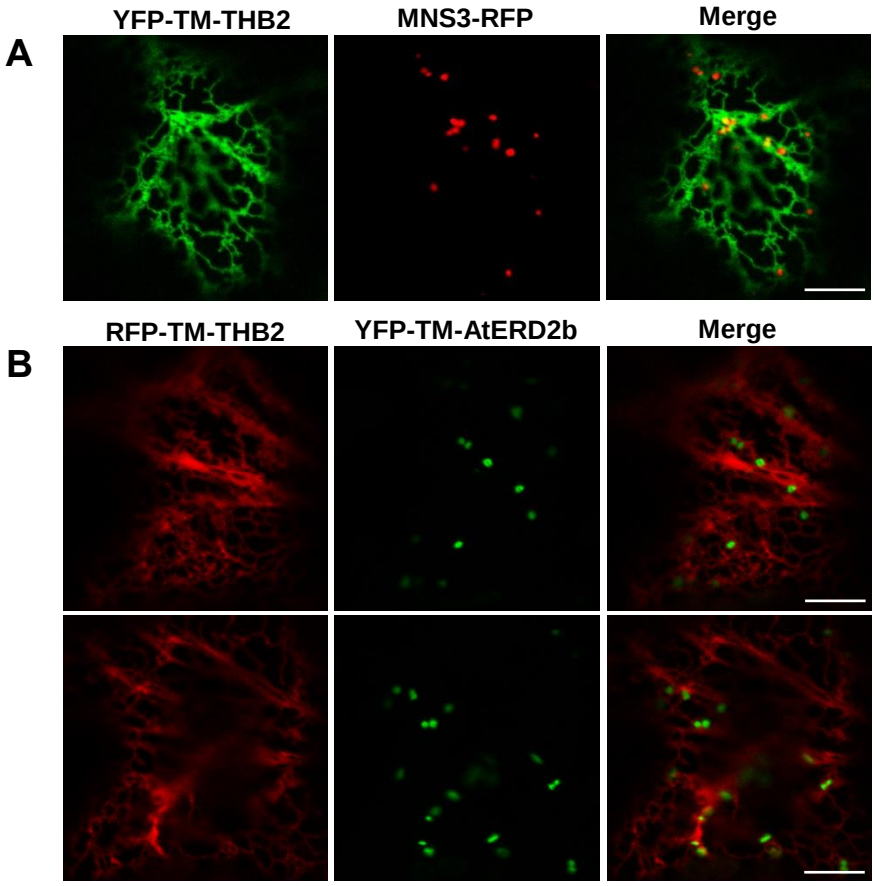


**Figure 31: Localisation of THB2 following the addition of an N-terminal ERP TM domain and fluorescent proteins.**
**(A)** CLSM analysis of YFP-TM-THB2 co-expressed with MNS3-RFP. In this case THB2 only localises to the ER and punctate structures are not visible. MNS3-RFP resides exclusively in Golgi punctate. Notice no co-localisation in the merge. **(B)** Co-expressed RFP-TM-THB2 and YFP-TM-AtERD2b. RFP-TM-THB2 is strictly localised in the ER and does not co-localise at all with YFP-TM-AtERD2b, as seen most clearly in the merge.

Similarly RFP-TM-THB2 completely localised to the ER when co-expressed with YFP-TM-ERD2 (Figure 32B), which itself exhibited the typical Golgi-only residency. Again, expression was weak for the THB2 construct. Thus THB2 is unable to mediate a predominant Golgi localisation independently. Perhaps an adequate display of the C-terminal di-leucine Golgi-retention signal requires interactions between THB1 and THB2 as well as ligand-interactions, none of which will be present when THB2 is expressed individually. This would explain why the addition of LPYS was crucial in revealing the altered-function properties leading to an induced secretion of Amy-HDEL.

### 5.2.8 LPYS-TM-THB2-YFP does not induce the secretion of Amy-HDEL

Even though I have shown previously that the LPYS motif transplants successfully onto other proteins, it is still important to validate Golgi retention for THB2 if this is to be the reason for the effects it mediates. As a research group we have repeatedly advocated that fusion proteins should be functionally validated following modification, therefore I first tested the LPYS-TM-THB2-YFP fluorescent fusion in our gain-of-function assays (Figure 32A). Given the last five amino acids of THB2 were not important for the induced Amy-HDEL secretion, it was quite a surprise that when a C-terminal YFP was added instead the induction effect was completely abolished, to the extent that even a reduction of Amy-HDEL secretion was observed. Yet when visualised in protoplasts (Figure 32B), the LPYS signal was clearly exposed at the cytosolic N-terminus because a Golgi localisation was enforced for the chimera. This further strengthens the argument for how important robust validation systems are when working with modified proteins. Since LPYS-TM-THB2ΔC5 actually caused the same induced Amy-HDEL secretion as LPYS-TM-THB2, the failure of the C-terminal YFP fusion to function in that way can only be explained by steric hindrance from the bulky fluorescent protein that prevents interaction with an ERD2 machinery component not specifically associated to Golgi-retention. At this stage all further work was to be carried out with LPYS-TM-THB2 to complete its characterisation.

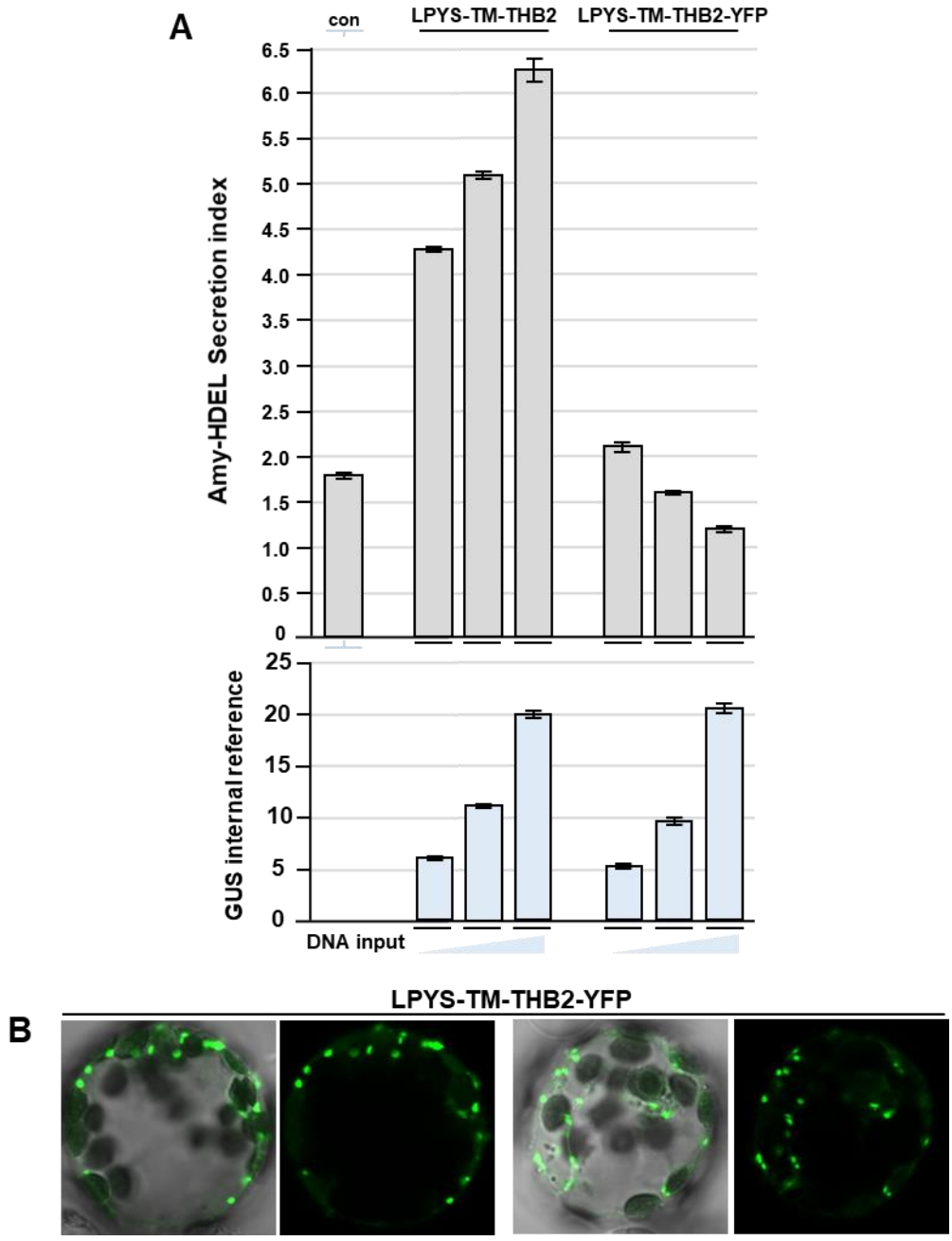


**Figure 32: A C-terminal YFP addition to LPYS-TM-THB2 abolishes the induction in Amy-HDEL secretion.**

**(A)** Dose response assays comparing Amy-HDEL retention when co-expressed with LPYS-TM-THB2 and the fluorescent LPYS-TM-THB2-YFP. Expression levels across the dose response are more than triple that in figure 29 which appears to cause an even steeper induction of secretion by LPYS-TM-THB2. However by fusing YFP to the C-terminus this effect is completely neutralised. In fact high concentrations of LPYS-TM-THB2-YFP even caused a minor reduction in the SI. **(B)** CLSM analysis of LPYS-TM-THB2-YFP expressed in N. benthamiana leaf protoplasts. Only Golgi punctate can be seen labelled, showing the LPYS signal is effective in this format.

### 5.2.9 Combining Golgi-localised THBs does not infer ERD2-like activity

The results so far indicate that THB1 and THB2 must interact with each other to display the C-terminal Golgi-retention signal and that each individual domain can significantly influence Amy-HDEL transport when stabilised by a proper TM anchor and forced to reside in the Golgi. Since earlier work demonstrated that the TM-ERD2 fusion has almost wild type activity and basically displays 8 transmembrane domains, I was still curious if LPYS-TM-THB1 and LPYS-TM-THB2 could oligomerise in the Golgi and create a complex resembling ERD2 which can mediate increased retention of Amy-HDEL.

In figure 33 I have combined LPYS-TM-THB2 with either LPYS-TM-THB1, TM-THB1 or THB1. The intention with TM-THB1 and THB1 was to also test if having just THB2 anchored to the cis-Golgi could capture these THB1 constructs and perhaps mediate Amy-HDEL retention in an ERD2-like fashion. However, what I saw in gain-of-function assays were simple combinations of the individual effects caused by each THB construct on the secretion index. LPYS-TM-THB1 when co-expressed with LPYS-TM-THB2 halves the induction effect compared to the control dose response of LPYS-TM-THB2, whereas the less impactful TM-THB1 only reduces Amy-HDEL induction by approximately one-third. This is reflective of the reduction in total activity and slight retention of Amy-HDEL for each THB1 construct, respectively. THB1 alone is incapable of causing any meaningful change to the induction in secretion by LPYS-TM-THB2, as to be expected when considering the original data on THB1 in figure 24. These experiments show that in all of the formats designed so far I am unable to initiate a joining of THB1 and THB2 domains to reconstitute an ERD2-like effect such as the retention of Amy-HDEL. Likewise there is also not another novel effect seen that is separate from the individual effects of each THB. In fact, my data suggests that the THBs are not interacting at all and may require proper joining via the TM4 domain as a fusion protein. If the reduced effect of LPYS-TM-THB2 is truly caused by an interaction from LPYS-TM-THB1 or TM-THB1, then I would expect a larger neutralisation of induced Amy-HDEL secretion since the THBs are available in roughly equal quantities.

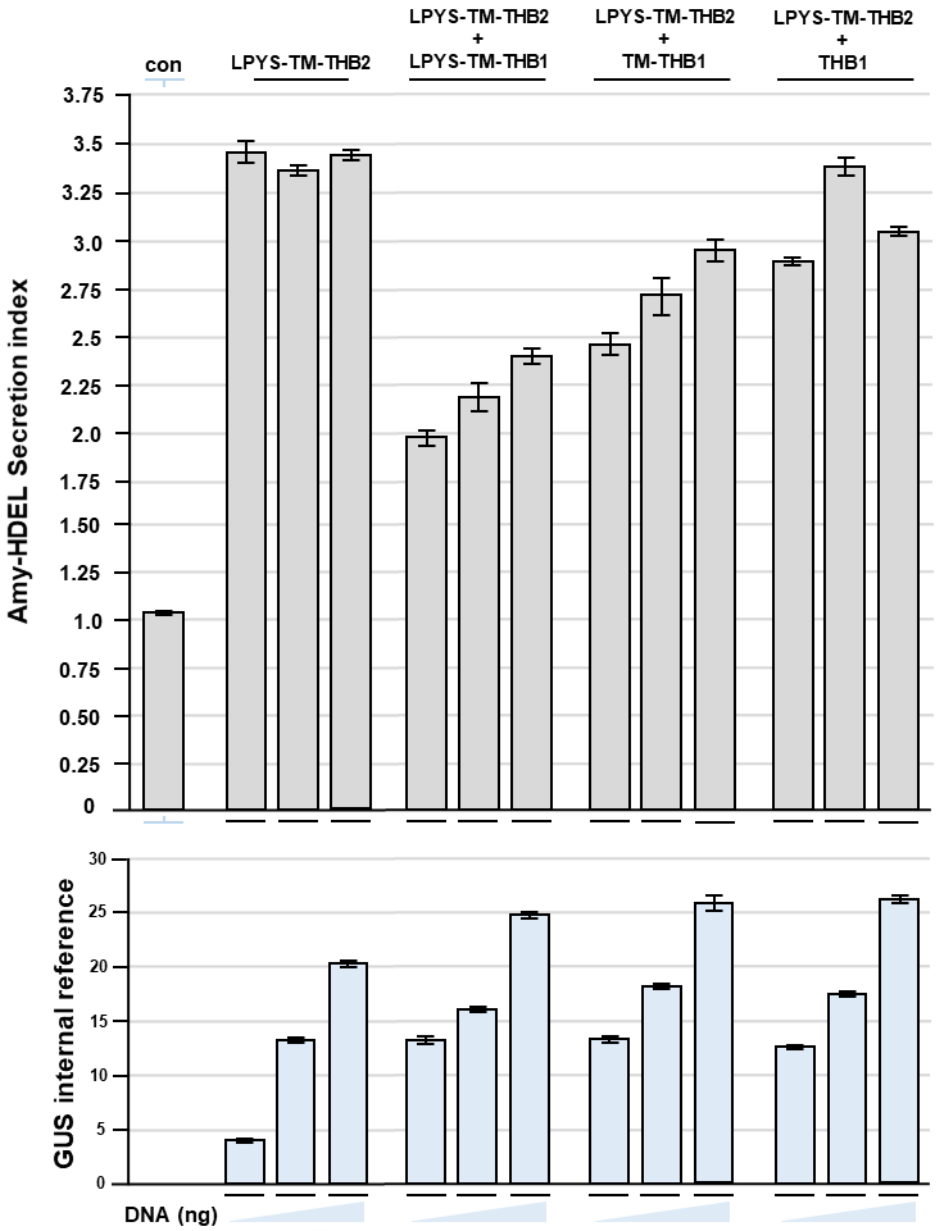


**Figure 33: Combining THB1 variants with LPYS-TM-THB2 does not lead to ERD2-like retention of Amy-HDEL.**

Comparable dose response assays of LPYS-TM-THB2 combined with LPYS-TM-THB1, TM-THB1 and THB1. When in combination with LPYS-TM-THB1 the induction in secretion caused by LPYS-TM-THB2 is roughly halved and most likely due to the effect it has on the total activity. The minor retention mediated by TM-THB1 reduced the induction by LPYS-TM-THB2 even less so and at high expression levels the induction is still approximately three-fold. Co-expressing THB1 alone has little to no effect on the induction of Amy-HDEL by LPY-TM-THB2.

### 5.2.10 LYPS-TM-THB2 also induces constitutive secretion

Clearly LPYS-TM-THB2 operates at least initially in the cis-Golgi, but this region is not exclusive to HDEL cargo and is accessed by secretory and vacuolar cargo too. To determine how general its influence is and whether it affects anterograde pathways I tested LPYS-TM-THB2 in gain-of-function assays with the model cargoes secreted amylase (Amy) and vacuolar amylase-sporamin (Amy-SPO) (figure 34). As a positive control Amy-HDEL displayed the reported 3-4-fold induction again in secretion. Interestingly a noticeable increase was also observed for constitutive secretion marker Amy. Relative to the Amy control, the co-expressed dose response of LPYS-TM-THB2 inducing Amy secretion 2-fold at the highest expression levels. I am unaware of any published molecular reagent that induces constitutive secretion, so this represents a novel phenotype seen for these transport assays. Relative to Amy-HDEL and Amy, AmySPO was only marginally affected, but a weak induction of secretion was observed at the highest effector concentration. AmySPO is traditionally expressed at low levels due to high turnover in the vacuole and the basal rate of secretion is very low to begin with due to high efficiency in vacuolar sorting in plants (Foresti *et al*., 2010). In all three cases, total activity was not much affected (data not shown), so an increase in the secretion index due to cell death is also unlikely.

This experiment tells us that LPYS-TM-THB2 probably does not affect vacuolar sorting, but it seems to have an agenda that is not as closely related to ERD2 as originally thought. Its ability to induce the secretion of the model cargo Amylase means it enhances the fastest rate of anterograde transport out of cells in a non-specific manner. To do this cannot involve simply redirecting traffic in the existing pathway because the quickest route is already favoured by Amylase. It is tempting to speculate that the answer may lie in the generation of a completely new set of transport carriers, and this may shed light on the way in which ERD2 normally recycles within the Golgi apparatus.

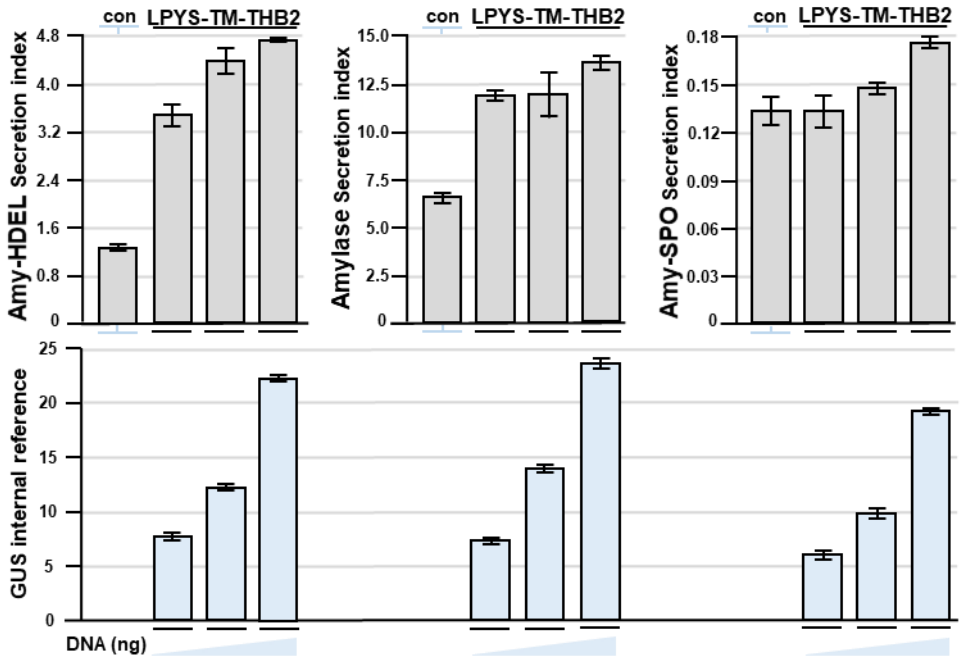


**Figure 34: LPYS-TM-THB2 induces an increase in the secretion of secretory and vacuolar cargo to a lesser extent than ER cargo.**

Repeated dose response assays for LPYS-TM-THB2 but testing the response by secreted Amylase (Amy) and vacuolar targeted Amy-sporamin (Amy-SPO) cargoes. As seen previously Amy-HDEL secretion is more than tripled in combination with LPYS-TM-THB2. For Amy, secretion is approximately doubled and for Amy-SPO only a small induction of approximately one third is seen. Expression levels are very similar between the Amy-HDEL and Amy dose responses, whilst expression is slightly lower for LPYS-TM-THB2 in the Amy-SPO dose response.

### 5.2.11 Increasing amounts of ERD2 will eventually neutralise the induction in Amy-HDEL secretion caused by LPYS-TM-THB2

It still remains unclear to what degree THB2 and ERD2 influence each other, whether it is spatial competition or an interaction that is more direct. One possible option is that it just runs rampant at the cis-Golgi which would naturally upset ERD2, or alternatively it harbours the same machinery but does not lead to the normal cross-talk with THB1 and this titrates certain key-players that are no longer available for endogenous ERD2. To test if LPYS-TM-THB2 and ERD2 compete for the same binding partners, I explored if ERD2 can suppress the effect of THB2-mediated Amy-HDEL secretion. Figure 35 shows a dose-response with wild type ERD2 containing its own Golgi-retention signal and the artificial chimera that depends on a fast COPII export signal to establish Golgi localisation (KK^SS mutant). In both cases, Amy-HDEL secretion by LPYS-TM-THB2 could be inhibited by expression of the full length ERD2 molecule, albeit better when the wild type Golgi retention signal was present. This was expected because even in the

absence of the THB2 construct, there is a significant difference between the two constructs (Figure 17).

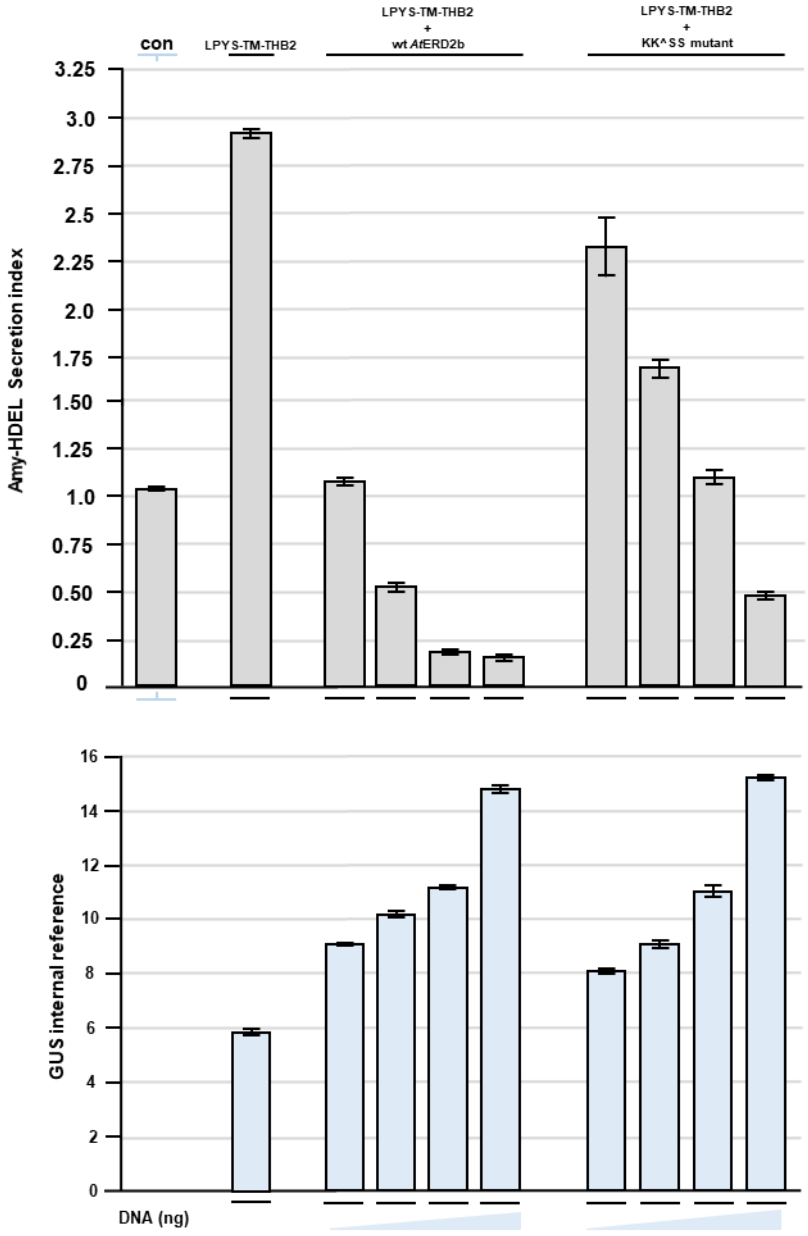


**Figure 35: Expressing wild type ERD2 can suppress the induction in secretion by LPYS-TM-THB2, whilst the ERD2KK^SS can do so less effectively.**

Dose responses with constant levels of LPYS-TM-THB2 and increasing concentrations of ERD2 and ERD2KK^SS can be compared with LYPS-TM-THB2 alone. Large amounts of ERD2 are needed to bring the secretion index down to wildtype levels and the typical amount of receptors necessary to reduce the SI down completely (see figure 12, chapter 3) are needed only to cancel out the effect of LPYS-TM-THB2 (first bar of dose response). ERD2KK^SS struggles to bring the SI down even at very high expression levels.

In the case of wild type ERD2, the lowest amount used in the dose response typically leads to maximum retention of Amy-HDEL, yet in the presence of LPYS-TH-THB2 it just suffices to restore the status quo. It is possible that the small THB2 construct is better expressed due to its small size, but it is more likely that it competes strongly for endogenous machinery. Since I have already established that this machinery component does not specify Golgi-retention of ERD2, the LPYS-TM-THB2 construct is imminently attractive as a bait for novel protein-protein interactions.

### 5.2.12 THB2 of ERD2 may share some similarity with the THB domain of the coronavirus M-protein

Whilst the THBs of SWEET transporters share similar structural traits such as PQ loops, the THBs of ERD2 are more divergent and THB1s from separate homologs are more closely related than with the THB2 of the same receptor. Given the unexpected effect of the THB2 constructs on constitutive secretion, I focused on the well-known effects of envelope viruses which manipulate membrane trafficking to maximise the production of virus particles. Coronavirus M proteins are necessary for internalised budding and the formation of virus-like particles (VLPs) at the ERGIC in mammalian cells (Klumperman *et al*., 1994). Interestingly, they contain a triple helix bundle and analysis of the M protein from SARS-CoV-2 in the wake of the COVID pandemic has elucidated that they share a similar structure to prokaryotic SemiSWEETs (Thomas, 2020).

When comparing THB1 and THB2 of ERD2, it was the latter that resembled the N-terminal THB domain of coronavirus M-proteins the most. This domain is followed by a cytosolic tail that eventually resides within the virus particle as it buds into the ERGIC lumen. The evolutionary conservation of M protein structure and thus internalisation at the ER-Golgi interface may offer some insights into the relevance of THBs in ERD2. For this reason I carried out gene synthesis to express the THB domain of the Coronavirus M-protein alone or supplemented by LPYS-TM at its N-terminus and compared it with LPYS-TM-THB2 generated from ERD2. Figure 36 shows that the THB domain alone had no effect on Amy-HDEL secretion. However, addition of the LPYS-TM domain resulted in a 2-fold induction of Amy-HDEL secretion. The effect was weaker compared to the ERD2 THB2 domain but it was

highly reproducible. It is likely that the Coronavirus M-protein THB may interfere with endogenous ERD2 machinery in a similar manner when forced to remain at the cis-Golgi. It is intriguing because it suggests that the machinery exploited by these virus particles may be conserved between human and plants, a fact that underlines the earlier observation that ERD2 function appears to be extremely conserved.

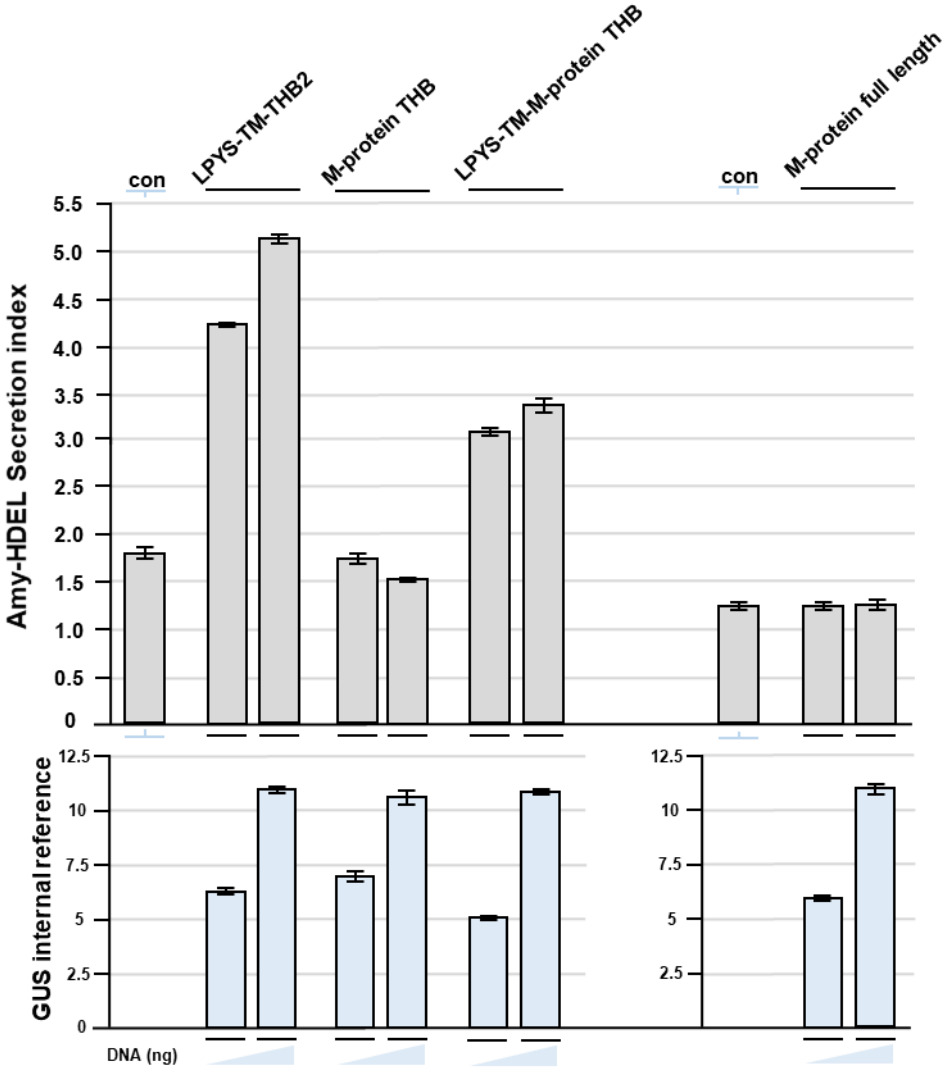


**Figure 36: The THB from SARS-CoV-2 can induce Amy-HDEL secretion when retained at the cis-Golgi.**

**(A)** Small dose responses comparing LPYS-TM-THB2, M-protein THB and the M-protein THB combined with LPYS-TM. The M-protein THB alone does not influence Amy-HDEL, however when combined with the LPYS signal it induces secretion 2-fold, visibly less so than the 3-fold induction by LPYS-TM-THB2. The full length M-protein was also tested, however it appears to have little influence much like when its THB is expressed alone.

To finalise the characterisation I expressed a fluorescent derivative of the Coronavirus M-protein, starting with a signal peptide and YFP (secYFP), followed by either the THB domain alone (secYFP-THB) or the full length M protein (SecYFP-Mfl). In each case I co-expressed MNS3-RFP for comparison. Figure 37 shows that the former construct reaches the plant Golgi apparatus but also labels the ER. Interestingly, the full length M-protein fusion accumulates exclusively in the Golgi apparatus, yet in Figure 36 it does not appear to have the same influence on Amy-HDEL as LPYS-TM-M protein THB. This remarkable outcome suggests that Coronavirus M-proteins may deploy ancient Golgi retention signals that could exploit the same machinery as ERD2 with less influence on endogenous protein sorting. It is possible that M-proteins and ERD2 evolved from a common precursor, or that M-proteins evolved from ERD2 itself.

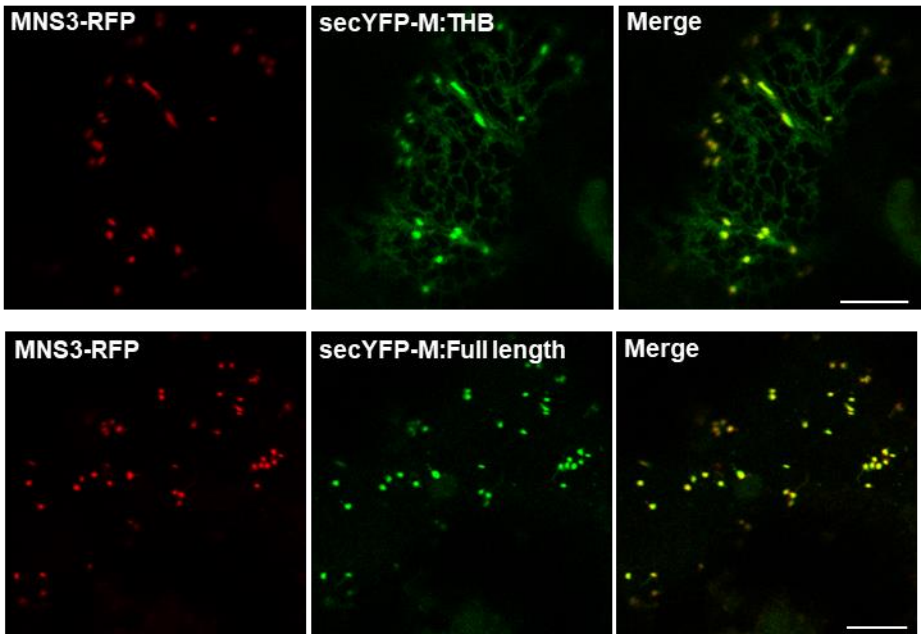


**Figure 37: The THB and Full length M-protein from SARS-CoV-2 localise differently.**
secYFP-M:THB and secYFP-M: full length co-expressed with MNS3-RFP. Whilst full length M protein co-localised with MNS3-RFP in Golgi punctate only, the M:THB partially localises to the ER as well as the Golgi as seen by the fluorescence in ER tubules.

## 5.3 Discussion

### 5.3.1 THB1 and THB2 do not behave like ERD2 and are unable to reside at the Golgi independently

A pursuit to establish whether the THBs of ERD2 could combine and mediate some degree of ER retention was inspired by a family of SWEET transporters who share the same structural subdomains. The THBs of SWEETs and SemiSWEETs are able to oligomerise after being expressed separately and support glucose transport across membranes (Hu Xuan *et al*., 2013). Numerous considerations were provided for both THB1 and THB2 to stabilise the smaller molecules within the membrane, however all attempts resulted in a failure to mimic the retention capabilities of the whole receptor. It seems these structures shared by ERD2 and SWEETs may be where the functional similarity ends.

Any expectations for THB1, THB2 or SPTHB2 to mediate retention of Amy-HDEL individually or when combined (Figure 24) was ambitious, but this at least served as an indicator that more structural stability was necessary, as found for the first THB of AtSWEET1 (Hu Xuan *et al*., 2013). Given the neutral position of TM4 in ERD2, I was initially more concerned for the stability of THB2 since THB1 is capable of determining the topology during the full synthesis of ERD2, which THB2 may usually be guided by. An additional TM domain sourced from ERP (Silva-Alvim *et al*., 2018) placed at the N-terminus of both THBs did appear to bring some form of stability as minor changes to Amy-HDEL secretion were observed for TM-THB1 and TM-THB2.

The likelihood of inducing ERD2-like behaviour was evidently much lower after the realisation that neither THB was predominantly localised to the Golgi (Figures 28, 31), so in a final attempt I fused the Golgi retention signal isolated from MNS3 (Chapter 4) to both subdomains. In doing so the only responsibility left for THB1 and THB2 was to interact with one another, possibly requiring an HDEL ligand in close proximity. However and regardless of both THBs containing a Golgi retention signal, or LPYS-TM-THB2 being co-expressed with TM-THB1 or just THB1, I was still unable to create conditions where the two subdomains combined and retained HDEL proteins. In fact when both THBs were localised to the Golgi the exact

opposite seemed to occur, as the phenotype for Amy-HDEL appeared as a mixed effect of the two subdomains, meaning they were operating separately.

Whether receptors specifically require TM4 or if other linkers can be used remains to be determined, but ultimately covalent bridging between the two subdomains appears to be a critical element for the intramolecular negotiations of ERD2 leading to the capture and retrograde transport of HDEL proteins to the ER.

### 5.3.2 THB1 can inhibit trafficking at the ER-Golgi interface when retained in the Golgi

Once THB1 was forcibly retained at the cis-Golgi via the N-terminal LPYS retention motif it did appear to reduce the secretion index of Amy-HDEL, however this effect was distinguishable from the usual characteristics of ERD2-mediated retention. On closer inspection LPYS-TM-THB1 had a wider influence that was more similar to the BFA-like effect initiated by ERD2 overexpression, with the only difference between the two constructs being the vast reduction of Amy-HDEL secretion seen for ERD2. What is significant is that LPYS-TM-THB1 caused this response at much lower concentrations, therefore it would be interesting to see if the construct is capable of an even stronger influence at higher expression levels, possibly beyond that of full length ERD2. It is clear that THB1 can mimic the structural configuration necessary for ERD2 to induce these effects, but perhaps it is easier to do so without the hindrance of THB2 or cross-talk with other retention components. Whilst the localisation of this construct was not analysed, Golgi clustering and apparent BFA bodies were exposed by a similar construct, YFP-TM-THB1. This fluorescent marker was without a Golgi retention signal, however the small population of fusions reaching this compartment may still be indicative of the grand-scale morphological effects THB1 is causing when Golgi residency occurs en masse.

What is clear for now is that the blockade on trafficking at the ER-Golgi interface, otherwise described as a BFA-like effect, doesn't seem to require the entire body of ERD2 but instead a smaller functional domain hidden within THB1. Further characterisation of this construct may fully potentiate its role in the BFA-like effect of ERD2 and also help to gain a better understanding of the events leading to a reduced yield of HDEL cargo, an observation made possible only by the quantitative nature of our validation system.

### 5.3.3 The effects of LPYS-TM-THB2 cannot be explained by the current understanding of ERD2 function

One of the few traits THB2 shared with THB1 is that the LPYS fusion was required for the subdomain to bestow a change to the trafficking of Amy-HDEL. Likewise, the fluorescent fusions highlighted a struggle for THB2 to mediate a Golgi localisation of its own accord, which is in support of previous reports (Alvim, 2018) that the di-leucine motif is not sufficient for Golgi residency outside the context of ERD2. It is also apparent that the subdomain doesn't carry an exposed ER export signal. Whilst fusion of YFP (LPYS-TM-THB2-YFP) nullified the huge induction of Amy-HDEL secretion by THB2, it did localise exclusively to punctate structures therefore it is safe to assume that a positioning at the cis-Golgi mediated by LPYS is critical to this novel phenotype.

The ability of ERD2 to gradually suppress the induction in secretion provided strong evidence in support of LPYS-TM-THB2 competing for machinery that is typically harnessed by endogenous receptors at the cis-Golgi. The much weaker degree of suppression by the KK^SS mutant pointed at a strict Golgi localisation to be of primary importance when competing for interactions with the unidentified machinery, because the KK^SS construct is known to have a reduced presence at the Golgi under HDEL saturation (Figure 18). The method of Golgi retention thus appeared less important, as did the di-leucine motif after being rendered completely unnecessary for inducing the secretion of Amy-HDEL in the context of LPYS-TM-THB2 (Figure 30).

Similar to THB1, It is also apparent that THB2 can mimic the conformational state ERD2 presents when actively recruiting other machineries in the cis-Golgi, but the frequency at which THB2 appears this way is likely random if the smaller protein is not regulated in the same manner as full length ERD2. Increasing concentrations of ERD2 outcompeting the effect of LPYS-TM-THB2 could thus be simply explained by a temporal dominance of ERD2 in the bound-state, if it is this conformation which is preferential for interacting partners.

Nonetheless, the question still remains as to what is causing such a large induction of Amy-HDEL by LPYS-TM-THB2. Since this construct may have the ability to maintain interactions for longer than a receptor switching states to handle the

constant onslaught of escaping chaperones, it may be a great candidate for capturing some of the machinery required for ERD2 cycling at the cis-Golgi.

### 5.3.4 Coronavirus M protein reveals a potential explanation for accelerated secretion by THB2

The major induction of Amy-HDEL secretion caused by THB2 is fathomable if it is considered to be competing for ERD2 binding partners in a dominant negative fashion. However this argument does not hold any weight with respect to the induction in constitutive secretion of Amy, because ERD2 is not involved with this pathway.

Besides the obvious properties shared with ERD2, THB2 also has detectable sequence similarity with the THB present in SARS-CoV-2 M protein. In gain-of-function assays the THB taken from M protein and combined with LPYS-TM was able to induce the secretion of Amy-HDEL even though it is functionally unrelated to ERD2. Meanwhile the full length M protein was neutral, which is particularly interesting since it can independently mediate a Golgi-only localisation while the M protein THB cannot. Perhaps there is an evolutionary trait in the full length membrane components of SARS-CoV-2 that mask the negative effect the THB could independently have on the host pathway during virus formation. This may mirror a similar divergence in function for THB2 when in combination with the other elements of ERD2.

Even though ERD2 and the M protein do not share any obvious functional traits, they both contain THBs which exploit the same machinery. If the THBs have a role in membrane manipulation similar to the generation of VLPs, this may offer some explanation for the non-specific induction in secretion seen for lumenal proteins. More importantly, why this property is necessary in the context of ERD2 function may give clues to how the receptor concentrates HDEL ligands into sub-compartments. Further investigation into the divergence between M protein and ERD2 may then help to understand why VLPs exocytose but receptors are able to remain at the cis-Golgi.

## 5.4 Conclusion

In this chapter my original approach was straight forward; could I bring forth a combination of THB1 and THB2 constructs in gain-of-function assays to retain HDEL cargo in an ERD2-like fashion? To do so would provide in-situ support for the intramolecular cohesion between subdomains stipulated in the crystal structure (Brauer *et al*., 2019; Gerondopoulos *et al*., 2021). It would open up interesting lines of research expanding on the conserved role of ERD2 between species. Mutant combinations could narrow down ERD2-specific functions to individual subdomains, similar to the investigations carried out for SWEET transporters. However the results I presented were not so simple to interpret. Instead they reflect a complex set of events within the pathway that are not yet characterised for ERD2, at least under steady-state conditions. Perhaps the method of expressing THBs has resulted in an exacerbation of typically transient interactions performed by ERD2. Or instead these structures have actually revealed an evolutionarily redundant set of functions that are not intended for the pathway as we know it. How closely related these effects are to ERD2 function may be revealed through further characterisation of the novel constructs generated in this chapter, followed by their use as baits for protein-protein interactions.

# Chapter 6 - General Discussion

In 2018 I quickly adopted a pragmatic approach to my research, having joined a laboratory with published findings which questioned some of the most dogmatic principles associated to ERD2 function. A fresh perspective was not appreciated nor welcomed by peers, quickly leading to a focus on the matters that the group were yet to address in the first publication. Critique was to be expected especially considering the ramifications our results posed for many in the field. Fortunately I and the group shared a very self-critical philosophy on the data, such that work immediately commenced on the remaining discrepancies between our research and the old model.

Just prior to my project, the di-leucine motif discovered by Alvim (2018) was confirmed by FRAP analysis as a Golgi retention motif positioned at the C-terminus of ERD2, as originally proposed. This was the final stride made by my predecessor before handing over the reins, leaving me still to challenge the premise behind receptor recycling (and lack of for the functional receptor), the receptor's association with COPI transport and finally the conservation of findings in mammalian models. Key to all of this was a practical rather than theoretical application of experiments, meaning functional validation of ERD2 was a fundamental prerequisite for all datasets. Taking this attitude has driven the partition in findings between myself and the field, the inconsistencies of which I have attempted to settle in two dedicated chapters. What remained to be addressed on the matter was a conceptual problem related to recycling cargo back to the point of origin, which has not been discussed previously in the literature but will form part of the general discussion. In the third results chapter I took an alternative approach and established a compelling dataset suggesting that ERD2 function strictly correlates with a permanent cis-Golgi residency. From there, I took the opportunity to move on and explore novel cis-Golgi interactions by ERD2-associated triple helix bundles, which may offer intriguing clues towards a new mode of function.

Central to the discoveries made in this thesis are the use of mesophyll protoplasts from *N. benthamiana* and the intact lower epidermal layer of leaves from *N.*

*tabacum*. With the exception of the human and Arabidopsis YFP-TM-ERD2 and ERD2-YFP fluorescent fusions, all localisation data on constructs presented in this thesis were acquired from microscopy in only transiently expressing *N. tabacum* leaves or *N. benthamiana* protoplasts. Whilst stringent conditions were in place for each set of experiments, there were still numerous uncontrollable factors in play at the point of imaging live tissues, such as the differing rates of growth and expression between individual plants and transformant lines of *Agrobacterium tumefaciens*. For these reasons there will always be some degree of uncertainty with this style of scientific interrogation, however the potential influences of model organisms on the research outcomes of future experiments could be mitigated by expanding subcellular observations into multiple tissues or better still, different species. One single tissue is not representative of the numerous cell types and associated organelle organisations of all eukaryotes, therefore caution should be taken when drawing conclusions from such isolated datasets. Establishing different localisations for ERD2-YFP and YFP-TM-ERD2 benefitted greatly from expanding the microscopy into human HeLa cells, offering justification that the same efforts should be made in the future to consolidate other important findings within this thesis. Also, the choices do not have to be limited to *N. tabacum* leaves or HeLa cells, as root cells from stable transgenic lines or caulonema from *Physcomitrium patens* offer suitable material for subcellular microscopy too.

Similarly, microscopy should not act as a stand-alone method for biological validation and as this thesis draws on heavily, one of the reasons for this is because tagging the same protein in different configurations can lead to different organelle residencies. Genetic validation via complementation on the other hand is a very robust method for determining the biological integrity and localisation of modified proteins, however it is still susceptible to disguising reduced function, as we have seen for the ERD2-c-myc fusion in yeast studies. Whilst I present another method of biological validation using Amy-HDEL secretion assays and normalised internal expression of ERD2 variants, this method also has its weaknesses. The use of protoplasts enables highly quantitative monitoring of ERD2 activity, however, they are a single subset of mesophyll cells from one plant species. As is the case with microscopy, this narrow sample size cannot be representative for all secreting eukaryotic cells and thus findings should be considered with that in mind. Other

properties of modification besides the effects on ERD2 function are also not considered in protoplast assays, such as regulation and degradation of receptors which would influence overall concentrations in cells. To consider this in the future, western blots of ERD2 variants could be carried out and presented alongside GUS activity to confirm consistent populations as well as plasmid expression levels between experiments. Finally, the model secretory cargo amylase and its variants (Amy-HDEL, Amy-SPO) are not native proteins of *N. benthamiana*, meaning they are technically generating an artificial stress on the retention system within protoplasts. To gain further insights on the native pathway, Western blot analysis would also be a useful tool for monitoring the populations of native ER residents within medium and total cell protoplast samples when expressing ectopic ERD2 and cargoes.

## 6.1 The “Sisyphus” Paradox

A burden which is Sisyphean by nature is described as one that can never be completed. This is clearly not the case for sorting receptors whereby the recycling principle is very popular, not least because it explains how few receptors can transport multiple ligands. Recycling is established for receptor-mediated endocytosis (Grant and Donaldson, 2009) and the segregation of lysosomal/vacuolar proteins from secreted proteins in the Golgi apparatus (Seaman, 2005; da Silva *et al*., 2005). In both cases receptors bind to ligands at the first point of contact, enter or even help form a directed transport vesicle, release the ligand on arrival to the acceptor compartment, and then recycle back to the donor membrane for new rounds of ligand-selection. One key factor is that the acceptor compartment is separate to any region that the cargo has been previously and thus can only gain access via a sorting receptor. Another is that once the cargo is delivered to the acceptor compartment it will not be passively transported back to the point of original sorting.

To explain the retrieval of ER chaperones from the Golgi apparatus, a similar receptor recycling model was proposed (Pelham, 1988) and gained traction after supporting evidence (Lewis and Pelham, 1992b) agreed with the type of trafficking described for other receptors operating under the same principle. However a fundamental difference was overlooked in the context of ERD2: Whilst vacuolar

proteins are sorted at the Golgi only once from other proteins, ER residents are recycled back to the ER where they were originally synthesized. This is the same organelle they are transported from in a manner of passive bulk flow (Crofts *et al*., 1999) meaning they can (and will) arrive at the Golgi again. Their perpetual escape to the Golgi would cause an endless “Sisyphus” task for ERD2. Not only that, the ER is the focal point of *de novo* synthesis within the pathway therefore newly synthesized ER residents would amplify the burden at each cycle. Given the high abundance of soluble ER residents (Macer and Koch, 1988), such odds would defeat even the most efficiently transported receptors, never mind those which are already vastly outnumbered. This conceptual problem has not been widely considered to date because any scientific evidence against the recycling model for ERD2 has been lacking.

## 6.2 ERD2 Behaves like a Gatekeeper

Colloquially, the classic “frequent flyer” model for receptor-mediated transport can be illustrated by a taxi-driver who takes only a limited number of passengers. The driver can return to the collection point for another shuttle service, but whilst in transit any additional passengers have to wait. Our results suggest that ERD2 does not function like a taxi driver but instead it acts like a “gatekeeper” at the cis-Golgi.

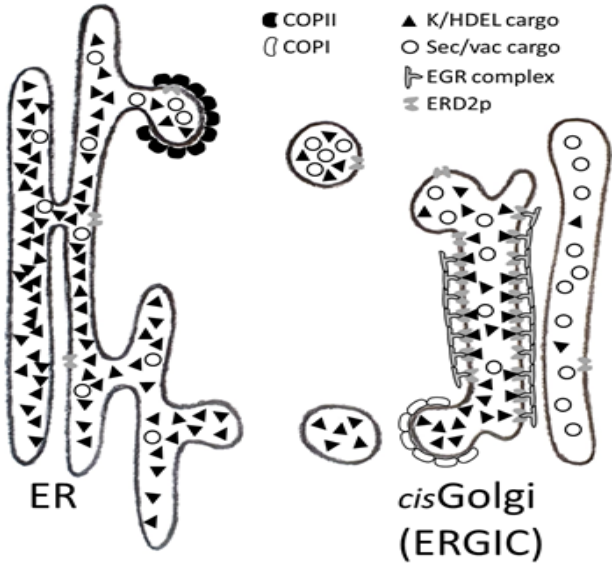


**Figure 38: ERD2 may operate as a “Gatekeeper” positioned at the cis-Golgi/ERGIC**
Receptors appear to be retained at the cis-Golgi by an unknown ERD2 Golgi retention (EGR) complex, via interaction with the C-terminal di-leucine motif. ERD2 remains in concentrated regions of the cis/ERGIC cisternae, binding K/HDEL cargo and then releasing them in the vicinity of COPI vesicle budding sites. A complex could explain the retention of other cis-Golgi localised proteins such as MNS3, however, such a structure is not in agreement with the cisternal maturation model for protein transport through the Golgi apparatus.

This can be illustrated by a bouncer who denies entry. Unlike a taxi driver, the bouncer holds its position at the gate and is able to repel a far greater crowd of individuals, including those making repeated attempts. In this sense permanent Golgi-residency requires a smaller population and thus lower turn-over of ERD2, which explains why so little is needed to be effective (Figure 10, 12) and expression under control of its own promoter is so difficult to detect in mammalian cells (Tang *et al*., 1993) and *P. patens* (Alvim *et al*., 2023). Therefore, the Golgi retention motif of ERD2 and its conservation is symbolic of its function in mediating ER retention of soluble proteins (Silva-Alvim *et al*., 2018). As it is exposed in the cytosol, the signal is likely recognised by a protein complex that contributes to the identity of the cis-Golgi/ ERGIC. Also the glycan modifying protein MNS3 is actively retained in Golgi structures by preventing Golgi to ER transport (Schoberer *et al*., 2019), and the N-terminal retention motif it contains can reactivate ERD2 when its own signal is masked (Figure 21). Each signal appears to respond differently to BFA treatment (Schoberer *et al*., 2019; Figure 23), therefore it would be interesting to determine the separate interactions taking place at the cis-Golgi which lead to this.

A precedent for a sorting facilitator that does not enter the budding carrier itself is TANGO1, promoting collagen loading for ER export whilst effectively remaining behind in the ER membrane (Saito *et al*., 2009; Saito *et al*., 2011; Raote *et al*., 2018). Collagen is a very abundant secretory cargo, and if Tango1 sorting was in analogy to the “taxi-driver” it could be equally overwhelmed, even when collagen is only transported once and facilitated by bulk flow. To facilitate packaging of larger molecules into COPII carriers the TANGO1 family members combine and form a corral around the COPII and translocon sub-units Sec16p, Sec12p, Sec22p and Sec23p. One of the three cytosolic domains of TANGO1 tethers directly to another complex for the recruitment of ERGIC membranes as the COPII carrier expands in size. This presents a system where cross-talk with transport machinery is delegated across numerous cytosolic domains of TANGO1, to the extent that it is able to modulate the process from one position. This may also be the case for ERD2 cytosolic domains alongside the established di-leucine motif.

An example of a Golgi-resident sorting component is Rer1p (Sato *et al*., 2001), which also depends on its C-terminus to accumulate in the Golgi apparatus whilst mediating the accumulation of membrane proteins such as Sec12 in the ER. It is

proposed that the Golgi localisation of Rer1p is dependent on interactions with coatomer, as it relocates to the vacuole when expressed in α and β' mutant lines. Similarly, Rer1p was seen to form complexes with coatomer in a separate manner to the putative dilysine motif after incubation with binding mutants but no further investigation was taken on this mechanism. It would be interesting to carry out a similar investigation with ERD2. The receptor must work synergistically with COPI machinery in order for HDEL cargo to be returned to the ER, but I have shown this cannot be via the recruitment strategies suggested by the field (Figures 13, 16).

## 6.3 Cycling at the cis-Golgi

It seems that THB1 and THB2 have a mutual disinterest or rather struggle to engage without a covalent force bringing them into close proximity. It is unlikely that the additional ERP TM domain and ectopic Golgi retention motif isolated from MNS3 prevents the possibility of an ERD2 configuration, as neither of these modifications vastly changed the biological activity of the wild type receptor (Figure 20). What still remains to be determined is the structural threshold which dictates when THB subdomains mediate the role of ERD2 or instead carry out their individual effects, and whether it can be mediated by something other than TM4.

The responses from forcing THB1 and THB2 to remain at the cis-Golgi were unexpected, particularly for THB2 since the magnitude of Amy-HDEL secretion and the two-fold induction of constitutive secretion has not been seen in these assays previously. Taking a pragmatic approach, my ideology shifted slightly as I realised that identifying competitors which directly or indirectly inhibit the retention of HDEL proteins was a sensible starting point for hunting candidates that assist ERD2 in its role as a cis-Golgi localised receptor. THBs may generate long lasting interactions that are typically transient for ERD2. They are not hindered by each other or the constant sorting of ligands, so may be able to mimic the bound conformation freely and for longer. It is assumed that such interactions are typical of active ERD2 in receptor-ligand complexes and this could be confirmed by testing binding mutants or even the di-leucine mutant as competitors (LLGG) as I've shown for wild type ERD2 (Figure 35).

The induction in constitutive secretion by THB2 forced me to consider that this subdomain is influencing more than just ER retention at the cis-Golgi. A change to the morphology of this sub-compartment is one potential explanation, which is a trait of SARS-CoV-2 during the generation of VLPs at the ER-Golgi interface. The resulting induction in Amy-HDEL secretion by the THB isolated from SARS-CoV-2 M protein gives an impression that the two effects might be related and a very adventurous argument could be made for the generation of nonspecific transport carriers. However, the M protein THB has not been characterised with other cargoes and the features enabling the full length M to localise to the cis-Golgi independently are still unknown. Identification and a thorough characterisation of any binding partners is necessary before a reasonable explanation can be offered for the induced secretion. This may be best investigated by the use of these constructs as baits in pull-down assays.

After the C-terminal fusion of YFP to LPYS-TM-THB2 abolished the induced secretion of Amy-HDEL it meant that at least some of the interactions are taking place on the cytosolic side of the membrane. Thus the same fusion could confirm this to be the case for LPYS-TM-THB1. Perhaps if instead an additional TM-domain at the C-terminus of THB1 or THB2 followed by a fluorescent protein was fused, novel cytosolic domains would not be masked and then a more reliable localisation of the constructs could be observed. The fact that the last five amino acids are not important for THB2 (Figure 30) suggests the fusion of a TM domain is also unlikely to cause much harm and could be a viable option.

The BFA-like effect caused by ERD2 is known to involve cytosolic interactions such as the recruitment of ARF1-GAP (Aoe *et al*., 1997), therefore if THB1 is triggering a similar effect then it is likely to influence cytosolic proteins too. The reduction in Amy-HDEL yield with increased expression of LPYS-TM-THB1 and overexpression of ERD2 is an interesting coincidence. One could imagine a scenario where the receptor is involved in a vacuolar signalling cascade for protein turn-over and the increase in HDEL proteins is interpreted as a stress cue for misfolded proteins. A visible localisation of RFP-TM-ERD2 in the vacuole following BFA incubation (Figure 23) supports such a mechanism and degradation here would explain a decrease in the total activity of Amy-HDEL. Similarly, the internalisation occurring for RFP to appear in the lumen aligns with the sort of membrane manipulation

taking place during the formation of VLPs. The common structural denominator in all of these instances is the THB, and I am hopeful these subdomains will elucidate novel functional properties for ERD2-mediated retention from the cis-Golgi, when employed as tools for detecting binding partners.

## 6.4 Concluding Remarks

It is now beyond reasonable doubt that ERD2 resides strictly at the Golgi apparatus. It is also clear that ERD2 does not interact with COPI transport in a traditional sense. Given its involvement in one of the earliest sorting mechanisms established for eukaryotic cells, big leaps in our understanding of ERD2 function may bring opportunities to further characterise the cis-Golgi, whose evolutionary origin is still unknown. As a starting point, the ERD2 subdomains are an exciting prospect for unravelling a new mode of function.

# Chapter 7 - Materials and Methods

## 7.1 Buffers and Solutions

- **LB (Luria Bertani) medium**: 10g/L tryptone; 5g/L yeast extract; 10g/L NaCl. Autoclave sterile, including 15g/l agar for solid medium
- **2xYT medium**: 16g/L tryptone; 10g/L yeast extract; 5g/L NaCl. pH 7.0 adjusted with NaOH. Autoclave sterile
- **TES solution**: 10mM Tris-HCl pH8.0, 5mM EDTA, 250mM sucrose; filter sterile
- **TE buffer**: 10mM Tris-HCl pH8.0, 0.1mM EDTA
- **TE 50/1 buffer**: 50mM Tris-HCl pH8.0, 1mM EDTA
- **TEX buffer 1L**: 500mg MES, 750mg $CaCl_2 \cdot 2H_2O$ 0.4M sucrose [13.7%], and Murishage and Skoog (1962) mix [100ml (10X) Macro, 10ml (100X) Ferro-EDTA, 1ml (1000X) micro] brought to pH5.7 with KOH.
- **Electroporation buffer**: 0.4M sucrose [13.7%], 2.4g/l HEPES, 6g/l KCl, and 600mg/l $CaCl_2$, brought to pH 7.2 with KOH
- **α-amylase extraction buffer**: 50mM malic acid, 50mM NaCl, 2mM CaCl2 and 0.02% sodium azide, 0.02% BSA
- **To 10ml of GUS Extraction buffer**: 5ml sodium phosphate buffer pH7.0, 1ml $Na_2EDTA$, 1ml 0.1% sodium lauryl sarcosine, 0.1ml 0.1% Triton X-100 and 7.8µl βMeEtOH added prior to use.
- **To 5ml of GUS Reaction buffer**: 2.5ml sodium phosphate buffer pH7.0, 0.1ml 0.1% Triton, 0.5ml PNPG, 3.9µl βMeEtOH added prior to use.
- **To 50ml GUS stop buffer**: 13.14g 2-amino-2-methylpropanediol into distilled water. 2.5M final concentration.
- **Leaf extraction buffer**: 100mM Tris-HCl, pH7.8, 200mM NaCl, 1mM EDTA, 0.2% Triton X-100, and 2% βMeEtOH)
- **ECL Solution 1**: 1ml 1M Tris-HCl pH 8.5, 100µl 250mM Luminol, 44µl 90mM p-coumaric acid, 8.85ml dH20
- **ECL Solution 2**: 6µl 30% $H_2O_2$, 1ml 1M Tris-HCl pH8.5, 9ml $dH_2O$
- **TFBI solution**: 30mM KC2H3O2; 100mM RbCl; 10mM $CaCl_2 \cdot 2H_2O$; 50mM $MnCl_2 \cdot 4H_2O$; 15% v/v glycerol. pH5.8 using 0.2M CH3COOH. Filter sterilised and stored at 4°C

- **TFBII solution**: 10mM MOPS; 10mM RbCl; 75mM $CaCl_2 \cdot 2H_2O$; 15% v/v glycerol. pH6.6 using 5M KOH. Filter sterilised and stored at 4°C

## 7.2 Molecular Biology

Common and well-established molecular biology techniques employed for DNA sub-cloning and buffers adapted from Sambrook *et al*. (1989) unless otherwise stated. 0.5X TBE (Tris, boric acid, EDTA) agarose gels and buffer used for DNA analysis. Restriction digestion and dephosphorylation was carried out in buffers compatible to the enzymes e.g. NEBuffer3.1, CutSmart or alkaline phosphatase buffer, as recommended by enzyme provider (New England Biolabs). *E.coli* strain MC1061 was transformed when generating new constructs (Casadaban & Cohen, 1980).

PCR was carried out as per the KOD DNA polymerase protocol from Novagen, Darmstadt, Germany (Novagen, 2011). Oligonucleotides were purchased from Eurogentec (Liege, Belgium). DNA was amplified using a thermocycler (GeneCycler BioRad, Hercules, CA, USA) and conditions were adjusted according to the reaction.

The following thermocycler protocol was used for sub-cloning mutagenesis constructs using corresponding quick-change primers:

1. Initial denaturing 95°C, 2 mins
2. Denaturing 95°C, 20sec
3. Annealing 55°C, 20sec
4. Extension 72°C, 60sec
5. Final extension 72°C, 10mins

Repeat steps 2-4 between 15-30 cycles to acquire ample amplification product. 2 hours digestion using DpNI restriction enzyme necessary to eliminate methylated parent plasmid prior to transformation of competent cells with product.

Chimaeric gene products were created with sense or anti-sense primers specifically designed for the replacement of N- or C-terminal regions, respectively, combined with common sense primers downstream of polyadenylation sites or upstream of promoter regions. Corresponding thermocycler protocol:

1. Initial denaturing 95°C, 2 mins

2. Denaturing 95°C, 20sec
3. Annealing 50°C, 20sec
4. Extension 72°C, 60sec
5. Final extension 72°C, 5mins

Repeat steps as in quick-change protocol. Amplicons were digested with specifically incorporated restriction sites for ligation into corresponding vectors prior to transformation of competent cells.

## 7.3 DNA Isolation

Mini-preparations (minipreps) of DNA were isolated from overnight inoculations of transformed MC1061 single colonies in ~3 ml of LB medium. 1.25ml of inoculum was transferred to eppendorf tubes and centrifuged for 1 minute at 14,000rpm, followed by removal of supernatant from pellets. Cell resuspension was in 150µl of TES, then 20µl of lysozyme solution was added and mixed quickly before a 5 minute incubation at room temperature. Addition of 300µl distilled water followed and tubes were incubated at 73°C for 15 minutes. Tubes were centrifuged at 14,000rpm for 15 minutes and supernatants transferred to new tubes. 50µl of 5M $NaClO_4$ (~10% volume) was added and tubes were vigorously shaken. The same shaking occurred after the next addition of 400µl isopropanol (80% volume), which was followed by 15 minutes centrifugation at 14,000rpm. Supernatants were removed as previously and a “pulse” spin was carried out prior to complete removal of supernatant with a fine micropipette. Finally, tubes were aerated at 37°C for 15 minutes and then DNA pellets were re-suspended in 50µl of TE buffer and stored at -20°C until use.

For larger yields of DNA and improved purity prior to sequencing, wizard-preparations (wizpreps) were instead carried out using a single colony inoculated in 10 ml of LB medium overnight and Promega Wizard® *PLUS* SV kits for DNA isolation and purification.

For the largest DNA preps (maxipreps) intended for transient expression assays, a single colony was used as pre-inoculum in 3 ml of LB and 150µg/ml ampicillin, grown for ~3 hours (until minimal turbidity) before inoculation into 500ml of 2xYT

medium and purification as in minipreps, with equivalent volume ratios of added components.

## 7.4 Competent E.coli Stocks

An aliquot of untransformed MC1061 E.coli was streaked out on a neutral LB-agar plate and incubated overnight at 37°C. 3ml of 2xYT medium was inoculated with a fresh colony and incubated at 37°C with vigorous shaking (180rpm). Once sufficiently turbid, the pre-inoculum was transferred into a final culture of 200ml pre-warmed 2xYT medium and incubated at 37°C. When the culture reached an O.D550nm of approximately 0.400-0.450, it was transferred into four sterile 50ml conical tubes and placed on ice for 5 minutes to arrest cell division. Cultures were then centrifuged at 3000g in a refrigerated swing-out rotor in sterile containers, for 20 minutes at 4°C. Cell pellets were re-suspended in a total of 80ml ice-cold TFBI solution and placed on ice for 5 minutes. The cell suspension was centrifuged as before and then re-suspended in a total of 8 ml of TFBII, pooled and left on ice for 15 minutes. Using pre-chilled pipettes tips, 100µl aliquots of homogenous cell suspension were transferred to pre-chilled eppendorfs (placed on ice). Aliquots were then frozen in dry ice and stored at -80°C.

## 7.5 Plant material and transient expression experiments

Sterile grown *Nicotiana tabacum* cv., Petit Havana (Maliga *et al*. 1973) and *Nicotiana benthamiana* (Goodin *et al*. 2008) plants were grown from surface-sterilized seeds. *N. tabacum* plants were used for leaf infiltration experiments with *Agrobacterium tumefaciens* and N. benthamiana for α-amylase secretion assays as described in previously published protocols, respectively (Leborgne-Castel *et al.,* 1999; Foresti *et al.,* 2006; Silva-Alvim *et al*., 2018).

### 7.5.1 Preparation of protoplasts

*N. benthamiana* leaf protoplasts were released by incubation with 0.25x digestion mix containing TEX buffer supplemented with 0.2% Macerozyme R10 and 0.4% Cellulase R10 (Yakult). 10X stock of concentrated digestion enzymes were

generated by adding lyophilized powders in TEX buffer and mixing for 2h, centrifuging at 5000 x g for 15min and finally filter sterilization (0.2 µm) of the suspension. Aliquots were 2.5ml and kept at −80°C for routine use. The 0.25x digestion mix was always prepared freshly by addition of 98ml of TEX buffer to aliquots.

Overnight digests of floating leaf cuttings were prepared with a scalpel and needle bed. Plates were lightly shaken to release protoplasts and then filtered through a 100-µm nylon mesh to remove connective and structural tissue. Mesh was rinsed with electroporation buffer to release further protoplasts from the tissue remnants, making sure not to surpass a volume of 105ml. Protoplast suspension was centrifuged in Falcon tubes (50 ml) for 15min, 100 x g, room temp in a swing-out rotor. Centrifugation was stopped without brake to prevent re-suspension of the floating protoplast layer. The pellet and the underlying medium were removed and discarded using a peristaltic pump and a sterile Pasteur pipette until the band of floating living protoplasts reached the bottom. Live protoplasts were pooled into one falcon tube by re-suspending each in 25ml of electroporation buffer and centrifugation was repeated. Resuspension and centrifugation repeated at least once more and until pellet is very minimal, meaning most excess material has been removed.

### 7.5.2 Electroporation of protoplasts

After the final wash, protoplasts were re-suspended in electroporation buffer at an expected concentration of $5 \times 10^6$ protoplasts/ml (usually a resuspension volume of 15.5ml for dense plate preparations). 500µl aliquots of protoplast electroporation mix were disseminated into single use 1ml plastic cuvette prior to the addition of 100µl electroporation buffer containing variable volumes of effector plasmid DNA (gene of interest) and a consistent cargo molecule volume (Amylase, AmyHDEL, AmySPO) depending on maxiprep concentration. Protoplast suspensions were incubated with plasmid DNA preparations for 15-30 minutes then electroporated for 5 seconds between stainless steel plate electrodes spanning 3.5mm apart. A complete exponential discharge of a 1000-µF capacitor charged at 160V was connected to the electrodes. Electroporated protoplasts were left to recover for 30 minutes before pouring from the cuvettes into 5 cm Petri dishes, washing cuvettes

in 1ml TEX buffer and transferring to petri dish, twice. The following incubation of transformed protoplasts were performed for at least 24h, otherwise specified.

### 7.5.3 Harvesting of electroporated protoplasts

Protoplasts were harvested in different conditions depending on the assay required. From the total volume of 2.5ml, 500µl was taken for analysis in a GUS-normalised assay. The remaining 2ml of protoplast suspension was transferred to a 10ml falcon tube and used for protein extraction or α-amylase secretion assays. Tubes were centrifuged for 5 minutes at low speed of 100 x g to reduce damage to cells. After centrifugation the underlying medium was removed at a volume of approximately 1ml, then centrifuged at 14000rpm, 4°C for 10 minutes. 500µl on uncontaminated medium was transferred to new tubes and stored on ice or frozen for analysis in α-amylase assays. After this the remaining medium and cell layer were diluted to a volume of approximately 10ml in 250mM NaCl and recentrifuged at low speed again. After removing supernatant with a peristaltic pump all remaining cells are now contained as a pellet, which could be stored on ice or frozen until analysis in protein extractions or α-amylase secretion assays.

### 7.5.4 α-amylase secretion assays

The quantifiable α-amylase assay reagents releasing p-nitrophenol in quantities relative to α-amylase availability were purchased from Megazyme (http://secure.megazyme.com). The isolated protoplast medium suspensions from harvesting were combined in equal volume with α-amylase extraction buffer and a 1:1 dilution was usually suitable to carry out a 25-minute assay that remains in the photometric linear range without exhausting substrate. For cell pellets resuspension was carried out in 1ml α-amylase extraction buffer avoiding any solution reaching the lids and then sonicated for 5 seconds (130W, 20 KHz – 60% amplitude). Centrifugation followed sonication and was 10 minutes, 14000 rpm, 4°C and supernatant was used in assays, keeping stored on ice otherwise. Secretion assays were carried out in a 45°C water bath using 30µl of sample supernatant from either cells or medium in a time range of approximately 20 minutes for cells, which required a 1:10 dilution of supernatant with α-amylase extraction buffer. The reaction involved the addition of 30µl substrate (product

code: R-CAAR4) consisting of blocked p-nitrophenyl maltoheptaoside (BPNPG7, 54.5 mg) and thermostable α-glucosidase (125 units at pH 6.0)) which was dissolved as in the manufacturer's instructions (add 10ml of autoclaved distilled water, stored at −80°C as 1ml aliquots). The reaction was stopped by the addition of 150µl of reaction stop buffer (1% (w/v) Trizma base) leaving a final volume of 210µl. 200µl was transferred to a 96-well plate for each sample and absorbance was measured at 405nm. Negative controls for correcting absorbance were obtained from mock-transformed protoplasts and subsequently subtracted from all active samples. Amylase activity was calculated for medium and cells in the units ΔOD/minute/millilitre, factoring in resuspension volume, reaction dilution, sample volume then conversion to per ml, and incubation time (in minutes) as follows:

Medium (resuspension is 500µl medium with 500µl Amy extraction buffer, so multiply by 2):

α-amylase activity = ΔOD*2*dilution factor/30µl*1000/incubation time

Cells (resuspension is 2ml of pelleted cells resuspended in 950µl Amy extraction buffer, so divide by 2):

α-amylase activity = ΔOD/2*dilution factor/30*1000/incubation time

Only raw absorbance readings between 0.05 and 2.25 were accepted to avoid substrate limitations, with all electroporated samples being tested in biological triplicate and technical duplicate at a minimum.

### 7.5.5 GUS-normalized internal reference assays

The assay is intended and carried out as described by Gershlick *et al*. (2014), with some modifications. B-glucuronidase is cytosolically expressed and harvested as an internal marker to normalise plasmid expression levels between samples. All the reagents used were made according to the previously mentioned paper. 500µl protoplasts are combined with 500µl of GUS extraction buffer and kept always on ice. They are then sonicated for 5 seconds (130W, 20 KHz – 60% amplitude), and

centrifuged (refrigerated microfuge 4°C, 14000 rpm, and 10 minutes). Supernatant is diluted 10-fold and into 100µl reaction volumes, then combined with 100µl GUS reaction buffer. Samples were incubated at 37°C for between 14-18 hours, then the reaction was ended with 80µl stop buffer. 200µl was transferred into individual wells of a 96-well microtiter plate and absorbance was recorded at 405nm. GUS activity was calculated as ∆OD*2*dilution factor/100µl*1000/incubation time (hr) to end with the units ΔOD/ml/hr. Only raw absorbance readings between 0.05 and 2.5 were accepted to avoid substrate limitations, with all electroporated samples being tested in biological triplicate and technical duplicate at a minimum.

Best transfection practice (BTP) for new dual expression plasmid preparations was designed as a method of transfection quality control in order to define adequate GUS activity/plasmid expression from a typical electroporation. This is because the point at which GUS activity starts to approach a plateau is highly variable and cannot be predicted from the DNA concentration, therefore a relative activity, defined empirically as 30 units (given in ΔOD/ml/hr) prior to plateau conditions was deemed acceptable for BTP. Note that plateau values of up to 200 units can be reached. Plasmids that reached the GUS activity plateau with lower than 30 units were deemed unsuitable and were discarded. For GUS-normalised comparisons of different effector plasmids and for dose–response assays, plasmid doses were strictly determined volumetrically relative to the default plasmid concentration resulting in 30 GUS units. Generally lower doses were used to avoid conditions of overexpression, unless overexpression was intended for a given experiment.

## 7.6 Tobacco leaf infiltration and microscopy

Tobacco leaves were infiltrated with *Agrobacterium tumefaciens* cultures transformed with plasmids. Prior to infiltration the optical density of grown cultures were altered to 0.05-0.1 depending on the number of cultures included in the infiltration. The cultures were also washed twice and resuspended in infiltration buffer (50mM MES pH 5.6, 10mM $MgCl_2$, 0.5% glucose 100µm acetosyringone). Infiltrated regions were analysed 48-60 hours later via confocal laser scanning microscopy (CLSM). Preparation of cultures for infiltration has strictly followed previously published protocol (Sparkes *et al*., 2006).

## 7.7 Generation of transgenic plants by leaf-disk transformation

Nicotiana benthamiana (Goodin *et al*. 2008) plants, were grown in Murashige and Skoog (MS) medium with 2% sucrose in a controlled room at 25°C with a 16-h day-length at a light irradiance of 200μE m2s. Stably transformed plants were obtained by Agrobacterium infection of leaf disks as described by Denecke *et al*. (1990). Selection of transformants was accomplished in MS medium supplemented with 3% sucrose and containing 100 μg/mL kanamycin and 250 μg/mL cefotaxime. Regenerated plants were analysed and scored by CLSM.

## 7.8 Organelle markers

The markers ST-RFP and Aleu-RFP were used as previously (Bottanelli *et al*., 2012). The ER marker used was RFP-HDEL (Gershlick *et al*., 2014) and for the Golgi MNS3-RFP (Schoberer *et al*., 2019)

## 7.9 Fluorescence confocal microscope imaging and analysis

Infiltrated tobacco leaf squares (0.5 x 0.5 cm) were mounted in tap water with the lower epidermis facing the thin cover glass (22 x 50 mm; No. 0). Confocal imaging was performed using an upright Zeiss LSM 880 Laser Scanning Microscope (Zeiss) with a PMT detector and a Plan-Apochromat 40x/1.4 oil DIC M27 objective. When YFP-fusions were imaged alone, the excitation wavelength was 514nm and fluorescence was detected with a bandpass filter of 519-620nm. When RFP-fusions were imaged alone, the excitation wavelength was 561nm and fluorescence was detected with a bandpass filter 585-650nm. To image YFP-fusions together with RFP-fusions, samples were excited using an Argon ion laser at the wavelength of 488 nm for YFP and a HeNe ion laser at 561 nm for RFP. A 488/543 dichroic beam splitter was used to detect fluorescence, YFP fluorescence was detected with a bandpass filter 493-529 nm and RFP fluorescence was detected with a bandpass filter 585-650 nm. All dual colour imaging was performed by line switching to obtain adequate live bio-imaging data that are not distorted by organelle motion. Post-acquisition image processing was performed with the Zen 2.3 lite blue edition (Zeiss) and ImageJ (Schneider *et al*. 2012). Image analysis was undertaken using the ImageJ analysis program and the PSC co-localization plug-

in (French *et al*. 2008) to calculate co-localization and to produce scatter plots as described before (Foresti *et al*. 2010).

## 7.10 Mammalian Cell culture and transfections

The coding regions for the two fluorescent variants of plant and human ERD2 were inserted into the mammalian cell expression vector pcDNA3.1 under the transcriptional control of the CMV promoter, resulting in pJCA108 (YFP-TM-AtERD2), pJCA109 (AtERD2-YFP), pRB36 (YFP-TM-HsERD2), pRB52 (HsERD2-YFP).

HeLa CCL-2 cells were purchased from the American Type Culture Collection (Manassas, VA). These cells were cultured in Dulbecco's modified Eagle's medium (Thermo Fisher Scientific), supplemented with 100 units of penicillin/ml, 0.1 mg of streptomycin/ml, and 10% (v/v) fetal bovine serum (FBS). HeLa cells were transiently transfected with the plasmids indicated in the figure legends by using Lipofectamine 2000 reagent (Thermo Fisher Scientific) according to the manufacturer's instructions.

For immunofluorescence assays, the following antibodies were used: the monoclonal mouse antibodies to GM130 (1:200 dilution; catalog no.: 610822; clone 35/GM130; BD Biosciences), sheep polyclonal anti-TGN46 (1:400 dilution; catalog no.: AHP500; Bio-Rad). Secondary antibodies conjugated to Alexa fluorophores were purchased from Thermo Fisher Scientific.

Immunofluorescence was performed as previously described (Tavarez *et al*., 2017). Briefly, cells were fixed for 15 min at RT with 4% (w/v) PFA in PBS. PFA-fixed cells were permeabilized with 0.01% (w/v) saponin in blocking solution (0.2% [w/v] pork skin gelatin in PBS) for 30 min at 37 °C, and double labeled with specific primary and secondary Alexa-conjugated antibodies. Cells were imaged on a Zeiss confocal laser-scanning microscope 780 (Zeiss). Post-acquisition image processing was performed with Fiji/ImageJ software (https://imagej.net/software/fiji/).

**Table 1 - List of Constructs Used in This Project**

All existing and new constructs generated in this thesis are listed in table 1. All vectors were confirmed with qualitative digest and sequencing by Source BioScience.

| Description | Reference/Generated by |
|---|---|
| 35s:α-amylase | (Crofts *et al*., 1999) |
| 35s:α-amylase-HDEL | (Phillipson *et al*., 2001) |
| 35s:α-amylase-SPORAMIN | (Pimpl *et al*., 2003) |
| TR2:GUS 35s:ERD2b | (An, 2015) |
| TR2:GUS 35s:TM-ERD2b | (Silva-Alvim *et al*., 2018) |
| TR2:RFP-TM-ERD2::p24tail KKSS | (Alvim, 2018) |
| TR2:RFP-TM-ERD2::p24tail | (Alvim, 2018) |
| TR2:ST-RFP | (An, 2015) |
| 35S: RFP-HDEL | (Gershlick *et al*., 2014) |
| TR2:GUS 35s:atERD2b-HA | (An, 2015) |
| CMV:YFP-TM-AtERD2b | (Alvim, 2018) |
| CMV:ERD2b-YFP | (Alvim, 2018) |
| TR2-YFP-TM-AtERD2b | (Silva-Alvim *et al*., 2018) |
| TR2-YFP-TM-AtERD2bΔC5 | (Alvim, 2018) |
| TR2-RFP-TM-ERD2 | (Alvim, 2018) |
| TR2-GUS-3'ocs-35S-ERD2KKLIadd-3'nos | R Bolt |
| TR2-YFP-TM-ERD2KCDrep-3'nos | R Bolt |
| TR2-YFP-TM-ERD2KKLIadd-3'nos | R Bolt |
| TR2-YFP-TM-ERD2KCDadd-3'nos | R Bolt |
| TR2-GUS-3'ocs:35S-ERD2p24tailKK^SS-3'nos | R Bolt |
| TR2-GUS-3'ocs:35S-ERD2G1-3'nos | R Bolt |
| TR2-GUS-3'ocs:35S-ERD2A1-3'nos | R Bolt |
| TR2-YFP-TM-ERD2bΔC5 R5A | R Bolt |
| TR2-YFP-TM-humanERD2-3'nos (KDELR2) | R Bolt |
| TR2-YFP-TM-hERD2S209A | R Bolt |
| TR2-YFP-TM-hERD2S209D | R Bolt |
| TR2-YFP-TM-hERD2LLGG | R Bolt |

| | |
|---|---|
| TR2-GUS-3'ocs:35S-(AtERD2)THB1-3'nos | R Bolt |
| TR2-GUS-3'ocs:35S-(AtERD2)THB2-3'nos | R Bolt |
| TR2-GUS-3'ocs:35S-(AtERD2)SPTHB2-3'nos | R Bolt |
| TR2::YFP-1TM-ERD2bK206A-3'nos | R Bolt |
| TR2::YFP-1TM-ERD2bK209A-3'nos | R Bolt |
| TR2::YFP-1TM-ERD2bK210A-3'nos | R Bolt |
| TR2-GUS-3'ocs:35S-HuERD2-HA-3'nos | D Hirsz |
| TR2-GUS-3'ocs:35S-HuERD2-myc-3'nos | D Hirsz |
| TR2-GUS-3'ocs:35S-HuERD2-FLAG-3'nos | D Hirsz |
| TR2-YFP-TM-huERD2-HA-3'nos | D Hirsz |
| TR2-YFP-TM-huERD2-myc-3'nos | D Hirsz |
| TR2-YFP-TM-huERD2-FLAG-3'nos | D Hirsz |
| TR2-GUS-3'ocs-35S-huERD2K206A^K207A-3'nos | N Bencka |
| TR2-YFP-TM-huERD2-K206A^K207A-3'nos | N Bencka |
| TR2-YFP-1TM-ERD2b-FLAG-3'nos | M Christaki |
| TR2-YFP-1TM-ERD2b-myc-3'nos | M Christaki |
| TR2-YFP-1TM-ERD2b-HA-3'nos | M Christaki |
| TR2-GUS-3'ocs-35S-hERD2-YFP-3'nos | R Bolt |
| TR2-GUS-3'OCS:35S-YFP-TM-huERD2-3'NOS | R Bolt |
| TR2-GUS-3'OCS:35S-LPYS-TM-ERD2-3'NOS | R Bolt |
| TR2-GUS-3'OCS:35S-LPYS-TM-ERD2-YFP-3'NOS | R Bolt |
| TR2-GUS-3'OCS:35S-LPYS-TM-ERD2LL^GG-3'NOS | R Bolt |
| TR2-ERD2b-YFP-3'nos | M Hu |
| CMV-YFP-TM-hERD2 | R Bolt |
| TR2-hERD2b-YFP-3'nos | R Bolt |
| TR2-NbMNS3-RFP-3'nos | R Bolt |
| TR2-LPYS-TM-ERD2-YFP-3'nos | R Bolt |
| TR2-TM-ERD2b-YFP-3'nos | R Bolt |
| TR2-GUS-35S-shortLPYS-TM-THB1-3'nos | R Bolt |
| TR2-GUS-35S-TM-THB1-3'NOS | R Bolt |
| CMV-hERD2b-YFP | R Bolt |
| TR2-YFP-TM-THB1-3'NOS | R Bolt |
| TR2-GUS-35S-TM-THB2-3'nos | R Bolt |

| | |
|---|---|
| TR2-RFP-TM4-THB2-3'nos | R Bolt |
| TR2-YFP-TM4-THB2-3'nos | R Bolt |
| TR2-GUS-35S-LPYS-1TM-THB2-3'nos | R Bolt |
| TR2-GUS-35S-ERD2b-deltaC5-3'nos | R Bolt |
| TR2-GUS-3'ocs-35S-TM4-THB2-3'nos | R Bolt |
| TR2-GUS-35S-LPYS-1TM-THB2deltaC5-3'nos | R Bolt |
| TR2-GUS-3'OCS-35S-LPYS-1TM-THB2-YFP-3'nos | R Bolt |
| TR2-ERD2b-YFP-3'ocs-35s-ERD2 AB hybrid AS-3'nos | R Bolt |
| 35S-Amy-3'nos-TR2-YFP-1TM-ERD2bΔC5 | R Bolt |
| 35S-Amy-HDEL-3'nos-TR2-YFP-1TM-ERD2bΔC5 | R Bolt |
| 35S-Amy-3'nos-TR2-YFP-1TM-ERD2b | R Bolt |
| 35S-Amy-HDEL-3'nos-TR2-YFP-1TM-ERD2b | R Bolt |
| TR2-hERD2b-YFP-3'ocs-35s-ERD2 AB hybrid AS-3'nos | R Bolt |
| TR2-GUS-35S-LPYS-1TM-Mprotein-3'nos | E Cooper |
| TR2-GUS-35S-LPYS-1TM-Mprotein THB-3'nos | B Potter |
| TR2-secYFP-Mprotein THB-3'nos | B Potter |
| TR2-secYFP-M protein-3'nos | B Potter |

Abbreviations: 35S: Cauliflower mosaic virus promoter; 3'nos: 3' untranslated end of nopaline synthase gene; TR2': TR-DNA derived mas 2'; CMV: cytomegalovirus immediate-early enhancer and promoter.

# Chapter 8 - Bibliography

ALVIM, J. C. 2018. On the mechanisms of receptor-mediated retention of soluble endoplasmic reticulum resident proteins in eukaryotes. University of Leeds, PhD, 213.

ALVIM, J. C., BOLT, R. M., AN, J., KAMISUGI, Y., CUMING, A., SILVA-ALVIM, F. A. L., CONCHA, J. O., daSILVA, L. L. P., HU, M., HIRSZ, D., DENECKE, J. 2023. The K/HDEL receptor does not recycle but instead acts as a Golgi-gatekeeper. *Nat Commun* **14**, 1612.

ALVIM KAMEI, C. L., BORUC, J., VANDEPOELE, K., VAN DEN DAELE, H., MAES, S., RUSSINOVA, E., INZÉ, D. & DE VEYLDER, L. 2008. The PRA1 gene family in Arabidopsis. Plant Physiol, 147, 1735-49.

AN, J. 2015. Elucidating the recycling mechanism of ER resident proteins with ERD2.

ANELLI, T. & SITIA, R. 2008. Protein quality control in the early secretory pathway. The EMBO Journal, 27, 315-327.

ANTONNY, B., MADDEN, D., HAMAMOTO, S., ORCI, L. & SCHEKMAN, R. 2001. Dynamics of the COPII coat with GTP and stable analogues. Nat Cell Biol, 3, 531-7.

AOE, T., CUKIERMAN, E., LEE, A., CASSEL, D., PETERS, P. J. & HSU, V. W. 1997. The KDEL receptor, ERD2, regulates intracellular traffic by recruiting a GTPase-activating protein for ARF1. Embo Journal, 16, 7305-7316.

AOE, T., LEE, A. J., VAN DONSELAAR, E., PETERS, P. J. & HSU, V. W. 1998. Modulation of intracellular transport by transported proteins: Insight from regulation of COPI-mediated transport. Proceedings of the National Academy of Sciences of the United States of America, 95, 1624-1629.

APPENZELLER-HERZOG, C. & HAURI, H. P. 2006. The ER-Golgi intermediate compartment (ERGIC): in search of its identity and function. Journal of Cell Science, 119, 2173-2183.

ARVAN, P. & CASTLE, D. 1998. Sorting and storage during secretory granule biogenesis: looking backward and looking forward. Biochem J, 332 ( Pt 3), 593-610.

BARLOWE, C., D'ENFERT, C. & SCHEKMAN, R. 1993. Purification and characterization of SAR1p, a small GTP-binding protein required for transport vesicle formation from the endoplasmic reticulum. J Biol Chem, 268, 873-9.

BARLOWE, C., ORCI, L., YEUNG, T., HOSOBUCHI, M., HAMAMOTO, S., SALAMA, N., REXACH, M. F., RAVAZZOLA, M., AMHERDT, M. & SCHEKMAN, R. 1994. COPII: A membrane coat formed by Sec proteins that drive vesicle budding from the endoplasmic reticulum. Cell, 77, 895-907.

BARLOWE, C. & SCHEKMAN, R. 1993. SEC12 ENCODES A GUANINE-NUCLEOTIDE-EXCHANGE FACTOR ESSENTIAL FOR TRANSPORT VESICLE BUDDING FROM THE ER. Nature, 365, 347-349.

BECKER, B., SHAEBANI, M. R., RAMMO, D., BUBEL, T., SANTEN, L. & SCHMITT, M. J. 2016. Cargo binding promotes KDEL receptor clustering at the mammalian cell surface. Scientific Reports, 6.

BETHUNE, J. & WIELAND, F. T. 2018. Assembly of COPI and COPII Vesicular Coat Proteins on Membranes. Annual Review of Biophysics, Vol 47, 47, 63-83.

BEZNOUSSENKO, G. V., RAGNINI-WILSON, A., WILSON, C. & MIRONOV, A. A. 2016. Three-dimensional and immune electron microscopic analysis of the secretory pathway in Saccharomyces cerevisiae. Histochem Cell Biol, 146, 515-527.

BI, X., CORPINA, R. A. & GOLDBERG, J. 2002. Structure of the Sec23/24-Sar1 pre-budding complex of the COPII vesicle coat. Nature, 419, 271-7.

BI, X., MANCIAS, J. D. & GOLDBERG, J. 2007. Insights into COPII coat nucleation from the structure of Sec23.Sar1 complexed with the active fragment of Sec31. Dev Cell, 13, 635-645.

BIELLI , A., HANEY , C. J., GABRESKI , G., WATKINS , S. C., BANNYKH , S. I. & ARIDOR , M. 2005. Regulation of Sar1 NH2 terminus by GTP binding and hydrolysis promotes membrane deformation to control COPII vesicle fission. Journal of Cell Biology, 171, 919-924.

BLOBEL, G. & DOBBERSTEIN, B. 1975. Transfer of proteins across membranes. I. Presence of proteolytically processed and unprocessed nascent immunoglobulin light chains on membrane-bound ribosomes of murine myeloma. J Cell Biol, 67, 835-51.

BLOBEL, G. & SABATINI, D. D. 1971. Ribosome-Membrane Interaction in Eukaryotic Cells. In: MANSON, L. A. (ed.) Biomembranes: Volume 2. Boston, MA: Springer US.

BOEVINK, P., OPARKA, K., CRUZ, S. S., MARTIN, B., BETTERIDGE, A. & HAWES, C. 1998. Stacks on tracks: the plant Golgi apparatus traffics on an actin/ER network. Plant Journal, 15, 441-447.

BONIFACINO, J. S. & LIPPINCOTT-SCHWARTZ, J. 2003. Coat proteins: shaping membrane transport. Nature Reviews Molecular Cell Biology, 4, 409-414.

BORGNE, R. L. & HOFLACK, B. 1997. Mannose 6-Phosphate Receptors Regulate the Formation of Clathrin-coated Vesicles in the TGN. Journal of Cell Biology, 137, 335-345.

BRACH, T., SOYK, S., MULLER, C., HINZ, G., HELL, R., BRANDIZZI, F. & MEYER, A. J. 2009. Non-invasive topology analysis of membrane proteins in the secretory pathway. Plant J, 57, 534-41.

BRANDIZZI, F. & BARLOWE, C. 2013. Organization of the ER-Golgi interface for membrane traffic control. Nat Rev Mol Cell Biol, 14, 382-92.

BRAULKE, T. & BONIFACINO, J. S. 2009. Sorting of lysosomal proteins. Biochim Biophys Acta, 1793, 605-14.

BRODSKY, F. M., HILL, B. L., ACTON, S. L., NÄTHKE, I., WONG, D. H., PONNAMBALAM, S. & PARHAM, P. 1991. Clathrin light chains: arrays of protein motifs that regulate coated-vesicle dynamics. Trends Biochem Sci, 16, 208-13.

BRÄUER, P., PARKER, J. L., GERONDOPOULOS, A., ZIMMERMANN, I., SEEGER, M. A., BARR, F. A. & NEWSTEAD, S. 2019. Structural basis for pH-dependent retrieval of ER proteins from the Golgi by the KDEL receptor. 363, 1103-1107.

CABRERA, M., MUÑIZ, M., HIDALGO, J., VEGA, L., MARTÍN, M. E. & VELASCO, A. 2003. The Retrieval Function of the KDEL Receptor Requires PKA Phosphorylation of Its C-Terminus. Molecular Biology of the Cell, 14, 4114-4125.

CASADABAN, M. J. & COHEN, S. N. 1980. Analysis of gene control signals by DNA fusion and cloning in Escherichia coli. J Mol Biol, 138, 179-207.

CANCINO, J., CAPALBO, A., DI CAMPLI, A., GIANNOTTA, M., RIZZO, R., JUNG, J. E., DI MARTINO, R., PERSICO, M., HEINKLEIN, P., SALLESE, M. & LUINI, A. 2014. Control systems of membrane transport at the interface between the endoplasmic reticulum and the Golgi. Dev Cell, 30, 280-94.

CERIOTTI, A. & COLMAN, A. 1988. Binding to membrane proteins within the endoplasmic reticulum cannot explain the retention of the glucose-regulated protein GRP78 in Xenopus oocytes. The EMBO journal, 7, 633-638.

CHEN, Y. & BRANDIZZI, F. 2013. IRE1: ER stress sensor and cell fate executor. Trends Cell Biol, 23, 547-55.

CLARY, D. O., GRIFF, I. C. & ROTHMAN, J. E. 1990. SNAPs, a family of NSF attachment proteins involved in intracellular membrane fusion in animals and yeast. Cell, 61, 709-21.

CONTRERAS, I., ORTIZ-ZAPATER, E. & ANIENTO, F. 2004a. Sorting signals in the cytosolic tail of membrane proteins involved in the interaction with plant ARF1 and coatomer. Plant Journal, 38, 685-698.

CONTRERAS, I., YANG, Y., ROBINSON, D. G. & ANIENTO, F. 2004b. Sorting signals in the cytosolic tail of plant p24 proteins involved in the interaction with the COPII coat. Plant Cell Physiol, 45, 1779-86.

COPIC, A., LATHAM, C. F., HORLBECK, M. A., D'ARCANGELO, J. G. & MILLER, E. A. 2012. ER Cargo Properties Specify a Requirement for COPII Coat Rigidity Mediated by Sec13p. Science, 335, 1359-1362.

COSSON, P. & LETOURNEUR, F. 1994. Coatomer interaction with di-lysine endoplasmic reticulum retention motifs. Science, 263, 1629-31.

CROFTS, A. J., LEBORGNE-CASTEL, N., HILLMER, S., ROBINSON, D. G., PHILLIPSON, B., CARLSSON, L. E., ASHFORD, D. A. & DENECKE, J. 1999. Saturation of the endoplasmic reticulum retention machinery reveals anterograde bulk flow. Plant Cell, 11, 2233-48.

CUKIERMAN, E., HUBER, I., ROTMAN, M. & CASSEL, D. 1995. The ARF1 GTPase-activating protein: zinc finger motif and Golgi complex localization. Science, 270, 1999-2002.

D'ENFERT, C., BARLOWE, C., NISHIKAWA, S., NAKANO, A. & SCHEKMAN, R. 1991a. Structural and functional dissection of a membrane glycoprotein required for vesicle budding from the endoplasmic reticulum. Mol Cell Biol, 11, 5727-34.

D'ENFERT, C., WUESTEHUBE, L. J., LILA, T. & SCHEKMAN, R. 1991b. Sec12p-dependent membrane binding of the small GTP-binding protein Sar1p promotes formation of transport vesicles from the ER. Journal of Cell Biology, 114, 663-670.

DASILVA, L. L., SNAPP, E. L., DENECKE, J., LIPPINCOTT-SCHWARTZ, J., HAWES, C. & BRANDIZZI, F. 2004. Endoplasmic reticulum export sites and Golgi bodies behave as single mobile secretory units in plant cells. Plant Cell, 16, 1753-71.

DASILVA, L. L. P., FORESTI, O. & DENECKE, J. 2006. Targeting of the plant vacuolar sorting receptor BP80 is dependent on multiple sorting signals in the cytosolic tail. The Plant cell, 18, 1477-1497.

DEAN, N. & PELHAM, H. R. B. 1990. RECYCLING OF PROTEINS FROM THE GOLGI COMPARTMENT TO THE ER IN YEAST. Journal of Cell Biology, 111, 369-377.

DENECKE, J., BOTTERMAN, J. & DEBLAERE, R. 1990. Protein secretion in plant cells can occur via a default pathway. Plant Cell, 2, 51-9.

DENECKE, J., DE RYCKE, R. & BOTTERMAN, J. 1992. Plant and mammalian sorting signals for protein retention in the endoplasmic reticulum contain a conserved epitope. Embo j, 11, 2345-55.

DODONOVA, S. O., ADERHOLD, P., KOPP, J., GANEVA, I., RÖHLING, S., HAGEN, W. J. H., SINNING, I., WIELAND, F. & BRIGGS, J. A. G. 2017. 9Å structure of the COPI coat reveals that the Arf1 GTPase occupies two contrasting molecular environments. eLife, 6, e26691.

DODONOVA, S. O., DIESTELKOETTER-BACHERT, P., VON APPEN, A., HAGEN, W. J. H., BECK, R., BECK, M., WIELAND, F. & BRIGGS, J. A. G. 2015. A structure of the COPI coat and the role of coat proteins in membrane vesicle assembly. Science, 349, 195-198.

DOMINGUEZ, M., DEJGAARD, K., FÜLLEKRUG, J., DAHAN, S., FAZEL, A., PACCAUD, J. P., THOMAS, D. Y., BERGERON, J. J. & NILSSON, T. 1998. gp25L/emp24/p24 protein family members of the cis-Golgi network bind both COP I and II coatomer. J Cell Biol, 140, 751-65.

DONOHOE, B. S., KANG, B.-H. & STAEHELIN, L. A. 2007. Identification and characterization of COPIa- and COPIb-type vesicle classes associated with plant and algal Golgi. 104, 163-168.

DUNCAN, J. R. & KORNFELD, S. 1988. Intracellular movement of two mannose 6-phosphate receptors: return to the Golgi apparatus. J Cell Biol, 106, 617-28.

ELAZAR, Z., SCHERZ-SHOUVAL, R. & SHORER, H. 2003. Involvement of LMA1 and GATE-16 family members in intracellular membrane dynamics. Biochim Biophys Acta, 1641, 145-56.

ELLGAARD, L., RIEK, R., HERRMANN, T., GÜNTERT, P., BRAUN, D., HELENIUS, A. & WÜTHRICH, K. 2001. NMR structure of the calreticulin P-domain. Proc Natl Acad Sci U S A, 98, 3133-8.

EUGSTER, A., FRIGERIO, G., DALE, M. & DUDEN, R. 2004. The α- and β′-COP WD40 Domains Mediate Cargo-selective Interactions with Distinct Di-lysine Motifs. Molecular Biology of the Cell, 15, 1011-1023.

FASSHAUER, D., SUTTON, R. B., BRUNGER, A. T. & JAHN, R. 1998. Conserved structural features of the synaptic fusion complex: SNARE proteins reclassified as Q- and R-SNAREs. Proc Natl Acad Sci U S A, 95, 15781-6.

FIEDLER, K., VEIT, M., STAMNES, M. A. & ROTHMAN, J. E. 1996. Bimodal interaction of coatomer with the p24 family of putative cargo receptors. Science, 273, 1396-9.

FLYNN, G. C., POHL, J., FLOCCO, M. T. & ROTHMAN, J. E. 1991. Peptide-binding specificity of the molecular chaperone BiP. Nature, 353, 726-730.

FORESTI, O., DASILVA, L. L. & DENECKE, J. 2006. Overexpression of the Arabidopsis syntaxin PEP12/SYP21 inhibits transport from the prevacuolar compartment to the lytic vacuole in vivo. Plant Cell, 18, 2275-93.

FORESTI, O., GERSHLICK, D. C., BOTTANELLI, F., HUMMEL, E., HAWES, C. & DENECKE, J. 2010. A Recycling-Defective Vacuolar Sorting Receptor Reveals an Intermediate Compartment Situated between Prevacuoles and Vacuoles in Tobacco. Plant Cell, 22, 3992-4008.

FRA, A. M., FAGIOLI, C., FINAZZI, D., SITIA, R. & ALBERINI, C. M. 1993. Quality control of ER synthesized proteins: an exposed thiol group as a three-way switch mediating assembly, retention and degradation. The EMBO Journal, 12, 4755-4761.

FRENCH, A. P., MILLS, S., SWARUP, R., BENNETT, M. J. & PRIDMORE, T. P. 2008. Colocalization of fluorescent markers in confocal microscope images of plant cells. Nat Protoc, 3, 619-28.

FRIGERIO, G., GRIMSEY, N., DALE, M., MAJOUL, I. & DUDEN, R. 2007. Two human ARFGAPs associated with COP-I-coated vesicles. Traffic, 8, 1644-55.

FRÜHOLZ, S., FÄßLER, F., KOLUKISAOGLU, Ü. & PIMPL, P. 2018. Nanobody-triggered lockdown of VSRs reveals ligand reloading in the Golgi. Nature Communications, 9, 643.

GAO, C. J., YU, C. K. Y., QU, S., SAN, M. W. Y., LI, K. Y., LO, S. W. & JIANG, L. W. 2012. The Golgi-Localized Arabidopsis Endomembrane Protein12 Contains Both Endoplasmic Reticulum Export and Golgi Retention Signals at Its C Terminus C. Plant Cell, 24, 2086-2104.

GARCÍA-MATA, R., SZUL, T., ALVAREZ, C. & SZTUL, E. 2003. ADP-Ribosylation Factor/COPI-dependent Events at the Endoplasmic Reticulum-Golgi Interface Are Regulated by the Guanine Nucleotide Exchange Factor GBF1. Molecular Biology of the Cell, 14, 2250-2261.

GERONDOPOULOS, A., BRÄUER, P., SOBAJIMA, T., WU, Z., PARKER, J. L., BIGGIN, P. C., BARR, F. A. & NEWSTEAD, S. 2021. A signal capture and proofreading mechanism for the KDEL-receptor explains selectivity and dynamic range in ER retrieval. eLife, 10, e68380.

GERSHLICK, D. C., LOUSA CDE, M., FORESTI, O., LEE, A. J., PEREIRA, E. A., DASILVA, L. L., BOTTANELLI, F. & DENECKE, J. 2014. Golgi-dependent transport of vacuolar sorting receptors is regulated by COPII, AP1, and AP4 protein complexes in tobacco. Plant Cell, 26, 1308-29.

GLICK, B. S. & LUINI, A. 2011. Models for Golgi traffic: a critical assessment. Cold Spring Harb Perspect Biol, 3, a005215.

GOODIN, M. M., ZAITLIN, D., NAIDU, R. A. & LOMMEL, S. A. 2008. Nicotiana benthamiana: its history and future as a model for plant-pathogen interactions. Mol Plant Microbe Interact, 21, 1015-26.

HAAS, I. G. & WABL, M. 1983. Immunoglobulin heavy chain binding protein. Nature, 306, 387-9.

HAMMAN, B. D., HENDERSHOT, L. M. & JOHNSON, A. E. 1998. BiP maintains the permeability barrier of the ER membrane by sealing the lumenal end of the translocon pore before and early in translocation. Cell, 92, 747-58.

HAMMOND, A. T. & GLICK, B. S. 2000. Dynamics of transitional endoplasmic reticulum sites in vertebrate cells. Mol Biol Cell, 11, 3013-30.

HARA-KUGE, S., KUGE, O., ORCI, L., AMHERDT, M., RAVAZZOLA, M., WIELAND, F. T. & ROTHMAN, J. E. 1994. En bloc incorporation of coatomer subunits during the assembly of COP-coated vesicles. J Cell Biol, 124, 883-92.

HARDING, H. P., ZHANG, Y. & RON, D. 1999. Protein translation and folding are coupled by an endoplasmic-reticulum-resident kinase. Nature, 397, 271-4.

HARDWICK, K. G., LEWIS, M. J., SEMENZA, J., DEAN, N. & PELHAM, H. R. B. 1990. ERD1, A YEAST GENE REQUIRED FOR THE RETENTION OF LUMINAL ENDOPLASMIC-RETICULUM PROTEINS, AFFECTS GLYCOPROTEIN PROCESSING IN THE GOLGI-APPARATUS. Embo Journal, 9, 623-630.

HARDWICK, K. G. & PELHAM, H. R. B. 1992. SED5 ENCODES A 39-KD INTEGRAL MEMBRANE-PROTEIN REQUIRED FOR VESICULAR TRANSPORT BETWEEN THE ER AND THE GOLGI-COMPLEX. Journal of Cell Biology, 119, 513-521.

HAWES, C., KIVINIEMI, P. & KRIECHBAUMER, V. 2015. The endoplasmic reticulum: a dynamic and well-connected organelle. J Integr Plant Biol, 57, 50-62.

HAZE, K., YOSHIDA, H., YANAGI, H., YURA, T. & MORI, K. 1999. Mammalian transcription factor ATF6 is synthesized as a transmembrane protein and activated by proteolysis in response to endoplasmic reticulum stress. Mol Biol Cell, 10, 3787-99.

HENDERSON, M. J., RICHIE, C. T., AIRAVAARA, M., WANG, Y. & HARVEY, B. K. 2013. Mesencephalic astrocyte-derived neurotrophic factor (MANF) secretion and cell surface binding are modulated by KDEL receptors. J Biol Chem, 288, 4209-25.

HETZ, C., MARTINON, F., RODRIGUEZ, D. & GLIMCHER, L. H. 2011. The Unfolded Protein Response: Integrating Stress Signals Through the Stress Sensor IRE1α. Physiological Reviews, 91, 1219-1243.

HEUCKEN, N. & IVANOV, R. 2018. The retromer, sorting nexins and the plant endomembrane protein trafficking. Journal of Cell Science, 131.

HICKE, L. & SCHEKMAN, R. 1989. Yeast Sec23p acts in the cytoplasm to promote protein transport from the endoplasmic reticulum to the Golgi complex in vivo and in vitro. Embo j, 8, 1677-84.

HICKE, L., YOSHIHISA, T. & SCHEKMAN, R. 1992. SEC23P AND A NOVEL 105-KDA PROTEIN FUNCTION AS A MULTIMERIC COMPLEX TO PROMOTE VESICLE BUDDING AND PROTEIN-TRANSPORT FROM THE ENDOPLASMIC-RETICULUM. Molecular Biology of the Cell, 3, 667-676.

HOFFMANN, N., KING, S., SAMUELS, A. L. & MCFARLANE, H. E. 2021. Subcellular coordination of plant cell wall synthesis. Dev Cell, 56, 933-948.

HSU, V. W., SHAH, N. & KLAUSNER, R. D. 1992. A brefeldin A-like phenotype is induced by the overexpression of a human ERD-2-like protein, ELP-1. Cell, 69, 625-35.

HU, J., SHIBATA, Y., ZHU, P. P., VOSS, C., RISMANCHI, N., PRINZ, W. A., RAPOPORT, T. A. & BLACKSTONE, C. 2009. A class of dynamin-like GTPases involved in the generation of the tubular ER network. Cell, 138, 549-61.

HUANG, M. D., WEISSMAN, J. T., BERAUD-DUFOUR, S., LUAN, P., WANG, C. Q., CHEN, W., ARIDOR, M., WILSON, I. A. & BALCH, W. E. 2001. Crystal structure of Sar1-GDP at 1.7 angstrom resolution and the role of the NH2 terminus in ER export. Journal of Cell Biology, 155, 937-948.

HUOTARI, J. & HELENIUS, A. 2011. Endosome maturation. Embo Journal, 30, 3481-3500.

HWANG, C., SINSKEY, A. J. & LODISH, H. F. 1992. Oxidized redox state of glutathione in the endoplasmic reticulum. Science, 257, 1496-502.

ITO, Y., UEMURA, T. & NAKANO, A. 2018. The Golgi entry core compartment functions as a COPII-independent scaffold for ER-to-Golgi transport in plant cells. J Cell Sci, 131.

JACKSON, L. P., KELLY, B. T., MCCOY, A. J., GAFFRY, T., JAMES, L. C., COLLINS, B. M., HÖNING, S., EVANS, P. R. & OWEN, D. J. 2010. A large-scale conformational change couples membrane recruitment to cargo binding in the AP2 clathrin adaptor complex. Cell, 141, 1220-9.

JACKSON, L. P., LEWIS, M., KENT, H. M., EDELING, M. A., EVANS, P. R., DUDEN, R. & OWEN, D. J. 2012. Molecular basis for recognition of dilysine trafficking motifs by COPI. Dev Cell, 23, 1255-62.

JACKSON, M. R., NILSSON, T. & PETERSON, P. A. 1990. Identification of a consensus motif for retention of transmembrane proteins in the endoplasmic reticulum. The EMBO journal, 9, 3153-3162.

JACKSON, M. R., NILSSON, T. & PETERSON, P. A. 1993. Retrieval of transmembrane proteins to the endoplasmic reticulum. J Cell Biol, 121, 317-33.

JAMIESON, J. D. & PALADE, G. E. 1967. Intracellular transport of secretory proteins in the pancreatic exocrine cell. II. Transport to condensing vacuoles and zymogen granules. J Cell Biol, 34, 597-615.

JANSON, I. M., TOOMIK, R., O'FARRELL, F. & EK, P. 1998. KDEL motif interacts with a specific sequence in mammalian erd2 receptor. Biochemical and Biophysical Research Communications, 247, 447-451.

JIA, J., YUE, X., ZHU, L., JING, S., WANG, Y., GIM, B., QIAN, Y. & LEE, I. 2021. KDEL receptor is a cell surface receptor that cycles between the plasma membrane and the Golgi via clathrin-mediated transport carriers. Cell Mol Life Sci, 78, 1085-1100.

JOHNSON, A. E. & WAES, M. A. V. 1999. The Translocon: A Dynamic Gateway at the ER Membrane. Annual Review of Cell and Developmental Biology, 15, 799-842.

KAUFMAN, R. J. 2004. Regulation of mRNA translation by protein folding in the endoplasmic reticulum. Trends in Biochemical Sciences, 29, 152-158.

KEENAN, R. J., FREYMANN, D. M., STROUD, R. M. & WALTER, P. 2001. The signal recognition particle. Annu Rev Biochem, 70, 755-75.

KELLY, B. T., GRAHAM, S. C., LISKA, N., DANNHAUSER, P. N., HÖNING, S., UNGEWICKELL, E. J. & OWEN, D. J. 2014. Clathrin adaptors. AP2 controls clathrin polymerization with a membrane-activated switch. Science, 345, 459-63.

KELLY, B. T., MCCOY, A. J., SPÄTE, K., MILLER, S. E., EVANS, P. R., HÖNING, S. & OWEN, D. J. 2008. A structural explanation for the binding of endocytic dileucine motifs by the AP2 complex. Nature, 456, 976-979.

KHALKHALL, Z. & MARSHALL, R. D. 1975. Glycosylation of ribonuclease A catalysed by rabbit liver extracts. Biochem J, 146, 299-307.

KIRCHHAUSEN, T. 1999. Adaptors for clathrin-mediated traffic. Annu Rev Cell Dev Biol, 15, 705-32.

KIRCHHAUSEN, T., HARRISON, S. C., CHOW, E. P., MATTALIANO, R. J., RAMACHANDRAN, K. L., SMART, J. & BROSIUS, J. 1987. Clathrin heavy chain: molecular cloning and complete primary structure. Proc Natl Acad Sci U S A, 84, 8805-9.

KIRSCH, T., PARIS, N., BUTLER, J. M., BEEVERS, L. & ROGERS, J. C. 1994. Purification and initial characterization of a potential plant vacuolar targeting receptor. 91, 3403-3407.

KIRSCH, T., SAALBACH, G., RAIKHEL, N. V. & BEEVERS, L. 1996. Interaction of a potential vacuolar targeting receptor with amino- and carboxyl-terminal targeting determinants. Plant Physiol, 111, 469-74.

KITAKURA, S., VANNESTE, S., ROBERT, S., LÖFKE, C., TEICHMANN, T., TANAKA, H. & FRIML, J. 2011. Clathrin mediates endocytosis and polar distribution of PIN auxin transporters in Arabidopsis. Plant Cell, 23, 1920-31.

KLUMPERMAN, J., LOCKER, J. K., MEIJER, A., HORZINEK, M. C., GEUZE, H. J. & ROTTIER, P. J. 1994. Coronavirus M proteins accumulate in the Golgi complex beyond the site of virion budding. J Virol, 68, 6523-34.

KORNFELD, S. 1992. Structure and function of the mannose 6-phosphate/insulinlike growth factor II receptors. Annu Rev Biochem, 61, 307-30.

KORNFELD, S. & MELLMAN, I. 1989. The biogenesis of lysosomes. Annu Rev Cell Biol, 5, 483-525.

KOVTUN, O., DICKSON, V. K., KELLY, B. T., OWEN, D. J. & BRIGGS, J. A. G. 2020. Architecture of the AP2/clathrin coat on the membranes of clathrin-coated vesicles. Sci Adv, 6, eaba8381.

LANGHANS, M., MARCOTE, M. J., PIMPL, P., VIRGILI-LOPEZ, G., ROBINSON, D. G. & ANIENTO, F. 2008. In vivo trafficking and localization of p24 proteins in plant cells. Traffic, 9, 770-85.

LATIJNHOUWERS, M., GILLESPIE, T., BOEVINK, P., KRIECHBAUMER, V., HAWES, C. & CARVALHO, C. M. 2007. Localization and domain characterization of Arabidopsis golgin candidates. Journal of Experimental Botany, 58, 4373-4386.

LEBORGNE-CASTEL, N., JELITTO-VAN DOOREN, E. P., CROFTS, A. J. & DENECKE, J. 1999. Overexpression of BiP in tobacco alleviates endoplasmic reticulum stress. The Plant cell, 11, 459-470.

LEE, H. I., GAL, S., NEWMAN, T. C. & RAIKHEL, N. V. 1993. The Arabidopsis endoplasmic reticulum retention receptor functions in yeast. Proc Natl Acad Sci U S A, 90, 11433-7.

LEE, M. C. S., MILLER, E. A., GOLDBERG, J., ORCI, L. & SCHEKMAN, R. 2004. Bi-directional protein transport between the ER and Golgi. Annual Review of Cell and Developmental Biology, 20, 87-123.

LETOURNEUR, F., GAYNOR, E. C., HENNECKE, S., DEMOLLIERE, C., DUDEN, R., EMR, S. D., RIEZMAN, H. & COSSON, P. 1994. COATOMER IS ESSENTIAL FOR RETRIEVAL OF DILYSINE-TAGGED PROTEINS TO THE ENDOPLASMIC-RETICULUM. Cell, 79, 1199-1207.

LEWIS, M. J. & PELHAM, H. R. 1990. A human homologue of the yeast HDEL receptor. Nature, 348, 162-3.

LEWIS, M. J. & PELHAM, H. R. 1992a. Ligand-induced redistribution of a human KDEL receptor from the Golgi complex to the endoplasmic reticulum. Cell, 68, 353-64.

LEWIS, M. J. & PELHAM, H. R. B. 1992b. SEQUENCE OF A 2ND HUMAN KDEL RECEPTOR. Journal of Molecular Biology, 226, 913-916.

LEWIS, M. J., SWEET, D. J. & PELHAM, H. R. 1990. The ERD2 gene determines the specificity of the luminal ER protein retention system. Cell, 61, 1359-63.

LI, J., ZHAO-HUI, C., BATOUX, M., NEKRASOV, V., ROUX, M., CHINCHILLA, D., ZIPFEL, C. & JONES, J. D. G. 2009. Specific ER quality control components required for biogenesis of the plant innate immune receptor EFR. Proceedings of the National Academy of Sciences, 106, 15973-15978.

LIPPINCOTT-SCHWARTZ, J., DONALDSON, J. G., SCHWEIZER, A., BERGER, E. G., HAURI, H.-P., YUAN, L. C. & KLAUSNER, R. D. 1990. Microtubule-dependent retrograde transport of proteins into the ER in the presence of brefeldin a suggests an ER recycling pathway. Cell, 60, 821-836.

LIU, S. H., WONG, M. L., CRAIK, C. S. & BRODSKY, F. M. 1995. Regulation of clathrin assembly and trimerization defined using recombinant triskelion hubs. Cell, 83, 257-67.

LLOPIS, J., MCCAFFERY, J. M., MIYAWAKI, A., FARQUHAR, M. G. & TSIEN, R. Y. 1998. Measurement of cytosolic, mitochondrial, and Golgi pH in single living cells with green fluorescent proteins. Proc Natl Acad Sci U S A, 95, 6803-8.

LODISH, H. F., KONG, N., SNIDER, M. & STROUS, G. J. A. M. 1983. Hepatoma secretory proteins migrate from rough endoplasmic reticulum to Golgi at characteristic rates. Nature, 304, 80-83.

LORD, C., BHANDARI, D., MENON, S., GHASSEMIAN, M., NYCZ, D., HAY, J., GHOSH, P. & FERRO-NOVICK, S. 2011. Sequential interactions with Sec23 control the direction of vesicle traffic. Nature, 473, 181-6.

LU, L. & HONG, W. 2014. From endosomes to the trans-Golgi network. Seminars in Cell & Developmental Biology, 31, 30-39.

LUJAN, P. & CAMPELO, F. 2021. Should I stay or should I go? Golgi membrane spatial organization for protein sorting and retention. Archives of Biochemistry and Biophysics, 707, 108921.

MA, W., GOLDBERG, E. & GOLDBERG, J. 2017. ER retention is imposed by COPII protein sorting and attenuated by 4-phenylbutyrate. eLife, 6, e26624.

MACER, D. R. & KOCH, G. L. 1988. Identification of a set of calcium-binding proteins in reticuloplasm, the luminal content of the endoplasmic reticulum. Journal of Cell Science, 91, 61-70.

MAINS, P. E. & SIBLEY, C. H. 1983. The requirement of light chain for the surface deposition of the heavy chain of immunoglobulin M. J Biol Chem, 258, 5027-33.

MAJOUL, I., STRAUB, M., HELL, S. W., DUDEN, R. & SOLING, H. D. 2001. KDEL-cargo regulates interactions between proteins involved in COPI vesicle traffic: Measurements in living cells using FRET. Developmental Cell, 1, 139-153.

MALHOTRA, V., ORCI, L., GLICK, B. S., BLOCK, M. R. & ROTHMAN, J. E. 1988. Role of an N-ethylmaleimide-sensitive transport component in promoting fusion of transport vesicles with cisternae of the Golgi stack. Cell, 54, 221-7.

MALIGA, P., SZ-BREZNOVITS, A. & MARTON, L. 1973. Streptomycin-resistant plants from callus culture of haploid tobacco. Nat New Biol, 244, 29-30.

MANNEVILLE, J.-B., CASELLA, J.-F., AMBROGGIO, E., GOUNON, P., BERTHERAT, J., BASSEREAU, P., CARTAUD, J., ANTONNY, B. & GOUD, B. 2008. COPI coat assembly occurs on liquid-disordered domains and the associated membrane deformations are limited by membrane tension. Proceedings of the National Academy of Sciences, 105, 16946-16951.

MARTINIÈRE, A. & MOREAU, P. 2020. Complex roles of Rabs and SNAREs in the secretory pathway and plant development: a never-ending story. J Microsc, 280, 140-157.

MATSUOKA, K. & NEUHAUS, J.-M. 1999. Cis-elements of protein transport to the plant vacuoles. Journal of Experimental Botany, 50, 165-174.

MATSUOKA, K., SCHEKMAN, R., ORCI, L. & HEUSER, J. E. 2001. Surface structure of the COPII-coated vesicle. Proceedings of the National Academy of Sciences of the United States of America, 98, 13705-13709.

MATTERA, R., BOEHM, M., CHAUDHURI, R., PRABHU, Y. & BONIFACINO, J. S. 2011. Conservation and diversification of dileucine signal recognition by adaptor protein (AP) complex variants. J Biol Chem, 286, 2022-30.

MAYER, A., WICKNER, W. & HAAS, A. 1996. Sec18p (NSF)-driven release of Sec17p (alpha-SNAP) can precede docking and fusion of yeast vacuoles. Cell, 85, 83-94.

MEI, M., ZHAI, C., LI, X. Z., ZHOU, Y., PENG, W. F., MA, L. X., WANG, Q. H., IVERSON, B. L., ZHANG, G. M. & YI, L. 2017. Characterization of aromatic residue-controlled protein retention in the endoplasmic reticulum of Saccharomyces cerevisiae. Journal of Biological Chemistry, 292, 20707-20719.

MONTESINOS, J. C., PASTOR-CANTIZANO, N., ROBINSON, D. G., MARCOTE, M. J. & ANIENTO, F. 2014. Arabidopsis p24 delta 5 and p24 delta 9 facilitate Coat Protein I-dependent transport of the K/HDEL receptor ERD2 from the Golgi to the endoplasmic reticulum. Plant Journal, 80, 1014-1030.

MOSSESSOVA, E., BICKFORD, L. C. & GOLDBERG, J. 2003. SNARE selectivity of the COPII coat. Cell, 114, 483-95.

MUNRO, S. & PELHAM, H. R. B. 1987. A C-TERMINAL SIGNAL PREVENTS SECRETION OF LUMINAL ER PROTEINS. Cell, 48, 899-907.

NAKANO, A. & MURAMATSU, M. 1989. A NOVEL GTP-BINDING PROTEIN, SAR1P, IS INVOLVED IN TRANSPORT FROM THE ENDOPLASMIC-RETICULUM TO THE GOLGI-APPARATUS. Journal of Cell Biology, 109, 2677-2691.

NILSSON, T., JACKSON, M. & PETERSON, P. A. 1989. Short cytoplasmic sequences serve as retention signals for transmembrane proteins in the endoplasmic reticulum. Cell, 58, 707-18.

NISHIMURA, N. & BALCH, W. E. 1997. A di-acidic signal required for selective export from the endoplasmic reticulum. Science, 277, 556-558.

OHNO, H., STEWART, J., FOURNIER, M. C., BOSSHART, H., RHEE, I., MIYATAKE, S., SAITO, T., GALLUSSER, A., KIRCHHAUSEN, T. & BONIFACINO, J. S. 1995. Interaction of tyrosine-based sorting signals with clathrin-associated proteins. Science, 269, 1872-5.

ORCI, L., GLICK, B. S. & ROTHMAN, J. E. 1986. A new type of coated vesicular carrier that appears not to contain clathrin: Its possible role in protein transport within the Golgi stack. Cell, 46, 171-184.

ORCI, L., STAMNES, M., RAVAZZOLA, M., AMHERDT, M., PERRELET, A., SOLLNER, T. H. & ROTHMAN, J. E. 1997. Bidirectional transport by distinct populations of COPI-coated vesicles. Cell, 90, 335-349.

OTERO, J. H., LIZÁK, B. & HENDERSHOT, L. M. 2010. Life and death of a BiP substrate. Semin Cell Dev Biol, 21, 472-8.

PAGE, L. J., SOWERBY, P. J., LUI, W. W. & ROBINSON, M. S. 1999. Gamma-synergin: an EH domain-containing protein that interacts with gamma-adaptin. J Cell Biol, 146, 993-1004.

PALADE, G. 1975. Intracellular aspects of the process of protein synthesis. Science, 189, 347-358.

PARSONS, H. T., STEVENS, T. J., MCFARLANE, H. E., VIDAL-MELGOSA, S., GRISS, J., LAWRENCE, N., BUTLER, R., SOUSA, M. M. L., SALEMI, M., WILLATS, W. G. T., PETZOLD, C. J., HEAZLEWOOD, J. L. & LILLEYA, K. S. 2019. Separating Golgi Proteins from Cis to Trans Reveals Underlying Properties of Cisternal Localization. Plant Cell, 31, 2010-2034.

PEARSE, B. M. 1975. Coated vesicles from pig brain: purification and biochemical characterization. J Mol Biol, 97, 93-8.

PEARSE, B. M. & ROBINSON, M. S. 1990. Clathrin, adaptors, and sorting. Annu Rev Cell Biol, 6, 151-71.

PELHAM, H. R. 1988. Evidence that luminal ER proteins are sorted from secreted proteins in a post-ER compartment. Embo j, 7, 913-8.

PELHAM, H. R. B. 1994. ABOUT TURN FOR THE COPS. Cell, 79, 1125-1127.

PELHAM, H. R. B., HARDWICK, K. G. & LEWIS, M. J. 1988. SORTING OF SOLUBLE ER PROTEINS IN YEAST. Embo Journal, 7, 1757-1762.

PFEFFER, S. R. 2007. Unsolved mysteries in membrane traffic. Annu Rev Biochem, 76, 629-45.

PFEFFER, S. R. & ROTHMAN, J. E. 1987. Biosynthetic protein transport and sorting by the endoplasmic reticulum and Golgi. Annu Rev Biochem, 56, 829-52.

PHILLIPSON, B. A., PIMPL, P., DASILVA, L. L., CROFTS, A. J., TAYLOR, J. P., MOVAFEGHI, A., ROBINSON, D. G. & DENECKE, J. 2001. Secretory bulk flow of soluble proteins is efficient and COPII dependent. Plant Cell, 13, 2005-20.

PIMPL, P., HANTON, S. L., TAYLOR, J. P., PINTO-DASILVA, L. L. & DENECKE, J. 2003. The GTPase ARF1p controls the sequence-specific vacuolar sorting route to the lytic vacuole. Plant Cell, 15, 1242-56.

PRYER, N. K., SALAMA, N. R., SCHEKMAN, R. & KAISER, C. A. 1993. CYTOSOLIC SEC13P COMPLEX IS REQUIRED FOR VESICLE FORMATION FROM THE ENDOPLASMIC-RETICULUM INVITRO. Journal of Cell Biology, 120, 865-875.

RABOUILLE, C. & KLUMPERMAN, J. 2005. Opinion: The maturing role of COPI vesicles in intra-Golgi transport. Nat Rev Mol Cell Biol, 6, 812-7.

REN, X., FARÍAS, G. G., CANAGARAJAH, B. J., BONIFACINO, J. S. & HURLEY, J. H. 2013. Structural basis for recruitment and activation of the AP-1 clathrin adaptor complex by Arf1. Cell, 152, 755-67.

RICE, L. M. & BRUNGER, A. T. 1999. Crystal structure of the vesicular transport protein Sec17: implications for SNAP function in SNARE complex disassembly. Mol Cell, 4, 85-95.

ROBINSON, D. G. & ANIENTO, F. 2020. A Model for ERD2 Function in Higher Plants. 11.

ROBINSON, D. G. & NEUHAUS, J. M. 2016. Receptor-mediated sorting of soluble vacuolar proteins: myths, facts, and a new model. J Exp Bot, 67, 4435-49.

ROJO, E. & DENECKE, J. 2008. What Is Moving in the Secretory Pathway of Plants? Plant Physiology, 147, 1493-1503.

SALAMA, N. R., CHUANG, J. S. & SCHEKMAN, R. W. 1997. SEC31 encodes an essential component of the COPII coat required for transport vesicle budding from the endoplasmic reticulum. Molecular Biology of the Cell, 8, 205-217.

SALAMA, N. R., YEUNG, T. & SCHEKMAN, R. W. 1993. THE SEC13P COMPLEX AND RECONSTITUTION OF VESICLE BUDDING FROM THE ER WITH PURIFIED CYTOSOLIC PROTEINS. Embo Journal, 12, 4073-4082.

SAMBROOK, J., FRITSCH, E.F. & MANIATIS, T., 1989. Molecular cloning: a laboratory manual., Cold Spring Harbor: Cold Spring Harbor laboratory.

SANDERFOOT, A. A., AHMED, S. U., MARTY-MAZARS, D., RAPOPORT, I., KIRCHHAUSEN, T., MARTY, F. & RAIKHEL, N. V. 1998. A putative vacuolar cargo receptor partially colocalizes with AtPEP12p on a prevacuolar compartment in Arabidopsis roots. Proc Natl Acad Sci U S A, 95, 9920-5.

SATO, K. & NAKANO, A. 2004. Reconstitution of Coat Protein Complex II (COPII) Vesicle Formation from Cargo-reconstituted Proteoliposomes Reveals the Potential Role of GTP Hydrolysis by Sar1p in Protein Sorting*. Journal of Biological Chemistry, 279, 1330-1335.

SATO, K. & NAKANO, A. 2005. Dissection of COPII subunit-cargo assembly and disassembly kinetics during Sar1p-GTP hydrolysis. Nature Structural & Molecular Biology, 12, 167-174.

SAUDEK, V. 2012. Cystinosin, MPDU1, SWEETs and KDELR belong to a well-defined protein family with putative function of cargo receptors involved in vesicle trafficking. PLoS One, 7, e30876.

SCHACHTER, H., JABBAL, I., HUDGIN, R. L., PINTERIC, L., MCGUIRE, E. J. & ROSEMAN, S. 1970. Intracellular Localization of Liver Sugar Nucleotide Glycoprotein Glycosyltransferases in a Golgi-rich Fraction. Journal of Biological Chemistry, 245, 1090-1100.

SCHEEL, A. A. & PELHAM, H. R. B. 1998. Identification of amino acids in the binding pocket of the human KDEL receptor. Journal of Biological Chemistry, 273, 2467-2472.

SCHOBERER, J., KONIG, J., VEIT, C., VAVRA, U., LIEBMINGER, E., BOTCHWAY, S. W., ALTMANN, F., KRIECHBAUMER, V., HAWES, C. & STRASSER, R. 2019. A signal motif retains Arabidopsis ER-alpha-mannosidase I in the cis-Golgi and prevents enhanced glycoprotein ERAD. Nat Commun, 10, 3701.

SCHNEIDER, C. A., RASBAND, W. S. & ELICEIRI, K. W. 2012. NIH Image to ImageJ: 25 years of image analysis. Nature Methods, 9, 671-675.

SCHRAG, J. D., BERGERON, J. J. M., LI, Y., BORISOVA, S., HAHN, M., THOMAS, D. Y. & CYGLER, M. 2001. The Structure of Calnexin, an ER Chaperone Involved in Quality Control of Protein Folding. Molecular Cell, 8, 633-644.

SCHWARZ, D. S. & BLOWER, M. D. 2016. The endoplasmic reticulum: structure, function and response to cellular signaling. Cellular and Molecular Life Sciences, 73, 79-94.

SEAMAN, M. N. 2012. The retromer complex - endosomal protein recycling and beyond. J Cell Sci, 125, 4693-702.

SEAMAN, M. N., MCCAFFERY, J. M. & EMR, S. D. 1998. A membrane coat complex essential for endosome-to-Golgi retrograde transport in yeast. J Cell Biol, 142, 665-81.

SEAMAN, M. N. J. 2005. Recycle your receptors with retromer. Trends in Cell Biology, 15, 68-75.

SEMENZA, J. C., HARDWICK, K. G., DEAN, N. & PELHAM, H. R. B. 1990. ERD2, A YEAST GENE REQUIRED FOR THE RECEPTOR-MEDIATED RETRIEVAL OF LUMINAL ER PROTEINS FROM THE SECRETORY PATHWAY. Cell, 61, 1349-1357.

SEMENZA, J. C. & PELHAM, H. R. 1992. Changing the specificity of the sorting receptor for luminal endoplasmic reticulum proteins. J Mol Biol, 224, 1-5.

SHEN, J. & PRYWES, R. 2005. ER stress signaling by regulated proteolysis of ATF6. Methods, 35, 382-389.

SHIBATA, Y., HU, J., KOZLOV, M. M. & RAPOPORT, T. A. 2009. Mechanisms shaping the membranes of cellular organelles. Annu Rev Cell Dev Biol, 25, 329-54.

SHIBATA, Y., SHEMESH, T., PRINZ, W. A., PALAZZO, A. F., KOZLOV, M. M. & RAPOPORT, T. A. 2010. Mechanisms determining the morphology of the peripheral ER. Cell, 143, 774-88.

SHINSHI, H., WENZLER, H., NEUHAUS, J.-M., FELIX, G., HOFSTEENGE, J. & MEINS, F. 1988. Evidence for N- and C-terminal processing of a plant defense-related enzyme: Primary structure of tobacco prepro-β-1,3-glucanase. Proceedings of the National Academy of Sciences, 85, 5541-5545.

SHOMRON, O., NEVO-YASSAF, I., AVIAD, T., YAFFE, Y., ZAHAVI, E. E., DUKHOVNY, A., PERLSON, E., BRODSKY, I., YEHESKEL, A., PASMANIK-CHOR, M., MIRONOV, A., BEZNOUSSENKO, G. V., MIRONOV, A. A., SKLAN, E. H., PATTERSON, G. H., YONEMURA, Y., SANNAI, M., KAETHER, C. & HIRSCHBERG, K. 2021. COPII collar defines the boundary between ER and ER exit site and does not coat cargo containers. J Cell Biol, 220.

SICARI, D., IGBARIA, A. & CHEVET, E. 2019. Control of Protein Homeostasis in the Early Secretory Pathway: Current Status and Challenges. Cells, 8.

SIEKEVITZ, P. & PALADE, G. E. 1960. A cytochemical study on the pancreas of the guinea pig. 5. In vivo incorporation of leucine-1-C14 into the chymotrypsinogen of various cell fractions. J Biophys Biochem Cytol, 7, 619-30.

SILVA-ALVIM, F. A. L., AN, J., ALVIM, J. C., FORESTI, O., GRIPPA, A., PELGROM, A., ADAMS, T. L., HAWES, C. & DENECKE, J. 2018. Predominant Golgi Residency of the Plant K/HDEL Receptor Is Essential for Its Function in Mediating ER Retention. Plant Cell, 30, 2174-2196.

SINGH, P., TANG, B. L., WONG, S. H. & HONG, W. J. 1993. TRANSMEMBRANE TOPOLOGY OF THE MAMMALIAN KDEL RECEPTOR. Molecular and Cellular Biology, 13, 6435-6441.

SPANG, A., MATSUOKA, K., HAMAMOTO, S., SCHEKMAN, R. & ORCI, L. 1998. Coatomer, Arf1p, and nucleotide are required to bud coat protein complex I-coated vesicles from large synthetic liposomes. Proceedings of the National Academy of Sciences, 95, 11199-11204.

SPARKES, I. A., RUNIONS, J., KEARNS, A. & HAWES, C. 2006. Rapid, transient expression of fluorescent fusion proteins in tobacco plants and generation of stably transformed plants. Nature Protocols, 1, 2019-2025.

SPARKES, I., TOLLEY, N., ALLER, I., SVOZIL, J., OSTERRIEDER, A., BOTCHWAY, S., MUELLER, C., FRIGERIO, L. & HAWES, C. 2010. Five Arabidopsis reticulon isoforms share endoplasmic reticulum location, topology, and membrane-shaping properties. Plant Cell, 22, 1333-43.

STAGG, S. M., GURKAN, C., FOWLER, D. M., LAPOINTE, P., FOSS, T. R., POTTER, C. S., CARRAGHER, B. & BALCH, W. E. 2006. Structure of the Sec13/31 COPII coat cage. Nature, 439, 234-238.

STANLEY, P. 2011. Golgi glycosylation. Cold Spring Harbor perspectives in biology, 3, a005199.

STRATING, J. R. P. M. & MARTENS, G. J. M. 2009. The p24 family and selective transport processes at the ER—Golgi interface. Biology of the Cell, 101, 495-509.

SUTTON, R. B., FASSHAUER, D., JAHN, R. & BRUNGER, A. T. 1998. Crystal structure of a SNARE complex involved in synaptic exocytosis at 2.4 A resolution. Nature, 395, 347-53.

SÖLLNER, T., WHITEHEART, S. W., BRUNNER, M., ERDJUMENT-BROMAGE, H., GEROMANOS, S., TEMPST, P. & ROTHMAN, J. E. 1993. SNAP receptors implicated in vesicle targeting and fusion. Nature, 362, 318-324.

TAKATSU, H., YOSHINO, K. & NAKAYAMA, K. 2000. Adaptor gamma ear homology domain conserved in gamma-adaptin and GGA proteins that interact with gamma-synergin. Biochem Biophys Res Commun, 271, 719-25.

TANG, B. L., WONG, S. H., QI, X. L., LOW, S. H. & HONG, W. J. 1993. MOLECULAR-CLONING, CHARACTERIZATION, SUBCELLULAR-LOCALIZATION AND DYNAMICS OF P23, THE MAMMALIAN KDEL RECEPTOR. Journal of Cell Biology, 120, 325-338.

TAO, Y., CHEUNG, L. S., LI, S., EOM, J.-S., CHEN, L.-Q., XU, Y., PERRY, K., FROMMER, W. B. & FENG, L. 2015. Structure of a eukaryotic SWEET transporter in a homotrimeric complex. Nature, 527, 259.

TAVARES, L. A., DA SILVA, E. M. L., DA SILVA-JANUÁRIO, M. E., JANUÁRIO, Y. C., DE CAVALHO, J. V., CZERNISZ, É. S., MARDONES, G. A. & DASILVA, L. L. P. 2017. CD4 downregulation by the HIV-1 protein Nef reveals distinct roles for the γ1 and γ2 subunits of the AP-1 complex in protein trafficking. Journal of Cell Science, 130, 429-443.

TAYLOR, S. C., FERGUSON, A. D., BERGERON, J. J. & THOMAS, D. Y. 2004. The ER protein folding sensor UDP-glucose glycoprotein-glucosyltransferase modifies substrates distant to local changes in glycoprotein conformation. Nat Struct Mol Biol, 11, 128-34.

TER HAAR, E., HARRISON, S. C. & KIRCHHAUSEN, T. 2000. Peptide-in-groove interactions link target proteins to the β-propeller of clathrin. Proceedings of the National Academy of Sciences, 97, 1096-1100.

THOMAS, S. 2020. The Structure of the Membrane Protein of SARS-CoV-2 Resembles the Sugar Transporter SemiSWEET. Pathog Immun, 5, 342-363.

THYBERG, J. & MOSKALEWSKI, S. 1999. Role of microtubules in the organization of the Golgi complex. Exp Cell Res, 246, 263-79.

TOUCHOT, N., CHARDIN, P. & TAVITIAN, A. 1987. Four additional members of the ras gene superfamily isolated by an oligonucleotide strategy: molecular cloning of YPT-related cDNAs from a rat brain library. Proc Natl Acad Sci U S A, 84, 8210-4.

TOWNLEY, A. K., FENG, Y., SCHMIDT, K., CARTER, D. A., PORTER, R., VERKADE, P. & STEPHENS, D. J. 2008. Efficient coupling of Sec23-Sec24 to Sec13-Sec31 drives COPII-dependent collagen secretion and is essential for normal craniofacial development. Journal of Cell Science, 121, 3025-3034.

TOWNSLEY, F. M., FRIGERIO, G. & PELHAM, H. R. B. 1994. RETRIEVAL OF HDEL PROTEINS IS REQUIRED FOR GROWTH OF YEAST-CELLS. Journal of Cell Biology, 127, 21-28.

TOWNSLEY, F. M., WILSON, D. W. & PELHAM, H. R. B. 1993. MUTATIONAL ANALYSIS OF THE HUMAN KDEL RECEPTOR - DISTINCT STRUCTURAL REQUIREMENTS FOR GOLGI RETENTION, LIGAND-BINDING AND RETROGRADE TRANSPORT. Embo Journal, 12, 2821-2829.

TRAUB, L. M. & KORNFELD, S. 1997. The trans-Golgi network: a late secretory sorting station. Current Opinion in Cell Biology, 9, 527-533.

VATTEM, K. M. & WEK, R. C. 2004. Reinitiation involving upstream ORFs regulates ATF4 mRNA translation in mammalian cells. Proceedings of the National Academy of Sciences of the United States of America, 101, 11269-11274.

VIOTTI, C., BUBECK, J., STIERHOF, Y. D., KREBS, M., LANGHANS, M., VAN DEN BERG, W., VAN DONGEN, W., RICHTER, S., GELDNER, N., TAKANO, J., JÜRGENS, G., DE VRIES, S. C., ROBINSON, D. G. & SCHUMACHER, K. 2010. Endocytic and secretory traffic in Arabidopsis merge in the trans-Golgi network/early endosome, an independent and highly dynamic organelle. Plant Cell, 22, 1344-57.

VITALE, A. & DENECKE, J. 1999. The endoplasmic reticulum - Gateway of the secretory pathway. Plant Cell, 11, 615-628.

VOELTZ, G. K., PRINZ, W. A., SHIBATA, Y., RIST, J. M. & RAPOPORT, T. A. 2006. A Class of Membrane Proteins Shaping the Tubular Endoplasmic Reticulum. Cell, 124, 573-586.

VON FIGURA, K. & HASILIK, A. 1986. Lysosomal enzymes and their receptors. Annu Rev Biochem, 55, 167-93.

VON HEIJNE, G. 1992. Membrane protein structure prediction. Hydrophobicity analysis and the positive-inside rule. J Mol Biol, 225, 487-94.

WAHEED, A., POHLMANN, R., HASILIK, A. & VON FIGURA, K. 1981. Subcellular location of two enzymes involved in the synthesis of phosphorylated recognition markers in lysosomal enzymes. J Biol Chem, 256, 4150-2.

WALCH-SOLIMENA, C., JAHN, R. & SÜDHOF, T. C. 1993. Synaptic vesicle proteins in exocytosis: what do we know? Curr Opin Neurobiol, 3, 329-36.

WANG, C., YAN, X., CHEN, Q., JIANG, N., FU, W., MA, B., LIU, J., LI, C., BEDNAREK, S. Y. & PAN, J. 2013. Clathrin light chains regulate clathrin-mediated trafficking, auxin signaling, and development in Arabidopsis. Plant Cell, 25, 499-516.

WANG, S. S., XIE, K., XU, G. Y., ZHOU, H. R., GUO, Q., WU, J. Y., LIAO, Z. W., LIU, N., WANG, Y. & LIU, Y. L. 2018. Plant G proteins interact with endoplasmic reticulum luminal protein receptors to regulate endoplasmic reticulum retrieval. Journal of Integrative Plant Biology, 60, 541-561.

WANG, Y. J., WANG, J., SUN, H. Q., MARTINEZ, M., SUN, Y. X., MACIA, E., KIRCHHAUSEN, T., ALBANESI, J. P., ROTH, M. G. & YIN, H. L. 2003. Phosphatidylinositol 4 phosphate regulates targeting of clathrin adaptor AP-1 complexes to the Golgi. Cell, 114, 299-310.

WATERS, M. G., SERAFINI, T. & ROTHMAN, J. E. 1991. 'Coatomer': a cytosolic protein complex containing subunits of non-clathrin-coated Golgi transport vesicles. Nature, 349, 248-51.

WEIGEL, A. V., CHANG, C.-L., SHTENGEL, G., XU, C. S., HOFFMAN, D. P., FREEMAN, M., IYER, N., AARON, J., KHUON, S., BOGOVIC, J., QIU, W., HESS, H. F. & LIPPINCOTT-SCHWARTZ, J. 2021. ER-to-Golgi protein delivery through an interwoven, tubular network extending from ER. Cell, 184, 2412-2429.e16.

WIELAND, F. T., GLEASON, M. L., SERAFINI, T. A. & ROTHMAN, J. E. 1987. The rate of bulk flow from the endoplasmic reticulum to the cell surface. Cell, 50, 289-300.

WILKINSON, B. & GILBERT, H. F. 2004. Protein disulfide isomerase. Biochimica et Biophysica Acta (BBA) - Proteins and Proteomics, 1699, 35-44.

WILSON, D. W., LEWIS, M. J. & PELHAM, H. R. 1993. pH-dependent binding of KDEL to its receptor in vitro. J Biol Chem, 268, 7465-8.

WOO, C. H., GAO, C., YU, P., TU, L., MENG, Z., BANFIELD, D. K., YAO, X. & JIANG, L. 2015. Conserved function of the lysine-based KXD/E motif in Golgi retention for endomembrane proteins among different organisms. Molecular Biology of the Cell, 26, 4280-4293.

XU, G. & LIU, Y. 2012. Plant ERD2s self-interact and interact with GTPase-activating proteins and ADP-ribosylation factor 1. Plant Signal Behav, 7, 1092-4.

XU, G. Y., LI, S. Z., XIE, K., ZHANG, Q., WANG, Y., TANG, Y., LIU, D., HONG, Y. G., HE, C. Y. & LIU, Y. L. 2012. Plant ERD2-like proteins function as endoplasmic reticulum luminal protein receptors and participate in programmed cell death during innate immunity. Plant Journal, 72, 57-69.

XUAN, Y. H., HU, Y. B., CHEN, L. Q., SOSSO, D., DUCAT, D. C., HOU, B. H. & FROMMER, W. B. 2013. Functional role of oligomerization for bacterial and plant SWEET sugar transporter family. Proc Natl Acad Sci U S A, 110, E3685-94.

YBE, J. A., BRODSKY, F. M., HOFMANN, K., LIN, K., LIU, S. H., CHEN, L., EARNEST, T. N., FLETTERICK, R. J. & HWANG, P. K. 1999. Clathrin self-assembly is mediated by a tandemly repeated superhelix. Nature, 399, 371-5.

YBE, J. A., GREENE, B., LIU, S. H., PLEY, U., PARHAM, P. & BRODSKY, F. M. 1998. Clathrin self-assembly is regulated by three light-chain residues controlling the formation of critical salt bridges. Embo j, 17, 1297-303.

YOSHIHISA, T., BARLOWE, C. & SCHEKMAN, R. 1993. REQUIREMENT FOR A GTPASE-ACTIVATING PROTEIN IN VESICLE BUDDING FROM THE ENDOPLASMIC-RETICULUM. Science, 259, 1466-1468.

# Appendix 1

nature communications

Article

https://doi.org/10.1038/s41467-023-37056-0

# The K/HDEL receptor does not recycle but instead acts as a Golgi-gatekeeper

Received: 29 June 2022

Accepted: 24 February 2023

Published online: 23 March 2023

Check for updates

Jonas C. Alvim[1,3,4], Robert M. Bolt[1,4], Jing An[1], Yasuko Kamisugi[1], Andrew Cuming[1], Fernanda A. L. Silva-Alvim[1,3], Juan O. Concha[2], Luis L. P. daSilva[2], Meiyi Hu[1], Dominique Hirsz[1] & Jurgen Denecke[1]

Accurately measuring the ability of the K/HDEL receptor (ERD2) to retain the ER cargo Amy-HDEL has questioned earlier results on which the popular receptor recycling model is based upon. Here we demonstrate that ERD2 Golgi-retention, rather than fast ER export supports its function. Ligand-induced ERD2 redistribution is only observed when the C-terminus is masked or mutated, compromising the signal that prevents Golgi-to-ER transport of the receptor. Forcing COPI mediated retrograde transport destroys receptor function, but introducing ER-to-Golgi export or *cis*-Golgi retention signals re-activate ERD2 when its endogenous Golgi-retention signal is masked or deleted. We propose that ERD2 remains fixed as a Golgi gatekeeper, capturing K/HDEL proteins when they arrive and releasing them again into a subdomain for retrograde transport back to the ER. An in vivo ligand:receptor ratio far greater than 100 to 1 strongly supports this model, and the underlying mechanism appears to be extremely conserved across kingdoms.

The Golgi apparatus plays a central role in sending and receiving membrane carriers to and from organelles of the secretory pathway. Its evolutionary origin is unknown, and how it maintains its identity despite the constant influx and efflux of transport carriers continues to fascinate and divide the field[1–3]. Membrane-spanning sorting receptors are a particularly interesting class of proteins as they mediate the sorting of cargo but need to be sorted themselves.

A central dogma to describe receptor-mediated transport was first derived from the principle of receptor-mediated endocytosis at the plasma membrane[4]. Another prominent example is the mannose-6-phosphate (M6P) receptor which binds lysosomal proteins in the Golgi, moves in clathrin-coated vesicles to early endosomes, followed by ligand-release and receptor recycling back to the Golgi[5,6]. Continuous recycling[7] permits few receptors to sort many lysosomal proteins, and this was shown to be essential for vacuolar sorting in yeasts[8] and plants[9]. Well-defined receptor mutants with defects in either anterograde or retrograde transport strongly support the recycling model[10,11].

Evidence that a similar recycling principle operates for highly abundant soluble ER residents bearing the KDEL or HDEL retention signal first arose from the detection of post-translational modifications that are Golgi-specific[12,13]. An elegant genetic screen led to the identification of the K/HDEL receptor (ERD2) in yeast[14], followed by the isolation of the human homologue[15]. Ligand-overproduction caused human ERD2 redistribution from the Golgi to the ER[16], and the receptor-recycling principle was generally accepted by the field. Since detection of endogenous ERD2 proved technically difficult[17,18], the field used C-terminal ERD2 fusions for subcellular localisation, to the extent that ligand-induced ERD2 redistribution was used to monitor its activity indirectly[19,20–22], rather than studying ligand-retention directly in function of ERD2 levels.

We have recently established a method that allows quantification of ERD2 activity by monitoring increased retention of HDEL or KDEL proteins[23]. This assay revealed that YFP or RFP fused to the ERD2 C-terminus inactivate the receptor. A fluorescent fusion (YFP-TM-ERD2) in which the ERD2 core remains unobstructed retains the ability

[1]Centre for Plant Sciences, School of Biology, Faculty of Biological Sciences, University of Leeds, Leeds LS2 9JT, UK. [2]Department of Cell and Molecular Biology, Ribeirão Preto Medical School, University of São Paulo, Ribeirão Preto, São Paulo, Brazil. [3]Present address: Laboratory of Plant Physiology and Biophysics, Bower Building, University of Glasgow, Glasgow G12 8QQ, UK. [4]These authors contributed equally: Jonas C. Alvim, Robert M. Bolt.
e-mail: j.denecke@leeds.ac.uk